

**Environmental and physiological controls over carbon
and oxygen isotope variations in plants**

Lucas Alexander Cernusak

January, 2004

*A thesis submitted for the degree of Doctor of Philosophy of
The Australian National University*



THE AUSTRALIAN NATIONAL UNIVERSITY

Statement of Originality

Data presented in Figure 3.4B were kindly provided by Mr. DJ Arthur and Professor JS Pate, School of Plant Biology, Faculty of Natural and Agricultural Sciences, The University of Western Australia. The derivation presented in the Appendix to Chapter 4 (4.6. Appendix: including phloem water export in the calculation of Δ_e) was kindly provided by Professor GD Farquhar, Environmental Biology Group, Research School of Biological Sciences, The Australian National University.

All other work presented in this thesis was carried out by myself.



Lucas Cernusak



Acknowledgments

Many people have contributed their time and energy generously over the course of my PhD program, without which I would not have been able to complete this thesis. John Pate and David Arthur provided essential assistance with all sample collections and field measurements conducted in Western Australia. Chin Wong constructed the gas exchange system used for measurements in Canberra, and provided invaluable assistance with day to day operation and trouble-shooting. Hilary Stuart-Williams and Sue Wood generously assisted with isotopic analyses in Canberra, as did Lidia Bednarek with isotopic analyses in Perth. Jeff Wood provided helpful advice for the statistical analysis of data presented in Chapter 5. Finally, Graham Farquhar was intimately involved in the planning and theoretical analysis of all experiments presented in this thesis. I gratefully acknowledge the assistance of these people.

I acknowledge the support of the Cooperative Research Center for Greenhouse Accounting, and thank its tireless staff, especially Janette Lindesay, for enriching my PhD course.

Many people contributed toward making my PhD experience very positive and enjoyable. I thank the members of the Environmental Biology Group, Research School of Biological Sciences, for stimulating scientific and non-scientific discussions. I especially thank Margaret Barbour and Sally Box for their insight, support, and friendship. I thank Graham Farquhar for continually challenging me, and for fostering a motivating, yet relaxed, research environment.

Finally, I thank Lisa for her kindness and her companionship, and my family for all of their support and encouragement.

Abstract

Small variations in the natural abundance of stable isotopes of carbon and oxygen in terrestrial ecosystems can provide important information about plant and ecosystem responses to environmental change. However, application of such variations requires a quantitative understanding of isotopic fractionations caused by plants. The aim of this thesis was to provide a better understanding of the biological and physical fractionation of carbon and oxygen stable isotopes during some physiological processes in plants. Key results are as follows:

- Phloem water was found to be enriched in ^{18}O relative to xylem water. However, the enrichments were rather variable among species, with *Lupinus angustifolius* and *Ricinus communis*, two herbaceous species, showing larger enrichments than *Eucalyptus globulus*, a long-lived, woody species. Results suggest that the potential influence of ^{18}O -enriched phloem water should be considered when interpreting $^{18}\text{O}/^{16}\text{O}$ of organic material in herbaceous plants.
- Leaf water $^{18}\text{O}/^{16}\text{O}$ was found to be more enriched at night than predictions of a steady state leaf water model under field conditions in both *Lupinus angustifolius* and *Eucalyptus globulus*. A non-steady state modification of the leaf water model resulted in improved predictions of nighttime leaf water $^{18}\text{O}/^{16}\text{O}$ in both species.
- Correlated changes were observed in phloem sap sugar concentration and phloem sap sugar $^{13}\text{C}/^{12}\text{C}$ in response to variation in plant water potential in *Eucalyptus globulus*. Results suggest that measurements of phloem sap sugar concentration may provide a simple, easily-obtained indicator of plant water status.
- The $^{18}\text{O}/^{16}\text{O}$ of phloem sap sugars exported from photosynthesizing *Ricinus communis* leaves was found to be very close to that predicted for organic molecules in equilibrium with average lamina leaf water. Similar results were obtained for *Eucalyptus globulus* in the field.
- Consistent variations in leaf organic material $^{18}\text{O}/^{16}\text{O}$ and $^{13}\text{C}/^{12}\text{C}$ between parasitic plants and their hosts were observed among different functional types of parasitic plants growing in southwestern Australia. In some cases these variations were easily interpretable using existing models of plant organic

material $^{18}\text{O}/^{16}\text{O}$ and $^{13}\text{C}/^{12}\text{C}$. However, in other cases, the observed variations could not be accounted for with such models.

- The carbon dioxide diffusing out of *Ricinus communis* leaves in the dark was found to be very enriched in ^{18}O compared to predictions made with a contemporary model of $^{18}\text{O}/^{16}\text{O}$ in leaf dark respiration that considers only the net CO_2 efflux from the leaf. Modification of the model to take into account the large flux of CO_2 that enters leaves, equilibrates with leaf water, and diffuses out of leaves without affecting the net CO_2 efflux, resulted in sensible interpretations of observed data.

Collectively, the results presented in this thesis should allow improved interpretation of $^{18}\text{O}/^{16}\text{O}$ and $^{13}\text{C}/^{12}\text{C}$ in plant organic material, and of $^{18}\text{O}/^{16}\text{O}$ in atmospheric CO_2 . It is ultimately hoped that this will improve the ability of the scientific community to detect and predict plant and ecosystem responses to environmental change.

Table of Contents

Chapter 1: General Introduction	1
1.1. Motivation	1
1.2. Isotope Notation	2
1.3. Research Topics	2
1.4. Structure of the Thesis	3
1.5. Publications	4
Chapter 2: Diurnal variation in the stable isotope composition of water and dry matter in fruiting <i>Lupinus angustifolius</i> under field conditions	6
2.1. Abstract	6
2.2. Introduction	7
2.3. Materials and Methods	8
2.3.1. Study site	8
2.3.2. Gas-exchange measurements	8
2.3.3. Sample collections	9
2.3.4. Isotopic analyses	11
2.3.5. Modeling leaf water isotopic enrichment	12
2.4. Results	14
2.4.1. Gas-exchange	14
2.4.2. Isotopic composition of dry matter components	15
2.4.3. Isotopic composition of water components within the system	18
2.5. Discussion	26
2.5.1. Isotopic composition of water components within the system	27
2.5.2. Isotopic composition of dry matter components	30
Chapter 3: Water relations link carbon and oxygen isotope discrimination to phloem sap sugar concentration in <i>Eucalyptus globulus</i>	36
3.1. Abstract	36
3.2. Introduction	36
3.3. Materials and Methods	40
3.4. Results	45
3.5. Discussion	52

Chapter 4: Oxygen isotope composition of phloem sap in relation to leaf water in <i>Ricinus communis</i>	59
4.1. Abstract	59
4.2. Introduction	59
4.3. Materials and Methods	63
4.3.1. Glasshouse experiment 1	63
4.3.2. Leaf chamber experiment 1	64
4.3.3. Glasshouse experiment 2	65
4.3.4. Leaf chamber experiment 2	66
4.3.5. Isotopic analyses	66
4.4. Results	67
4.4.1. Enrichment of ^{18}O in leaf water and phloem sap dry matter	67
4.4.2. Enrichment of ^{18}O in phloem water	72
4.5. Discussion	72
4.6. Appendix: including phloem water export in the calculation of Δ_e	78
 Chapter 5: Oxygen and carbon isotope composition of parasitic plants and their hosts in southwestern Australia	 81
5.1. Abstract	81
5.2. Introduction	81
5.3. Materials and Methods	85
5.4. Results	88
5.4.1. Mistletoe $\delta^{18}\text{O}$	88
5.4.2. Mistletoe $\delta^{13}\text{C}$	91
5.4.3. Root hemiparasite $\delta^{18}\text{O}$	93
5.4.4. Root hemiparasite $\delta^{13}\text{C}$	93
5.4.5. Holoparasite $\delta^{18}\text{O}$	94
5.4.6. Holoparasite $\delta^{13}\text{C}$	94
5.4.7. All species $\delta^{18}\text{O}$ and $\delta^{13}\text{C}$	95
5.5. Discussion	97
5.5.1. Mistletoe $\delta^{18}\text{O}$	98
5.5.2. Mistletoe $\delta^{13}\text{C}$	100
5.5.3. Root hemiparasite $\delta^{18}\text{O}$ and $\delta^{13}\text{C}$	101

5.5.4. Holoparasite $\delta^{18}\text{O}$	102
5.5.5. Holoparasite $\delta^{13}\text{C}$	103
5.5.6. All species $\delta^{18}\text{O}$ and $\delta^{13}\text{C}$	105

Chapter 6: Environmental and physiological controls over the oxygen and carbon isotope composition of the Tasmanian blue gum, <i>Eucalyptus globulus</i>	106
6.1. Abstract	106
6.2. Introduction	106
6.3. Theory	107
6.4. Materials and Methods	110
6.4.1. Sampling campaign 1	110
6.4.2. Sampling campaign 2	112
6.4.3. Sampling campaign 3	112
6.4.4. Isotopic analyses	115
6.4.5. Isotopic calculations	116
6.5. Results	117
6.5.1. Xylem water $\delta^{18}\text{O}$	117
6.5.2. Leaf water $\Delta^{18}\text{O}$	119
6.5.3. Phloem sap $\Delta^{18}\text{O}_{\text{pw}}$	123
6.5.4. Phloem sap $\Delta^{18}\text{O}_{\text{suc}}$	123
6.5.5. Leaf $\Delta^{18}\text{O}_{\text{p}}$ and $\Delta^{18}\text{O}_{\text{c}}$	126
6.5.6. Wood and bark $\Delta^{18}\text{O}_{\text{p}}$ and $\Delta^{18}\text{O}_{\text{c}}$	128
6.5.7. Phloem sap, leaf, and wood $\Delta^{13}\text{C}$	129
6.5.8. Correlations between $\Delta^{18}\text{O}$ and $\Delta^{13}\text{C}$	133
6.6. Discussion	133
6.6.1. Xylem water $\delta^{18}\text{O}$	134
6.6.2. Leaf water $\Delta^{18}\text{O}$	134
6.6.3. Phloem sap $\Delta^{18}\text{O}_{\text{pw}}$	135
6.6.4. Phloem sap $\Delta^{18}\text{O}_{\text{suc}}$	136
6.6.5. Leaf $\Delta^{18}\text{O}_{\text{p}}$ and $\Delta^{18}\text{O}_{\text{c}}$	136
6.6.6. Wood and bark $\Delta^{18}\text{O}_{\text{p}}$ and $\Delta^{18}\text{O}_{\text{c}}$	140
6.6.7. Phloem sap, leaf, and wood $\Delta^{13}\text{C}$	141
6.6.8. Correlations between $\Delta^{18}\text{O}$ and $\Delta^{13}\text{C}$	142

Chapter 7: Measurement and interpretation of the oxygen isotope composition of carbon dioxide respired by leaves in the dark	144
7.1. Abstract	144
7.2. Introduction	144
7.3. Theory	146
7.4. Methods	150
7.4.1. Plant material and gas exchange measurements	150
7.4.2. Isotope measurements	152
7.4.3. Calculation of the oxygen isotope composition of dark-respired CO ₂	152
7.4.4. Calculation of photosynthetic discrimination against ¹³ C and ¹⁸ O	153
7.4.5. Calculation of the conductance from c _i to c _e	154
7.4.6. Calculation of the oxygen isotope composition of average lamina leaf water	155
7.5. Results	156
7.5.1. Dark respiration with CO ₂ free air entering the leaf chamber	156
7.5.2. Dark respiration at atmospheric CO ₂ concentration	159
7.5.3. Carbon and oxygen isotope discrimination during photosynthesis	160
7.6. Discussion	162
7.7. Appendix	170
7.7.1. Predicting the δ ¹⁸ O of dark-respired CO ₂	170
7.7.2. Calculating δ _R from on-line gas-exchange measurements	171
Chapter 8: General Conclusions	173
8.1. Conclusions to Questions Posed in Chapter 1	173
8.1.1. Question 1	173
8.1.2. Question 2	174
8.1.3. Question 3	174
8.1.4. Question 4	174
8.1.5. Question 5	175
8.1.6. Question 6	175
8.2. Future Research Questions	176
Bibliography	174

Chapter 1: General Introduction

1.1. Motivation

Anthropogenic activity has impacted upon many aspects of terrestrial ecosystems. For example, dramatic alterations in productivity, nutrient cycling, and species composition have occurred in many places. In the coming century, terrestrial ecosystems will undoubtedly continue to experience extensive biophysical and biological change. It is important to understand and predict ecosystem responses to such changes, in order to avoid irreparable degradation of ecosystem goods and services. Sound predictions of ecosystem responses to environmental change must be based on reliable knowledge of the mechanisms that control ecosystem processes, particularly the transfer of energy and mass among ecosystem components.

Within this context, it is important to consider plant physiological processes. Plants control the transfer of carbon, water, and nutrients between ecosystem biota and the abiotic environment. Plant physiological processes can be studied over a range of spatial and temporal scales and organizational levels. It is important to consider all of these scales and levels in order to gain multiple insights into how plants regulate ecosystem processes and responses to different types of change.

Variation in the natural abundance of stable isotopes provides a useful tool for investigating the controls on plant physiological processes at scales ranging from the leaf to globe (Griffiths 1998). Recent technological advances have allowed measurements of stable isotope ratios to be made more quickly and efficiently than was previously possible. As a result, isotopic measurements can be easily combined with other physiological measurements to make novel insights into the mechanisms that regulate ecosystem function.

Stable isotopes of the elements carbon (C) and oxygen (O) occur naturally in the environment. The stable isotope ^{13}C contains one neutron more than the much more abundant ^{12}C , and comprises about 1% of carbon in terrestrial ecosystems. Similarly, the stable isotope ^{18}O contains two neutrons more than ^{16}O , and comprises about 0.2% of oxygen in terrestrial ecosystems. The stable isotopes ^{13}C and ^{18}O are incorporated into biological cycles along side their much more abundant counterparts, ^{12}C and ^{16}O . The ratios of the minor to major isotopes ($^{13}\text{C}/^{12}\text{C}$ and $^{18}\text{O}/^{16}\text{O}$) are modified to varying extents during transfer between the abiotic environment and plants, and among different components within plants. These modifications are termed fractionations; alternatively the term discrimination can be applied, which specifically denotes the proportional

deviation from unity of the isotope ratio of a reactant relative to a product (Farquhar and Richards 1984). For many processes, discrimination against ^{13}C or ^{18}O varies according to how plants respond physiologically to changes in their environment. Such variations in isotopic discrimination can therefore reveal important information about plant and ecosystem responses to environmental change (Yakir and Sternberg 2000; Adams and Grierson 2001; Dawson et al. 2002; Ehleringer et al. 2002; Maguas and Griffiths 2003).

1.2. Isotope Notation

Because the natural variations that occur in stable isotope ratios are very small in absolute terms, the isotopic composition of a material (δ_X) is typically expressed as its relative deviation from that of a standard:

$$\delta_X = \frac{R_X}{R_{Std}} - 1, \quad (1.1)$$

where R_X is the isotope ratio of material X , and R_{Std} is that of the standard. The resulting δ value is then multiplied by 1000, giving it the dimension per mil (‰), in order to avoid the use of very small numbers. Although different isotope laboratories often use different secondary standards, the δ values are always related back to a primary standard, so that values can be compared among laboratories. For example, in the case of $\delta^{13}\text{C}$, values are related to the primary standard Pee Dee Belemnite (Craig 1957), which has a $^{13}\text{C}/^{12}\text{C}$ ratio of 0.01124.

In some cases, it is convenient to express the isotope ratio of a material as the relative deviation from a previous state following some process or reaction, rather than as the relative deviation from a standard. Farquhar and Richards (1984) suggested that the isotope discrimination associated with a process or reaction (Δ_Y) could be expressed as

$$\Delta_Y = \frac{R_{reactant}}{R_{product}} - 1, \quad (1.2)$$

where $R_{reactant}$ is the isotope ratio of material X before process Y , and $R_{product}$ is the isotope ratio afterward. The resulting Δ values are also typically expressed as per mil.

1.3. Research Topics

Application of stable isotope variations to the study of plant and ecosystem physiology requires a quantitative understanding of the fractionation events that take

place during the transfer of energy and mass within plants and ecosystems. The aim of research presented in this thesis is to provide a better understanding of the biological and physical fractionations of carbon and oxygen isotope ratios during some plant physiological processes. To this end, the following questions were addressed:

1. Is water enriched in ^{18}O by transpiration exported from leaves in phloem sap? If so, is the level of enrichment such that this process should be considered when interpreting variation in $^{18}\text{O}/^{16}\text{O}$ of plant organic material?
2. Can leaf water $^{18}\text{O}/^{16}\text{O}$ be predicted under field conditions using a steady state model over a full diel cycle? If not, can the model be modified to take into account non-steady state variation?
3. What is the physiological basis for a previously-observed, strong correlation between phloem sap sugar concentration and $^{13}\text{C}/^{12}\text{C}$ of phloem sap sugars?
4. Is the fractionation of $^{18}\text{O}/^{16}\text{O}$ between leaf water and sugars exported from leaves in the phloem sap predictable based on a known isotope effect between organic molecules and the water in which they form?
5. Can the models that are currently available for carbon and oxygen isotope discrimination be applied to plants in the field that are taxonomically and functionally very diverse, and still provide sensible interpretations in terms of physiological processes?
6. What are the controls over the oxygen isotope composition of carbon dioxide respired by leaves in the dark? Can a theoretical model be developed that explains observed variation in $^{18}\text{O}/^{16}\text{O}$ of leaf dark respiration?

1.4. Structure of the Thesis

With regard to Questions 1 to 6 above, this thesis is structured as follows: Chapter 2 presents measurements of phloem water $^{18}\text{O}/^{16}\text{O}$ in phloem sap samples collected from pod tips of *Lupinus angustifolius* periodically over a full diel cycle. The oxygen isotope composition of leaf water, in addition to other plant components, is also presented, and the departure from steady state predictions of leaf water $^{18}\text{O}/^{16}\text{O}$ assessed. Observations are then compared against results of a non-steady state leaf water enrichment model. Chapter 2 thus addresses questions 1 and 2 in the species *Lupinus angustifolius*, an annual legume commonly grown as a grain crop in Western Australia.

In Chapter 3, I present measurements of phloem sap sugar concentrations and phloem sap sugar $^{13}\text{C}/^{12}\text{C}$ in *Eucalyptus globulus*, thus addressing question 3. I explain the relationship between phloem sap sugar concentration and phloem sap sugar $^{13}\text{C}/^{12}\text{C}$ in terms of correlated changes in the two parameters caused by variation in plant water potential.

Chapter 4 presents measurements, under controlled laboratory conditions, of the $^{18}\text{O}/^{16}\text{O}$ of phloem sap sugar and phloem water in relation to leaf water in *Ricinus communis*. Questions 1 and 4 are thus addressed in Chapter 4.

In Chapter 5, I present measurements of the carbon and oxygen isotope composition of parasitic plants and their hosts in southwestern Australia. The plants sampled represent a very broad range in terms of plant form and function. I apply current models of ^{18}O and ^{13}C discrimination in an attempt to interpret observed variation in the isotope ratios, thereby addressing question 5.

In Chapter 6, I present measurements of $^{18}\text{O}/^{16}\text{O}$ of leaf water, phloem sugar, and phloem water in *Eucalyptus globulus*, sampled under field conditions. Results are applied to questions 1, 2, and 4 for a long-lived, woody plant species. These results are then contrasted with the results obtained in Chapters 2 and 4 for *Lupinus angustifolius* and *Ricinus communis*.

Finally in Chapter 7, I present measurements and a model of the oxygen isotope composition of carbon dioxide respired in the dark by leaves of *Ricinus communis*. Chapter 7 thus addresses question 6.

1.5. Publications

Chapters 2 to 5 represent manuscripts that have been published, or are in press, in peer-reviewed journals. These publications are detailed below:

- Chapter 2: Cernusak LA, Pate JS, Farquhar GD (2002) Diurnal variation in the stable isotope composition of water and dry matter in fruiting *Lupinus angustifolius* under field conditions. *Plant, Cell & Environment* 25:893-907
- Chapter 3: Cernusak LA, Arthur DJ, Pate JS, Farquhar GD (2003) Water relations link carbon and oxygen isotope discrimination to phloem sap sugar concentration in *Eucalyptus globulus*. *Plant Physiology* 131:1544-1554

Chapter 4: Cernusak LA, Wong S-C, Farquhar GD (2003) Oxygen isotope composition of phloem sap in relation to leaf water in *Ricinus communis*. *Functional Plant Biology* 30:1059-1070

Chapter 5: Cernusak LA, Pate JS, Farquhar GD (in press) Oxygen and carbon isotope composition of parasitic plants and their hosts in southwestern Australia. *Oecologia*

Chapters 6 and 7 represent manuscripts that are in the final stages of revision before being submitted to peer-reviewed journals for publication.

Chapter 2: Diurnal variation in the stable isotope composition of water and dry matter in fruiting *Lupinus angustifolius* under field conditions

2.1. Abstract

In this chapter, I present an integrated account of the diurnal variation in the stable isotopes of water (δD and $\delta^{18}O$) and dry matter ($\delta^{15}N$, $\delta^{13}C$, and $\delta^{18}O$) in the long-distance transport fluids (xylem sap and phloem sap), leaves, pod walls, and seeds of *Lupinus angustifolius* under field conditions in Western Australia. The δD and $\delta^{18}O$ of leaf water showed a pronounced diurnal variation, ranging from early morning minima near 0‰ for both δD and $\delta^{18}O$ to early afternoon maxima of 62‰ and 23‰, respectively. Xylem sap water showed no diurnal variation in isotopic composition and had mean values of -13.2‰ and -2.3‰ for δD and $\delta^{18}O$. Phloem sap water collected from pod tips was intermediate in isotopic composition between xylem sap and leaf water and exhibited only a moderate diurnal fluctuation. Isotopic compositions of pod wall and seed water were intermediate between those of phloem and xylem sap water. A model of average leaf water enrichment in the steady state (Craig and Gordon 1965; Dongmann et al. 1974; Farquhar and Lloyd 1993) agreed closely with observed leaf water enrichment in the morning and early afternoon, but poorly during the night. A modified model taking into account non-steady state effects (Farquhar and Cernusak, unpublished) gave better predictions of observed leaf water enrichments over a full diel cycle. The $\delta^{15}N$, $\delta^{13}C$, and $\delta^{18}O$ of dry matter varied appreciably among components. Dry matter $\delta^{15}N$ was highest in xylem sap and lowest in leaves, whereas dry matter $\delta^{13}C$ was lowest in leaves and highest in phloem sap and seeds, and dry matter $\delta^{18}O$ was lowest in leaves and highest in pod walls. Phloem sap, leaf, and fruit dry matter $\delta^{18}O$ varied diurnally, as did phloem sap dry matter $\delta^{13}C$. Results demonstrate the importance of considering the non-steady state when modeling biological fractionation of stable isotopes in the natural environment.

2.2. Introduction

There is currently major interest in understanding the role of plants in the global carbon cycle (Prentice et al. 2001), and it has already become evident that small variations in the natural abundances of the stable isotopes of C, N, O, and H can provide unique insights into the processes controlling carbon uptake and release from vegetation (Griffiths 1998). However, meaningful interpretation of isotopic data requires a sound understanding of the biological fractionation of stable isotopes over relatively short time periods and between the component parts of a plant.

It is well known, for example, that the water contained in leaves becomes enriched in the heavy isotopes of O and H (^{18}O and D) during transpiration. Theory has been developed to account for such enrichments (Craig and Gordon 1965; Dongmann et al. 1974; Farquhar and Lloyd 1993). The organic matter of plants partly reflects the ^{18}O enrichment of leaf water, essentially by tracking and integrating differences in ^{18}O signals generated under varying evaporative conditions and transpiration rates during the growth of the plant (Barbour and Farquhar 2000). The same oxygen isotope signal of leaf water is also reflected in the portion of gaseous CO_2 which, having entered into leaves via stomata, then diffuses back out again without being captured by photosynthetic enzymes. This enrichment in the $^{18}\text{O}/^{16}\text{O}$ ratio of atmospheric CO_2 by plants has important implications for estimating carbon fluxes between the biosphere and the atmosphere (Farquhar et al. 1993). Finally, the $^{18}\text{O}/^{16}\text{O}$ ratio of leaf water is also recorded in the gaseous O_2 that is evolved during photosynthesis, and variations in $^{18}\text{O}/^{16}\text{O}$ of atmospheric O_2 provide a basis for constructing historic estimates of terrestrial and marine productivity (Bender et al. 1994).

The heavier isotope of carbon (^{13}C) is discriminated against during photosynthesis, with the degree of discrimination depending in part on the type of photosynthetic pathway (Bender 1968). In C_3 plants, the fractionation correlates positively with the gaseous concentration ratio between intercellular and ambient CO_2 (Farquhar et al. 1982), and thereby negatively with plant water use efficiency (Farquhar and Richards 1984). Extents of discrimination against ^{13}C also differ when CO_2 is fixed by terrestrial versus marine organisms (Francey et al. 1995), and to a lesser extent among different classes of terrestrial ecosystems (Lloyd and Farquhar 1994, Bowling et al. 2002). Consequently, ^{13}C discrimination can be an important parameter in global and ecosystem carbon budgets. Since assimilated carbon can cycle through plants and ecosystems in different ways before returning to the atmosphere, detailed consideration

of daily and seasonal fractionation events taking place within plants becomes important when constructing carbon budgets based on $^{13}\text{C}/^{12}\text{C}$ ratios.

The availability of nitrogen in an ecosystem plays an important role in determining ecosystem productivity (Vitousek and Howarth 1991), and related natural abundance ratios for $^{15}\text{N}/^{14}\text{N}$ in soil and plant components have been shown to comprise potentially useful integrators of the types and turnover rates of nitrogen cycling involved (Robinson 2001). Yet again, understanding is required of how isotopic fractionations of nitrogen are mediated during daily transformation and transport events, from initial assimilation right through to incorporation into specific organic components of different plant organs.

In this investigation, I set out to understand more fully the biological fractionations of these stable isotopes which occur during the functioning of a plant under field conditions, where environmental parameters vary considerably with time of day and plants adjust accordingly in terms of their gaseous exchanges and partitioning processes. I specifically report on daily variation in the stable isotopes of C, N, O and H in the water and dry matter of xylem, phloem, leaves, and fruits of lupin, a legume commonly grown as a grain crop in Western Australia, and already subject to extensive earlier studies on the carbon, nitrogen, and water economies of fruits under both glasshouse and field conditions (Pate et al. 1977; Pate et al. 1980; Pate et al. 1985).

2.3. Materials and Methods

2.3.1. Study site

The study was conducted on a uniform stand of *Lupinus angustifolius* L. var. *Tangil* grown as part of a breeding trial at the Mount Barker Research Station (34°38'02" S, 117°32'00" E). This facility is operated by Agriculture Western Australia and is located approximately 20 km from the township of Mount Barker, Western Australia. The crop was sown on June 6, 2000. All measurements and sap and biomass collections were undertaken during November 1 and 2, 2000 when fruits were well-developed and estimated to be approximately one month away from harvest maturity.

2.3.2. Gas-exchange measurements

Gas exchanges of source leaves and filling fruits on main stems were monitored at one- to two-hour intervals during the 26-hour study period, except during the night

when dew was present on leaves and atmospheric vapor pressure approached saturation (Figure 2.1). Fluxes of CO₂ and water vapor during daylight were measured using an LCA 4 Portable Gas Exchange System (ADC BioScientific Ltd, Hertfordshire, England). Approximately 5 cm² of leaf or pod surface (two to three leaflets or one to two fruits) were detached and immediately placed inside the gas exchange cuvette and measurements were repeated on eight to ten such sets of leaflets or fruits at each sampling time. Measurements were completed within approximately five minutes of detachment. No decline in gas exchange rates following detachment was observed within this time period.

Ambient air temperature and relative humidity were measured periodically throughout the experiment using a Vaisala temperature and humidity probe (Vaisala Inc., Helsinki, Finland). Leaf and pod temperatures were measured concurrently on three to six leaflets or pods using a 0.13 mm diameter chromel-constantan thermocouple (Omega Engineering, Stamford, Connecticut, USA).

2.3.3. *Sample collections*

Xylem sap and phloem sap were sampled at one- to two-hour intervals throughout the 26-hour study period commencing at 0900. Xylem sap was collected from the lower main stems of 10 individuals at each sampling time using the mild-vacuum extraction technique developed by Jeschke & Pate (1995) and Pate, Jeschke & Aylward (1995). Phloem sap was obtained by cutting the distal tips of 30-50 fruits and immediately collecting the exudate (Pate et al. 1974). Sap samples from individual plants were pooled to form bulk samples (5-10 mL for xylem sap, 30-50 µL for phloem sap) from each sampling time, and samples were immediately decanted into sealable tubes and frozen at -20°C. Sucrose concentrations of phloem sap were measured at the time of collection using a hand-held refractometer (Pate et al. 1998). Refractometer readings were corrected for the presence of amino acids and amides by measuring the nitrogen concentration of each phloem sap dry matter sample and by assuming amino acids and amides were present in similar proportionality profiles to those recorded previously for phloem sap of lupins (Pate et al. 1974; Sharkey and Pate 1976). Combined amino acid and amide concentration estimates ranged from 19 to 28 g L⁻¹, similar to those values previously recorded (Pate et al. 1974; Sharkey and Pate 1976).

Leaves, pod walls, and seeds were collected for isotopic analysis of tissue water and dry matter at the same time when xylem sap and phloem sap were being collected.

Ten leaflets were randomly selected at each time of sampling and placed in gas-tight collection vials before being frozen. Four to six fruits were similarly collected and their pod walls quickly separated from seeds. Sets of samples were collected in duplicate; one randomly allocated for tissue water extraction and δD and $\delta^{18}O$ analyses, the other for analyses of $\delta^{13}C$, $\delta^{18}O$, and $\delta^{15}N$ in dry matter. The relative water content (RWC) of the leaves collected for dry matter analyses was determined by dividing the difference between fresh and dry weights by fresh weight. Leaf area was determined with a Li-Cor leaf area meter (Li-Cor Inc, Lincoln, NE, USA), thus enabling data to be expressed in terms of areal concentrations of water within the leaf samples.

I am aware of the substantial alterations in isotope signals of water which can occur during exposure of liquid interfaces to the atmosphere and of the errors which such alterations might introduce when interpreting data. For xylem sap samples, the mild vacuum extraction technique involved an entirely sealed system which siphoned tracheal fluid progressively into a tube of 5 to 10 ml volume over a period of a few seconds. Samples were then removed from the collection apparatus and immediately decanted into sealable vials. For phloem sap samples, evaporation from exuding droplets was minimized by immediately attracting them (within 5 seconds) into micro-capillary tubes that have extremely small exposed-liquid-surface : volume ratios. The contents of the capillaries were then expelled into small-volume vials (0.1 ml) that were sealed except in the few seconds when additional samples were introduced. In the case of plant tissue samples, transfer within seconds from plants into sealed tubes would be expected to virtually eliminate the opportunity for evaporative enrichment of water isotope ratios during harvest. All samples were immediately frozen at the field site following collection and remained frozen until isotopic analyses were conducted.

To test the possible extent to which evaporative enrichment of water isotope ratios might have occurred during the brief exposure of samples to the atmosphere during sap collection, I performed regression analyses of the δD and $\delta^{18}O$ of xylem sap samples against the vapor pressure deficit at the time of sap collection. Vapor pressure deficits ranged from 0 to 28 mbar over the course of the study. If the isotopic composition of the xylem sap samples had been markedly altered by evaporative enrichment during sap collection, one would expect the isotopic composition of the samples to correlate with the vapor pressure deficit (and therefore the evaporation rate) at the time of collection. I observed no relationship between xylem sap isotopic

composition and vapor pressure deficit ($P=0.22$ for $\delta^{18}\text{O}$; $P=0.65$ for δD), suggesting that the sap samples were not affected by evaporative enrichment during sap collection.

2.3.4. Isotopic analyses

Tissue water was extracted from leaves, pod walls, and seeds by azeotropic distillation with toluene (Revesz and Woods 1990). Traces of toluene remaining in the water following the distillation were removed by adding wax to the water and warming the water to the melting point of the wax. The $\delta^{18}\text{O}$ of the water samples extracted from leaves, pod walls, and seeds was measured by a continuous-flow isotope ratio mass spectrometer (CF-IRMS) (Micromass Isochrom-EA, Manchester, UK) following pyrolysis in a Carlo Erba elemental analyzer (CE Instruments, Milan, Italy) (Farquhar et al. 1997). Xylem water $\delta^{18}\text{O}$ was similarly measured by this technique. The oxygen isotope ratio of phloem sap water was determined using a method recently described by Gan, Wong & Farquhar (in press) for the determination of the $\delta^{18}\text{O}$ of the water component of a homogeneous mixture of water and dry matter. In this procedure, the $\delta^{18}\text{O}$ of one aliquot of phloem sap solution was measured by pyrolysis. A second aliquot of sap was then evaporated overnight at 60°C , and the resulting dry matter component assayed for $\delta^{18}\text{O}$. Isotope composition of the water in the original sap sample was then estimated by mass balance.

Hydrogen isotope ratios of water samples were measured in Perth using a CF-IRMS system (Delta Plus XL, Finnigan Mat, Bremen, Germany) incorporating an elemental analyzer with pyrolysis reactor (Thermoquest PYRO/EA, Finnigan Mat, Bremen, Germany). For phloem sap water δD , the phloem sap remaining after the $\delta^{18}\text{O}$ analyses was distilled cryogenically under vacuum to collect water separately from dry matter. The δD of the phloem water was then determined as for the other water samples.

The $\delta^{15}\text{N}$ and $\delta^{13}\text{C}$ of xylem sap and phloem sap dry matter were determined by CF-IRMS using the Perth-based ANCA combustion system (PDZ Europa Ltd, Cheshire, UK) coupled to a dual-inlet mass spectrometer (SIRA9, VG Isogas, Cheshire, UK). The $\delta^{15}\text{N}$ and $\delta^{13}\text{C}$ of leaf, pod wall, and seed dry matter were determined by CF-IRMS with an Isochrom mass spectrometer (Micromass, Manchester, UK) coupled to a Carlo Erba elemental analyzer (CE Instruments, Milan, Italy) housed at the Australian National University.

The $\delta^{18}\text{O}$ of leaf, pod wall, and seed dry matter was determined using the method described by Farquhar et al. (1997). Xylem sap dry matter $\delta^{18}\text{O}$ was similarly determined after evaporation of sap water at 60°C . Isotope ratios were expressed using delta (δ) notation with respect to the standards of air for nitrogen, Pee Dee Belemnite for carbon, and Vienna Standard Mean Ocean Water for oxygen and hydrogen. Carbon isotope ratios were converted to discrimination values (Δ) (Farquhar et al. 1989a) by assuming an isotopic composition for atmospheric CO_2 of -7.8‰ .

I tested for differences between isotope ratios of various dry matter components using analysis of variance. If significant differences were detected, Tukey's method was used for pair-wise comparisons. Statistical analyses were conducted in SYSTAT 9.0 (SPSS Inc, Chicago, IL, USA).

2.3.5. Modeling leaf water isotopic enrichment

Observations of the isotopic enrichments of leaf water over that of source water ($\Delta^{18}\text{O}$ or ΔD for oxygen or hydrogen, respectively) were compared to the predictions of steady state and non-steady state models. Steady state isotopic enrichment at leaf evaporative sites (Δ_{es}) was modeled as described previously (Craig and Gordon 1965; Dongmann et al. 1974; Farquhar et al. 1989b) using the expression

$$\Delta_{es} = \varepsilon^* + \varepsilon_k + (\Delta_v - \varepsilon_k) \frac{e_a}{e_i}, \quad (2.1)$$

where ε^* is the equilibrium fractionation factor between liquid and vapor, ε_k the kinetic fractionation that occurs during diffusion from the leaf to the atmosphere, Δ_v the isotopic discrimination between atmospheric vapor and source water (i.e. $\Delta_v = R_v/R_s - 1$; $R_v = {}^{18}\text{O}/{}^{16}\text{O}$ or D/H of vapor and $R_s = {}^{18}\text{O}/{}^{16}\text{O}$ or D/H of source water), and e_a/e_i the ratio of ambient to intercellular vapor pressures. The ε^* was estimated using the regression equations of Bottinga and Craig (1969) for oxygen and Majoube (1971) for hydrogen. The ε_k was calculated for oxygen according to the equation (Farquhar et al. 1989b)

$$\varepsilon_k = \frac{28r_s + 19r_b}{r_s + r_b}, \quad (2.2)$$

where r_s and r_b are the stomatal and boundary layer resistances for diffusion of water vapor in air. The coefficients 28 and 19 in the above equation represent discrimination factors (scaled to per mil) for the respective diffusions of H_2^{18}O through stomata (Merlivat 1978) and leaf boundary layer (Farquhar et al. 1989b). The corresponding coefficients used for calculating ε_k for HDO were 25 and 17.

I predicted the average steady state leaf water enrichment from the estimated enrichment at the evaporative sites using the following formula (Farquhar and Lloyd 1993):

$$\Delta_{Ls} = \frac{\Delta_{es}(1 - e^{-\phi})}{\phi}. \quad (2.3)$$

The ϕ is a dimensionless number termed the Péclet number which is defined as $EL/(CD)$, where E is transpiration rate, L a scaled effective path length, C the molar concentration of water, and D the diffusivity of $H_2^{18}O$ or HDO in water.

The steady-state model of isotopic enrichment at the evaporative sites can then be further modified to take into account non-steady state effects (Farquhar and Cernusak, unpublished) as follows:

$$\Delta_{en} = \Delta_{es} - \left[\frac{\frac{d(W\Delta_{en})}{dt}}{gw_i} \right], \quad (2.4)$$

where Δ_{en} is the non-steady state enrichment (‰), W the leaf water concentration (mol m^{-2}), t time (s), g total conductance of stomata plus boundary layer ($\text{mol m}^{-2} \text{s}^{-1}$), and w_i the mole fraction of water vapor in the leaf intercellular spaces (mol mol^{-1}). By analogy, the average leaf water isotopic enrichment in the non-steady state (Δ_{Ln}) can be modeled as

$$\Delta_{Ln} = \Delta_{Ls} - \left[\frac{\frac{d(W\Delta_{Ln})}{dt}}{gw_i} \right]. \quad (2.5)$$

Equations (2.1) through (2.5) were parameterized to develop steady state and non-steady state predictions of evaporative site and average leaf water isotopic enrichment. For equation (2.2), ε_k was estimated using gas exchange data; estimates of boundary layer conductance were based on measurements of average leaf dimensions and wind speed at the adjacent weather station (Mount Barker, Western Australia). I estimated Δ_v by assuming that atmospheric water vapor was in isotopic equilibrium at the mean daily temperature with source water as inferred from measurements of the isotopic composition of xylem sap water. Values for e_a/e_i were estimated from measurements of relative humidity, air temperature, and leaf temperature. Transpiration rates from the gas exchange measurements conducted during daylight hours were used in equation (2.3). In the same equation, I assumed a scaled effective path length of 8

mm (Flanagan et al. 1994). Equations (2.4) and (2.5) were solved iteratively using the Solver function in Microsoft Excel and assuming starting values for Δ_{en} and Δ_{Ln} of 15‰ and 40‰ for oxygen and hydrogen at 0930 on day 1 (the start of the study). Values for W and g were measured during the day. At times in the night when gas exchange measurements were not possible, I assumed a g of $75 \text{ mmol m}^{-2} \text{ s}^{-1}$. The predicted enrichment values were compared to observed enrichment values (Δ_o), calculated as

$$\Delta_o = \frac{\delta_o - \delta_s}{\delta_s + 1}, \quad (2.6)$$

where δ_o is the observed δD or $\delta^{18}\text{O}$ of leaf water, and δ_s is the δD or $\delta^{18}\text{O}$ of source water.

The relationship between the enrichments of δD and $\delta^{18}\text{O}$ provides an additional means of evaluating predictions made from the models. Theoretical predictions of δD - $\delta^{18}\text{O}$ slopes in leaf water have been compared to measured values in earlier studies (Allison et al. 1985; Walker et al. 1989; Yakir et al. 1990; Walker and Lance 1991), but by using equations (2.1) to (2.5), this approach can be extended to include kinetic fractionation of the boundary layer outside the stomata, the differential diffusivities of HDO and H_2^{18}O in water, and non-steady state effects. For a series of measurements under varying conditions, a regression line can be drawn through the points yielding a slope and intercept in ΔD - $\Delta^{18}\text{O}$ space. The slope of such a line is sensitive to changes or errors in the estimate of atmospheric vapor isotopic composition, and so should provide a means of validating assumptions relating to isotopic equilibria between source water and atmospheric vapor. I tested for discrepancies between regression slopes stemming from modeled versus measured data using analysis of covariance in SYSTAT 9.0 (SPSS Inc, Chicago, IL, USA).

2.4. Results

2.4.1. Gas-exchange

As expected during the approach to summer in a mediterranean environment, large diel variations in ambient air temperature and relative humidity occurred (Figures 2.1A and 2.1B). Air temperature varied markedly, peaking near 27°C in mid-afternoon and then falling below 8°C at night. Relative humidity decreased during the day to near 20% by afternoon, but then recovered fully to 100% early in the night.

The highest photosynthetic rates of source leaves occurred in the early morning (Figure 2.1C) followed by a progressive decrease during the rest of the morning through

to mid afternoon. As leaf-to-air vapor pressure deficits moderated in the late afternoon a second, albeit smaller, peak in photosynthesis occurred. A negative linear correlation existed between mean leaf photosynthetic rates and vapor pressure deficit ($R=-0.75$, $P=0.01$, $n=10$), presumably reflecting increasingly reduced stomatal conductance under increasing water stress. Intact whole fruits exhibited slight net gaseous gains of carbon early in the mornings, but incurred continuous net losses of CO_2 for the remainder of the day. However, since these losses were consistently less during the day than after dark, pod wall photosynthesis appeared capable of significant refixation of CO_2 respired to the fruit interior by the seeds. Transpiration losses of leaves and fruits tended to be greater in the morning and early afternoon than in late afternoon, again indicating progressive decreases in stomatal conductances during the day (Figure 2.1D).

As to be expected, leaf RWC decreased during the morning hours when transpiration rates were highest, reaching a minimum in the early afternoon (Figure 2.2A). It then increased until the following morning as the water balance of leaves was progressively restored. The sucrose concentration of phloem sap increased throughout the morning with a sharp peak at 0.38 mol L^{-1} in the early afternoon (Figure 2.2B) preceding a steady decline until the following morning. Although apparently diminishing through the night, phloem sap sucrose concentration did not fall below 0.30 mol L^{-1} , despite photosynthesis having ceased many hours earlier. A negative relationship was observed between daytime phloem sap sucrose concentration and leaf photosynthetic rates ($R=-0.72$, $P=0.02$, $n=10$), namely the opposite of what one might expect if the current rate of sugar production in photosynthesis were directly determining sap concentration. Phloem sap sugar concentration was also negatively correlated with leaf RWC ($R=-0.85$, $P<0.0001$, $n=15$) and positively correlated with atmospheric vapor pressure deficit ($R=0.73$, $P=0.002$, $n=15$).

2.4.2. *Isotopic composition of dry matter components*

The $\delta^{15}\text{N}$ values of bulk dry matter of transport fluids, leaves, and fruits changed only marginally during the day. But as seen from the mean values given in Figure 2.3A, the organic matter of fruits and especially leaves was consistently more depleted

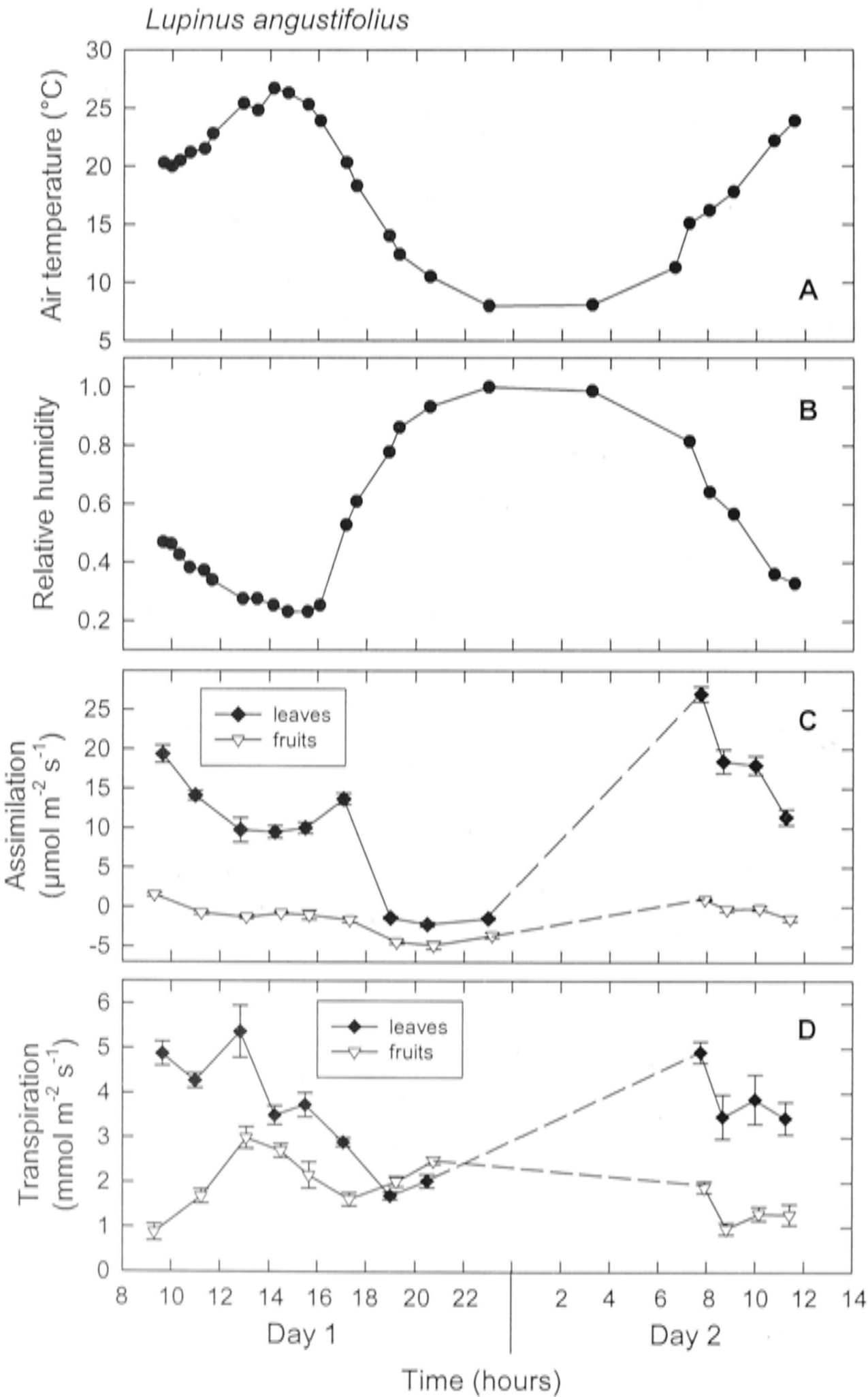


Figure 2.1. (A) Air temperature, (B) relative humidity, (C) carbon dioxide exchange, and (D) transpiration for five-month old *Lupinus angustifolius* grown under field conditions in Western Australia. Measurements were made on November 1 and 2, 2000. Gas exchange was measured on both leaves and fruits and data are expressed on a projected area basis; each point is an average of eight to ten measurements. Error bars are ± 1 SE.

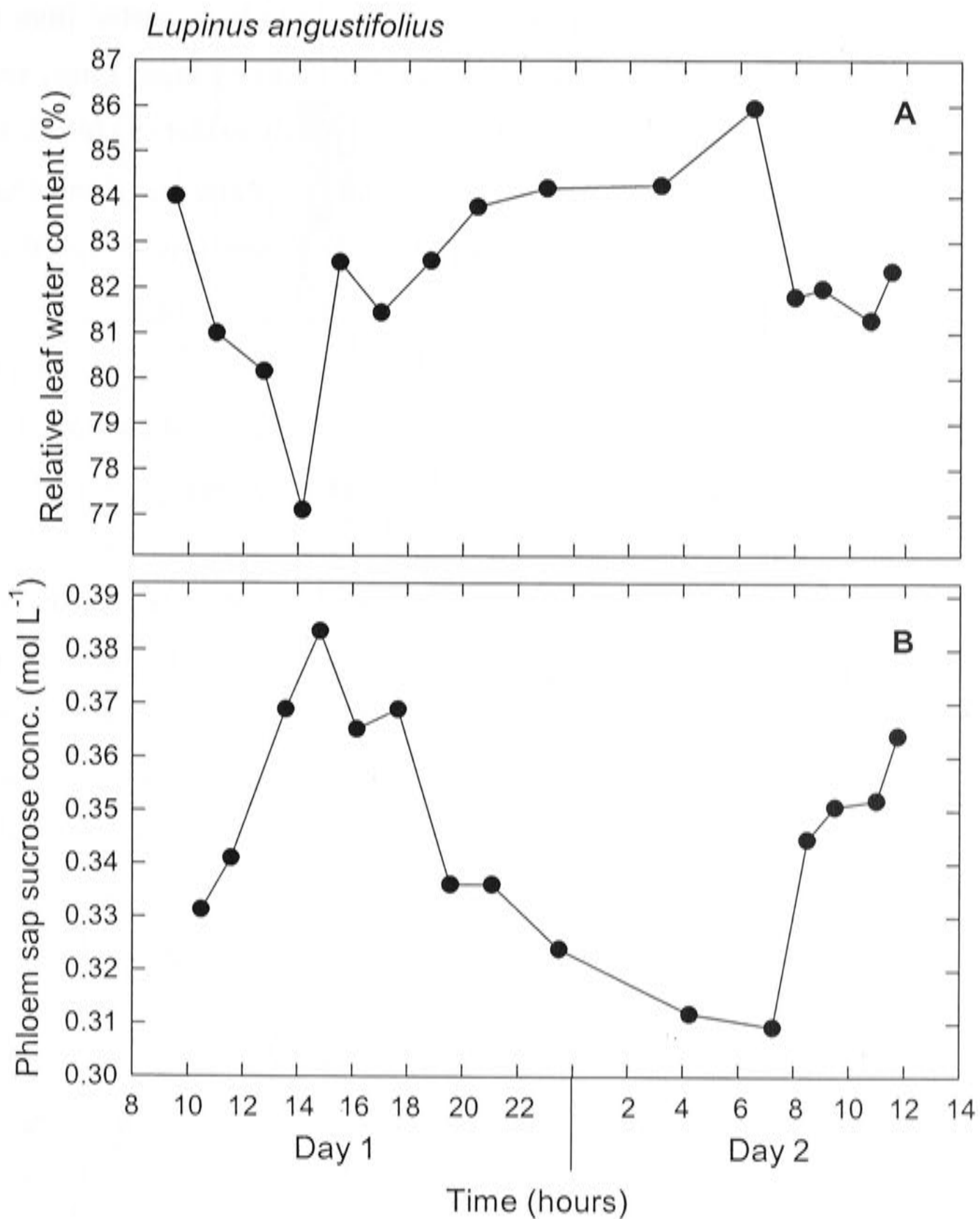


Figure 2.2. Diel variation in (A) relative leaf water content and (B) phloem sap sucrose concentration of *Lupinus angustifolius*. Relative water content was calculated as the difference between fresh and dry weight divided by fresh weight. Phloem sap was collected from the distal tips of attached pods. Samples were collected on November 1 and 2, 2000.

in ^{15}N than that of either xylem sap or phloem sap. Of the transport fluids, phloem sap was depleted in ^{15}N by more than 1‰ compared to xylem sap.

The corresponding mean $\delta^{13}\text{C}$ values for dry matter components showed phloem sap to be less negative than xylem sap (Figure 2.3B). As to be expected from earlier studies showing phloem dominated import of organic solutes by lupin fruits, seed dry matter showed a carbon isotope ratio conforming more closely to that of phloem sap dry matter than xylem sap dry matter. The $\delta^{13}\text{C}$ of pod-wall dry matter was about 1‰ more negative than that of seed dry matter, whereas $\delta^{13}\text{C}$ of source leaves was 3‰ more negative than that of seeds. The $\delta^{13}\text{C}$ values for samples of phloem sap dry matter collected through the study were positively correlated with sucrose concentration for samples taken during daylight hours (Figure 2.4). However, $\delta^{13}\text{C}$ values did not show a significant correlation with sucrose concentration for those few sap collections made at night (Figure 2.4).

Mean oxygen isotope ratios differed amongst all dry matter components with the exception of the similar values recorded for phloem sap and seeds (Figure 2.3C). The values ranked somewhat similarly in relative magnitude to those mentioned above for $\delta^{13}\text{C}$, with leaf dry matter least enriched, pod wall dry matter most enriched, and mean values for phloem sap, xylem sap, and seeds intermediate between leaves and pod walls. Marked fluctuations were observed in time courses for $\delta^{18}\text{O}$ in dry matter for both phloem sap (Figure 2.5A) and leaves (Figure 2.5B). Thus, dry matter of phloem sap was least enriched in the morning, increased in the afternoon, and then remained enriched throughout the night before decreasing again the following morning. The $\delta^{18}\text{O}$ values for leaf dry matter also increased in the morning, but then decreased throughout the night before increasing the following morning. Diel changes in $\delta^{18}\text{O}$ of pod-wall and seed dry matter (Figure 2.5C) were similar to, but less pronounced, than those for leaves.

2.4.3. *Isotopic composition of water components within the system*

A strong diel variation was observed in the oxygen and hydrogen isotope ratios of leaf water (Figures 2.6A and 2.6B), encompassing maxima of 23‰ and 62‰ respectively in the early afternoon, followed by almost linear decreases in both entities to well defined minima near 0‰ just before sunrise. By contrast, xylem water, presumably recently accessed from the soil by roots, showed no appreciable diel

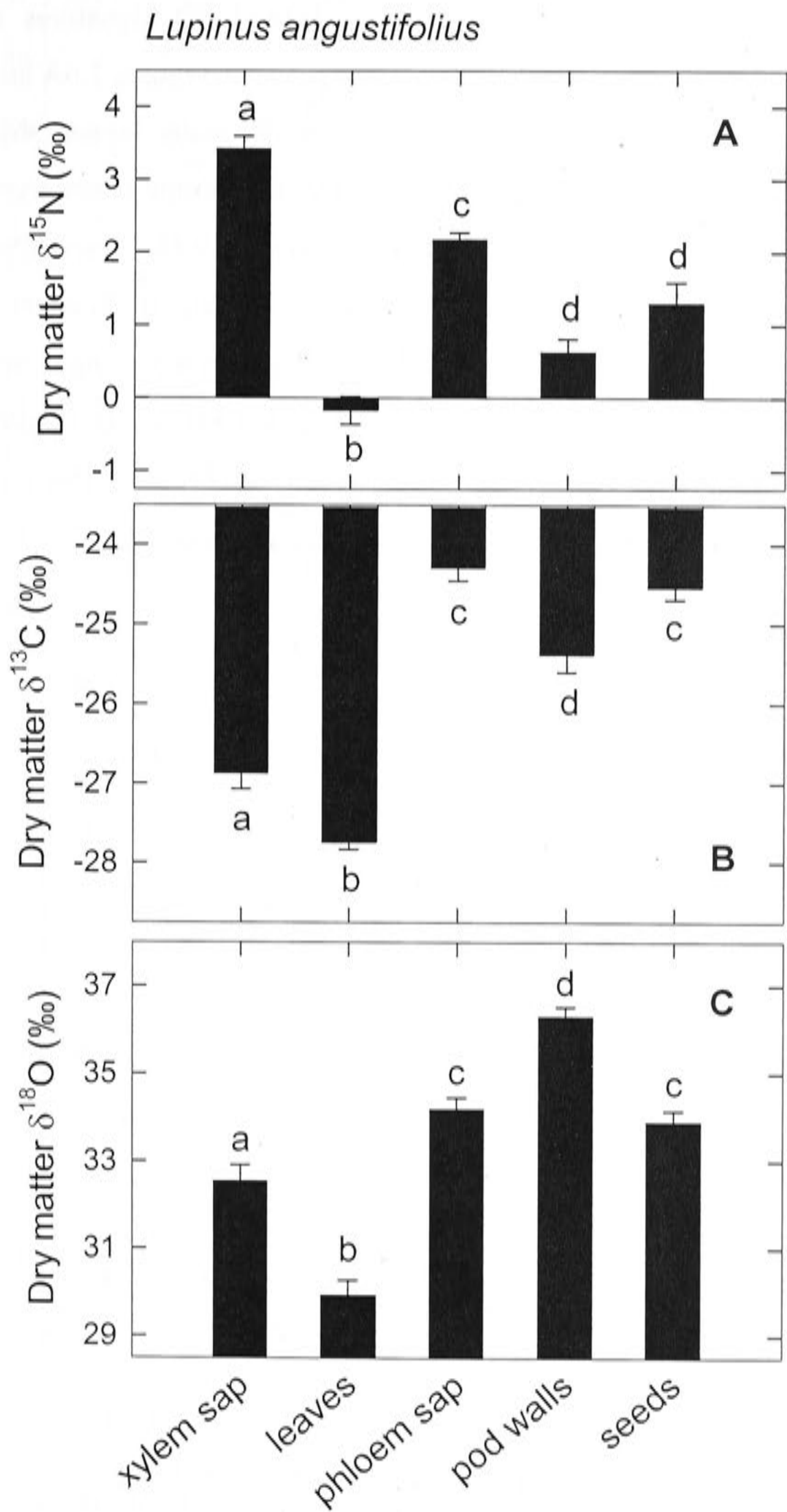


Figure 2.3. (A) Nitrogen, (B) carbon, and (C) oxygen stable isotope ratios for dry matter components of *Lupinus angustifolius*. Values are averaged over a diel cycle. Error bars are ± 1 SE. Bars within a panel followed by different letters are significantly different at $P < 0.05$.

variation in either $\delta^{18}\text{O}$ or δD with values fluctuating only marginally around means of -2.3‰ and -13.2‰ , respectively.

Phloem sap water generally showed $\delta^{18}\text{O}$ and δD signatures intermediate between current values for leaf water and xylem sap water (Figures 2.6A and 2.6B), and the moderate diurnal variations shown for phloem sap water lagged slightly behind those for bulk leaf water. Maximum phloem sap water isotope ratios were 15.2‰ for $\delta^{18}\text{O}$ and 48‰ for δD , with minimum values of 7.6‰ and 19.8‰ , respectively.

Isotopic compositions ($\delta^{18}\text{O}$ and δD) differed only slightly in water of pod walls and seeds, showing relatively slight diurnal fluctuations encompassing a range of values intermediate between those for water in phloem sap and xylem sap (Figures 2.6A and 2.6B). Mean values of $\delta^{18}\text{O}$ were 6.6‰ for pod-wall water and 6.9‰ for seed water, while mean values of δD were 12.3‰ for the same components.

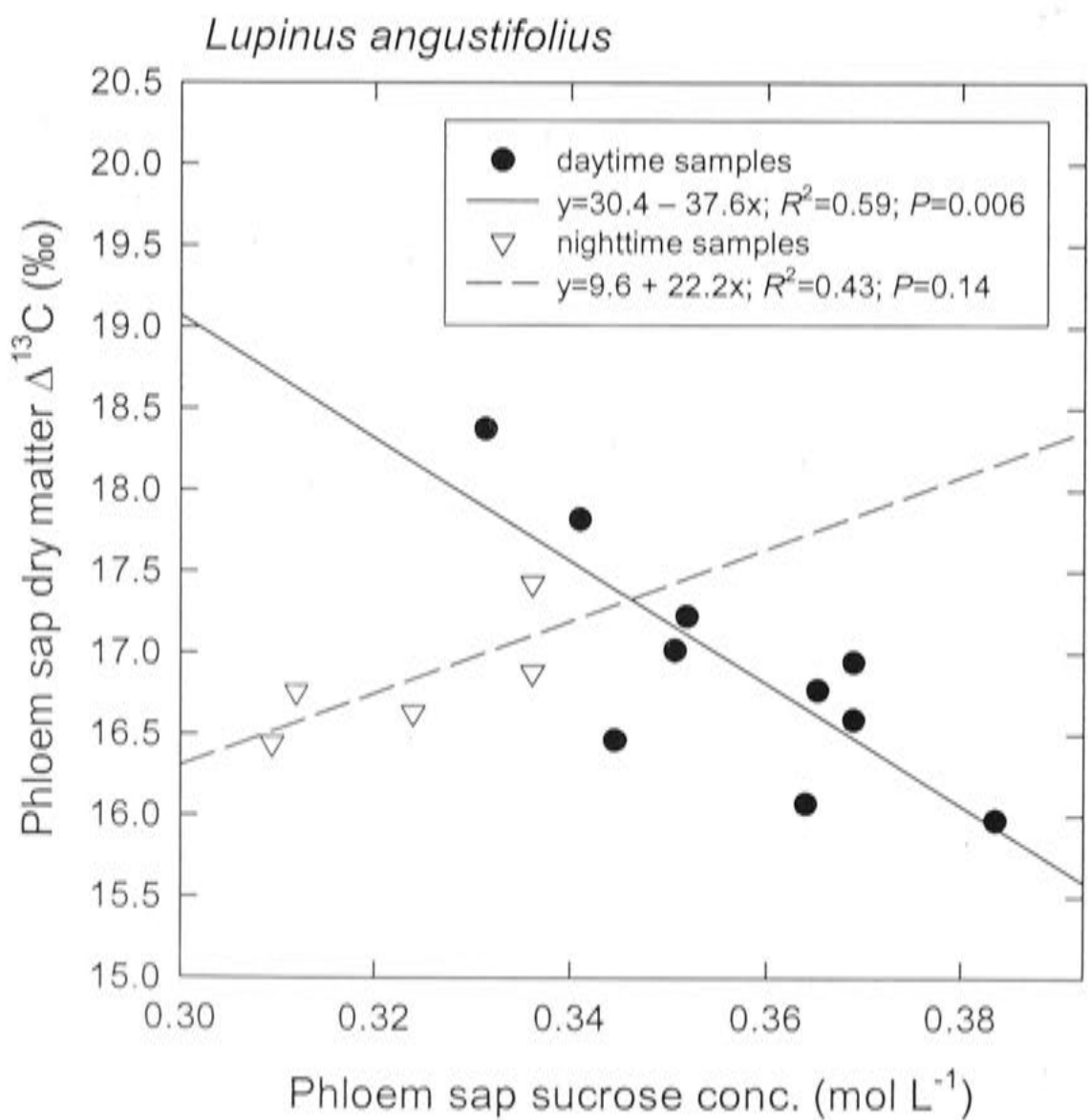


Figure 2.4. Carbon isotope discrimination ($\Delta^{13}\text{C}$) of phloem sap dry matter collected from pod tips plotted against the sucrose concentration of the phloem sap. Each point is the average of two bulk collections from several individuals. Samples are plotted separately as nighttime samples or daytime samples.

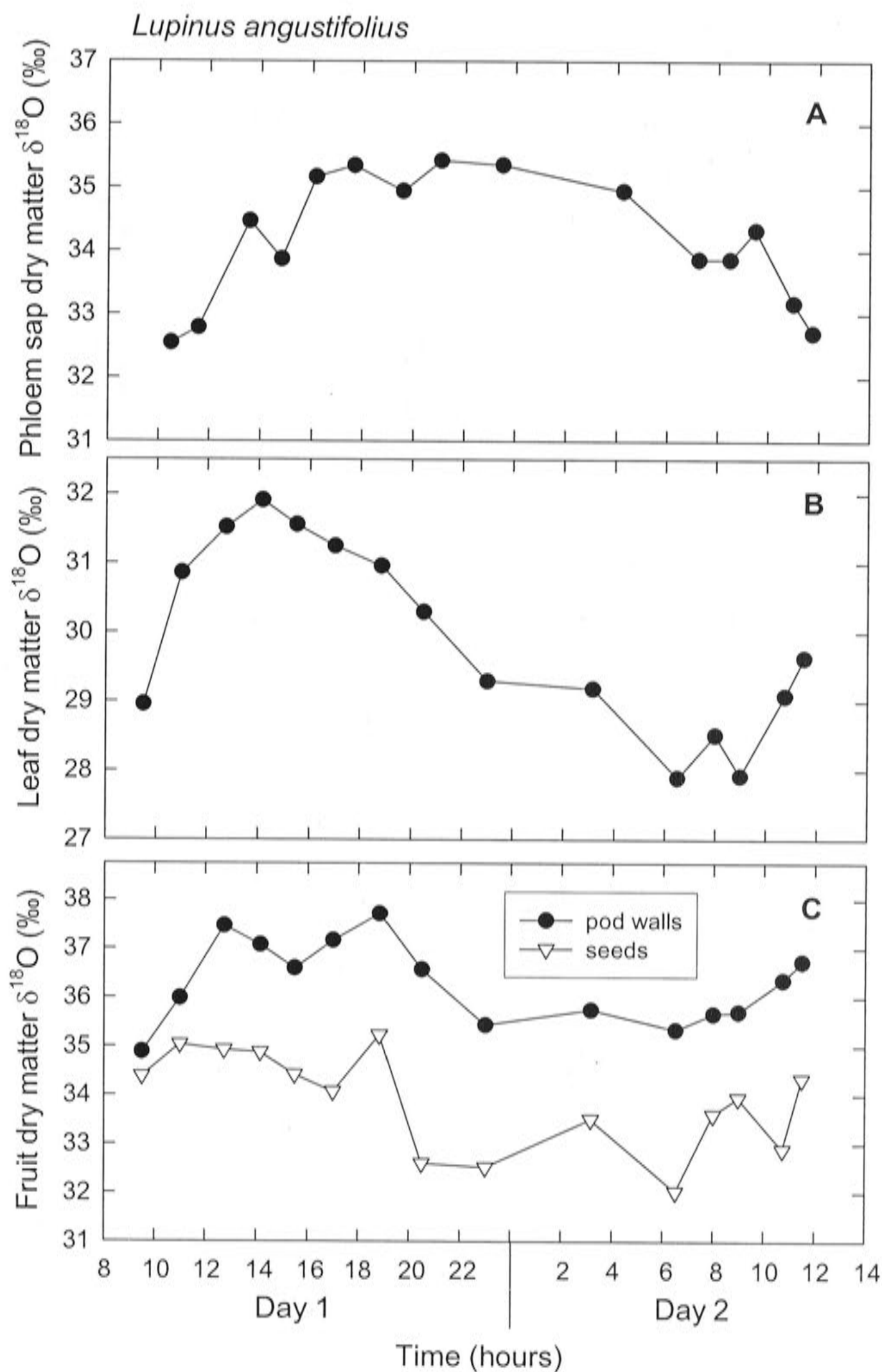


Figure 2.5. Diel variation in the oxygen isotope ratio of (A) phloem sap dry matter, (B) leaf dry matter, and (C) fruit dry matter. Samples were collected on November 1 and 2, 2000 from field-grown *Lupinus angustifolius*. Each point represents a bulk sample collected from several individuals.

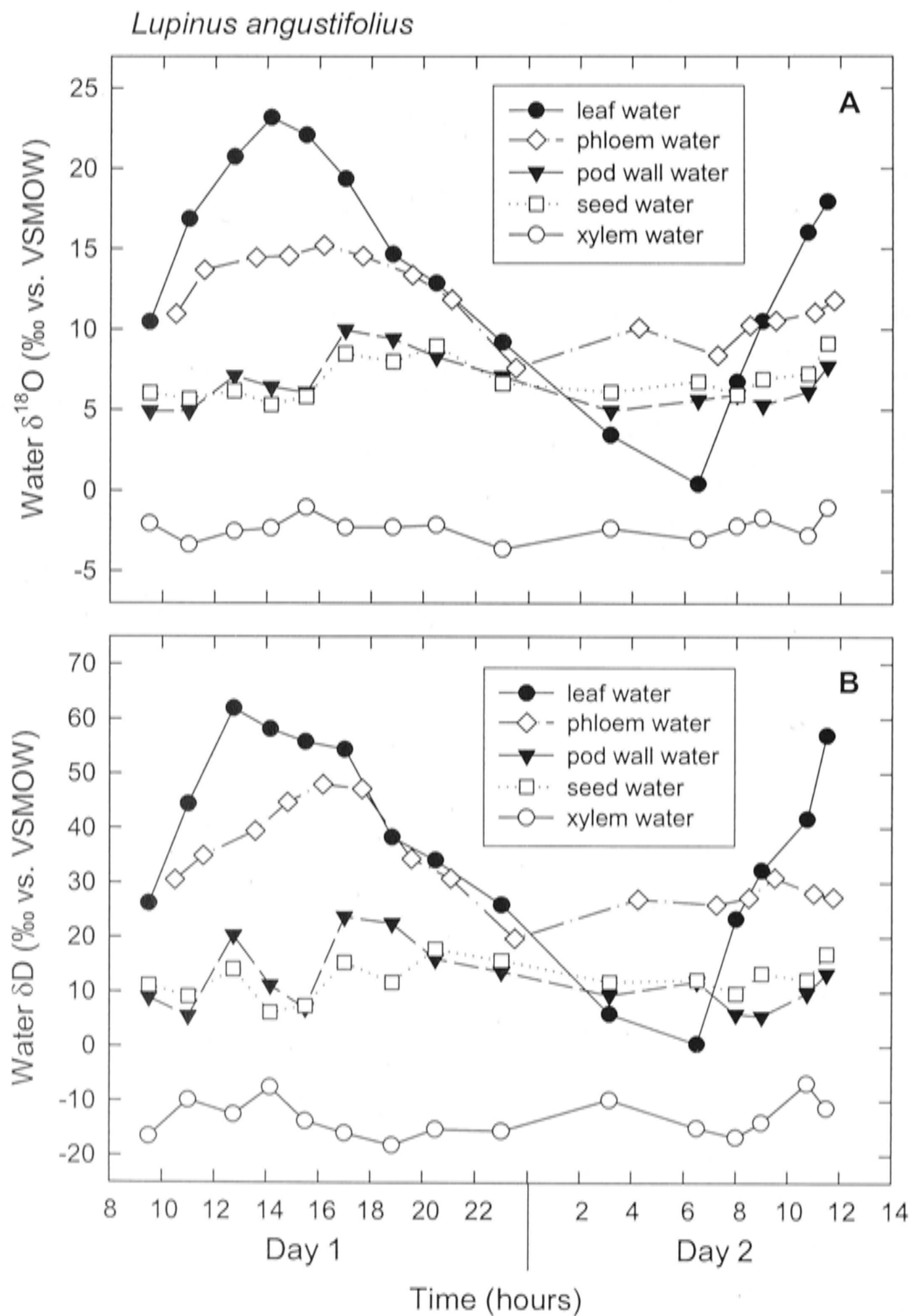


Figure 2.6. Diel variation in (A) oxygen and (B) hydrogen isotope ratios of various water components in *Lupinus angustifolius*. Leaf water samples were collected in bulk from 10 leaflets; pod-wall and seed water samples were collected in bulk from 4 to 6 fruits. Xylem and phloem water were also collected in bulk from several individuals at each sampling time. Samples were collected on November 1 and 2, 2000.

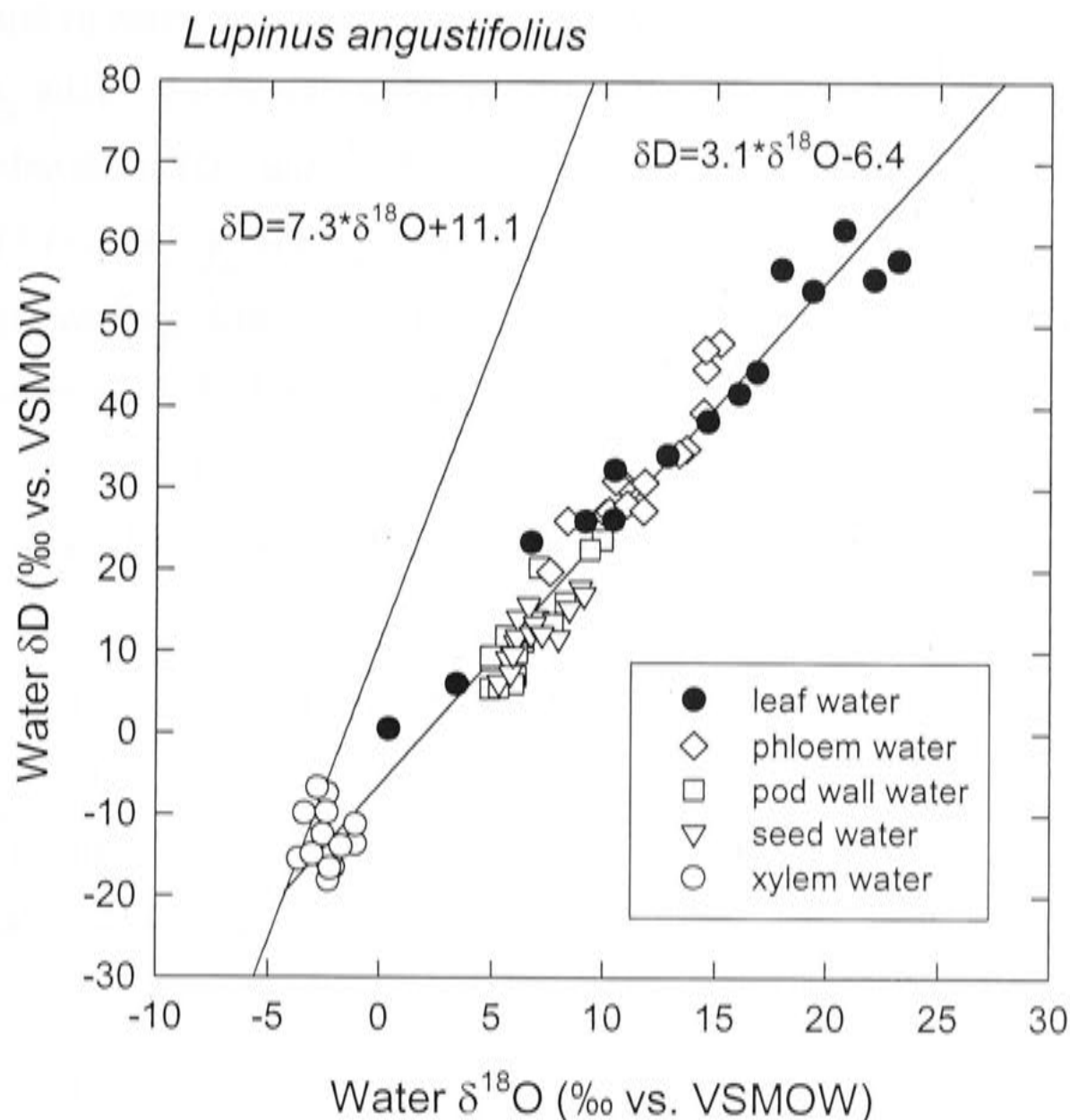


Figure 2.7. Relationship between hydrogen and oxygen isotope ratios for various water components sampled over a 26-hour period from *Lupinus angustifolius* grown in Western Australia. Also shown is the local meteoric water line for precipitation in Perth, Western Australia.

When $\delta^{18}O$ and δD values for all water components were matched against each other, the data resolved as a single regression line with a slope of 3.1 (Figure 2.7). Slopes and intercepts were not appreciably altered when xylem sap water was included in or excluded from the analyses ($P=0.55$ for slope; $P=0.81$ for intercept). However, as seen in the itemized data points of Figure 2.7, the slope of the regression line relating specifically to leaf water differed significantly ($P=0.005$) from that drawn through data for both leaf water and xylem sap water. Figure 2.7 also shows that δD values for xylem sap water fall slightly below those predicted by the local meteoric water line, $\delta D = 7.3 * \delta^{18}O + 11.1$ (Townley et al. 1993), for Perth, Western Australia (420 km north of Mount Barker). Based on the observed $\delta^{18}O$ of xylem sap water, the predicted δD

for precipitation water would be -5.7‰ , which can then be compared to the observed value of -13.2‰ for δD of xylem sap water entering shoots from roots of lupin plants.

Predictions from steady state and non-steady state leaf water models for evaporative site and average leaf water enrichment ($\Delta^{18}\text{O}$ and ΔD) are detailed in Figure 2.8. For ^{18}O enrichment, the steady state prediction of water at the site of evaporation (Δ_{es}) was generally exceeding that actually observed for bulk leaf water during the course of the day, but was much lower than that shown by leaf water at night (Figure 2.8A). The steady state prediction of average leaf water (Δ_{Ls}) for $\delta^{18}\text{O}$ was close to that observed during the day, particularly in the morning and early afternoon. As transpiration eased off in the late afternoon and evening, the Δ_{Ls} prediction converged with the Δ_{es} prediction. Non-steady state predictions of the site of evaporation and average leaf water ^{18}O enrichment were close to observed ^{18}O enrichments through the diel cycle. The Δ_{Ln} was consistently less than the Δ_{en} with the magnitude of difference between the two being noticeably larger at times of high transpiration and lower at times of low transpiration. Patterns of the predictions from the various models for ΔD were qualitatively similar to those for $\Delta^{18}\text{O}$, but tended to be shifted down relative to observed enrichments.

The slopes and intercepts of the regression lines drawn in ΔD - $\Delta^{18}\text{O}$ space are presented in Table 2.1. The regression slope of the Δ_{es} predictions differed slightly from that of the Δ_{Ls} predictions ($P=0.03$), reflecting the different diffusivities of HDO and H_2^{18}O in water [i.e., $2.34 \times 10^{-9} \text{ m}^2 \text{ s}^{-1}$ for HDO compared to $2.66 \times 10^{-9} \text{ m}^2 \text{ s}^{-1}$ for H_2^{18}O (Wang, 1954)]. Thus, taking the Péclet effect into account results in a slightly lower regression slope. However, the difference was small, judging from the overlap in the 95% confidence intervals around the two estimates. The inclusion of non-steady state effects had a negligible influence on the predicted regression slopes for both evaporative site enrichment and average leaf water enrichment ($P=0.73$ for Δ_{en} ; $P=0.82$ for Δ_{Ln}). The ΔD - $\Delta^{18}\text{O}$ regression slope of the observed enrichment (Δ_o) was higher than the predicted slopes for both Δ_{es} and Δ_{Ls} ($P=0.003$ for Δ_{es} ; $P<0.001$ for Δ_{Ls}). Results were similar when non-steady state effects were taken into account ($P=0.02$ for Δ_{en} ; $P=0.009$ for Δ_{Ln}).

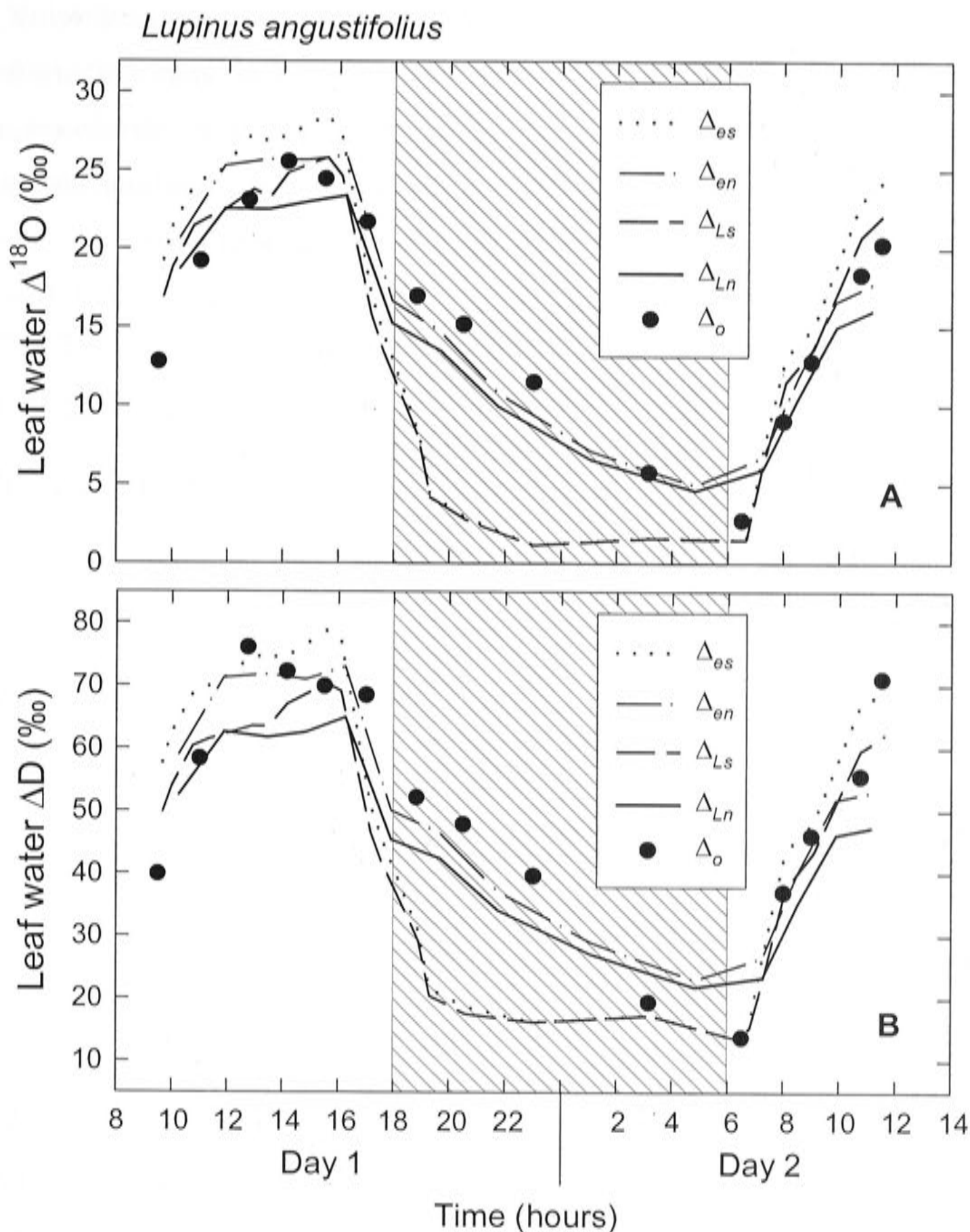


Figure 2.8. Comparison of modeled and observed (A) oxygen and (B) hydrogen isotope enrichment in leaf water of *Lupinus angustifolius*. Nighttime hours are shaded. Symbols are as follows: predicted steady state evaporative site enrichment (Δ_{es}); predicted non-steady state evaporative site enrichment (Δ_{en}); predicted steady state average leaf water enrichment (Δ_{Ls}); predicted non-steady state average leaf water enrichment (Δ_{Ln}); and observed enrichment (Δ_o).

Table 2.1. Slopes and intercepts for ΔD - $\Delta^{18}O$ leaf water isotope enrichment relationships from model predictions and observations, and their respective 95% confidence intervals. Symbols are as follows: predicted steady state evaporative site enrichment (Δ_{es}); predicted non-steady state evaporative site enrichment (Δ_{en}); predicted steady state average leaf water enrichment (Δ_{Ls}); predicted non-steady state average leaf water enrichment (Δ_{Ln}); and observed enrichment (Δ_o).

	slope	95% confidence limits		intercept	95% confidence limits	
		lower	upper		lower	upper
Δ_{es}	2.35	2.30	2.40	11.80	10.82	12.77
Δ_{en}	2.33	2.27	2.39	11.83	10.77	12.89
Δ_{Ls}	2.26	2.20	2.32	11.48	10.44	12.52
Δ_{Ln}	2.25	2.18	2.32	11.43	10.31	12.55
Δ_o	2.73	2.39	3.08	7.49	1.54	13.44

2.5. Discussion

This study represents an integrated account of diel variations in stable isotope ratios of O and H in water and C, N, and O in dry matter of translocation streams and source and sink organs of the grain legume *Lupinus angustifolius*. Sampling fruiting plants over a full diel cycle, $\delta^{18}O$ and δD of the rapidly exchanging water of transpiring leaves and phloem sap were shown to fluctuate through the day to a much greater extent than the bulk tissue water of less actively transpiring pod walls and essentially non-transpiring seeds. As to be expected, soil-derived source water moving up from the roots, and intercepted as stem xylem sap, showed highly consistent $\delta^{18}O$ and δD signals, indicating that diurnal oscillations observed for plant components emanated from fractionation processes within rather than outside the plant. Diel variations in isotope composition were also observed in the $\delta^{13}C$ and $\delta^{18}O$ of phloem sap dry matter, and in the $\delta^{18}O$ of leaf and fruit dry matter, but not in the $\delta^{13}C$ of bulk dry matter components other than phloem sap. The data collectively indicated complex fractionation and

mixing phenomena geared principally around diurnal changes in rates of transpiration and CO_2 exchange by leaves and pod walls. Parallel observations of $\delta^{15}\text{N}$ in transport and source and sink components indicated consistently maintained differences in isotopic composition, probably related to fractionation processes during mixing of fixed atmospheric and soil derived nitrogen, and therefore only marginally related to the processes alluded to above. In the following sections the principal findings will be discussed in further detail.

2.5.1. Isotopic composition of water components within the system

In those few studies in which both $\delta^{18}\text{O}$ and δD of leaf water have been assessed simultaneously under field conditions (Allison et al. 1985; Bariac et al. 1989; Bariac et al. 1990; Yakir et al. 1990; Walker and Lance 1991; Flanagan et al. 1993; Bariac et al. 1994), the diurnal patterns of enrichment have typically shown mid-afternoon maxima and early morning minima in composition of both isotopes. My present data conform to this general pattern. The use of a steady state model for average leaf water enrichment, represented by equations (2.1) to (2.3), resulted in reasonably accurate predictions of leaf water $\delta^{18}\text{O}$, and to a lesser extent δD , during times when the evaporative flux term gw_i was relatively large. However, as gw_i decreased in the afternoon and on through the night, the discrepancy increased between observed values and those predicted by the steady-state model. I conclude that in modeling exercises in which nighttime leaf water enrichment is an important component, such as when evaluating components of dark respiration of ecosystems (Flanagan et al. 1997; Flanagan et al. 1999), it will be necessary to adjust for potential errors related to assuming steady-state isotopic enrichment. Yakir (1998) has addressed this problem, and a recent further extension of the approach by Farquhar and Cernusak (unpublished) indicates that the correction for non-steady state effects is much more influenced by changes in Δ_{en} and Δ_{Ln} [see equations (2.4) and (2.5)] than by changes in W . For example, in the present study, proportional changes in W over the diurnal cycle were only about 10% (Figure 2.2A), whereas the Δ_{en} and Δ_{Ln} changed by nearly 80% (Figure 2.8).

I believe that the data summarized in Figure 2.6 represent the first measurements of the stable isotope composition of water collected from phloem bleeding sap. Adar et al. (1995) reported $\delta^{18}\text{O}$ values for phloem water of tamarisk using a collection technique involving vacuum distillation of tissues from stems and roots. The latter technique could result in contamination of water samples from components other than

translocating cells. Data from the above study suggested that ^{18}O enriched phloem water could be detected in tamarisk roots up to 12 m below the soil surface. In the present study, based on phloem sap water exuded from cut tips of lupin fruits, variation in $\delta^{18}\text{O}$ and δD over a diurnal cycle encompassed a range of values intermediate between those of leaf water and xylem water. However, water of the phloem stream appeared slightly more enriched than leaf water in the very early morning, probably reflecting slow translocatory rates from leaf to fruit through the previous night, with phloem sap water accordingly reflecting earlier loading conditions when the leaf water was more enriched. In any event, data for *Lupinus* and those mentioned above for tamarisk suggest that the fluid contents of the sieve tubes remain sufficiently isolated from surrounding tissue water to transmit enrichment signals from source leaves to sink organs such as fruits or roots to which the translocate is passing.

Judging from earlier models of the economies of water, carbon, and nitrogen of lupin fruits (Pate et al. 1977; Pate et al. 1985), water accumulated in pod walls and seeds should be derived from water entering through both phloem and xylem. Measurements of water isotopes recorded here confirm this suggestion, although the large water content of the fruit tissues appears to effectively buffer fruit water against the relatively large diurnal fluctuations concurrently recorded in $\delta^{18}\text{O}$ and δD of the leaf water (Figure 2.6). Complications due to fractionation during transpiration of pods are to be expected, but were difficult to resolve in the present study.

Plotting of hydrogen and oxygen isotope ratios of different plant water components recorded through the diel cycle produced a single mixing line (Figure 2.7), just as observed earlier for water in the stem, sheath, and various leaves of barley plants on a single occasion at midday in South Australia (Walker and Lance 1991). The resulting regression line drawn through all water components for lupin intersected almost perfectly that of incoming xylem water, as to be expected if the variations in enrichment among phloem and sink tissues resulted specifically from the mixing of enriched leaf water with un-enriched xylem water (see also Yakir et al. 1990; Yakir et al. 1994b). In my analysis, the regression line based solely on values for leaf water intercepted the meteoric water line slightly above the xylem sap water. Dealing more generally with soil-plant-atmospheric systems, Bariac et al. (1994) found that plots of leaf water δD against $\delta^{18}\text{O}$ varied in slope according to whether samples were collected during the day or night. However, this effect did not appear as a feature that could be resolved in the present data set.

Theory relating to the enrichment for δD relative to that for $\delta^{18}O$ has been discussed for water in lakes by Gat (1971), and for the water in leaves by subsequent authors (Allison et al. 1985; Walker et al. 1989; Yakir et al. 1990; Walker and Lance 1991). In the simplest scenario, where atmospheric vapor remains in equilibrium with source water, the expression denoting the slope (S) of the relative enrichments of δD and $\delta^{18}O$ at evaporative sites simplifies from $S=[\varepsilon^*+\varepsilon_k+(\Delta_v-\varepsilon_k)e_a/e_i]_H/[\varepsilon^*+\varepsilon_k+(\Delta_v-\varepsilon_k)e_a/e_i]_O$ to $S=(\varepsilon^*)_H/(\varepsilon^*)_O$, where the subscripts H and O denote fractionation factors for δD and $\delta^{18}O$, respectively (Gat 1971; Allison et al. 1985). In this simple case, small variations in S will still apply at different temperatures since the quotient $(\varepsilon^*)_H/(\varepsilon^*)_O$ decreases with increasing temperature, for example from 9.33 at 10°C to 8.88 at 20°C. In contrast, the effect of the partitioning of ε_k between stomata and leaf boundary layer is negligible because the changes are proportionally very similar for HDO and $H_2^{18}O$. Thus, for the range of boundary layer and stomatal conductances encountered in the present study, the quotient $(\varepsilon_k)_H/(\varepsilon_k)_O$ varied only from 0.8929 to 0.8932. Overall then, S should vary little for water at evaporative sites where atmospheric vapor remains in equilibrium with source water, namely an S value of 3.20 at 10°C versus 2.97 at 20°C. However, as noted previously, when the Péclet effect is taken into account the estimate for average leaf water will differ slightly from that for evaporative sites.

In practice, however, there is likely to be diel variation in temperature such that Δ_v will not equal $-\varepsilon^*$ at all times during the diel cycle. In addition, if e_a varies, identical values for e_a/e_i may occur at different leaf temperatures. In such cases the relative changes in δD and $\delta^{18}O$ will differ through the day (Walker and Lance 1991). Moreover, although it is generally expected to be the case that atmospheric vapor is close to isotopic equilibrium with source water in natural systems (Jouzel et al. 1991), there may be specific situations that will not conform to this generalization (White and Gedzelman 1984).

The regression slopes drawn in ΔD - $\Delta^{18}O$ space and listed in Table 2.1 differ from the slope (S) as defined by Gat (1971) in that they are drawn through several points collected through a diel cycle and plotted as enrichment over source water (i.e., Δ). For the values in Table 2.1, the modeled regression slope differed slightly from the observed slope, namely with a predicted value for Δ_{Ln} of 2.25 versus an observed value of 2.73. This small discrepancy may have resulted from the assumption that isotopic

equilibrium existed between atmospheric vapor and source water. My estimate of $\delta^{18}\text{O}$ of water vapor, based on the equilibrium fractionation factor at the mean daily temperature, was -11.85‰ . This is close to the mean vapor $\delta^{18}\text{O}$ observed in Perth between July 1996 and January 1998 for measurements conducted on a semi-weekly basis ($\text{mean} = -12.26\text{‰}$, $SD = 1.63\text{‰}$, $n = 56$; John Rich, PhD dissertation, unpublished). The slight under prediction of ΔD for average leaf water could then have resulted from an error in the estimate of atmospheric vapor δD and this would also account for the discrepancy between the modeled and observed ΔD - $\Delta^{18}\text{O}$ slope. My equilibrium estimate for vapor δD was -97.6‰ , which differs from the mean value observed in Perth of -85.0‰ ($SD = 10.1\text{‰}$, $n = 107$; John Rich, PhD dissertation, unpublished). However, use of the mean Perth value in the ΔD models resulted in larger discrepancies between the predicted and observed ΔD - $\Delta^{18}\text{O}$ slope and larger errors in the diurnal ΔD predictions.

The predicted steady-state evaporative site enrichment for $\delta^{18}\text{O}$ of water in transpiring leaves was larger than the observed leaf water enrichments in the morning and early afternoon (Figure 2.8A). Previous authors have reconciled similar discrepancies by assuming that some fraction of the water of leaves comprises un-enriched vein water recently derived from the xylem and not yet subject to evaporation (Allison et al. 1985; Leaney et al. 1985; Walker et al. 1989; Walker and Lance 1991; Yakir 1992; Roden and Ehleringer 1999; Roden et al. 2000). In the present study, I took a different approach in that variations between predicted evaporative site enrichment and observed leaf water enrichment were partly reconciled by considering the Péclet and non-steady state effects.

2.5.2. Isotopic composition of dry matter components

The $\delta^{18}\text{O}$ of oxygen atoms in carbonyl groups of organic molecules is influenced by exchange with those in surrounding free water, involving an equilibrium fractionation factor estimated to be $+27\text{‰}$ (Sternberg and DeNiro 1983; Sternberg et al. 1986). The specific possibilities for such exchanges during synthesis of sucrose have been outlined in detail by Farquhar, Barbour & Henry (1998), who ascribe particular importance to processes whereby triose phosphates are exported from chloroplasts and subsequently consumed in sucrose synthesis in the cytoplasm of mesophyll cells. As suggested by the above authors, exchange rates for oxygen atoms in triose phosphates are expected to be fast, so that under high rates of assimilation the equilibrium of

oxygen of triose molecules with cytosolic water should be completed well before their incorporation into sucrose. It is expected that there should be no further major exchanges of oxygen atoms occurring until the translocated sucrose is broken down in the sink tissues of the system. Consistent with this, Barbour et al. (2000b) found that phloem sap sucrose exported from castor bean leaves was in close isotopic equilibrium with predicted average leaf water.

In the present study, I observed a relatively large diurnal variation in the $\delta^{18}\text{O}$ of total leaf dry matter (Figure 2.5B), apparently indicating that carbohydrates were accumulated and exported with $\delta^{18}\text{O}$ values consistently more enriched than that of the bulk structural dry matter of leaves. This would be expected if the $\delta^{18}\text{O}$ signals of assimilated sugars were in close isotopic equilibrium with the $\delta^{18}\text{O}$ of leaf water at the time of fixation. Earlier data recorded by Sharkey & Pate (1976) for lupin leaves showed a 15% diurnal increase from dawn to dusk in dry matter concentration, with about half the marked afternoon increase accountable as starch deposited in chloroplasts and half as sugar in the cytosol of leaf tissues. In the present study, I observed a 19% increase (12.3 g m^{-2}) in dry matter concentration of leaves from predawn ($64.8 \pm 1.5 \text{ g m}^{-2}$) to late afternoon ($77.1 \pm 3.8 \text{ g m}^{-2}$). This observation is reasonable considering that a rough integration of the photosynthetic rates shown in Figure 2.1C suggests a daily fixation of $18.5 \text{ g dry matter m}^{-2} \text{ day}^{-1}$.

To illustrate how the accumulation and export of sucrose and starch could potentially alter the $\delta^{18}\text{O}$ of total dry matter of leaves, I performed the following simplified calculation. I began by assuming that photosynthesis, averaged over the day, occurred at a leaf water value of 20‰ (Figure 2.6A). Taking the equilibrium fractionation between medium water and organic molecules into account, the assimilated sugars should then have an average $\delta^{18}\text{O}$ value of 47‰. The predawn leaves had a total dry matter $\delta^{18}\text{O}$ value of 28‰ (Figure 2.5B). Assuming equivalent oxygen concentrations between the assimilated sugars and the predawn leaf, the addition of 12.3 g m^{-2} of dry matter having an average $\delta^{18}\text{O}$ of 47‰ would raise the $\delta^{18}\text{O}$ of total leaf dry matter from 28‰ to 31‰ by the end of the day. This additional photosynthate would then be exported through the night and the leaf would return to its initial value of 28‰ by predawn the next day. I speculate that there may additionally be some rapid turnover of oxygen atoms in organic compounds not subject to export from the leaf that would in turn contribute to the diurnally fluctuating $\delta^{18}\text{O}$ of total leaf

dry matter. The accumulation and export of enriched carbohydrates, combined with perturbations of this nature, would then be sufficient to account for the 4‰ diurnal variation in total leaf dry matter $\delta^{18}\text{O}$ that I observed for *Lupinus angustifolius*. It is worth noting, however, that such a pronounced diurnal fluctuation in the $\delta^{18}\text{O}$ of leaf dry matter would probably only occur in crop plants such as lupin that have high photosynthetic rates, low leaf mass per area, and pronounced day/night cycles of carbohydrate accumulation and export. Long-lived, perennial plants that do not possess these traits would not be expected to show a marked diurnal fluctuation in total leaf dry matter $\delta^{18}\text{O}$, and of course no diurnal fluctuation would be expected in $\delta^{18}\text{O}$ of leaf cellulose for any plant.

Somewhat surprisingly, the $\delta^{18}\text{O}$ signal of phloem sap sucrose collected from pod tips appeared closer to equilibrium with tissue water in pod walls and seeds than with average leaf water. One explanation would be that the phloem sap dry matter at the tips of fruits does not entirely comprise sucrose exported directly from leaves. Unfortunately, unlike *Lupinus albus* (Pate 1986), *Lupinus angustifolius* fails to bleed sap from leaf petioles, so it is not possible to intercept translocate immediately at its point of exit and thereby compare its isotopic composition with that of translocate collected 20 to 30 cm away in recipient fruits.

The sucrose concentration of phloem sap collected in this study from fruits of *Lupinus angustifolius* showed a strong diurnal variation, as observed previously for *Lupinus albus* (Sharkey and Pate 1976), and *Lupinus angustifolius* (Hocking et al. 1978). While correlating negatively with leaf photosynthetic rate, variations in sucrose concentration tracked closely with leaf water status, as affected by diurnal changes in leaf-to-air vapor pressure deficit and RWC. A response was reported previously for *Ricinus communis* in which the onset of water stress was shown to induce a net increase in the solute content of sieve tubes, so that positive turgor pressure was maintained in phloem despite steeply declining water potential in the surrounding tissues (Smith and Milburn 1980).

One would expect that in any translocatory system, sugar concentrations in the phloem sap should increase to a threshold value at which the osmotic pressure of sieve tubes is sufficient to drive the translocation process. It would then follow that as water potentials in the surrounding tissues continue to fall, higher sugar concentrations would be necessary for continued functioning of the transport system. Pate et al. (1998) reported a strong correlation between values for $\delta^{13}\text{C}$ of phloem sap sugars and

concurrent phloem sap sugar concentrations across a wide range of seasonal and habitat conditions for plantation-grown *Eucalyptus globulus*. This strong relationship is indicative of close coupling between stress and osmotically mediated parameters, particularly since $\delta^{13}\text{C}$ of plant photosynthate increases consistently with water stress (Farquhar and Richards 1984). In the present study, I observed a similar positive linear relationship between phloem sap sugar concentration and phloem sap sugar $\delta^{13}\text{C}$ for samples collected over a relatively narrow range of environmental conditions during daylight hours. The observed uncoupling of the relationship at night might then be resolved if nighttime translocate were derived, at least in part, from the mobilization of starch stored in leaves during previous photoperiods (Sharkey and Pate 1976; Hocking et al. 1978).

The regression line relating carbon isotope discrimination to sucrose concentration for the daytime samples was $\Delta^{13}\text{C}=30 - 38 [\text{sucrose}]$ (Figure 2.4). This relationship suggests that $\Delta^{13}\text{C}$ will decrease to 4.4‰, the value expected when stomata are completely closed, at a sucrose concentration of 0.69 mol L^{-1} . At 20°C , this sucrose concentration corresponds to an osmotic pressure of approximately 2.1 MPa (Nobel 1999), suggesting that canopy gas exchange should cease at leaf water potentials of -2.1 MPa , assuming no excess turgor in sieve tubes at that point. The analysis is simplified insofar as it ignores the osmotic pressure exerted by molecules other than sucrose in the phloem sap. Furthermore, there is no *a priori* reason to assume that the relationship between $\Delta^{13}\text{C}$ and phloem sap sugar concentration should be linear over its full range. More detailed analyses of this relationship could prove useful in future investigations.

Mean differences observed in $\delta^{13}\text{C}$ values for different dry matter components of the *Lupinus angustifolius* system spanned a range of more than 3‰, with leaves most negative (-27.7‰) and seeds least negative (-24.5‰). Differences of similar magnitude and direction between $\delta^{13}\text{C}$ of leaves and fruits have been reported for *Glycine max* (Yoneyama et al. 2000), *Cicer arietinum* (Behboudian et al. 2000), *Ricinus communis* (Yoneyama et al. 1998), and for a range of legume species (Yoneyama and Ohtani 1983). In the present study, the $\delta^{13}\text{C}$ of seeds of *Lupinus angustifolius* matched almost exactly that of the phloem sap carbon, whereas the negative values recorded for dry matter of donor leaves might simply have resulted from the structural dry matter of the foliar canopy having been laid down earlier in the growing season when plants were subject to consistently lower water stress. A similar situation where leaves were reported to contribute carbon to phloem sap with less negative $\delta^{13}\text{C}$ values than their

own dry matter was reported by Pate and Arthur (1998) for a study of Tasmanian Blue Gum (*Eucalyptus globulus*) carried out under essentially similar seasonal and climatic conditions to those experienced at Mount Barker. The above authors also showed that seasonal variations in carbon isotope ratios of phloem sap sugar were consistently reproduced in $\delta^{13}\text{C}$ values of the new dry matter laid down in shoot tissue and secondary xylem. It is likely that similar seasonal changes in $\delta^{13}\text{C}$ of phloem sap carbon of *Lupinus angustifolius* would be progressively recorded in the isotopic signatures of seed dry matter. However, one cannot for the present exclude the possibility of appreciable, albeit probably minor, fractionation events during export from leaves, translocation to fruits, and eventual conversion of sugars to dry matter.

Pod walls of *Lupinus angustifolius* showed a $\delta^{13}\text{C}$ for their dry matter that was almost 1‰ more negative than that of the seeds. A similar differential has also been observed between pod walls and seeds of *Cicer arietinum* (Behboudian et al. 2000). The gas exchange measurements made here, in conjunction with earlier studies on lupin fruits (Pate et al. 1977), indicate a significant refixation of seed-respired CO_2 by the pod. Cernusak et al. (2001) recently developed theory describing carbon isotope discrimination during refixation in photosynthetic bark, a process presumably analogous to refixation in pod walls. Their model suggests that refixation should contribute carbon with a $\delta^{13}\text{C}$ more negative than that of the respiratory carbon source. A greater proportional contribution of refixed carbon relative to carbon originating from source leaves in the dry matter of pod walls compared to seeds could then explain the difference in $\delta^{13}\text{C}$ between the two tissues.

Nitrogen isotope ratios varied among dry matter components across a surprisingly large range (3.6‰), with nitrogen accumulated in the dry matter of leaves and fruits more depleted in ^{15}N than that currently flowing in the xylem and phloem. A similar tendency for $\delta^{15}\text{N}$ of vegetative tissue to be depleted relative to incoming xylem $\delta^{15}\text{N}$ has also been observed for other species: *Ptilotus polystachyus* (Pate et al. 1993), *Triticum aestivum* (Yoneyama et al. 1997), and *Glycine max* (Yoneyama et al. 2000). Between the two transport fluids of *Lupinus angustifolius*, phloem sap was more depleted in ^{15}N than xylem sap, as similarly recorded for *Ricinus communis* at different times of plant development (Yoneyama et al. 1998), and for *Triticum aestivum* during grain filling (Yoneyama et al. 1997). In my study at Mount Barker, root systems were well nodulated and therefore able to feed their shoots with fixed nitrogen ($\delta^{15}\text{N}$ close to 0‰) whilst also accessing mineral nitrogen from the soil ($\delta^{15}\text{N}$ for $\text{NO}_3\text{-N}$ recorded for

the site in the range of 5.3-5.5‰; J.S. Pate, unpublished data). Differential partitioning of fixed nitrogen to certain plant parts combined with targeting of soil derived nitrogen to other parts earlier in the growing season might then explain the observed differences in $\delta^{15}\text{N}$ between different organs of plants sampled at the fruiting stage.

Of the stable isotope ratios that I examined progressively through a diurnal cycle, some components such as $\delta^{18}\text{O}$ and δD in leaf water showed a pronounced and distinctly diurnal variation, whereas others such as $\delta^{13}\text{C}$ and $\delta^{18}\text{O}$ in phloem sap dry matter showed more complex oscillations, possibly reflecting fractionations associated with the daily sugar/starch storage cycles of the leaves. Further insight into the effects of internal cycling and acquisition processes on isotopic fractionation within the source and sink organs of plants will undoubtedly contribute to the successful interpretation of multiple isotopic data sets in terms of plant performance under field conditions.

Chapter 3: Water relations link carbon and oxygen isotope discrimination to phloem sap sugar concentration in *Eucalyptus globulus*

3.1. Abstract

A strong correlation was previously observed between carbon isotope discrimination ($\Delta^{13}\text{C}$) of phloem sap sugars and phloem sap sugar concentration in the phloem-bleeding tree *Eucalyptus globulus* Labill. (Pate et al. 1998). I hypothesized that correspondence between these two parameters results from co-varying responses to plant water potential. I expected $\Delta^{13}\text{C}$ to decrease with decreasing plant water potential, and phloem sap sugar concentration to increase thereby maintaining turgor within sieve tubes. The hypothesis was tested with analyses of *E. globulus* trees growing on opposite ends of a rainfall gradient in southwestern Australia. The $\Delta^{13}\text{C}$ of phloem sap sugars was closely related to phloem sap sugar concentration ($r=-0.90$, $P<0.0001$, $n=40$). As predicted, daytime shoot water potential was positively related to $\Delta^{13}\text{C}$ ($r=0.70$, $P<0.0001$, $n=40$) and negatively related to phloem sap sugar concentration ($r=-0.86$, $P<0.0001$, $n=40$). Additional measurements showed a strong correspondence between predawn shoot water potential and phloem sap sugar concentration measured at midday ($r=-0.87$, $P<0.0001$, $n=30$). The $\Delta^{13}\text{C}$ of phloem sap sugars collected from the stem agreed well with that predicted from instantaneous measurements of c_i/c_a on subtending donor leaves. Accordingly, instantaneous c_i/c_a correlated negatively with phloem sap sugar concentration ($r=-0.91$, $P<0.0001$, $n=27$). Oxygen isotope enrichment ($\Delta^{18}\text{O}$) in phloem sap sugars also varied with phloem sap sugar concentration ($r=0.91$, $P<0.0001$, $n=39$), consistent with predictions from a theoretical model of $\Delta^{18}\text{O}$. I conclude that drought induces correlated variation in the concentration of phloem sap sugars and their isotopic composition in *E. globulus*.

3.2. Introduction

Measurement of stable carbon and oxygen isotope ratios in plant material provides a valuable tool for studying the performance of terrestrial plants. For example, the strong correlation between discrimination against ^{13}C ($\Delta^{13}\text{C}$) and the ratio of intercellular to ambient carbon dioxide concentrations (c_i/c_a) has been relied upon

extensively to assess plant water use efficiency under a variety of experimental and natural conditions (for reviews, see Farquhar et al. 1989a; Ehleringer 1993; Brugnoli and Farquhar 2000). Farquhar et al. (1982) derived an expression relating $\Delta^{13}\text{C}$ to c_i/c_a for C_3 photosynthesis such that,

$$\Delta^{13}\text{C} = a + (b - a) \frac{c_i}{c_a}, \quad (3.1)$$

where a is the fractionation caused by gaseous diffusion (4.4‰), and b is the effective fractionation caused by carboxylating enzymes (~27‰). The $\Delta^{13}\text{C}$ is defined with respect to atmospheric CO_2 as $\Delta^{13}\text{C} = R_a/R_p - 1$, where R_a is $^{13}\text{C}/^{12}\text{C}$ of atmospheric CO_2 and R_p is $^{13}\text{C}/^{12}\text{C}$ of plant material. Equation (3.1) suggests that $\Delta^{13}\text{C}$ decreases linearly as c_i/c_a decreases. Because c_i/c_a represents a balance between the supply of CO_2 via stomata and the photosynthetic demand for CO_2 , $\Delta^{13}\text{C}$ is often employed as an indicator of the extent of drought stress experienced by a plant. Thus, as stomata close to conserve water, $\Delta^{13}\text{C}$ decreases as a function of decreasing c_i/c_a . The advantage of measuring $\Delta^{13}\text{C}$ of plant material is that it provides a time-integrated, rather than instantaneous, estimate of c_i/c_a .

Oxygen isotope enrichment in plant material ($\Delta^{18}\text{O}$), on the other hand, is partly controlled by the evaporative enrichment of ^{18}O in leaf water. Sugars immediately exported from the leaf are presumed to be in close isotopic equilibrium with the water in which they formed (Farquhar et al. 1998; Barbour et al. 2000b; Barbour et al. in press-a), after taking into account an equilibrium fractionation of approximately +27‰ (Sternberg and DeNiro 1983; Sternberg et al. 1986). A proportion of the oxygen atoms in the exported sugars exchanges with local water during subsequent metabolism; however, the leaf water signal is expected to persist unaltered during translocation until the sugar molecules are broken down into derivative molecules containing carbonyl bonds (Barbour et al. in press-a). Leaf water heavy isotope enrichment at evaporative sites ($\Delta^{18}\text{O}_e$) has been modeled as (Craig and Gordon 1965; Dongmann et al. 1974; Farquhar et al. 1989b)

$$\Delta^{18}\text{O}_e = \varepsilon^* + \varepsilon_k + \left(\Delta^{18}\text{O}_v - \varepsilon_k \right) \frac{e_a}{e_i}, \quad (3.2)$$

where ε^* is the equilibrium fractionation between liquid and vapor, ε_k is the kinetic fractionation that occurs during diffusion from the leaf to the atmosphere, $\Delta^{18}\text{O}_v$ is the isotopic enrichment of atmospheric vapor compared to source water, and e_a/e_i is the ratio of ambient to intercellular vapor pressures. The ε_k can be calculated as

$\varepsilon_k(\text{‰}) = (28r_s + 19r_b)/(r_s + r_b)$, where r_s and r_b are the stomatal and boundary layer resistances to water vapor diffusion, and the coefficients 28 and 19 are the associated fractionation factors (Farquhar et al. 1989b). The $\Delta^{18}\text{O}$ in atmospheric water vapor, plant water, and plant organic material is defined with respect to the oxygen isotope ratio of source water as $\Delta^{18}\text{O}_x = R_x/R_s - 1$, where R_x is $^{18}\text{O}/^{16}\text{O}$ of atmospheric vapor, plant water, or organic material and R_s is $^{18}\text{O}/^{16}\text{O}$ of source water. The average isotopic enrichment of water in the leaf mesophyll ($\Delta^{18}\text{O}_L$) can then be related to the isotopic enrichment at evaporative sites by (Farquhar and Lloyd 1993)

$$\Delta^{18}\text{O}_L = \frac{\Delta^{18}\text{O}_e (1 - e^{-\wp})}{\wp} \quad (3.3)$$

The \wp is a dimensionless number termed the Péclet number which is defined as $EL/(CD)$, where E is transpiration rate ($\text{mol m}^{-2} \text{s}^{-1}$), L is a scaled effective path length (m), C is the molar concentration of water (mol m^{-3}), and D is the diffusivity of H_2^{18}O in water ($\text{m}^2 \text{s}^{-1}$).

A potentially useful application of $\Delta^{18}\text{O}$ in plant material is as an integrated measure of stomatal conductance and transpiration rate (Barbour and Farquhar 2000). At a given air temperature and humidity, equation (3.2) suggests that $\Delta^{18}\text{O}_e$ will decrease with increasing stomatal conductance (and therefore transpiration rate) as a result of evaporative cooling of the leaf and consequent lowering of e_a/e_i . Additionally, increased stomatal conductance decreases ε_k , thereby further decreasing $\Delta^{18}\text{O}_e$. Finally, increased transpiration increases the Péclet number, which decreases $\Delta^{18}\text{O}_L$, as seen in equation (3.3). The influence of increased stomatal conductance on e_a/e_i , ε_k , and \wp is opposed by an increase in ε^* with decreasing leaf temperature; however, the increase in ε^* is rather small, namely a change from 9.2‰ at 25°C to 9.6‰ at 20°C. Thus, $\Delta^{18}\text{O}$ can potentially compliment the use of $\Delta^{13}\text{C}$ by providing information about stomatal conductance independently of the effects of photosynthetic demand for CO_2 on c_i/c_a .

Significant variation in $\Delta^{13}\text{C}$ of phloem sap sugars was recently observed in the phloem-bleeding tree *Eucalyptus globulus* Labill. growing in southwestern Australia (Pate and Arthur 1998); variation occurred between rain-fed plantations experiencing drought-stress and irrigated plantations, as well as seasonally within rain-fed plantations in correspondence with seasonal rainfall patterns. Based on the data provided by Pate and Arthur (1998), phloem sap sugar $\Delta^{13}\text{C}$ appeared to integrate drought stress more directly, and over more physiologically relevant timescales, than did whole tissue $\Delta^{13}\text{C}$.

An additional advantage was the relative ease of analyzing phloem sap, which was so dominated by photosynthetic sugars that it did not require further extraction, as would be the case in the analysis of leaf soluble sugars or starch.

In a companion paper, Pate et al. (1998) reported a strong relationship between phloem sap sugar $\Delta^{13}\text{C}$ and phloem sap sugar concentration in *E. globulus*. According to the pressure-flow hypothesis of phloem translocation (Münch, 1930), photosynthate is distributed from source to sink regions within a plant via gradients in turgor within sieve tubes generated by the loading and unloading of sugars. The amount of turgor borne by a sieve tube depends, in part, on the water potential of the apoplastic reservoir surrounding it:

$$P = \Psi + \Pi, \quad (3.4)$$

where P is the hydrostatic pressure within the sieve tube, Ψ is the symplastic water potential (assumed equal to that of the apoplast when the system is in stationary state), and Π is the osmotic pressure within the sieve tube. The importance of the apoplastic water potential in the phloem system has been explicitly recognized in formal descriptions of the Münch hypothesis (eg., Christy and Ferrier 1973; Tyree et al. 1974; Goeschl et al. 1976; Smith et al. 1980; Sheehey et al. 1995), and attention has been drawn to the role of water potential gradients in determining the partitioning of photosynthate among multiple sinks (Lang and Thorpe 1986; Daudet et al. 2002). One might then hypothesize that as the water potential of a plant decreases during drought stress, the osmotic pressure within the sieve tubes will increase to provide the turgor necessary for continued functioning of the phloem. Experimental evidence in support of this concept was obtained for *Ricinus communis*, wherein the concentration of solutes in phloem sap increased in response to withholding water (Hall and Milburn 1973), and the loading of sucrose into the phloem appeared to be turgor pressure dependent (Smith and Milburn 1980).

These considerations led me to investigate the possibility that variation in plant water potential causes correlated changes in phloem sap sugar concentration and phloem sap sugar $\Delta^{13}\text{C}$ in *E. globulus*. The hypothesis is conceptualized in Figure 3.1. Additionally, I compared the $\Delta^{13}\text{C}$ measured in the phloem sap sugars with that predicted from instantaneous measurements of c_i/c_a , in order to assess the validity of applying equation (3.1) to the *E. globulus* system. Finally, I report on a strong relationship between $\Delta^{18}\text{O}$ in phloem sap sugars and the phloem sap sugar

concentration, and postulate that this relationship can also be mechanistically accounted for through consideration of plant water relations.

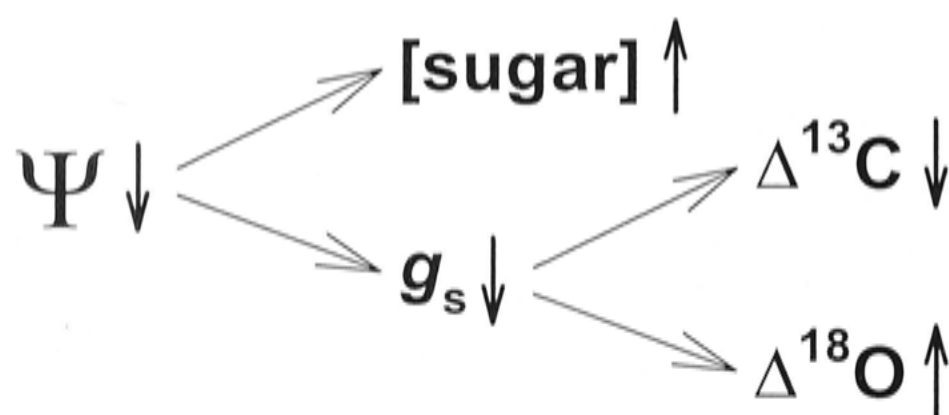


Figure 3.1. A conceptual diagram showing the hypothesized relationships among investigated variables. I expected phloem sap sugar concentration ($[sugar]$) and stomatal conductance (g_s) to vary in response to variation in plant water potential, and carbon ($\Delta^{13}C$) and oxygen ($\Delta^{18}O$) isotope discrimination to vary consequently in response to variation in stomatal conductance.

3.3. Materials and Methods

I measured daytime shoot water potential, phloem sap sugar concentration, phloem sap sugar $\Delta^{13}C$, phloem sap sugar $\Delta^{18}O$, and instantaneous gas exchange in 40 *Eucalyptus globulus* Labill. trees selected from three rain-fed plantations located in southwestern Australia. The three plantations were chosen such that the study would encompass a selection of trees ranging from relatively unstressed to very stressed. Sampling took place between February 21 and 23, 2002, a time that would ordinarily correspond to peak drought stress in the Mediterranean-type environment of southwestern Australia. Site 1 was located near Mount Barker, Western Australia ($34^{\circ}32'28''$ S, $117^{\circ}30'24''$ E), a region on the lower rainfall limit of *E. globulus* plantations averaging approximately 600 mm annual precipitation. Trees were planted in 1999, and were approximately 6 m tall at the time of sampling. Site 2, the wettest of the plantations, was located near the township of Denmark, Western Australia ($34^{\circ}58'45''$ S, $117^{\circ}20'06''$ E) in a region that averages approximately 1400 mm annual precipitation. The sampled trees at site 2 were located at the base of a small hill where I

expected soil moisture content to be relatively high. Trees were planted in 1999 and were approximately 10 m tall at the time of sampling. Trees from a third plantation (site 3), thought to be intermediate between the wet and dry plantations, were also sampled. Site 3 was also located near Denmark, Western Australia ($34^{\circ}58'43''$ S, $117^{\circ}19'02''$ E), but sampled trees were located high on the slope of a hill, and were thus expected to have a lower soil water availability than those at site 2. This plantation was also a 1999 planting. Average weather conditions in the vicinity of the sampling sites over the three weeks preceding sampling are given in Table 3.1.

Trees were sampled sequentially through the day over a single day at each plantation, starting in the early morning and concluding in the late afternoon. The study thus comprised 10 to 15 trees from each plantation. Shoot water potential was measured on four twigs of approximately 5 mm diameter from each tree using a Scholander-type pressure chamber (Scholander et al. 1965). A large ladder was used to access the canopy. Twig samples for water potential measurements were collected from a single canopy height that was approximately two-thirds the height of the live crown. At the same canopy level, phloem sap was collected from the main stem using the bleeding technique described previously (Pate et al. 1998). Phloem sap sugar concentration (w/v) was measured at the time of sap collection using a temperature-compensated, hand-held refractometer (Bellingham and Stanley, London, UK), previously calibrated against HPLC measurements of sugar concentration (Pate et al. 1998). Gas exchange was measured on five to ten leaves per tree at the same canopy level using an LCA 4 Portable Gas Exchange System (ADC BioScientific Ltd, Hertfordshire, England) at the same time that water potential and sugar concentration measurements were taking place. Sugar concentration values measured on a weight per volume basis on the refractometer were converted to molar concentrations by assuming the sugar fraction of the sap to comprise 70% sucrose and 30% raffinose on a weight basis (see Tables 2 and 3, Pate et al. 1998). This was the mean value for the relative concentrations of the two sugars observed across a range of 29 *E. globulus* plantations in southwestern Australia. The standard deviation of the ratio was 10%; an error of two standard deviations would lead to approximately a 7% difference in my calculated molar sugar concentrations.

Table 3.1. Average meteorological conditions over the first three weeks of February reported by weather stations in Mount Barker (34°37'30" S, 117°38'10" E) and Albany (34°56'35" S, 117°48'03" E), Western Australia. Albany is a coastal town approximately 50 km west of Denmark that should experience similar weather patterns to Denmark, and is the nearest operating weather station to Denmark. Total precipitation over the period was 8.0 mm at Mount Barker and 8.4 mm at Albany.

Parameter	Mount Barker 9am	Mount Barker 3pm	Albany 9am	Albany 3pm
Relative humidity (%)	67	49	67	51
Air temperature (°C)	17	21	18	21
Wind speed (m s ⁻¹)	4.2	4.4	5.8	7.5

Additional measurements were made of predawn shoot water potential followed by measurements of midday phloem sap sugar concentration in order to further investigate the relationship between the two parameters, and to see whether predawn or daytime shoot water potential correlated more strongly with daytime sugar concentration. Phloem sap was collected from stems at approximately 1.4 m height above the ground. These measurements took place at various *E. globulus* plantations in southwestern Australia in close proximity (within 100 km) to the primary study plantations in which the more detailed measurements took place.

Phloem sap sugar concentrations were converted to osmotic pressures according to the relationship given by Nobel (1991), which was based on measurements of the freezing point depression of sucrose solutions at 20°C (Weast and Lide 1989). Raffinose was assumed to have the same relationship between molar concentration and osmotic pressure as sucrose. Data for photosynthesis, stomatal conductance, and c_i/c_a were averaged for each tree. Measurements taken at irradiances less than 400 μmol photosynthetically active radiation (PAR) $\text{m}^{-2} \text{s}^{-1}$ were excluded from the analyses so that the effects of water stress on gas exchange could be analyzed independently of the effects of low irradiance. The value of 400 μmol PAR $\text{m}^{-2} \text{s}^{-1}$ was chosen based on a plot of photosynthesis versus irradiance for the unstressed plantation, in which there

appeared to be little increase in photosynthesis with increasing irradiance beyond PAR values of $400 \mu\text{mol m}^{-2} \text{s}^{-1}$.

The stable carbon and oxygen isotope ratios of phloem sap dry matter were determined on 5 μL phloem sap samples from which the water was evaporated overnight in a drying oven at 60°C . Carbon isotope analyses were conducted with an Isochrom mass spectrometer (Micromass, Manchester, UK) coupled to a Carlo Erba elemental analyzer (CE Instruments, Milan, Italy) operating in continuous-flow mode. Oxygen isotope ratios were measured by a second Isochrom mass spectrometer following pyrolysis in a Carlo Erba elemental analyzer (Farquhar et al. 1997). Carbon and oxygen isotope ratios were obtained in δ notation, where $\delta = R/R_{\text{standard}} - 1$, and R and R_{standard} are the isotope ratios of the sample and standard (PDB for carbon, VSMOW for oxygen), respectively. The $\delta^{13}\text{C}$ values were then converted to $\Delta^{13}\text{C}$ values using the equation $\Delta^{13}\text{C} = (\delta_a - \delta_p)/(1 + \delta_p)$, where δ_a is the $\delta^{13}\text{C}$ of atmospheric CO_2 and δ_p is the $\delta^{13}\text{C}$ of phloem sap dry matter. The $\delta^{13}\text{C}$ of atmospheric CO_2 was assumed to be -7.8‰ . The $\delta^{18}\text{O}$ values were converted to $\Delta^{18}\text{O}$ values using the equation $\Delta^{18}\text{O} = (\delta_o - \delta_s)/(1 + \delta_s)$, where δ_o is the $\delta^{18}\text{O}$ of phloem sap dry matter and δ_s is the $\delta^{18}\text{O}$ of source water. Xylem sap water $\delta^{18}\text{O}$ was measured in the Mount Barker plantation on two previous occasions in November 2000 and March 2001, and in the wetter Denmark plantation on one previous occasion in December 2001 (detailed in Chapter 6). Xylem sap water $\delta^{18}\text{O}$ values did not differ between sampling dates at the Mount Barker plantation ($P=0.09$, $n=11$), or between the Mount Barker plantation and the Denmark plantation ($P=0.65$, $n=41$). Therefore a mean source water $\delta^{18}\text{O}$ value of -3.6‰ was used in all calculations of $\Delta^{18}\text{O}$.

After analyzing the oxygen isotope composition of the phloem sap dry matter, I discovered from a separate set of analyses that the measured $\delta^{18}\text{O}$ of phloem sap sugars varies depending on whether the tin sample cup is sealed under argon immediately upon removal from the drying oven, or whether it is folded so that it does not form a gas-tight seal. I presume that the difference is caused by adsorption of water vapor from the atmosphere onto the surface of the dried sugars when the sample is not enclosed in a gas-tight cup. Of the phloem sap samples originally analyzed for this Chapter, 18 had sufficient sample remaining for an additional analysis. I re-analyzed these samples in tin cups sealed under argon immediately upon removal from the drying oven. The resulting $\delta^{18}\text{O}$ values were enriched by 5.5‰ on average compared to the first set of

analyses; however, the two data sets were very well correlated ($r=0.98$, $P<0.0001$, $n=18$). Therefore, I corrected the first set of analyses for the effect of not enclosing the dried sugar samples under a gas-tight seal using the results from the subset of samples that I was able to re-analyze. The regression equation used in the calculations was $\delta^{18}\text{O}_{\text{sealed}}=1.19\delta^{18}\text{O}_{\text{unsealed}}-0.89$, where $\delta^{18}\text{O}_{\text{sealed}}$ is the calculated value for the sealed-cup analysis and $\delta^{18}\text{O}_{\text{unsealed}}$ is the value from the initial unsealed-cup analysis.

Unfortunately, the *Lupinus angustifolius* phloem sap samples that were analyzed for dry matter $\delta^{18}\text{O}$ in Chapter 2 were completely consumed in the original analyses. Therefore it was not possible to re-analyze a subset of the phloem sap samples to test for differences in dry matter $\delta^{18}\text{O}$ between sealed and unsealed cups after discovering the possibility of a measurement bias associated with the former. However, from this point forward in the thesis, all phloem sap dry matter samples were analyzed in gas-tight tin cups sealed under argon immediately upon removal from the drying oven.

I produced theoretical estimates of phloem sap sugar $\Delta^{18}\text{O}$ in order to determine if a change in stomatal conductance alone could account for the range of variation in $\Delta^{18}\text{O}$ values observed in the study. The difference between leaf and air temperatures (ΔT) was predicted using a method developed by DGG dePury and GD Farquhar (unpublished) and described by Barbour et al. (2000a):

$$\Delta T = \frac{r_{bH}^* [Q_0(r_s + r_b) - LD]}{C_p(r_s + r_b + \varepsilon r_{bH}^*)}, \quad (3.5)$$

where r_{bH}^* is the sum of resistances to sensible and radiative heat transfer, Q_0 is the isothermal net radiation at the leaf surface, r_s is the stomatal resistance to water vapor, r_b is the boundary layer resistance to water vapor, L is the latent heat of vaporization, D is the vapor concentration deficit of the air, C_p is the specific heat of air at constant pressure, and ε is the proportional change in latent heat content of saturated air for a given change in sensible heat content. Boundary layer resistance was calculated as summarized by Barbour et al. (2000a) using an average leaf surface area of 60 cm^2 and wind speed of 6 m s^{-1} . The Q_0 was estimated as described by Barbour et al. (2000a) assuming canopy-averaged PAR to equal $1000 \mu\text{mol m}^{-2} \text{ s}^{-1}$. For equation (3.2), average air temperature and relative humidity values were assumed to be 20°C and 55%, respectively, based on data recorded in Table 3.1. The $\Delta^{18}\text{O}_v$ was assumed equal to $-\varepsilon^*$, which produced a $\delta^{18}\text{O}$ estimate for atmospheric water vapor of -13.2% . For comparison, the average vapor $\delta^{18}\text{O}$ in Perth, WA (approximately 400 km from the

study site), based on weekly measurements over a 1.5 year period from 1996 to 1998, was -12.3‰ with a standard deviation of 1.6‰ (John Rich, PhD dissertation, unpublished). An error of one such standard deviation in my vapor $\delta^{18}\text{O}$ estimate would lead to a difference of approximately 0.6‰ in predicted $\Delta^{18}\text{O}$ of phloem sap sugars, whereas a variation of two standard deviations would lead to a difference of approximately 1.2‰. The scaled effective path length for equation (3.3) was assumed to be 25 mm. This estimate was based on measurements in *Eucalyptus globulus* of the discrepancy between predicted $\Delta^{18}\text{O}_e$ and observed leaf water enrichment in the steady state (see Chapter 6 for details). Transpiration rate (E) for equation (3.3) was estimated as (DGG dePury and GD Farquhar, unpublished)

$$E = \frac{\frac{\varepsilon_{bH}^* Q_0}{L} + D}{r_s + r_b + \varepsilon_{bH}^*} \quad (3.6)$$

Relationships among measured parameters were assessed using Pearson correlation and least-squares regression analyses. Statistical analyses were performed in SYSTAT 9.0 (SPSS Inc, Chicago, IL, USA).

3.4. Results

The strong relationship between phloem sap sugar $\Delta^{13}\text{C}$ and phloem sap sugar concentration previously observed by Pate et al. (1998) featured prominently in the present data set (Figure 3.2A). Values for $\Delta^{13}\text{C}$ spanned a range of 10‰, and values for sugar concentration spanned a range of 0.3 mol L⁻¹. The Pearson correlation coefficient (r) relating the two variables was -0.90 ($P < 0.0001$, $n = 40$), indicating a very strong, negative, linear covariance. There was also a very strong correlation between phloem sap sugar concentration and instantaneous c_i/c_a (Figure 3.2B), with a correlation coefficient of -0.91 ($P < 0.0001$, $n = 27$). Additionally, significant correlation was observed between $\Delta^{13}\text{C}$ of phloem sap sugars and shoot water potential ($r = 0.70$, $P < 0.0001$, $n = 40$).

Stomatal conductance, photosynthesis, and c_i/c_a varied among trees growing in the three plantations. The lowest stomatal conductance values were recorded at the Mount Barker plantation and the drier Denmark plantation, and the highest values at the wetter Denmark plantation. Average stomatal conductances for individual trees ranged from 0.02 mol H₂O m⁻² s⁻¹ to 0.56 mol H₂O m⁻² s⁻¹. Average photosynthetic rates ranged from 1.7 μmol CO₂ m⁻² s⁻¹ to 13.0 μmol CO₂ m⁻² s⁻¹. Curvature in the

relationship between average values for stomatal conductance and photosynthesis suggested variation in c_i/c_a among the population of trees sampled.

The measured variation in instantaneous c_i/c_a correlated with $\Delta^{13}\text{C}$ of phloem sap sugars (Figure 3.3). The observed relationship was close to that predicted by equation (3.1). A linear regression through the data yielded the relationship $\Delta^{13}\text{C}=1.7+25.3c_i/c_a$, with the 95% confidence intervals extending from -1.5 to 4.9‰ for the intercept and 20.1 to 30.5‰ for the slope. With the intercept forced through 4.4‰ (the theoretical value for a), the regression yielded a slope estimate of 21.0‰, with the 95% confidence interval extending from 19.9 to 22.2‰.

Both daytime and predawn shoot water potential correlated strongly with daytime phloem sap sugar concentration (Figures 3.4A and 3.4B), with correlation coefficients of -0.86 ($P<0.0001$, $n=40$) and -0.87 ($P<0.0001$, $n=30$), respectively. Recall that the two sets of measurements took place on different trees. As seen in Figure 3.4A, the data for daytime shoot water potential and sugar concentration tended to separate into two populations when plotted against each other, with the trees from the two Denmark plantations having less negative water potentials and lower sugar concentrations than those from the Mount Barker plantation. The slope of the relationship between shoot water potential and daytime phloem sap sugar concentration did not differ significantly depending on whether shoot water potential was measured predawn or during the day ($P=0.07$, $n=70$). However, intercepts for the two relationships were significantly different ($P<0.0001$, $n=70$).

The osmotic pressure exerted by phloem sap sugars sampled from the stem was generally in excess of that required to balance the daytime apoplastic shoot water potential for the trees in the two Denmark plantations, but not greatly in excess for trees in the Mount Barker plantation, which showed the most negative daytime shoot water potentials (Figure 3.5). The slope of the relationship between daytime phloem sap sugar osmotic pressure and daytime shoot water potential had a value of -0.61, which was significantly different from -1 ($P<0.0001$). This suggested significant variation in the amount of turgor borne by sieve tubes in the stems across the range of shoot water potentials encountered in the study.

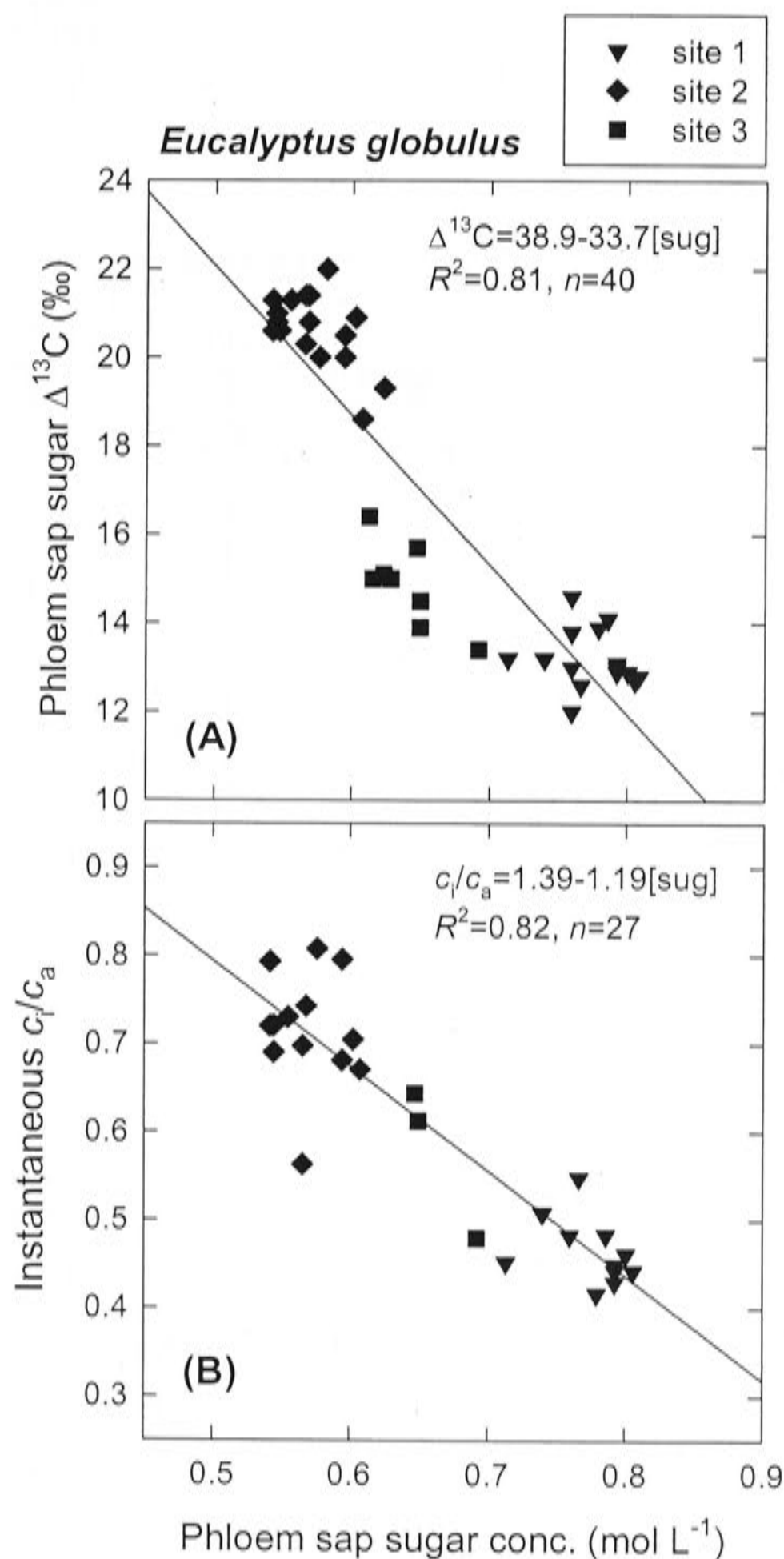


Figure 3.2. (A) Carbon isotope discrimination ($\Delta^{13}\text{C}$) measured in phloem sap sugars, and (B) instantaneous c_i/c_a plotted against phloem sap sugar concentration for *E. globulus* samples collected from three plantations in southwestern Australia in February 2002. Site 1 is the drought-stressed Mount Barker plantation; site 2 is the relatively unstressed Denmark plantation; and site 3 is the intermediate Denmark plantation. Each datum corresponds to one tree. Phloem sap was collected from the stem at approximately two-thirds the height of the live crown. Instantaneous c_i/c_a was measured on five to ten leaves at the same canopy height and averaged for each tree.

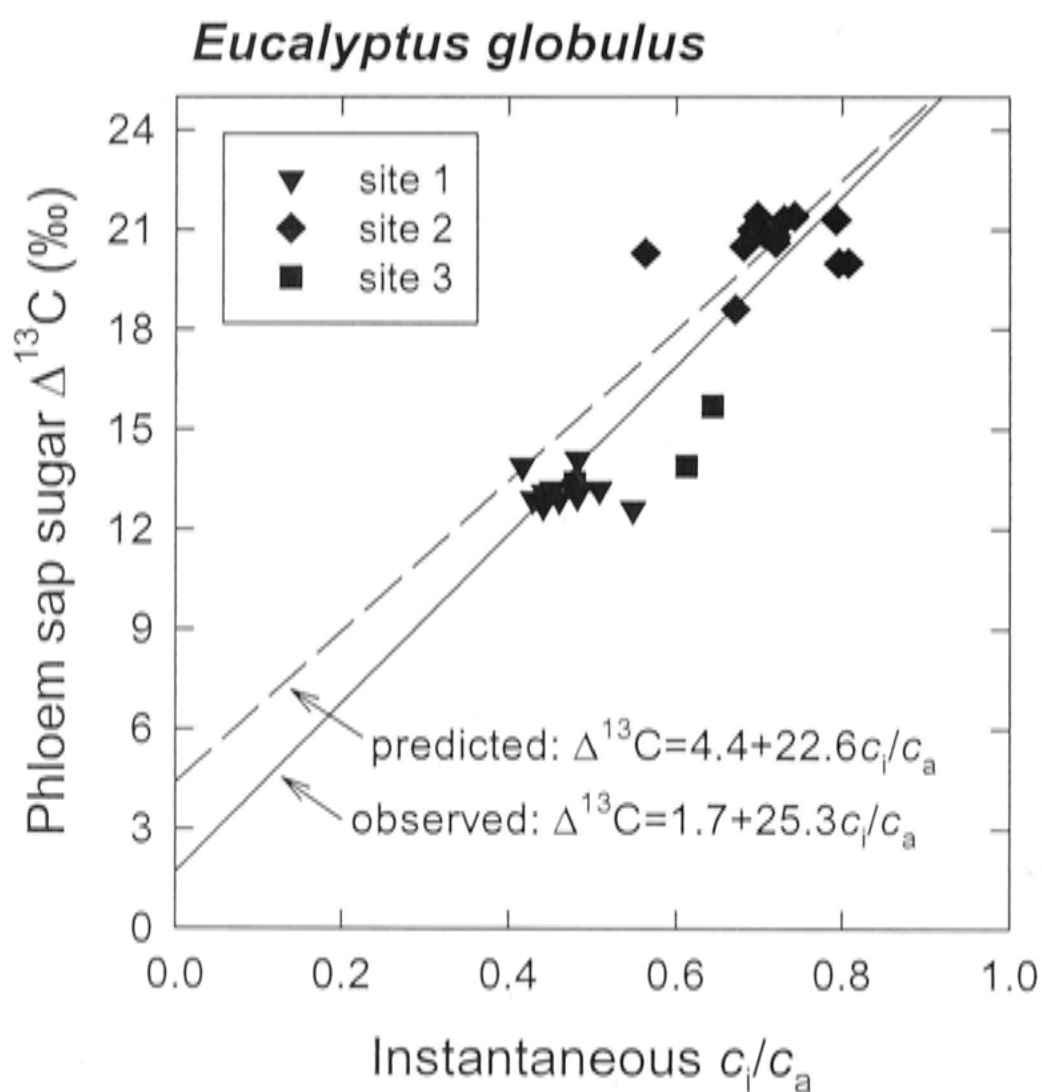


Figure 3.3. Carbon isotope discrimination ($\Delta^{13}\text{C}$) measured in phloem sap sugars collected from *E. globulus* stems plotted against instantaneous c_i/c_a . Gas exchange measurements took place at the same canopy height as the phloem sap collections; instantaneous c_i/c_a values are the average of five to ten measurements per tree. Each datum represents one tree. Site numbers refer to different plantations, as described in the caption of Figure 3.2.

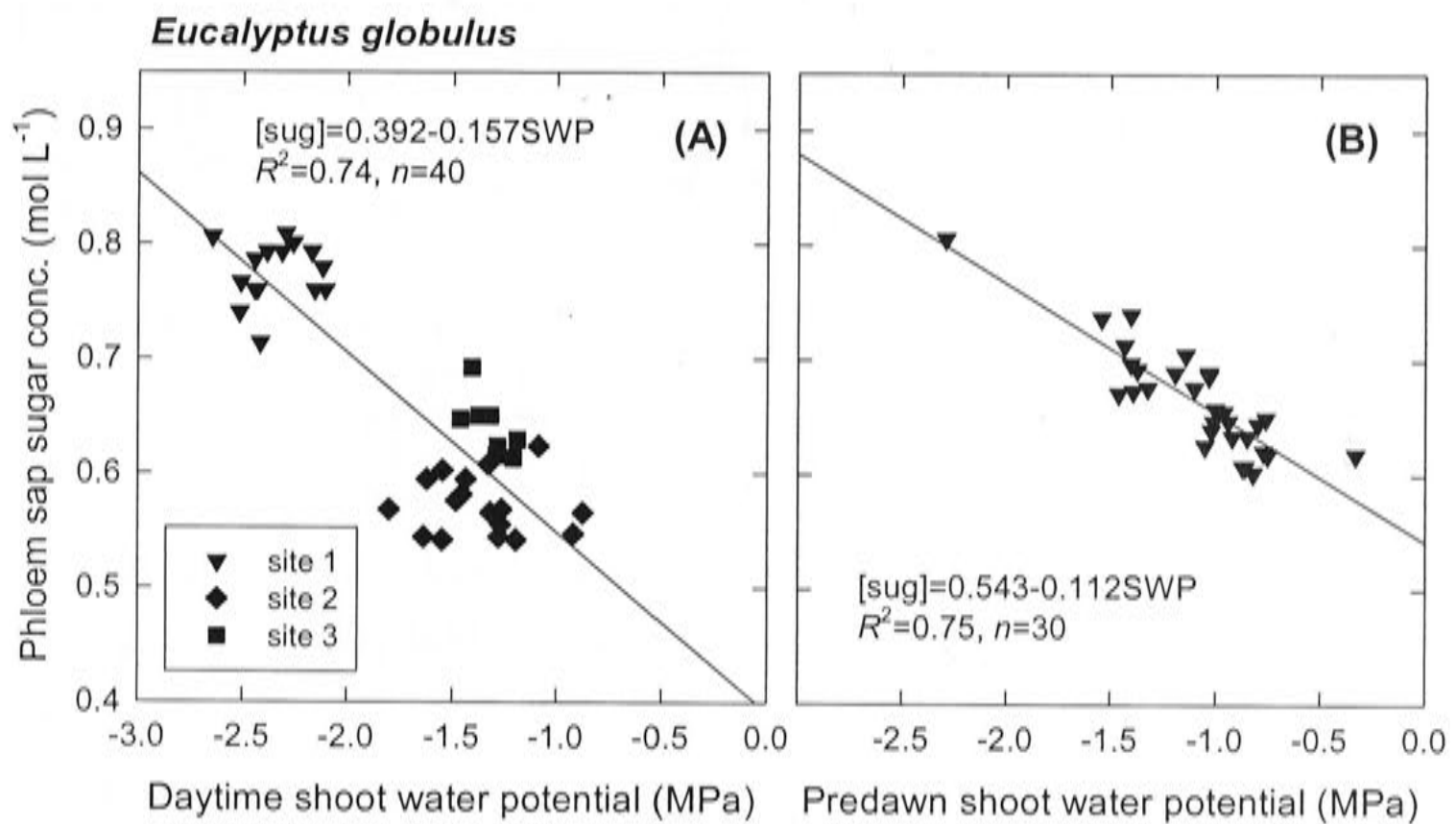


Figure 3.4. *Phloem sap sugar concentration plotted against (A) daytime and (B) predawn shoot water potential for *E. globulus* growing in southwestern Australia. Phloem sap was collected from the main stem at about two-thirds the height of the live crown for (A), and at approximately 1.4 m height for (B). Shoot water potential was measured on four twigs per tree at the same canopy height as the phloem sap was collected from and averaged for each tree. Each datum corresponds to one tree. Daytime and predawn measurements were conducted on different trees at different plantations. Different symbols in (A) show the separation among plantations; site 1 is the Mount Barker plantation, whereas sites 2 and 3 are the two Denmark plantations.*

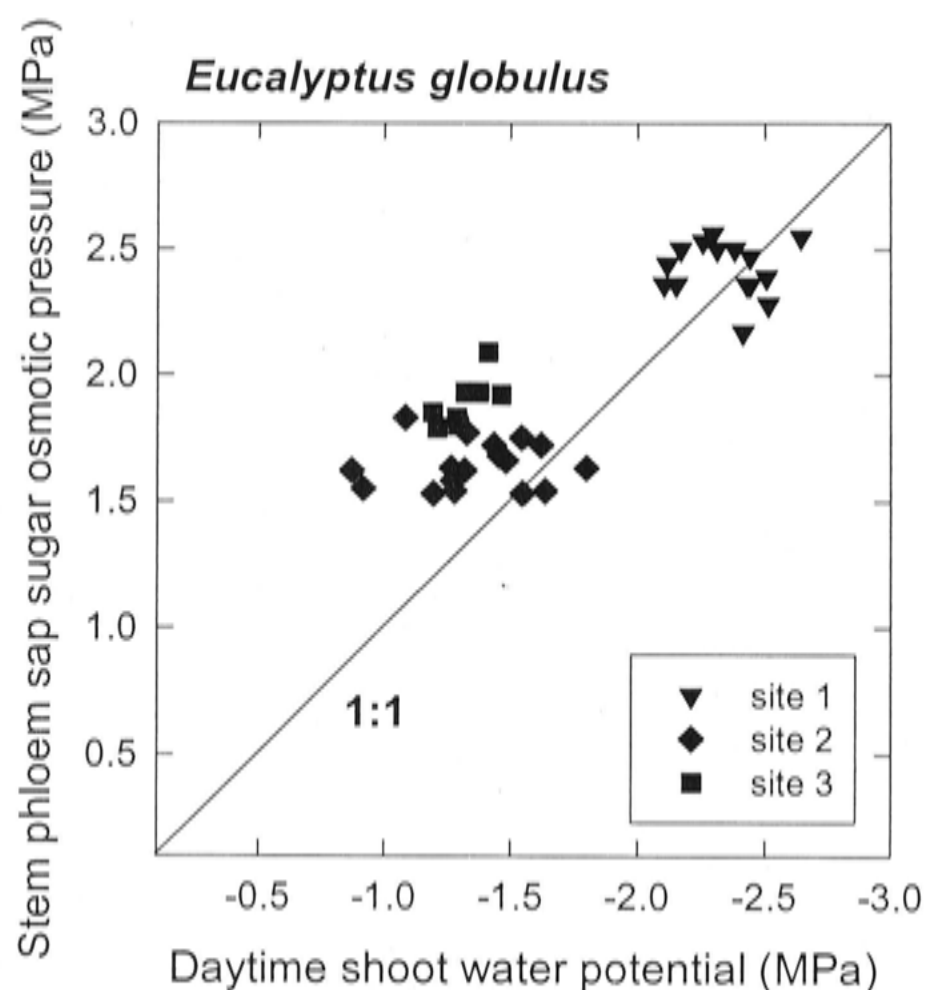


Figure 3.5. Phloem sap sugar osmotic pressure plotted against daytime shoot water potential. Osmotic pressure estimates were derived from measurements of phloem sap sugar concentration. Note that phloem sap was collected from the stem, whereas shoot water potential was measured in terminal shoots. Each datum represents one tree. Site 1 is the Mount Barker plantation; sites 2 and 3 are the two Denmark plantations.

The $\Delta^{18}\text{O}$ of phloem sap sugars correlated strongly with the phloem sap sugar concentration (Figure 3.6A), with a correlation coefficient of 0.91 ($P < 0.0001$, $n = 39$), and with daytime shoot water potential ($r = -0.78$, $P < 0.0001$, $n = 39$). Values of phloem sap sugar $\Delta^{18}\text{O}$ spanned a range of 8‰, with the lowest values (39.0 to 41.7‰) being recorded at the wetter Denmark plantation, intermediate values (42.3 to 43.7‰) at the drier Denmark plantation, and highest values (43.7 to 47.0‰) at the Mount Barker plantation. The $\Delta^{13}\text{C}$ and $\Delta^{18}\text{O}$ of phloem sap sugars correlated negatively with each other (Figure 3.6B) ($r = -0.92$, $P < 0.0001$, $n = 39$). The phloem sap sugar $\Delta^{18}\text{O}$ also correlated negatively with the instantaneous, cuvette-based measurements of transpiration rate (Figure 3.6C), with a correlation coefficient of -0.85 ($P < 0.0001$, $n = 27$). The theoretical model of $\Delta^{18}\text{O}$, summarized in equations (3.2), (3.3), (3.5), and (3.6) predicted values ranging from 47.3 to 38.3‰ over the observed range of stomatal

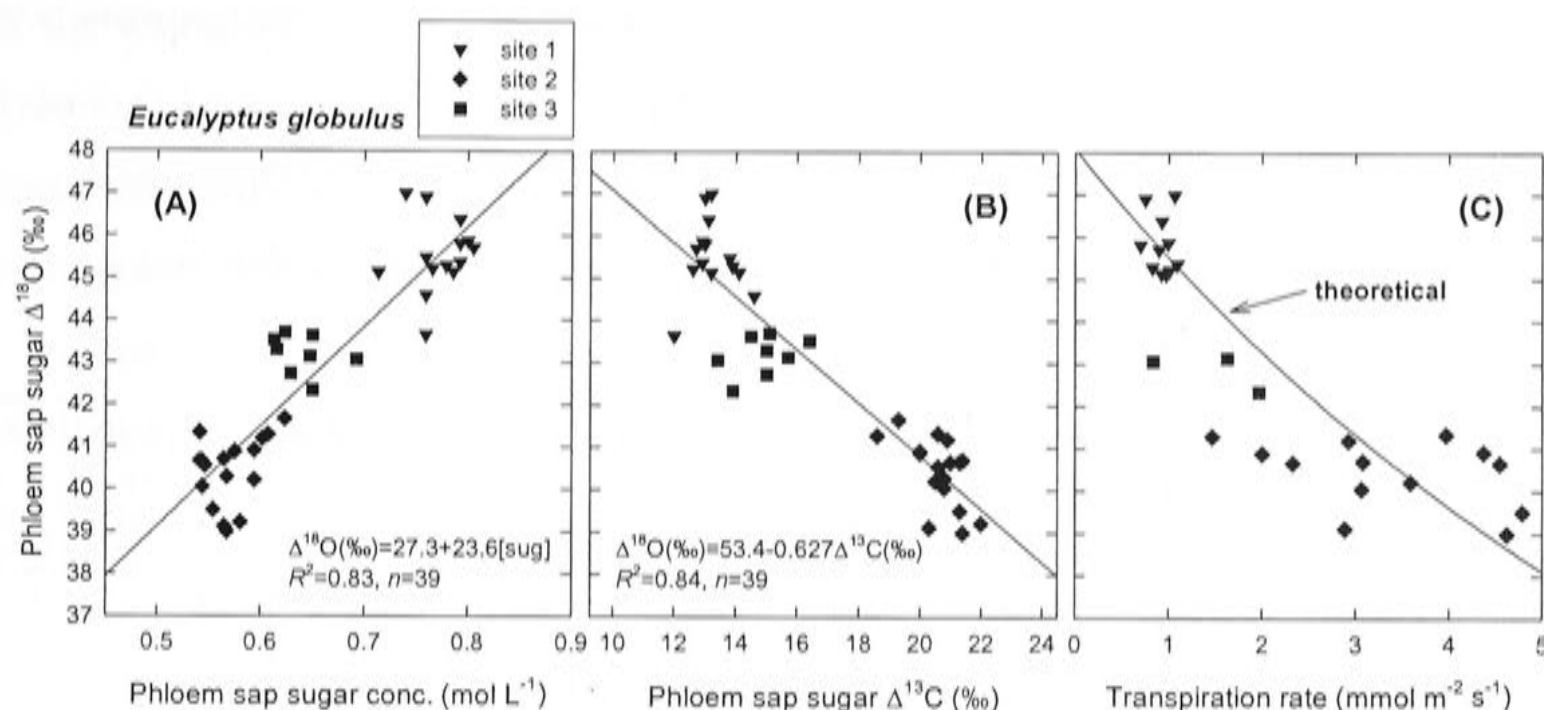


Figure 3.6. Oxygen isotope enrichment ($\Delta^{18}\text{O}$) of phloem sap sugars in *E. globulus* plotted against (A) the sugar concentration of the phloem sap, (B) the carbon isotope discrimination ($\Delta^{13}\text{C}$) of the phloem sap sugars, and (C) cuvette-based measurements of transpiration rate made concurrently with the phloem sap collections. Samples were collected in February 2002 from trees growing in three plantations in southwestern Australia. Site numbers are as described in the caption to Figure 3.2. Each datum corresponds to one tree. Transpiration was measured on five to ten leaves and averaged for each tree. The theoretical line in (C) was derived from equations (3.2), (3.3) and (3.5) in the main text. The theoretical relationship is that expected if variation in phloem sap sugar $\Delta^{18}\text{O}$ resulted exclusively from variation in stomatal conductance and therefore transpiration rate.

conductances (0.02 to 0.56 mol H₂O m⁻² s⁻¹). This predicted range of $\Delta^{18}\text{O}$ values agreed well with the observed range (47.0 to 39.0‰), suggesting that the observed variation in $\Delta^{18}\text{O}$ could in fact be accounted for by varying only one term in the model, i.e. stomatal conductance. For comparison, a sensitivity analysis is presented in Table 3.2 showing the effect of varying terms in the model other than stomatal conductance. The amount of variation in leaf temperature predicted by equation (3.5) over the observed range of stomatal conductances was 2.8°C. This can be compared with observed differences in leaf temperature of approximately 1°C in *Eucalyptus pauciflora* for stomatal conductance values ranging from 0.3 to 0.6 mol m⁻² s⁻¹ (J. Egerton, personal communication); over that range, equation (3.5) predicts a difference of 1.1°C. The best fit between modeled and observed $\Delta^{18}\text{O}$ values was found when the equilibrium fractionation between leaf water and exported sugars was assumed to be 28‰. Note that varying this parameter from 27 to 28‰ affects the absolute values predicted for $\Delta^{18}\text{O}$, but does not affect the range of values predicted.

Table 3.2. A sensitivity analysis showing the effect of varying different parameters in the phloem sap sugar $\Delta^{18}\text{O}$ model, in relation to the effect of varying stomatal conductance over the observed range of conductance values. Parameters were varied one at a time. When a parameter was not being varied, the median value in the selected range was used.

Parameter	Model component affected	Change to value of parameter	Predicted change in $\Delta^{18}\text{O}$ (‰)
stomatal conductance (mol $\text{H}_2\text{O m}^{-2} \text{ s}^{-1}$)	equations (3.2), (3.5), (3.6) ^a	0.02 to 0.56	-9.0
wind speed (m s^{-1})	equations (3.2), (3.5), (3.6)	2 to 10	-0.4
leaf area (cm^2)	equations (3.2), (3.5), (3.6)	20 to 100	0.2
air temperature ($^{\circ}\text{C}$)	equations (3.2), (3.5), (3.6)	15 to 25	-2.9
relative humidity (%)	equations (3.2), (3.5), (3.6)	50 to 60	-1.8
barometric pressure (mbar)	equations (3.5), (3.6)	950 to 1050	0.4
photosynthetically active radiation ($\mu\text{mol m}^{-2} \text{ s}^{-1}$)	equations (3.5), (3.6)	500 to 1500	0.9
scaled effective path length (mm)	equation (3.3)	20 to 40	-2.4
atmospheric vapor $\Delta^{18}\text{O}$ (‰)	equation (3.2)	-8.6 to -10.6	-0.8

^aNote that any parameter affecting equation (3.6), which predicts transpiration rate, also affects equation (3.3), which predicts the Péclet effect.

3.5. Discussion

Although further experimental testing is warranted, the results obtained in this study strongly support my hypothesis as conceptualized in Figure 3.1. Thus, it appears that variation in plant water potential induces correlated changes in phloem sap sugar concentration and the current $\Delta^{13}\text{C}$ and $\Delta^{18}\text{O}$ of *E. globulus* trees. The resulting correspondence between these parameters suggests the intriguing possibility of interpreting phloem sap sugar concentration in terms of plant responses to the environment, and in particular to drought stress.

The relationship between phloem sap sugar concentration and $\Delta^{13}\text{C}$ of phloem sap sugars appears to be extremely well conserved for *E. globulus* growing in southwestern Australia. Pate et al. (1998) reported the regression equation $[\text{sug}] = 1.05 - 0.025\Delta^{13}\text{C}(\text{‰})$, where $[\text{sug}]$ is phloem sap sugar concentration expressed as mol L^{-1} ,

and the regression has an R^2 value of 0.69. For the present data set I obtained the regression equation $[\text{sug}] = 1.06 - 0.024\Delta^{13}\text{C}(\text{‰})$, with an R^2 value of 0.81. The relationship that I observed was nearly identical to that observed previously. The Pate et al. (1998) data were derived from bulked phloem sap samples collected from 37 plantations distributed across southwestern Australia, such that each datum represented one plantation. The present data set therefore serves to confirm on an individual tree basis what was found previously on a plantation basis.

Phloem bleeding sap has also been collected from *Fagus sylvatica* growing in the south of Germany and assayed for both its sugar concentration and the $\Delta^{13}\text{C}$ of the sugars (Gessler et al. 2001). In that study, stand density was manipulated to varying degrees, which was expected to impact on soil water availability, and therefore $\Delta^{13}\text{C}$. Sampling also took place on slopes of differing aspect, which introduced further variation in $\Delta^{13}\text{C}$. Combining data from the different basal area treatments, slope aspects, and sampling dates resulted in a negative correlation between $\Delta^{13}\text{C}$ in phloem sap sugars and phloem sap sugar concentration for *F. sylvatica*, as expected from the hypothesis described by Figure 3.1. Although Gessler et al. do not provide a statistical analysis of the combined data set, the relationship does not appear to be as strong as the one that I observed. For *F. sylvatica*, sugar concentrations ranged from 0.1 to 0.4 mol L⁻¹, whereas in the present study concentrations ranged from 0.5 to 0.8 mol L⁻¹. The relationship between phloem sap sugar concentration and $\Delta^{13}\text{C}$ has also been observed to become weaker in *E. globulus* when phloem sap sugar concentrations are lower and soil water more plentiful (Arthur and Pate, unpublished data); this presumably reflects a more limited role of stomata in causing variation in c_i/c_a at such times.

A negative relationship between phloem sap sugar concentration and phloem sap sugar $\Delta^{13}\text{C}$ was previously observed in *Lupinus angustifolius*, where the sap was collected at different times over a diurnal cycle, and sugar concentrations varied over a relatively narrow range of from 0.33 to 0.38 mol L⁻¹ (Chapter 2). In the present study with *E. globulus*, I could not resolve a diurnal pattern of variation in either the concentration or $\Delta^{13}\text{C}$ of phloem sap sugars. This result contrasts with earlier results for *E. globulus* reported by Pate and Arthur (2000), in which a diurnal pattern in phloem sap sugar concentrations of stems and to a greater extent branches was observed, particularly between samples collected during the day and those collected at night. It is probable that in the present study such a diurnal pattern was obscured by inter-tree variability within the sampled plantations because all sequential sampling occurred on

different trees. In addition, a diurnal pattern may have been less apparent because I only sampled stems and only sampled during the day.

An apparently strong relationship was previously observed between shoot water potential and $\Delta^{13}\text{C}$ of phloem sap sugars in *F. sylvatica* (Gessler et al. 2001). The relationship reported in terms of $\delta^{13}\text{C}$ was $\delta^{13}\text{C}(\text{‰}) = -3.93\text{SWP} - 30.7$, where SWP is shoot water potential (MPa). If I express my data in the same terms, I obtain a relationship for *E. globulus* of $\delta^{13}\text{C}(\text{‰}) = -4.60\text{SWP} - 32.0$ ($R^2 = 0.49$, $P < 0.0001$, $n = 40$), reasonably similar to that obtained for *F. sylvatica*. Extrapolating the regression equations to their respective values at which $\Delta^{13}\text{C} = 4.4\text{‰}$ (or $\delta^{13}\text{C} = -12.2\text{‰}$) results in shoot water potential estimates of -4.7 MPa for *F. sylvatica* and -4.3 MPa for *E. globulus*. The discrimination value of 4.4‰ is the value expected when stomata are completely closed, foregoing issues associated with molecular flow at very low stomatal conductances (Farquhar and Lloyd 1993). These values can be compared to a water potential estimate of -2.1 MPa for *L. angustifolius* when $\Delta^{13}\text{C} = 4.4\text{‰}$ (Chapter 2). Not surprisingly, the estimates of water potential values at complete stomatal closure for the two long-lived, woody tree species are substantially lower than for the herbaceous annual. Such analyses could prove useful in determining the extent of drought stress that different species or genotypes are capable of tolerating.

Slopes of the relationship between shoot water potential and $\delta^{13}\text{C}$ have also been reported for $\delta^{13}\text{C}$ of leaf tissue and wood. A slope of -0.18‰ MPa^{-1} was reported for leaves of *Quercus pubescens* and *Quercus ilex* growing in southern France (Damesin et al. 1998), whereas slopes ranging from -1.8 to -3.1‰ MPa^{-1} were reported for wood of *Pinus radiata* and *Pinus pinaster* growing in southwestern Australia (Warren et al. 2001). The slope that I report for phloem sap sugars of *E. globulus* of -4.6‰ MPa^{-1} differs from those just mentioned in that it was derived from measurements of daytime shoot water potential, rather than predawn shoot water potential. Nonetheless, slopes among species appear to vary over a large range. It is possible that some of the variation can be accounted for by considering the different sampling techniques. Whole-tissue measurements potentially include considerable uncertainty about the period during which the carbon comprising the tissue was assimilated. On the other hand, the strong correspondence between phloem sap sugar $\Delta^{13}\text{C}$ and instantaneously measured c_i/c_a presently reported for *E. globulus* provides clear evidence that phloem sap sugars indeed provide an accurate estimate of the current $\Delta^{13}\text{C}$ of the plant.

I observed a slope for the relationship between $\Delta^{13}\text{C}$ of phloem sap sugars and instantaneous c_i/c_a of 21.0‰ when the intercept was forced through 4.4‰, as prescribed by equation (3.1). This relationship yields a value for b , the effective discrimination by carboxylating enzymes, of 25.4‰. This is consistent with the value of 25.7‰ estimated for b from measurements of leaf soluble sugars in *Populus nigra* \times *deltoids*, *Gossypium hirsutum*, and *Phaseolus vulgaris* (Brugnoli et al. 1988), and 25.0‰ estimated from leaf soluble sugars in *Gossypium hirsutum* and *Oryza sativa* (Brugnoli and Farquhar 2000). Possible reasons for the deviation of b values estimated from analyses of leaf soluble sugars from the suggested value of 27‰ have been discussed in detail by Brugnoli and Farquhar (2000). They include the effects of low mesophyll conductance to CO_2 , and possibly fractionation during dark respiration and photorespiration. The same set of potential mechanisms affecting apparent values of b observed in leaf soluble sugars should also apply to those observed in phloem sap sugars, with the one possible exception being the potential for fractionation during phloem loading. However, to date, such a phenomenon has not been demonstrated.

Data plotted in Figure 3.5 suggest that the amount of turgor conferred by sugars in the phloem sap is not homeostatically maintained across the range of apoplastic shoot water potentials sampled in *E. globulus*. The relationship between daytime phloem sap osmotic pressure in the stem and daytime shoot water potential had a slope greater than negative one, suggesting more turgor at less negative water potentials than at more negative water potentials. This pattern was also reflected in the bleeding behavior of the trees, with trees that had less negative water potentials bleeding more profusely than those with more negative water potentials. In their earlier *E. globulus* sampling efforts, Pate et al. (1998) remarked, “Failure to bleed was rare but encountered occasionally when severely water stressed plantations were sampled during very hot afternoons of late summer and autumn. Even then, the same trees produced sap when sampled after recovery of water stress the following evening.” This would suggest that only under the most severe conditions of drought stress is there a lack of turgor in the sieve tubes of *E. globulus*.

There are some complications involved in attempting to make precise quantitative estimates of stem phloem turgor based on the data plotted in Figure 3.5. Phloem sap was collected from main stems, whereas shoot water potential was measured on terminal shoots. One would expect the daytime water potential in the stem to be less negative than that in the terminal twigs, which would tend to shift the

relationship in Figure 3.5 toward a less negative apoplastic water potential for a given osmotic pressure, thereby resulting in higher estimated turgor pressures in the sieve tubes. However, it also seems likely that the effective osmotic pressure will be less than that estimated from the sugar concentration of the sap because the reflection coefficient of the sieve tube membranes and sieve plates is likely less than unity. The quantitative significance of these two factors is difficult to estimate, particularly since the associated biases are in opposing directions.

However, if I ignore these complications, sieve tube turgor estimates for *E. globulus* range from -0.2 to 0.8 MPa. These can be compared to previously reported values ranging from 0.7 to 1.2 MPa for stem phloem in *Fraxinus americana*, 0.9 to 1.1 MPa for stem phloem in *Ricinus communis* (Milburn 1980), and a value of 1.1 MPa for leaf phloem in *Hordeum vulgare* (Pritchard 1996). In those studies, xylem water potentials were -0.7, -0.5, and -0.2 MPa respectively; all somewhat less negative than the shoot water potentials recorded in the present study. However, in peduncles of *Triticum aestivum* sieve tube turgor pressures of 2.4 and 1.4 MPa were observed at apoplastic water potentials of -0.4 and -2.1 MPa, respectively (Fisher and Cash-Clark, 2000). This decrease in phloem sap turgor with increasing drought stress, as also seen for *E. globulus* in Figure 3.5, is likely to be qualitatively meaningful. If one assumes that the net assimilation rate of the canopy of a tree determines the translocation rate from the canopy, and that the translocation rate is proportional to the turgor gradient from source to sink, then it follows that a reduction in canopy photosynthesis due to stomatal closure will reduce the amount of photosynthate available for translocation and result in a smaller turgor gradient between the source and sink, likely caused by less turgor at the source.

I found that the observed variation in stomatal conductance across the study was sufficient to account for the range of values observed in $\Delta^{18}\text{O}$ of phloem sap sugars. Meteorological data from Mount Barker and Albany, WA suggest very little or no difference in average relative humidity among the study sites for the three weeks preceding measurements (Table 3.2). Similarly, there is no *a priori* reason to expect the isotopic composition of atmospheric water vapor to differ between the Mount Barker and Denmark sites; and, as noted previously, I have observed no difference in xylem water $\delta^{18}\text{O}$ between the Mount Barker plantation and the wetter Denmark plantation. Thus, there would not appear to be a basis for invoking variation in parameters in the $\Delta^{18}\text{O}$ model other than stomatal conductance and transpiration rate in seeking the most

parsimonious explanation for the observed variation in $\Delta^{18}\text{O}$ of phloem sap sugars. The separation of $\Delta^{18}\text{O}$ values in the two Denmark plantations provides further support for this interpretation, as these two sites were only 2 km apart and therefore would have likely experienced identical source water, atmospheric vapor $\delta^{18}\text{O}$, and temperature and humidity regimes.

The $\Delta^{18}\text{O}$ of total dry matter in leaves collected from the Mount Barker plantation and the wetter Denmark plantation was measured in a separate set of experiments (detailed in Chapter 6). Values were $33.5 \pm 0.3\text{‰}$ (mean \pm 1SE) for the Mount Barker plantation and $31.0 \pm 0.1\text{‰}$ for the Denmark plantation, showing that the difference in $\Delta^{18}\text{O}$ observed in phloem sap sugars is also reflected in leaf dry matter. Whereas the average difference between the two plantations for phloem sap sugars was 5.1‰, that for leaf dry matter was 2.5‰. This difference is to be expected, given that during the conversion of phloem sap sugars to leaf dry matter some of the oxygen atoms of the sugars are replaced by those of medium water. Additionally, leaf dry matter would integrate over a longer time period than would phloem sap sugars, most likely encompassing periods when differences in drought stress between the two plantation were less pronounced than at the time of phloem sap sampling.

Because stomatal conductance impacts upon the $\Delta^{18}\text{O}$ model at multiple points, the predicted effect of variation in this parameter was relatively large compared to that which might have been caused by variation in other model parameters (Table 3.1). The modeling exercise allowed me to partition the predicted variation in $\Delta^{18}\text{O}$ owing to variation in stomatal conductance into components due to variation in e_a/e_i (resulting from variation in leaf cooling), ε_k , and \wp . The ε_k varied from 27.9‰ at a stomatal conductance of $0.02 \text{ mol H}_2\text{O m}^{-2} \text{ s}^{-1}$ to 26.4‰ at a conductance of $0.56 \text{ mol H}_2\text{O m}^{-2} \text{ s}^{-1}$. Because I assumed that $\Delta^{18}\text{O}_v = -\varepsilon^*$, equation (3.2) simplifies to $\Delta^{18}\text{O}_e = (\varepsilon^* + \varepsilon_k)(1 - e_a/e_i)$. At a common e_a/e_i of 0.5, the variation in ε_k would equate to a difference of 0.8‰ in $\Delta^{18}\text{O}_e$. The variation in $\Delta^{18}\text{O}_e$ resulting from variation in e_a/e_i due to differences in evaporative cooling of the leaf at the minimum and maximum observed stomatal conductances for a given ε_k of 27‰ would be 2.9‰. Finally, the difference in $\Delta^{18}\text{O}_L$ between the minimum and maximum observed stomatal conductances resulting from variation in \wp for a given $\Delta^{18}\text{O}_e$ of 17‰ would be 5.7‰. Thus, it can be seen that most of the variation in $\Delta^{18}\text{O}$ of phloem sap sugars occurring as a result of variation in

stomatal conductance across the natural rainfall gradient in southwestern Australia was likely caused by variation in ϕ and leaf temperature.

I found that an equilibrium fractionation between predicted leaf water $\delta^{18}\text{O}$ and phloem sap sugar $\delta^{18}\text{O}$ of 28‰, rather than the commonly assumed value of 27‰, resulted in the best fit of modeled to observed data. The possibility exists that the $\delta^{18}\text{O}$ of the leaf water in the cytosol of the mesophyll cells with which sucrose equilibrates prior to export differs slightly from the bulk leaf water $\delta^{18}\text{O}$, as suggested in previous and recent leaf water modeling efforts (Leaney et al. 1985; Yakir et al. 1989; Yakir et al. 1990; Yakir 1992; Farquhar and Gan 2003).

Phloem exudation following an incision in the bark has been demonstrated for many tree species (Zimmerman 1960). Pate et al. (1998) observed exudation of collectable amounts of sap in 14 *Eucalyptus* species, in addition to *E. globulus*. Phloem bleeding for the purpose of sap collection has also been demonstrated in herbaceous plants, for example *Ricinus communis* (Milburn 1970), and several legumes (Pate et al. 1974). Results of this study, and those conducted previously with *E. globulus* (Pate and Arthur 1998; Pate et al. 1998; Pate and Arthur 2000) (Arthur and Pate, unpublished data) highlight the potential of phloem sap analyses for revealing information about the current physiological status of the plant. Such analyses could prove very useful in optimizing the management of *E. globulus* plantations, and the potential exists for their application in other cropping systems as well. The measurement of phloem sap sugar concentrations, in particular, is rapid and inexpensive and can be easily achieved in a field setting. I have demonstrated strong correspondence between the phloem sap sugar concentration of *E. globulus* and several measures of its physiological response to drought stress. Results suggest a very strong potential for the application of the measurement and interpretation of phloem sap sugar concentrations for the purposes of both plantation management and ecophysiological research.

Chapter 4: Oxygen isotope composition of phloem sap in relation to leaf water in *Ricinus communis*

4.1. Abstract

I measured the oxygen isotope composition of both the water and dry matter components of phloem sap exported from photosynthesizing *Ricinus communis* L. leaves. I found that the $^{18}\text{O}/^{16}\text{O}$ composition of exported dry matter matched almost exactly that expected for equilibrium with average lamina leaf water (leaf water exclusive of water associated with primary veins) with an isotope effect of $\alpha_o=1.027$, where $\alpha_o=R_o/R_w$, and R_o and R_w are $^{18}\text{O}/^{16}\text{O}$ of organic molecules and water, respectively. Average lamina leaf water was enriched compared to source water by 14 to 22‰ under my experimental conditions, and depleted compared to evaporative site water by 4 to 7‰, allowing me to resolve that it is indeed the average lamina leaf water $^{18}\text{O}/^{16}\text{O}$ signal that is exported from photosynthesizing leaves, rather than a signal more closely related to that of evaporative site water or source water. Additionally, I found that water exported in phloem sap from photosynthesizing leaves was enriched compared to source water; the mean phloem water enrichment observed for leaf petioles was $4.0 \pm 1.5\text{‰}$ (mean $\pm 1SD$, $n=27$). Phloem water collected from stem bases was also enriched compared to source water; however, the enrichment was about 0.8 times that observed for leaf petioles, suggesting some mixing between enriched phloem water and unenriched xylem water during translocation. Results indicate that the assumption that organic molecules exported from photosynthesizing leaves are enriched by 27‰ compared to average lamina leaf water is valid. Furthermore, results suggest that the potential influence of enriched phloem water should be considered when interpreting the $^{18}\text{O}/^{16}\text{O}$ signatures of plant organic material and plant cellulose.

4.2. Introduction

Measurement and interpretation of the oxygen isotope ratio ($^{18}\text{O}/^{16}\text{O}$) of plant cellulose was undertaken initially with the aim of reconstructing palaeoclimates (Gray and Thompson 1976; Libby *et al.* 1976; Epstein *et al.* 1977). More recently, it has been recognized that oxygen isotope ratios of plant material likely contain useful information about the physiological performance of plants in relation to their growth environments

(Sternberg 1989; Yakir 1992; Farquhar *et al.* 1998). Contemporary models of the oxygen isotope composition of plant organic material and/or plant cellulose from terrestrial plants indicate that any particular part of the plant dry matter is likely to contain a mixture of isotopic signals originating both from source water and from evaporatively enriched leaf water (Saurer *et al.* 1997; Barbour and Farquhar 2000; Roden *et al.* 2000).

The ^{18}O enrichment of water at the evaporative sites within leaves (Δ_e) can be modeled as (Craig and Gordon 1965; Dongmann *et al.* 1974; Farquhar and Lloyd 1993)

$$\Delta_e = \varepsilon^+ + \varepsilon_k + (\Delta_v - \varepsilon_k) \frac{e_a}{e_i}, \quad (4.1)$$

where ε^+ is the equilibrium fractionation between liquid and vapor at the air-water interfaces, ε_k is the kinetic fractionation that occurs during diffusion from the leaf intercellular air space through to the atmosphere, Δ_v is the isotopic enrichment of atmospheric vapor compared to source water, and e_a/e_i is the ratio of ambient to intercellular vapor pressures. The ε_k can be calculated as $\varepsilon_k(\text{‰}) = (32r_s + 21r_b)/(r_s + r_b)$ (Farquhar *et al.* 1989), where r_s and r_b are the stomatal and boundary layer resistances to water vapor diffusion, and the coefficients 32 and 21 are the associated fractionation factors scaled to per mil [Note that the fractionation factors for water vapor diffusion through stomata and boundary layer have been revised from 28 and 19, respectively, to 32 and 21, respectively; this reflects recent measurements showing the isotope effect for diffusion of H_2^{18}O in air to be 1.032 (Cappa *et al.* 2003), rather than 1.028 (Merlivat 1978)]. I express the oxygen isotope enrichment of any water or dry matter component of a plant (Δ_x) relative to source water as $\Delta_x = R_x/R_s - 1$, where R_x is $^{18}\text{O}/^{16}\text{O}$ of that component and R_s is $^{18}\text{O}/^{16}\text{O}$ of source water. Equation (4.1) is a convenient approximation of the mathematically correct form of this particular model [given in the Appendix as equation (A4.3)], which it underestimates by about 0.1‰ (Farquhar and Lloyd 1993). In the present context, I consider this bias to be negligible. I explain why in more detail in the discussion. Farquhar and Lloyd (1993), and more recently Farquhar and Gan (2003), related the average lamina mesophyll water enrichment (Δ_L) to Δ_e as

$$\Delta_L = \frac{\Delta_e (1 - e^{-\wp})}{\wp}, \quad (4.2)$$

where \wp is a lamina radial Péclet number (Farquhar and Gan 2003), defined as $EL/(CD)$, where E is transpiration rate ($\text{mol m}^{-2} \text{s}^{-1}$), L is a scaled effective path length

(m), C is the molar concentration of water (mol m^{-3}), and D is the diffusivity of H_2^{18}O in water ($\text{m}^2 \text{s}^{-1}$).

The ^{18}O enrichment of cellulose (Δ_c) in any sink tissue, whether it be a tree ring, a developing leaf, or a root, can then be related to Δ_L as (Barbour and Farquhar 2000)

$$\Delta_c = \Delta_L(1 - p_{\text{ex}}p_x) + \varepsilon_o, \quad (4.3)$$

where p_{ex} is the proportion of oxygen atoms exchanging with medium water in the sink tissue during cellulose synthesis, and p_x is the proportion of unenriched source water in the sink tissue. The term ε_o represents the equilibrium fractionation between carbonyl oxygen and medium water. Equation (4.3) essentially describes the mixing of the enriched leaf water signal with the unenriched source water signal in the sink tissue during cellulose synthesis. It is similar in this regard to equations presented elsewhere (Saurer *et al.* 1997; Roden *et al.* 2000); however, it differs in the inclusion of the term p_x , which I discuss below. Equation (4.3) can be extended to predict the ^{18}O enrichment of total dry matter by adding the term ε_{cp} to the right side of the equation (Barbour and Farquhar 2000), which accounts for the difference in ^{18}O enrichment between cellulose and the bulk dry matter from which it was extracted.

The term ε_o in equation (4.3) is estimated to have a value of +27‰. This value is the average of several measurements of the difference in oxygen isotope composition between cellulose extracted from aquatic plants and animals and the water in which they grew (Epstein *et al.* 1977; Deniro and Epstein 1981; Yakir and Deniro 1990); a similar value was obtained for terrestrial plants when comparing leaf cellulose to leaf water for plants grown under controlled conditions (Deniro and Epstein 1979; Helliker and Ehleringer 2002), and in tissue culture (Sternberg *et al.* 1986). Sternberg and Deniro (1983) found that the hydration reaction for the carbonyl oxygen of acetone had an isotope effect, α_o (defined as R_o/R_w , where R_o is $^{18}\text{O}/^{16}\text{O}$ of organic oxygen and R_w is $^{18}\text{O}/^{16}\text{O}$ of water), of 1.028, 1.028, and 1.026 at 15, 25, and 35°C, respectively. This experiment appeared to provide strong support for the hypothesis that hydration of carbonyl oxygen groups is the mechanism by which organic molecules record the oxygen isotope signature of the water in which they form. It also reinforced the notion that ε_o (defined as $\alpha_o - 1$) for such reactions is indeed very close to 27‰.

Equation (4.3) assumes that photosynthate exported from source leaves is in complete isotopic equilibrium with water having an enrichment of Δ_L . For an α_o value of 1.027, this assumption can be summarized as

$$\frac{R_{suc}}{R_L} = 1.027, \quad (4.4)$$

where R_{suc} is the $^{18}\text{O}/^{16}\text{O}$ of sucrose exported in the phloem and R_L is that of average lamina mesophyll leaf water. Multiplying both sides of equation (4.4) by R_L and dividing through by R_s , the $^{18}\text{O}/^{16}\text{O}$ of source water, then scaling to per mil, gives the following result:

$$\Delta_{suc} = 1.027\Delta_L + 27\text{‰}, \quad (4.5)$$

which describes the assumed relationship between ^{18}O enrichment of sucrose exported in the phloem sap and ^{18}O enrichment of average lamina leaf water. In the present study, I extended this assumption to the sum total of all organic molecules exported in the phloem sap, not just sucrose.

The term p_x in equation (4.3) allows for the possibility that some enriched water will be translocated in the phloem to the sink tissue along with sucrose, thereby altering $^{18}\text{O}/^{16}\text{O}$ of the medium water with which organic molecules exchange to a value somewhat more enriched in ^{18}O than source water. Little is known about the isotopic composition of phloem water exported from photosynthesizing leaves; however, this may be an important component in the quantitative assessment of processes contributing to the oxygen isotope composition of plant organic material and plant cellulose.

I had two primary objectives in this investigation: the first was to test the assumption articulated in equation (4.5) that exported photosynthate is in oxygen isotope equilibrium with average lamina leaf water; the second was to characterize the oxygen isotope composition of phloem water exported along with photosynthate from photosynthesizing leaves, particularly in relation to that of source water and average lamina leaf water. Measurements were conducted on phloem sap and leaf water samples collected from *Ricinus communis* L. An earlier paper reported observations of $^{18}\text{O}/^{16}\text{O}$ in phloem sap dry matter of *R. communis*, and made comparisons with predicted $^{18}\text{O}/^{16}\text{O}$ of lamina leaf water (Barbour *et al.* 2000). This chapter goes beyond those results by providing a direct comparison between measured lamina leaf water $^{18}\text{O}/^{16}\text{O}$ and measured phloem sap dry matter $^{18}\text{O}/^{16}\text{O}$; additionally, I report observations of phloem water $^{18}\text{O}/^{16}\text{O}$, which was not measured in the earlier paper.

4.3. Materials and Methods

I conducted four experiments aimed at achieving these objectives. For all four experiments, *Ricinus communis* L. plants were grown from seeds for six to 10 weeks in 10 L pots containing sterilized potting mix and a slow release fertilizer (Scotts Osmocote Plus, Sierra Horticultural Products, Heerlen, The Netherlands). Plants were grown in a temperature and humidity controlled glasshouse; daytime temperature and humidity were $27 \pm 2^\circ\text{C}$ and $40 \pm 10\%$, respectively. Nighttime temperature was 20°C with the same humidity as for the daytime. Plants were approximately one meter tall at the time of sampling.

4.3.1. Glasshouse experiment 1

Experiment 1 was conducted in the glasshouse and will be termed Glasshouse 1. In this experiment, the variables necessary for parameterization of the Δ_e model [equation (4.1)] were measured for the leaf that was the youngest fully expanded at the time of sampling (usually the sixth leaf up from the base of the plant). Stomatal conductance was measured with an LI-6400 portable photosynthesis system (Li-Cor Inc., Lincoln, NE, USA). Leaf temperature was measured under ambient conditions with a 0.13 mm diameter chromel-constantan thermocouple (Omega Engineering, Stamford, CT, USA). Relative humidity in the vicinity of the leaf was measured with a temperature and humidity probe (Humitter 50Y, Vaisala Inc., Helsinki, Finland). Irrigation water on the day of measurement and atmospheric water vapor inside the glasshouse were collected; vapor was collected by drawing air through a dry ice-ethanol cold trap at a flow rate of approximately 1 L min^{-1} . Phloem sap was then obtained from the leaf petiole by making a 1 to 2 mm deep incision with a sharp razor blade and immediately attracting the exuding sap into a micro capillary tube. The process was repeated until approximately 30 μL of sap was obtained. The leaf was then harvested for leaf water extraction. In Glasshouse 1, the leaf lamina was quickly separated from the primary vein network by cutting around the primary veins with scissors. The leaf lamina was then immediately sealed in a glass tube by a rubber stopper embedded in a screw cap. Finally, phloem sap was collected from the stem at the base of the plant in the manner described for the leaf petiole. All samples were frozen on dry ice immediately upon collection. Leaf lamina water was later extracted by vacuum distillation. Glasshouse 1 was repeated on eight plants over the course of three days in September 2002.

4.3.2. Leaf chamber experiment 1

The second experiment, which was conducted in a leaf chamber connected to a gas exchange system in the laboratory, will be termed Leaf Chamber 1. The gas exchange system has been described previously (Boyer *et al.* 1997; Barbour *et al.* 2000), except one modification: a large chamber (60 x 50 x 10 cm) was constructed to accommodate the large leaves of *R. communis*. The projected leaf areas for leaves measured in this experiment ranged from 329 to 808 cm². A bypass drying loop was connected to the chamber, such that chamber air was continuously cycled through a series of dry ice-ethanol cold traps at a rate of up to 45 L min⁻¹ to remove water vapor and prevent condensation within the system. The through-flow rate of air in the chamber ranged from 2 to 8 L min⁻¹. In Leaf Chamber 1, the water captured in the traps was collected for isotopic analysis. Importantly, the traps were not efficient enough to remove all of the vapor from the air stream, such that a small amount was recycled to the chamber after passage through the bypass drying loop.

For Leaf Chamber 1, an *R. communis* plant was brought into the laboratory on the evening before measurements were to take place and placed under illumination overnight to stimulate phloem sap bleeding the next day. In the morning a leaf was placed in the chamber and gas exchange was monitored. The CO₂ concentration inside the chamber was maintained at approximately 400 μmol mol⁻¹. Irradiance was approximately 500 μmol PAR m⁻² s⁻¹. Leaf temperature was measured by eight thermocouples positioned at various places on the underside of the leaf. After the leaf had reached a steady state with respect to CO₂ and water vapor exchange, it was left in the chamber for at least four hours. In a previous experiment with *R. communis*, Barbour *et al.* (2000) found that under very similar conditions, it took approximately three hours for phloem sap sucrose bled from the leaf petiole to come to a constant oxygen isotope ratio after a step change in the vapor pressure of chamber air. After 4 hours at steady state, approximately 30 μL of phloem sap was collected from the leaf petiole where it emerged from the chamber. The chamber lid was then removed, and the leaf lamina quickly separated from the primary vein network with scissors and sealed in a glass tube. Leaf water was later extracted from the leaf lamina by vacuum distillation. Leaf Chamber 1 was repeated on five plants during December 2002. Leaf temperatures were varied (from 22 to 30°C), as was the flow rate through the bypass drying loop, such that a range in values of e_a/e_i was obtained among different leaves.

This was done so that the relationships between ^{18}O enrichment in phloem sap and Δ_L could be assessed over a range of Δ_L values.

After Glasshouse 1 and Leaf Chamber 1 had been completed, I conducted an experiment to determine whether my method of leaf lamina sampling might be biasing the leaf water isotopic analyses due to evaporation from the leaf lamina during separation from the primary veins. The *R. communis* leaves that I sampled typically had nine primary veins radiating from the point where the petiole joined the leaf; it generally took two to three minutes to cut around them with a pair of scissors. To test for bias in the sampling procedure, I installed a balance in the glasshouse and determined the fresh weight of a leaf immediately after separating it from a plant. The lamina was then separated from the primary veins as had been done for Glasshouse 1 and Leaf Chamber 1. The veins and lamina were then placed together on the balance and their combined weight determined. This was repeated for 10 leaves from each of 10 plants. I calculated that the total mass of water in the leaves decreased by $8.5 \pm 2.5\%$ (mean $\pm 1SD$, $n=10$) during the time taken for lamina/primary vein separation; it was therefore judged likely that the leaf water sampling method had biased the leaf water isotopic analyses in Glasshouse 1 and Leaf Chamber 1.

4.3.3. Glasshouse experiment 2

The glasshouse experiment was then repeated, and this will be termed Glasshouse 2. For Glasshouse 2, the same procedure was followed as for Glasshouse 1, except that stomatal conductance was measured with an Li-1600 steady state porometer (Li-Cor Inc., Lincoln, NE, USA), and leaf temperature was measured with an infrared thermometer (Infracouple Model M50, Mikron Instruments, Oakland, NJ, USA). For leaf water sampling in Glasshouse 2, the entire leaf including the primary veins was immediately sealed in a glass tube and frozen. The primary vein network was then separated with scissors from five independent leaves for which the parameters necessary for predicting Δ_e had been measured. I calculated the proportion of leaf water associated with primary veins by assuming that no evaporation had taken place from the veins during separation from lamina for the leaves for which the mass was weighed before and after vein/lamina separation. The proportion of total leaf water associated with the primary veins was 0.22 ± 0.02 (mean $\pm 1SD$, $n=10$). Water was then extracted from the whole leaves and from the independently isolated veins by vacuum distillation. The enrichment of the primary vein water was measured and expressed as a proportion

of Δ_e ; the mean value was 0.04 ± 0.08 (mean $\pm 1SD$, $n=5$). The Δ_L for the leaf lamina of the whole leaves was then calculated by mass balance assuming the primary veins accounted for 22% of the total leaf water and had an enrichment of $0.04\Delta_e$. Glasshouse 2 was repeated on nine plants over the course of three days in January 2003.

4.3.4. Leaf chamber experiment 2

The leaf chamber experiment was also repeated and this experiment will be termed Leaf Chamber 2. Oxygen isotope analyses of the water vapor collected in the cold traps in the bypass drying loop in Leaf Chamber 1 indicated some fractionation of vapor in the air stream during passage through the traps; i.e. vapor retained in trap 1 was isotopically depleted compared to vapor retained in trap 2, etc. Because the proportion of vapor removed by the traps was slightly less than unity, the air inside the chamber was expected to contain vapor slightly enriched compared to source water. Therefore in Leaf Chamber 2, water vapor was collected for measurement of Δ_v from the air stream exiting the chamber en route to the IRGA. The flow rate of air through this dry ice-ethanol cold trap was 0.5 to 1 L min⁻¹, such that complete trapping of the vapor was easily achieved. I used the average value of Δ_v obtained from these measurements for calculations of Δ_e for leaves measured in Leaf Chamber 1; the average value was $1.2 \pm 1.1\text{‰}$ (mean $\pm 1SD$; $n=5$). In Leaf Chamber 2, after a leaf had been in the chamber under steady-state conditions for at least 4 hours, the chamber lid was removed and the leaf was immediately severed from the petiole and submerged in a bath of toluene. A scalpel was then used to separate the leaf lamina from the primary veins while at the same time ensuring that the leaf remained below the toluene surface. The lamina samples were then stored in reagent bottles filled with toluene until the leaf water could be extracted by azeotropic distillation (Revesz and Woods 1990). This procedure ensured a complete transfer of the lamina water without loss by evaporation during the sampling process. Leaf Chamber 2 was the same as Leaf Chamber 1 in all other aspects and was repeated on five plants during March 2003.

4.3.5. Isotopic analyses

Oxygen isotope ratios of water and dry matter samples were measured using the on-line pyrolysis method described by Farquhar *et al.* (1997). Analyses were conducted in an Isochrom mass spectrometer (Micromass, Manchester, UK) following pyrolysis in a Carlo Erba elemental analyzer (CE Instruments, Milan, Italy) or in a custom built

furnace at 1200°C with a glassy carbon tube. Phloem sap dry matter was obtained by drying the sap samples overnight at 60°C in smooth walled tin cups. The cups were then sealed under argon immediately upon removal from the drying oven to prevent hydration of the samples by water vapor in the ambient air (Chapter 3). The oxygen isotope composition of phloem sap water was measured as described previously (Chapter 2), using the technique developed by Gan *et al.* (in press) for the determination of $^{18}\text{O}/^{16}\text{O}$ of the water component of a homogenous mixture of water and dry matter. Oxygen isotope ratios were obtained in delta (δ) notation, referenced against Vienna Standard Mean Ocean Water. The $\delta^{18}\text{O}$ values for water and dry matter were then converted to enrichment above source water (Δ_x) by the relationship $\Delta_x = (\delta_x - \delta_s) / (1 + \delta_s)$, where δ_x is the $\delta^{18}\text{O}$ of the sample of interest and δ_s is that of source water. The δ_s values were obtained by analysis of the irrigation water on the day of leaf water and phloem sap collection. Analytical precision for $\delta^{18}\text{O}$ analyses, based on repeated measurements of laboratory standards for sucrose and water, was $\pm 0.3\text{‰}$.

I tested for differences among experiments in the terms $1 - \Delta_L / \Delta_e$ and $1 - \Delta_{\text{suc-L}} / \Delta_e$ with analyses of variance. The term $\Delta_{\text{suc-L}}$ refers to the water enrichment value inferred by subtracting 27‰ from Δ_{suc} and dividing by 1.027, as prescribed by equation (4.5). Differences among individual experiments were then assessed with Tukey's method for pair-wise comparisons. Variation between phloem sap collections made from leaf petioles and stem bases in Glasshouse 1 and Glasshouse 2 were assessed with paired *t*-tests. Statistical analyses took place in SYSTAT 9.0 (SPSS Inc., Chicago, IL, USA).

4.4. Results

4.4.1. Enrichment of ^{18}O in leaf water and phloem sap dry matter

The observed leaf lamina water ^{18}O enrichment (Δ_L) for all four experiments is shown in Figure 4.1A plotted against the predicted evaporative site enrichment (Δ_e). Viewing the data in this way reveals a clear separation between the experiments in which the leaf lamina was separated from the primary veins in the open air (open symbols in Figure 4.1A), and that in which Δ_L was calculated indirectly after extraction of the total leaf water (closed circles in Figure 4.1A), or in which the lamina was separated from the primary veins while submerged in toluene (closed triangles in Figure

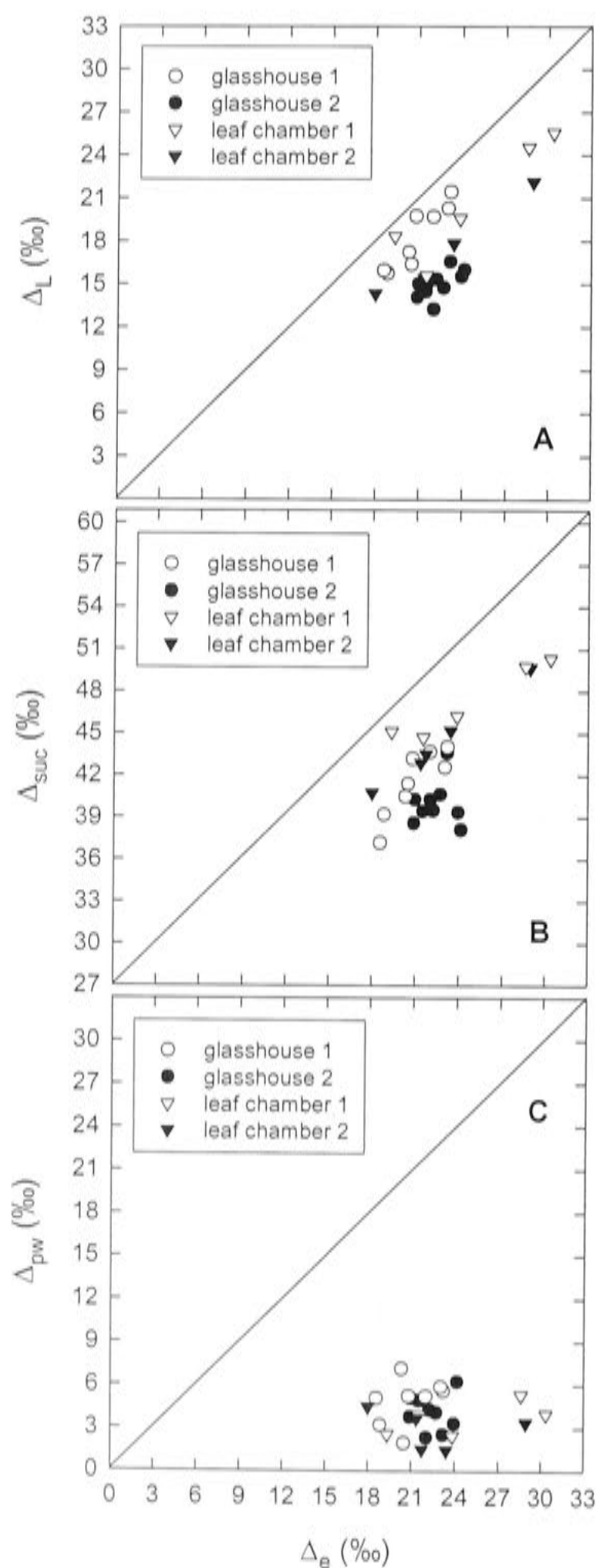


Figure 4.1. (A) Oxygen isotope enrichment of average lamina leaf water (Δ_L) plotted against predicted evaporative site enrichment (Δ_e) for leaves of *Ricinus communis*; different symbols refer to different experiments that employed different methods for sampling Δ_L . (B) Oxygen isotope enrichment of phloem sap dry matter (Δ_{suc}) for phloem sap collected from petioles of photosynthesizing leaves of *R. communis* plotted against Δ_e . The line drawn is that expected if exported photosynthate was in oxygen isotope equilibrium with evaporative site water. (C) Oxygen isotope enrichment of phloem water (Δ_{pw}) collected from petioles of photosynthesizing leaves of *R. communis* plotted against Δ_e .

Table 4.1. Mean values among experiments for the proportional deviation of observed lamina leaf water ^{18}O enrichment from predicted evaporative site enrichment ($1-\Delta_L/\Delta_e$), and for the proportional deviation of lamina leaf water enrichment inferred from phloem sap sucrose from predicted evaporative site enrichment ($1-\Delta_{\text{suc-L}}/\Delta_e$). Values are expressed as mean \pm 1SD for each experiment, followed in parentheses by the number of plants sampled. Values within a row followed by different letters are significantly different at $P < 0.05$.

	Glasshouse experiment 1	Glasshouse experiment 2	Leaf chamber experiment 1	Leaf chamber experiment 2
$1-\Delta_L/\Delta_e$	0.13 ± 0.05 (8) a	0.33 ± 0.04 (9) b	0.16 ± 0.08 (5) a	0.25 ± 0.04 (5) b
$1-\Delta_{\text{suc-L}}/\Delta_e$	0.33 ± 0.07 (8) a	0.43 ± 0.07 (9) c	0.20 ± 0.06 (5) b	0.26 ± 0.02 (5) ab

4.1A). Mean values from each of the experiments for the proportional deviation of the observed Δ_L from the predicted Δ_e ($1-\Delta_L/\Delta_e$) are given in Table 4.1, along with the results of an analysis of variance. Table 4.1 indicates that $1-\Delta_L/\Delta_e$ for Glasshouse 1 and Leaf Chamber 1 differs significantly from that for Glasshouse 2 and Leaf Chamber 2. This result confirmed my previous assessment that separation of primary veins from leaf lamina in the open air caused a bias in the analyses of Δ_L in Glasshouse 1 and Leaf Chamber 1.

The observed ^{18}O enrichment in phloem sap dry matter (Δ_{suc}) for all experiments is shown plotted against the Δ_e in Figure 4.1B. The solid line in Figure 4.1B represents the relationship that would be expected if sucrose exported from *R. communis* leaves was in full isotopic equilibrium with evaporative site water. The Figure shows that Δ_{suc} for measurements made in the glasshouse (open and closed circles in Figure 4.1B) was generally lower in relation to Δ_e than that for measurements made in the leaf chamber (open and closed triangles in Figure 4.1B). This observation is also apparent in the analysis of variance results for $1-\Delta_{\text{suc-L}}/\Delta_e$ (Table 4.1). Table 4.1 shows that $1-\Delta_{\text{suc-L}}/\Delta_e$ for Glasshouse 2 was higher than for either Leaf Chamber 1 or Leaf Chamber 2, and that $1-\Delta_{\text{suc-L}}/\Delta_e$ for Glasshouse 1 was higher than for Leaf Chamber 1. I attribute these differences to non-steady state conditions in the glasshouse that caused the Δ_e and Δ_L measured at the time when I intercepted organic molecules in the petiole phloem sap to differ from the Δ_e and Δ_L that existed previously at the time when those organic

molecules were synthesized in the leaf lamina. Specifically, there was a tendency for the relative humidity in the glasshouse to decrease from morning to afternoon, and this pattern was particularly apparent during sampling for Glasshouse 2; on the three sampling days for Glasshouse 2 the relative humidity decreased by up to 10% from mid-morning to mid-afternoon. This caused a sampling bias resulting in an overestimate of $1-\Delta_{\text{suc-L}}/\Delta_e$ that was particularly pronounced in Glasshouse 2.

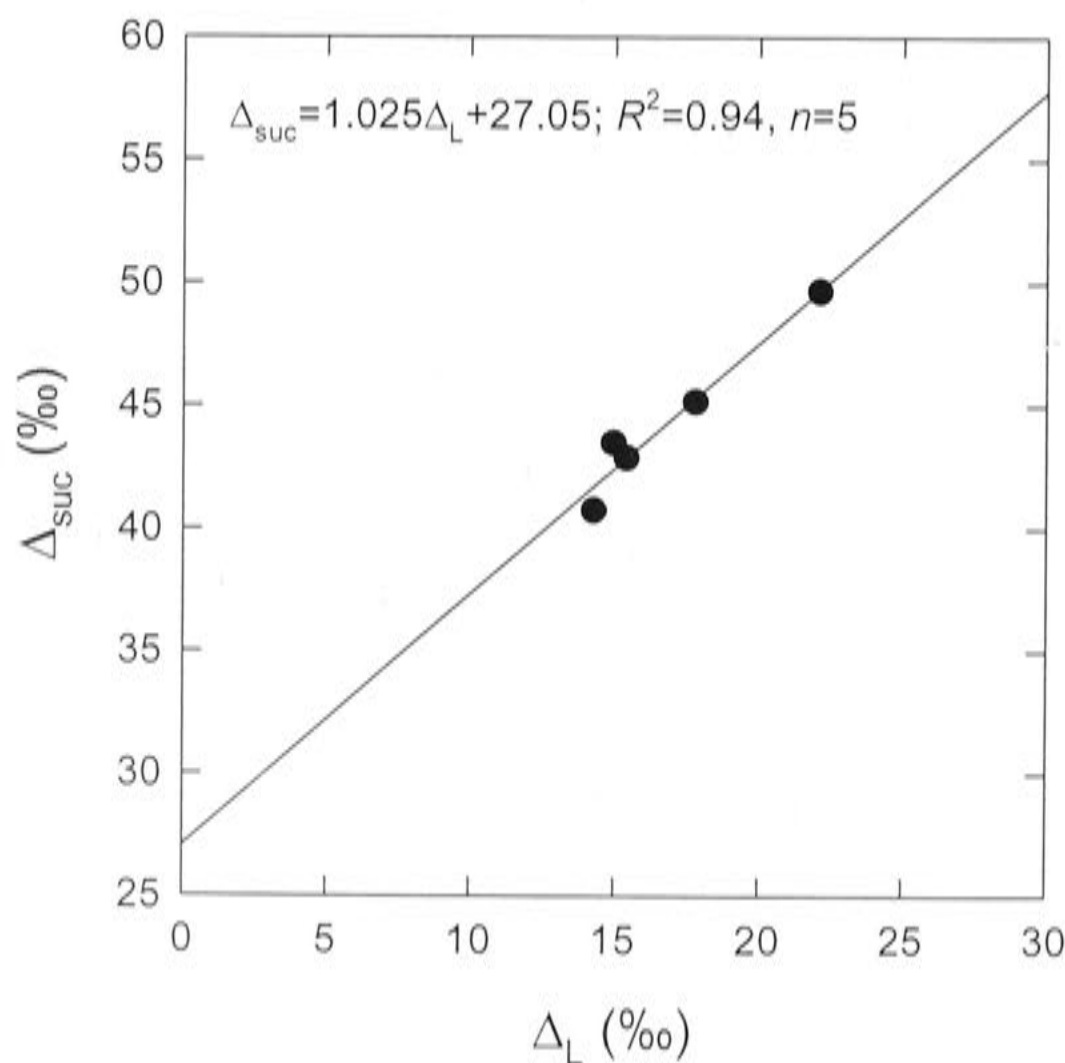


Figure 4.2. Oxygen isotope enrichment measured in phloem sap dry matter (Δ_{suc}) exported from photosynthesizing *Ricinus communis* leaves plotted against the observed lamina leaf water enrichment (Δ_L); both were sampled after the leaf was placed in a gas exchange cuvette under steady state conditions for approximately 4 hours. Assuming an equilibrium isotope effect between organic molecules and water of 1.027, the expected relationship between Δ_{suc} and Δ_L is $\Delta_{\text{suc}} = 1.027\Delta_L + 27\text{‰}$. The equation on the graph shows the observed relationship, which matches this prediction almost exactly.

Based on the above results, I concluded that there was only one experiment that produced reliable data describing the relationship between Δ_L and Δ_{suc} , and this was Leaf Chamber 2. The results for Δ_{suc} in relation to Δ_L for Leaf Chamber 2 are shown in Figure 4.2. The regression line drawn through the data ($\Delta_{\text{suc}}=1.025\Delta_L+27.05\text{‰}$; $R^2=0.94$, $n=5$) shows that the observed relationship matches almost exactly that expected if exported organic molecules are in full isotopic equilibrium with average lamina leaf water with $\alpha_0=1.027$. The Δ_L values observed in Leaf Chamber 2 ranged from 14.3 to 22.1‰, with a mean value of 16.9‰. Corresponding values for Δ_e ranged from 18.0 to 28.9‰, with a mean of 22.7‰. Differences between Δ_e and Δ_L ranged from 3.7 to 6.8‰, with a mean of 5.8‰. The relationship between Δ_L and Δ_e was $\Delta_L=0.77\Delta_e-0.46\text{‰}$ ($R^2=0.90$, $P=0.009$, $n=5$). The intercept of -0.46‰ was not significantly different from zero ($P=0.88$), confirming the expectation that there should be no enrichment in the leaf lamina water when Δ_e is zero.

The oxygen isotope composition of phloem sap dry matter collected in the glasshouse from leaf petioles did not differ from that collected concurrently from stem bases ($P=0.85$, $n=17$). This observation confirms that there is no exchange of oxygen atoms in sucrose with those of phloem water during translocation. This is the expected result because the sucrose molecule contains no carbonyl bonds.

Transpiration rates for Glasshouse 1 ranged from 3.6 to 5.8 $\text{mmol m}^{-2} \text{s}^{-1}$, with a mean of 4.7. Those for Glasshouse 2 were slightly higher, ranging from 4.0 to 6.5 $\text{mmol m}^{-2} \text{s}^{-1}$, with a mean of 5.6. For Leaf Chamber 1, transpiration rates ranged from 3.4 to 13.9 $\text{mmol m}^{-2} \text{s}^{-1}$, with a mean of 8.9. Finally, for Leaf Chamber 2, the range was from 4.3 to 8.0 $\text{mmol m}^{-2} \text{s}^{-1}$, with a mean of 6.3. Transpiration rate was not significantly correlated with $1-\Delta_L/\Delta_e$ or with $1-\Delta_{\text{suc-L}}/\Delta_e$ within individual experiments, or among all experiments. However, although the results were not statistically significant, the two leaf chamber experiments in which measurements were made over a range of vapor pressure deficits did show positive relationships between $1-\Delta_L/\Delta_e$ and $1-\Delta_{\text{suc-L}}/\Delta_e$ and transpiration rate. For Leaf Chamber 1, the correlation coefficient between $1-\Delta_L/\Delta_e$ and transpiration rate was 0.53 ($P=0.35$, $n=5$), and that between $1-\Delta_{\text{suc-L}}/\Delta_e$ and transpiration rate was 0.74 ($P=0.15$, $n=5$). For Leaf Chamber 2, the correlation coefficient between $1-\Delta_L/\Delta_e$ and transpiration rate was 0.49 ($P=0.40$, $n=5$), and that between $1-\Delta_{\text{suc-L}}/\Delta_e$ and transpiration rate was 0.80 ($P=0.10$, $n=5$).

4.4.2. Enrichment of ^{18}O in phloem water

The mean phloem water enrichment (Δ_{pw}) across all experiments for phloem sap collected from leaf petioles was $4.0 \pm 1.5\text{‰}$ (mean \pm 1SD, $n=27$), with values ranging from 1.5 to 7.2‰ (Figure 4.1C). There was no significant variation among experiments in petiole Δ_{pw} ($P=0.10$, $n=27$). The mean value for petiole Δ_{pw} expressed as a proportion of Δ_{e} was 0.18 ± 0.07 . Expressed as a proportion of Δ_{L} , mean petiole Δ_{pw} was 0.24 ± 0.09 . When I converted the petiole sap Δ_{suc} values to average lamina leaf water enrichment values ($\Delta_{\text{suc-L}}$) using equation (4.5) and $\alpha_0=1.027$, Δ_{pw} expressed as a proportion of $\Delta_{\text{suc-L}}$ was 0.28 ± 0.13 . I did not observe significant correlations between petiole Δ_{pw} and Δ_{e} , Δ_{L} , or $\Delta_{\text{suc-L}}$.

The mean Δ_{pw} for phloem sap collected from the bases of stems was $3.4 \pm 1.2\text{‰}$ (mean \pm 1SD, $n=17$). This Δ_{pw} value was significantly less than the corresponding Δ_{pw} value for petiole sap collected concurrently ($P=0.002$, $n=17$); the mean difference between Δ_{pw} for petioles and Δ_{pw} for stem bases from the same plants was 1.1‰. Stem base Δ_{pw} expressed as a proportion of petiole Δ_{pw} was 0.79 ± 0.27 , and the two were significantly and positively correlated ($r=0.59$, $P=0.01$, $n=17$). With the two expressed as proportions of their respective values for $\Delta_{\text{suc-L}}$, the difference was still significant ($P=0.008$, $n=17$), suggesting that the difference in Δ_{pw} between petioles and stem bases was not the result of non-steady state effects in the glasshouse.

4.5. Discussion

I tested the assumption that organic molecules exported in the phloem from photosynthesizing *R. communis* leaves are in full oxygen isotope equilibrium with average lamina leaf water. After my sampling technique had been appropriately improved, I found that this assumption held surprisingly well. I also observed that water exported in the phloem sap from photosynthesizing leaves was enriched compared to source water; however, the degree of enrichment was much less than that observed for the average lamina leaf water. Enrichment in the phloem water persisted during translocation within the plant, as evidenced by phloem water collected from stem bases also showing an enrichment relative to source water. Phloem water enrichment at the stem base was approximately 0.8 times that in the leaf petioles, possibly indicating some mixing of phloem water with xylem water during translocation.

I observed that Δ_L was less than Δ_e for all of the leaves that I sampled, including those observations where observed Δ_L was likely overestimated due to evaporation during lamina/vein separation (Figure 4.1A). Having bulk leaf water less enriched than predicted evaporative site water is a common feature among most leaf water investigations (Flanagan 1993). This trend has been attributed by different authors to the presence of unfractionated vein water in the bulk leaf water (Leaney *et al.* 1985), isotopic gradients within the leaf caused by the interplay between advection and diffusion of isotopically heavy molecules (Farquhar and Lloyd 1993), and compartmentation and incomplete mixing of the bulk leaf water (Yakir *et al.* 1989). Because chloroplasts are located close to evaporating surfaces, it has been suggested that chloroplast water should show an enrichment closer to Δ_e than to Δ_L , or somewhere between Δ_e and Δ_L (Farquhar *et al.* 1993); however, another study suggested that the enrichment of chloroplast water may in fact be very close to Δ_L , or that it might even lie somewhere between Δ_L and source water (Yakir *et al.* 1994). Thus, there remains considerable interest in resolving the precise isotopic signature of chloroplast water, and additionally in relating that to the isotopic signature of organic molecules exported from photosynthesizing leaves (Farquhar *et al.* 1998; Yakir 1998).

The initial products of the calvin cycle are expected to reflect nearly complete oxygen isotope exchange with chloroplast water (Farquhar *et al.* 1998; Barbour *et al.* in press-a). Upon export from the chloroplast, oxygen atoms in intermediate molecules in the sucrose synthesis pathway may undergo further exchange with cytosolic water. Farquhar *et al.* (1998) estimated that approximately 1/3 of the oxygen atoms that eventually become non-exchangeable in sucrose would have had opportunity to exchange with cytosolic water while in carbonyl groups of hexose phosphates. Thus, to a first approximation, oxygen atoms in sucrose should reflect ~2/3 chloroplast water and ~1/3 cytosolic water. It follows that one might expect the isotopic composition of sucrose exported from photosynthesizing leaves to have a signature closer to Δ_L than to Δ_e . Barbour *et al.* (2000) provided preliminary evidence for such a pattern by observing that sucrose exported from *R. communis* leaves carried an isotopic signature less enriched than would be the case for equilibrium with Δ_e ; moreover, the difference between Δ_{suc} and Δ_e increased with increasing e_a/e_i , as would be expected if Δ_{suc} reflected Δ_L . However, Barbour *et al.* (2000) did not sample the leaf water itself, only the sucrose exported from the leaf. Thus, the data presented in Figure 4.2 provide the

first direct evidence that the enrichment of exported organic molecules is indeed very near, if not exactly, that expected for equilibrium with Δ_L .

In addition to sucrose, phloem sap of *R. communis* also contains amino acids and organic acids, as well as inorganic anions and cations (Hall and Baker 1972). Hall and Baker (1972) reported that sucrose comprised 80 to 90% of the phloem sap dry matter, with a concentration of approximately 270 mM. The total amino acid concentration was approximately 35 mM, and the organic acid concentration, made up mainly of malic acid, was approximately 19 mM. These compounds should comprise almost all of the oxygen in the phloem sap dry matter of *R. communis*. My measurements indicate that the sum total of all of these compounds is in oxygen isotope equilibrium with average lamina leaf water. Preliminary measurements indicate little or no difference in oxygen isotope composition between sucrose purified from *R. communis* phloem sap and the bulk sap dry matter (L. Cernusak, unpublished data). Nonetheless, it may prove interesting to examine the organic components of the sap individually to determine whether there are subtle differences in the oxygen isotope signature carried by each of them.

Calculation of the lamina radial Péclet number in equation (4.2) requires estimation of L , the scaled effective path length over which mixing of evaporatively enriched water with unenriched source water occurs within the leaf lamina. This term is difficult to quantify from leaf anatomy alone. In practice, L values are estimated from the discrepancy between Δ_L and Δ_e while the leaf is at isotopic steady state. Assuming Δ_{suc} reflected Δ_L , Barbour *et al.* (2000) estimated that L for *R. communis* was 13.5 mm. Using data for Δ_L and Δ_e from Leaf Chamber 2, I estimate that L for the *R. communis* plants that I measured was 15.0 ± 3.5 mm (mean \pm 1SD, $n=5$), in reasonably good agreement with the estimate of Barbour *et al.* (2000) based on measurements of Δ_{suc} and Δ_e . However, to make my estimate strictly comparable to that of Barbour *et al.* (2000), I repeated the calculation using the previously accepted values of 28 and 19‰ for kinetic fractionation during water vapor diffusion through the stomata and boundary layer; recalculation of Δ_e with these values for ε_k yielded an estimate for L of 11.1 ± 2.6 mm.

Equation (4.2) predicts that the proportional discrepancy between Δ_L and Δ_e should increase with increasing transpiration rate. I did not observe statistically significant variation between $1-\Delta_L/\Delta_e$ and transpiration rate, or between $1-\Delta_{\text{suc-L}}/\Delta_e$ and transpiration rate, although the data did trend toward positive correlations with

transpiration rate for both parameters. However, my experiments were not aimed specifically at investigating these relationships. Because my aim was to assess relationships between Δ_L and Δ_{pw} and Δ_{suc} , it was necessary to harvest leaves immediately after collection of the phloem sap. A more appropriate experiment for assessing the relationship between $1-\Delta_{suc-L}/\Delta_e$ and transpiration rate is to expose the same leaf to different vapor pressures deficits while collecting phloem sap, as done by Barbour *et al.* (2000). This allows any variation caused by anatomical differences among leaves to be removed from the data set, thereby enabling a more powerful analysis of the relationship between $1-\Delta_{suc-L}/\Delta_e$ and transpiration rate. For the experiment conducted in this way, Barbour *et al.* (2000) observed that indeed $1-\Delta_{suc-L}/\Delta_e$ did increase significantly with increasing transpiration rate in *R. communis*.

I found that separating the leaf lamina from the primary veins in *R. communis* in the open air in Glasshouse 1 and Leaf Chamber 1 led to significant overestimation of Δ_L . Because there is significant spatial variation in Δ_L across the leaf lamina of dicotyledonous leaves (Wang and Yakir 1995; Gan *et al.* 2002), and because I was interested in sampling the average Δ_L for the entire leaf, separation of the entire leaf lamina from the primary vein network was necessary. This would probably not be the case in many comparative leaf water studies. Gan *et al.* (2002) concluded that the vein network is an integral part of the leaf water system and that comparative studies would be best conducted on total leaf water without separation of the primary veins. Such a sampling strategy would also avoid possible biases caused by evaporation during vein removal, and therefore may be worth considering. In my study, however, I was interested in sampling the lamina water specifically, so that it was necessary to somehow remove or factor out the influence of the primary veins.

In Glasshouse 2, I sampled total leaf water then subsequently factored out the influence of the primary veins based on independent measurements of the proportion of vein water contained in primary veins and its oxygen isotope enrichment relative to source water. Total leaf water ($\Delta_{L-total}$) showed an average enrichment of $11.9 \pm 0.8\text{‰}$ (mean \pm 1SD, $n=9$), and a proportional difference from Δ_e ($1-\Delta_{L-total}/\Delta_e$) of 0.47 ± 0.03 . This can be compared to a value of $1-\Delta_{L-total}/\Delta_e$ for *Gossypium hirsutum* sampled under essentially similar conditions of approximately 0.30 (Gan *et al.* 2002). The enrichment value that I observed in the primary vein water of $0.04\Delta_e$ was similar to that observed for *G. hirsutum*; however, the proportion of total leaf water associated with primary veins was higher in *R. communis*, estimated at 22%, as opposed to 15% for *G. hirsutum*.

(Gan *et al.* 2002). Also, my calculations of Δ_e used the newly revised, higher fractionation factors for calculation of ε_k . Using the previous, lower values for calculating Δ_e resulted in an estimate for $1-\Delta_{L\text{-total}}/\Delta_e$ for *R. communis* of 0.42 ± 0.03 .

I noted in the introduction that equation (4.1) is a convenient approximation of the mathematically correct form of the modified Craig-Gordon equation (Craig and Gordon 1965; Farquhar and Lloyd 1993), which is given in the Appendix as equation (A4.3). As discussed by Farquhar *et al.* (1998), the modified Craig-Gordon equation is itself an approximation of the evaporative site ^{18}O enrichment in a leaf because it does not consider the additions of oxygen to the leaf water by CO_2 uptake and respiration, or losses by the Hill reaction and sucrose export. It was shown that under normal conditions these corrections are very small (Farquhar *et al.* 1998); however, the effect of export of enriched phloem water from the leaf was not considered. An equation is derived in the Appendix of this chapter to examine the effect of phloem water export on the Δ_e calculations that I performed. I estimated the phloem water flux out of the leaf from the concentration of water in the phloem sap relative to dry matter, and by assuming that the carbon export in phloem sap dry matter was equal to carbon uptake by photosynthesis. For Leaf Chamber 2, I found that the difference in calculating Δ_e without taking account of phloem water export, as opposed to with taking account of phloem water export, was $0.05 \pm 0.03\text{‰}$ (mean $\pm 1\text{SD}$, $n=5$). This bias is very small, and partially compensates for the bias arising from the use of equation (4.1) in place of equation (A4.3). If the phloem water enrichment is hypothetically increased to 6‰ for the plants measured in Leaf Chamber 2 (a value well within the range of Δ_{pw} that I observed for *R. communis*), with all other conditions remaining the same as measured in Leaf Chamber 2, the export of enriched phloem water exactly compensates for the bias introduced by the use of equation (4.1). In this context, the bias arising from the use of equation (4.1), in place of its mathematically correct antecedent, does seem truly negligible.

There are few reports on the oxygen isotope composition of phloem water. Adar *et al.* (1995) reported $\delta^{18}\text{O}$ values for phloem water, xylem water, and leaf water of a tamarisk tree growing in the Negev Desert, Israel. Calculation of Δ_{pw} and Δ_L from their data gives values of 13.4 and 27.8‰, respectively; this yields a value for Δ_{pw}/Δ_L of 0.48. Calculation of Δ_{pw}/Δ_L for phloem water collected from pod tips of *Lupinus angustifolius* at midday yields a value of 0.66 (Chapter 2). These values can be compared to the mean value that I observed in *R. communis* for $\Delta_{pw}/\Delta_{\text{suc-L}}$ of 0.28. Expressing Δ_{pw} as a

proportion of $\Delta_{\text{suc-L}}$, as opposed to observed Δ_{L} , accounts for possible non-steady state effects in Glasshouse 1 and Glasshouse 2, and bias in Δ_{L} measurements in Glasshouse 1 and Leaf Chamber 1, assuming that water and dry matter are transported together by bulk flow in the phloem (Münch 1930). Thus, there appears to be a rather large range of values for $\Delta_{\text{pw}}/\Delta_{\text{L}}$ among the three species for which data are so far available. These differences may be caused by variation in phloem loading mechanisms, vein structure in leaves, or sieve tube permeability. In the case of *Lupinus angustifolius*, physiological processes in the fruits may also have influenced the observed Δ_{pw} .

The significance of Δ_{pw} for interpreting oxygen isotope variations in plant organic material and plant cellulose lies in its potential influence on the oxygen isotope composition of water in developing sink tissues; it is this water pool with which a proportion of oxygen originating in sucrose will exchange during new tissue synthesis. Evidence of this concept was demonstrated for developing seeds in *Lupinus angustifolius* (Chapter 2); seed water was enriched by $9.2 \pm 1.2\text{‰}$ (mean $\pm 1\text{SD}$, $n=15$) compared to xylem water. Estimates of the proportion of water in developing cells originating from phloem range from 50 to 80% (Schmalstig and Cosgrove 1990; Bret-Harte and Silk 1994; Pritchard *et al.* 2000). Thus, when water and organic molecules are unloaded together from phloem into sink tissues, the isotopic composition of water in the developing cells may differ substantially from source water. The term p_{x} in equation (4.3) allows this effect to be incorporated when modeling ^{18}O enrichment of organic material and cellulose, as described by Barbour and Farquhar (2000). An analogous term does not exist in other models of ^{18}O enrichment. For example, the tree ring model proposed by Roden *et al.* (2000) contains no term that could account an influence of Δ_{pw} . This may be an important omission given the observation of Adar *et al.* (1995) that phloem water in stems and roots of tamarisk trees can be enriched by as much as 14‰ compared to xylem water.

Gan *et al.* (2002) measured ^{18}O enrichment in the veins of *G. hirsutum* and found that xylem water near the ends of second order veins could be enriched by as much as $0.19\Delta_{\text{e}}$. The mean value of Δ_{pw} that I observed across all experiments was $0.18\Delta_{\text{e}}$ (or $0.20\Delta_{\text{e}}$, if calculating Δ_{e} with the previously accepted values for ϵ_{k}). The coincidence of these two numbers suggests that the xylem of second and possibly third order veins could be the source of water for phloem translocation out of dicotyledonous leaves. I acknowledge, however, that the situation may well be more complicated, particularly considering the structural and physiological complexities of phloem loading

(Wang and Canny 1985; van Bel 1993). Additionally, the measurements of Gan *et al.* (2002), and theory developed by Farquhar and Gan (2003), suggest that vein water enrichment, when expressed as a proportion of Δ_e , will change with variation in transpiration rate and variation in Δ_e . Thus, there may not be a unique relationship between vein water enrichment in higher order veins of the leaf lamina and Δ_e or Δ_L . This may explain why I failed to observe significant correlations between Δ_{pw} and Δ_e , Δ_L , or Δ_{suc-L} .

In conclusion, organic molecules (mainly sucrose) exported from photosynthesizing *R. communis* leaves had an isotopic signature that reflected almost exactly that of the average lamina leaf water, assuming an equilibrium isotope effect for oxygen exchange between organic molecules and water of 1.027. Phloem sap water collected from leaf petioles was enriched compared to source water, as was phloem sap water collected from stem bases. The average petiole phloem water enrichment was 4‰, or approximately 0.28 times that inferred for the average lamina leaf water at the time of phloem loading. Phloem water collected from stem bases showed an enrichment that was approximately 0.8 times that observed for leaf petioles, possibly indicating some mixing between phloem water and xylem water during translocation between leaf petioles and stem bases. These results have implications for the prediction and interpretation of oxygen isotope enrichment in plant dry matter and plant cellulose.

4.6. Appendix: including phloem water export in the calculation of Δ_e

I start with an intermediate equation in the derivation of the modified Craig-Gordon equation [for a recent example of the derivation to this point, see Farquhar and Gan (2003)]:

$$R_e = \alpha^+ \left[\alpha_k \left(1 - \frac{e_a}{e_i} \right) R_E + R_v \frac{e_a}{e_i} \right], \quad (\text{A4.1})$$

where R_e is $^{18}\text{O}/^{16}\text{O}$ of evaporative site water, α^+ is the equilibrium isotope effect associated with evaporation, α_k is the kinetic isotope effect associated with diffusion, R_E is $^{18}\text{O}/^{16}\text{O}$ of transpired water, R_v is $^{18}\text{O}/^{16}\text{O}$ of vapor and e_a/e_i is the ratio of ambient to intercellular vapor pressures. Following the derivation of Craig and Gordon (1965), in the steady state R_E can be replaced by R_s , the $^{18}\text{O}/^{16}\text{O}$ of source water:

$$R_e = \alpha^+ \left[\alpha_k \left(1 - \frac{e_a}{e_i} \right) R_s + R_v \frac{e_a}{e_i} \right]. \quad (\text{A4.2})$$

Dividing both sides of the equation by R_s gives (Farquhar and Lloyd 1993)

$$\Delta_e = (1 + \varepsilon^+) \left[1 + \varepsilon_k + (\Delta_v - \varepsilon_k) \frac{e_a}{e_i} \right] - 1, \quad (\text{A4.3})$$

which is the mathematically correct form of the modified Craig-Gordon equation that is conveniently approximated by equation (4.1) of the main text. To include the effect of the export of enriched phloem water in the calculation of Δ_e , I define the flux of water from the soil into the plant (J_s) as

$$J_s = E + P, \quad (\text{A4.4})$$

where E is the transpiration rate and P is the flux of water from the leaf into the phloem (strictly that which goes into growth, and does not recycle back into xylem). The analogous flux for H_2^{18}O is given by

$$R_s J_s = R_E E + R_P P, \quad (\text{A4.5})$$

where R_P is $^{18}\text{O}/^{16}\text{O}$ of phloem water. I define the isotope effect for phloem water enrichment (α_p) with respect to R_s :

$$\alpha_p = \frac{R_P}{R_s} = 1 + \Delta_{pw}, \quad (\text{A4.6})$$

such that $\alpha_p > 1$. Substituting from equations (A4.4) and (A4.6), equation (A4.5) can be rewritten as

$$R_E = R_s (1 + p) - \alpha_p R_s P, \quad (\text{A4.7})$$

where $p = P/E$. Equation (A4.7) indicates that the isotope ratio of transpired water will be slightly less than that of source water, due to export of enriched water in the phloem. Substituting equation (A4.7) into equation (A4.1) gives

$$R_e = \alpha^+ \left\{ \alpha_k \left(1 - \frac{e_a}{e_i} \right) \left[R_s (1 + p) - \alpha_p R_s P \right] + R_v \frac{e_a}{e_i} \right\}. \quad (\text{A4.8})$$

Expanding equation (A4.8), rearranging, and substituting from equation (A4.2) gives

$$R_e = R_c - \alpha^+ \alpha_k \left(1 - \frac{e_a}{e_i} \right) \Delta_{pw} R_s P, \quad (\text{A4.9})$$

where R_c is the modified Craig-Gordon expression given in equation (A4.2). Dividing equation (A4.9) by R_s gives

$$\Delta_e = \Delta_c - \alpha^+ \alpha_k \left(1 - \frac{e_a}{e_i} \right) p \Delta_{pw}, \quad (\text{A4.10})$$

where Δ_c is the modified Craig-Gordon expression as written in equation (A4.3). Equation (A4.10) can then be used to calculate evaporative site water enrichment,

taking into account the effect of phloem water export. To a close approximation, equation (A4.10) can be replaced by

$$\Delta_e = \Delta_c - \left(1 - \frac{e_a}{e_i}\right) p \Delta_{pw} , \quad (\text{A4.11})$$

which is a more convenient form for first approximations aimed at assessing the order of magnitude of the effect of phloem water export on Δ_e . Equation (A4.11) underestimates the difference between Δ_c and Δ_e by about 4% compared to equation (A4.10). The phloem water flux, P , can be estimated from the photosynthetic rate of the leaf and the sucrose concentration of the phloem sap, if one assumes that carbon export in the phloem is equal to carbon uptake by photosynthesis, such that $P=A/S$, where S is the sucrose concentration of the phloem sap ($\mu\text{mol C mmol}^{-1} \text{H}_2\text{O}$) and A is the photosynthetic rate of the leaf ($\mu\text{mol C m}^{-2} \text{s}^{-1}$). The dimensionless term p is then obtained by dividing P by E ($\text{mmol H}_2\text{O m}^{-2} \text{s}^{-1}$). I noted in the main text that my observations for *R. communis* indicated that the difference between Δ_c and Δ_e , as defined by equation (A4.10), was roughly 0.05‰. A more extreme case can be illustrated using the observations of Adar *et al.* (1995) in which Δ_{pw} for a Tamarisk tree was 13‰. Assuming Δ_c was 30‰ (based on the observation that Δ_L was 28‰), e_a/e_i was 0.25, and p was 0.05, equation (A4.11) indicates that the difference between Δ_c and Δ_e would have been 0.5‰, some ten-fold higher than the difference I estimated for *R. communis*.

Chapter 5: Oxygen and carbon isotope composition of parasitic plants and their hosts in southwestern Australia

5.1. Abstract

I measured leaf dry matter $\delta^{18}\text{O}$ and $\delta^{13}\text{C}$ in parasitic plants and their hosts growing in southwestern Australia. Parasite/host pairs included two mistletoe species, three species of holoparasites, and five species of root hemiparasites. Among these parasite functional types, significant variation was observed in parasite/host isotopic differences for both $\delta^{18}\text{O}$ ($P < 0.0001$, $n = 65$) and $\delta^{13}\text{C}$ ($P < 0.0001$, $n = 64$). Mistletoes were depleted in both ^{18}O and ^{13}C compared to their hosts; parasite/host differences were -4.0‰ for $\delta^{18}\text{O}$ ($P < 0.0001$) and -1.9‰ for $\delta^{13}\text{C}$ ($P < 0.0001$). The lower $\delta^{18}\text{O}$ in mistletoe leaf dry matter compared to their hosts is consistent with the frequently observed high transpiration rates of these parasites. Root hemiparasites were also depleted in ^{18}O and ^{13}C compared to their hosts, but not to the same extent as mistletoes; parasite/host differences were -1.0‰ for $\delta^{18}\text{O}$ ($P = 0.04$) and -1.2‰ for $\delta^{13}\text{C}$ ($P = 0.0006$). In contrast to mistletoes and root hemiparasites, holoparasites were enriched in both ^{18}O and ^{13}C compared to their hosts; parasite/host differences were $+3.0\text{‰}$ for $\delta^{18}\text{O}$ ($P < 0.0001$) and $+1.5\text{‰}$ for $\delta^{13}\text{C}$ ($P = 0.02$). The enrichment in ^{18}O for holoparasite dry matter did not result from more enriched tissue water; holoparasite tissue water $\delta^{18}\text{O}$ was less than host leaf water $\delta^{18}\text{O}$ by a difference of -3.8‰ when sampled at midday ($P = 0.0003$). Enrichment of holoparasites in ^{13}C compared to their hosts is consistent with a generally observed pattern of enrichment in heterotrophic plant tissues. Results provide insights into the ecology of parasitic plants in southwestern Australia; additionally, they provide a context for the formulation of specific hypotheses aimed at elucidating mechanisms underlying isotopic variations among plants.

5.2. Introduction

The evolution of a parasitic habit has been widespread in flowering plants, with examples found in 18 families and encompassing over 3000 species (Kuijt 1969). The common feature uniting almost all parasitic angiosperms is the presence of a haustorium, an organ that attaches the parasite to its host and allows for extraction of

water and solutes from the host's vascular system. Parasitic plants are often classified as hemiparasitic or holoparasitic, depending on the extent of their inability to produce their own reduced carbon for growth and respiration. Hemiparasites can be further divided into facultative or obligate parasites, depending on whether or not they are capable of completing their lifecycle in the absence of a host. In some cases, a distinction between holoparasitism and hemiparasitism is not easily made (Stewart and Press 1990). Parasitic plants may be further categorized as stem or root parasites depending on their position of haustorial attachment to the host. In the present study, I analyzed two species of mistletoes, which are obligate stem hemiparasites; three species of holoparasites, one root-feeding and two stem-feeding; and five species of facultative root hemiparasites, two annual and three perennial. The range in parasitic habits represented a diversity of strategies in parasite resource acquisition from the hosts, or from hosts and the surrounding environment.

Analyses of stable isotope ratios have already played an important role in providing information about the carbon, water, and nutrient relations of parasitic plants and their hosts (Ehleringer et al. 1985; Press et al. 1987; Marshall and Ehleringer 1990; Schulze et al. 1991; Richter et al. 1995; Ducharme and Ehleringer 1996; Tennakoon and Pate 1996b; Bannister and Strong 2001; Pate 2001). Analyses to date have primarily focused on stable isotopes of carbon for estimating water use efficiency and heterotrophic carbon gain, and nitrogen for identifying sources of nitrogen used by parasites. In the present study, I extended the use of stable isotopes in analyzing parasite/host interactions by measuring oxygen isotope ratios ($\delta^{18}\text{O}$), in order to obtain time-integrated estimates of variation in transpiration rates (Barbour and Farquhar 2000; Barbour et al. 2000; Chapter 3). Such analyses are simplified when plants are exposed to the same evaporative conditions, source water $\delta^{18}\text{O}$ ($\delta^{18}\text{O}_s$), and atmospheric vapor $\delta^{18}\text{O}$ ($\delta^{18}\text{O}_v$), as is likely the case for parasitic plants growing along side their hosts. Leaf water $\delta^{18}\text{O}$ at the evaporative sites in leaves ($\delta^{18}\text{O}_e$) has been modeled as (Craig and Gordon 1965; Dongmann et al. 1974; Farquhar and Lloyd 1993)

$$\delta^{18}\text{O}_e = \delta^{18}\text{O}_s + \varepsilon^* + \varepsilon_k + \left(\delta^{18}\text{O}_v - \delta^{18}\text{O}_s - \varepsilon_k \right) \frac{e_a}{e_i}, \quad (5.1)$$

where ε^* is the equilibrium fractionation between liquid and vapor, ε_k is the kinetic fractionation during diffusion through the stomata and leaf boundary layer, and e_a/e_i is the ratio of ambient to intercellular vapor pressures. The ε_k can be calculated as $\varepsilon_k(\text{‰}) = (32r_s + 21r_b)/(r_s + r_b)$, where r_s and r_b are the stomatal and boundary layer

resistances to water vapor diffusion (Farquhar et al. 1989), and the coefficients 32‰ and 21‰ are fractionation factors for water vapor diffusion through stomata and boundary layer, respectively (Cappa et al. 2003). The $\delta^{18}\text{O}$ of leaf water at the evaporative sites in leaves has in turn been related to the average $\delta^{18}\text{O}$ of leaf mesophyll water ($\delta^{18}\text{O}_L$) by (Farquhar and Lloyd 1993)

$$\delta^{18}\text{O}_L = \delta^{18}\text{O}_s + \frac{(\delta^{18}\text{O}_e - \delta^{18}\text{O}_s)(1 - e^{-\phi})}{\phi}, \quad (5.2)$$

where ϕ is a Péclet number, defined as $EL/(CD)$, where E is transpiration rate ($\text{mol H}_2\text{O m}^{-2} \text{s}^{-1}$), L is a scaled effective path length (m), C is the molar concentration of water (mol m^{-3}), and D is the diffusivity of H_2^{18}O in water ($\text{m}^2 \text{s}^{-1}$).

Equations (5.1) and (5.2) predict that at a given air temperature and humidity, an increase in stomatal conductance (and therefore transpiration rate) will cause a decrease in $\delta^{18}\text{O}_L$ as a result of increasing e_a/e_t (caused by evaporative cooling of the leaf), decreasing ε_k , and increasing ϕ . The $\delta^{18}\text{O}_L$ can then be related to the $\delta^{18}\text{O}$ of plant cellulose ($\delta^{18}\text{O}_c$) as follows (Barbour and Farquhar 2000):

$$\delta^{18}\text{O}_c = \delta^{18}\text{O}_s + (\delta^{18}\text{O}_L - \delta^{18}\text{O}_s)(1 - p_{ex}p_x) + \varepsilon_{wc}, \quad (5.3)$$

where p_{ex} is the proportion of oxygen atoms exchanging with medium water during cellulose synthesis, p_x is the proportion of unenriched water in the developing cell (coming from xylem rather than leaf mesophyll), and ε_{wc} is the equilibrium fractionation between carbonyl oxygen and medium water, estimated as 27‰ (Sternberg and DeNiro 1983; Sternberg et al. 1986). I have presented equations (5.1) to (5.3) in terms of little delta values (δ). In the present study, I relied upon the assumption that the parasite and host had the same source water, so that comparison of δ values implies a direct comparison of enrichment above source water ($\Delta^{18}\text{O}$).

The model presented in equation (5.3) can be extended to total leaf dry matter $\delta^{18}\text{O}$ by adding the term ε_{cp} , which describes the difference between dry matter $\delta^{18}\text{O}$ ($\delta^{18}\text{O}_p$) and cellulose $\delta^{18}\text{O}$ (Barbour and Farquhar 2000):

$$\delta^{18}\text{O}_p = \delta^{18}\text{O}_s + (\delta^{18}\text{O}_L - \delta^{18}\text{O}_s)(1 - p_{ex}p_x) + \varepsilon_{wc} + \varepsilon_{cp}. \quad (5.4)$$

Although the mechanisms contributing to ε_{cp} are not well understood, $\delta^{18}\text{O}_p$ and $\delta^{18}\text{O}_c$ have been strongly correlated when measured on the same samples in both leaves and wood (Borella et al. 1999; Barbour and Farquhar 2000; Barbour et al. 2000; Barbour et al. 2001). Moreover, $\delta^{18}\text{O}_p$ was found to be more sensitive to variation in stomatal conductance than $\delta^{18}\text{O}_c$ by a factor of two (Barbour et al. 2000). Additionally, $\delta^{18}\text{O}_p$

was found to be an excellent integrator of spatial (Gan et al. 2002) and temporal (Chapter 2) variation in $\delta^{18}\text{O}_L$. Accordingly, recent studies have begun taking advantage of the simplicity of analyzing $\delta^{18}\text{O}_p$ without the additional step of cellulose extraction (Saurer et al. 2000; Scheidegger et al. 2000; Saurer et al. 2001; Saurer et al. 2002). This is the approach that I took in the present study of parasite/host interactions. However, I analyzed $\delta^{18}\text{O}_c$ in approximately half the samples that I collected in order to determine whether similar patterns in parasite/host differences existed for both $\delta^{18}\text{O}_p$ and $\delta^{18}\text{O}_c$.

The carbon isotope ratio of C_3 plants ($\delta^{13}\text{C}_p$) is correlated with the ratio of intercellular to ambient carbon dioxide concentrations (c_i/c_a) in photosynthesizing leaves (Farquhar et al. 1982):

$$\delta^{13}\text{C}_p = \delta^{13}\text{C}_a - a - (b-a)\frac{c_i}{c_a}, \quad (5.5)$$

where $\delta^{13}\text{C}_a$ is the carbon isotope ratio of atmospheric CO_2 ($\sim 8\text{‰}$), a is the fractionation caused by gaseous diffusion (4.4‰), and b is the effective fractionation caused by carboxylating enzymes ($\sim 27\text{‰}$). In turn, the ratio c_i/c_a can be related to the instantaneous water use efficiency of a plant (A/E) as

$$\frac{A}{E} = \frac{c_a \left(1 - \frac{c_i}{c_a}\right)}{1.6v}, \quad (5.6)$$

where A is the photosynthetic rate ($\mu\text{mol CO}_2 \text{ m}^{-2} \text{ s}^{-1}$), E is the transpiration rate ($\text{mmol H}_2\text{O m}^{-2} \text{ s}^{-1}$), and v is the vapor pressure difference between the leaf and air ($\text{mmol H}_2\text{O mol}^{-1}$). The ambient carbon dioxide concentration, c_a , is expressed as $\mu\text{mol mol}^{-1}$. Equations (5.5) and (5.6) indicate that for plants experiencing the same v , $\delta^{13}\text{C}_p$ of the leaves can be used to make integrated comparisons of water use efficiency. For parasitic plants growing along side their hosts, the assumption of a common v is reasonable; however, I note that small differences in leaf temperature caused by different transpiration rates will cause variation in v between plants.

I used $\delta^{18}\text{O}_p$ and $\delta^{13}\text{C}_p$ in leaves of parasitic plants and their hosts growing in southwestern Australia to make inferences about contrasting strategies of resource acquisition, both within and among different functional types of parasites. Additionally, results indicated some situations in which variation in $\delta^{18}\text{O}_p$ and $\delta^{13}\text{C}_p$ could not be accounted for using equations (5.1) to (5.6). These discrepancies were used to highlight

areas in which further research into the mechanisms causing isotopic variations would be helpful.

5.3. Materials and Methods

The locations of sampling sites, names of species sampled at each site and their authorities, and the functional type of the parasite are given in Table 5.1. Of the root hemiparasite species, three were perennial (*E. odoratus*, *E. sparteus*, and *O. phyllanthi*), and two were annual (*B. trixago*, and *P. viscosa*). William Bay National Park, Ocean Beach, and Lights Beach are coastal heath sites in close proximity to the township of Denmark, Western Australia. The Pate Property is located on Mount Shadforth near Denmark and is an open woodland dominated by a mixture of marri and karri, *Corymbia calophylla* (Lindl.) K.D.Hill & L.A.S.Johnson and *Eucalyptus diversicolor* F.Muell., respectively. The Tunney site is an open woodland dominated by *Eucalyptus wandoo* Blakely and *Eucalyptus marginata* Sm., and the Williams site is native shrubland bordering farmland. The root hemiparasites were chosen such that the individuals sampled were growing in close proximity to only a single putative host. Several of the parasitic plant species have been studied previously in these same habitats with regard to various aspects of their biology and strategies of resource acquisition and use (Pate et al. 1990a; Pate et al. 1990b; Pate et al. 1990c; Pate et al. 1991; Tennakoon and Pate 1996a; Pate and Bell 2000; Pate 2001). Sampling took place between 7 and 13 December 2001, and again between 19 and 25 February 2002.

In the December sampling, a representative sample of 10 to 20 leaves was collected from both parasite and host and oven dried at 80°C. In the case of the annual root hemiparasites and their hosts, the whole aboveground biomass was sampled. The whole biomass was sampled for the *Cuscuta* and *Cassytha* holoparasites, and the whole aboveground biomass for the *Orobanche* holoparasite. For the mistletoes, host leaves were collected from the same branch that the mistletoe was parasitizing. In the February sampling, leaves of parasites and their hosts were immediately placed into gas-tight glass vials and frozen at -20°C. Leaf water sampling took place between 1100 and 1600 hours local time. Samples remained frozen until tissue water was extracted by cryogenic vacuum distillation. The dry matter was retained for carbon and oxygen isotope analyses. Dry matter samples were ground to a fine powder and analyzed for carbon isotope ratio in an Isochrom mass spectrometer (Micromass, Manchester, UK) following combustion in a Carlo Erba elemental analyzer (CE Instruments, Milan,

Table 5.1. Locations of sampling sites and pairs of species sampled at each site.

Site	Location	Parasite species	Host species	Type of parasite
William Bay National Park	35°01'25" S, 117°14'12" E	<i>Cassytha</i> sp.	<i>Acacia littorea</i> Maslin	holoparasite
			<i>Leucopogon capitellatus</i> DC.	
			<i>Spyridium globulosum</i> (Labill.) Benth.	
		<i>Cuscuta campestris</i> Yunck.	<i>Cakile maritima</i> Scop.	holoparasite
Ocean Beach	35°02'12" S, 117°19'53" E		<i>Euphorbia paralias</i> L.	
			<i>Muehlenbeckia adpressa</i> (Labill.) Meisn.	
			<i>Pecarisonium</i> sp.	
			<i>Senecio elegans</i> L.	
			Unknown host	
		<i>Exocarpos odoratus</i> (Miq.) A.DC.	<i>Spyridium globulosum</i> (Labill.) Benth.	root hemiparasite
		<i>Olax phyllanthi</i> (Labill.) R.Br.	<i>Acacia littorea</i> Maslin	root hemiparasite
			<i>Spyridium globulosum</i> (Labill.) Benth.	
		<i>Cassytha</i> sp.	<i>Exocarpos odoratus</i> (Miq.) A.DC.	holoparasite
		<i>Exocarpos odoratus</i> (Miq.) A.DC.	<i>Bossiaea linophylla</i> R.Br.	root hemiparasite
Lights Beach	35°01'20" S, 117°16'31" E		<i>Hibbertia</i> sp.	
			<i>Spyridium globulosum</i> (Labill.) Benth.	
		<i>Exocarpos sparteus</i> R.Br.	<i>Pelargonium australe</i> Willd.	root hemiparasite
			<i>Spyridium globulosum</i> (Labill.) Benth.	
		<i>Olax phyllanthi</i> (Labill.) R.Br.	<i>Hibbertia</i> sp.	root hemiparasite
			<i>Leucopogon parviflorus</i> (Andrews) Lindl.	
Pate Property	34°57'55" S, 117°17'19" E		<i>Spyridium globulosum</i> (Labill.) Benth.	
		<i>Bartsia trixago</i> L.	<i>Conocephalum</i> sp.	root hemiparasite
			<i>Senecio lautus</i> Willd.	
		<i>Exocarpos sparteus</i> R.Br.	<i>Scaevola nitida</i> R.Br.	root hemiparasite
		<i>Olax phyllanthi</i> (Labill.) R.Br.	<i>Scaevola nitida</i> R.Br.	root hemiparasite
		<i>Orobancha minor</i> Sm.	<i>Ribes sanguineum</i>	holoparasite
Tunney Williams	32°33'19" S, 119°17'55" E 32°59'49" S, 116°51'01" E	<i>Parentucellia viscosa</i> (L.) Caruel	<i>Anthoxanthum odoratum</i> L.	root hemiparasite
			<i>Hypochaeris radicata</i> L.	
			<i>Ricinocarpus</i> sp.	
			<i>Senecio</i> sp.	
		<i>Amyema miquelii</i> (Miq.) Tiegh.	<i>Eucalyptus wandoo</i> Blakely	mistletoe
		<i>Amyema preissii</i> (Miq.) Tiegh.	<i>Acacia acuminata</i> Benth.	mistletoe

Italy). Oxygen isotope analyses of both tissue water and dry matter took place in an Isochrom mass spectrometer following pyrolysis in a Carlo Erba elemental analyzer (Farquhar et al. 1997). Isotope ratios have been expressed in delta (δ) notation using Pee Dee Belemnite as the standard for carbon and Vienna Standard Mean Ocean Water as the standard for oxygen. Analytical precision was $\pm 0.1\text{‰}$ for $\delta^{13}\text{C}$ and $\pm 0.3\text{‰}$ for $\delta^{18}\text{O}$. The nitrogen concentration of leaf dry matter was measured for the mistletoes and their hosts in a Carlo Erba elemental analyzer (CE Instruments, Milan, Italy).

I extracted cellulose for isotopic analysis from the leaf samples collected in the December sampling, except the annual root hemiparasites and their hosts. Cellulose extractions were performed as described by Barbour and Farquhar (2000), based on the modified technique of Loader et al. (1997). The term ϵ_{cp} , describing the difference in $\delta^{18}\text{O}$ between total dry matter and cellulose, was calculated as $\epsilon_{\text{cp}} = \delta^{18}\text{O}_{\text{p}} - \delta^{18}\text{O}_{\text{c}}$.

I used equations (5.1) through (5.4) to estimate proportional differences in transpiration rates between mistletoes and their hosts from measurements of $\delta^{18}\text{O}_{\text{p}}$ and $\delta^{18}\text{O}_{\text{c}}$. The average November to February midday temperature and humidity for a weather station near to the mistletoe collection sites (Narrogin, Western Australia) were used to parameterize the model; values were 44% and 22°C, respectively. The $\delta^{18}\text{O}_{\text{v}}$ was assumed to be in equilibrium with $\delta^{18}\text{O}_{\text{s}}$ at the midday air temperature. The difference between leaf temperature and air temperature and the transpiration rate were calculated as described by Barbour et al. (2000). The photosynthesis-weighted average stomatal conductance of the hosts was assumed to be $50 \text{ mmol m}^{-2} \text{ s}^{-1}$. Boundary layer conductance for mistletoes and hosts was assumed to be $2.5 \text{ mol m}^{-2} \text{ s}^{-1}$. The scaled effective path length in equation (5.2) was assumed to be 25 mm for both mistletoes and hosts (Flanagan et al. 1993). After a leaf water enrichment had been calculated for the hosts, stomatal conductance of the mistletoe was increased in the model until the modeled $\delta^{18}\text{O}_{\text{L}}$ difference between host and mistletoe was equal to that inferred from measurements of $\delta^{18}\text{O}_{\text{p}}$ or $\delta^{18}\text{O}_{\text{c}}$, calculated as $\delta^{18}\text{O}_{\text{L(h)}} - \delta^{18}\text{O}_{\text{L(m)}} = (\delta^{18}\text{O}_{\text{p(h)}} - \delta^{18}\text{O}_{\text{p(m)}}) / (1 - p_{\text{exp}})$, where subscripts (h) and (m) refer to host and mistletoe, respectively; the $\delta^{18}\text{O}_{\text{p}}$ was replaced by $\delta^{18}\text{O}_{\text{c}}$ for measurements of cellulose, rather than dry matter. The p_{exp} was assumed to be 0.4 (Barbour and Farquhar 2000), such that a 1.67‰ difference in $\delta^{18}\text{O}_{\text{L}}$ between host and mistletoe was inferred from a 1‰ difference in $\delta^{18}\text{O}_{\text{p}}$ or $\delta^{18}\text{O}_{\text{c}}$. Proportional enhancements in mistletoe transpiration rates were calculated by dividing the mistletoe transpiration rate by the host transpiration rate and subtracting one. Thus,

a proportional enhancement in transpiration rate of zero indicates equivalent transpiration rates between mistletoe and host, whereas a proportional enhancement of 2, for example, indicates that the mistletoe transpiration rate was three times that of the host.

Parasite/host variation in isotopic parameters was investigated with analyses of variance. The parasite/host difference in $\delta^{13}\text{C}$ or $\delta^{18}\text{O}$ was taken as the dependent variable. Independent variables were parasite functional type and parasite species nested within parasite functional type. After the analysis of variance model was estimated, Tukey's method for pairwise comparisons was used to determine which parasite functional types or species within functional types differed from one another. Additionally, hypothesis tests were conducted to determine whether the parasite/host isotopic difference for each parasite functional type was significantly different from zero. Sampling date (December or February) was initially considered as a factor in the models, but was not significant in analyses of parasite/host differences in either $\delta^{18}\text{O}_p$ or $\delta^{13}\text{C}_p$, and thus was not considered further. Although parasite/host isotopic differences did not change with sampling date, there did appear to be a shift in $\delta^{18}\text{O}_p$ values for all species between December and February. Analysis of variance was used to test whether this difference was significant, using sampling date and species as independent variables. Variation in foliar nitrogen concentrations between mistletoes and their hosts and between mistletoe species was assessed using analysis of variance. Statistical analyses were conducted in SYSTAT 9.0 (SPSS Inc., Chicago, IL, USA).

5.4. Results

5.4.1. Mistletoe $\delta^{18}\text{O}$

There were strongly contrasting patterns in parasite/host isotopic differences for $\delta^{18}\text{O}_p$ among the different parasite functional types ($P < 0.0001$, $n = 65$); data are shown in Figure 5.1. Parasite species within functional types was not a significant term in this analysis ($P = 0.47$). Mistletoe $\delta^{18}\text{O}_p$ values were less than those of their hosts by a mean parasite/host difference of -4.0‰ ($P < 0.0001$); this value differed significantly from corresponding values for both holoparasites ($P < 0.0001$) and root hemiparasites ($P < 0.0001$). The transpiration modeling exercise based on $\delta^{18}\text{O}_p$ measurements suggested proportional enhancements in transpiration rates for *A. preissii* and *A. miquelii* compared to their hosts of 2.8 and 3.9, respectively. Note that this analysis assumed that ϵ_{cp} was invariant between mistletoe and host.

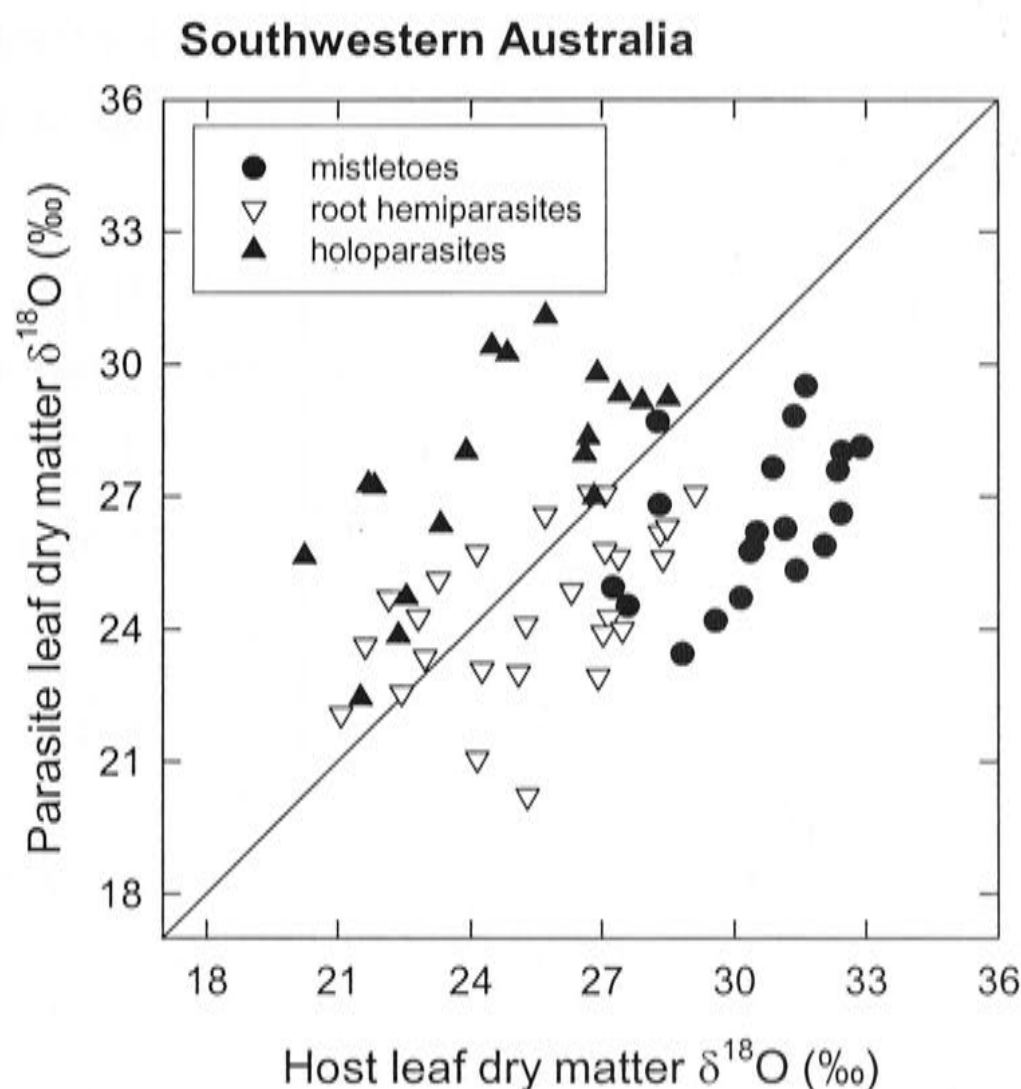


Figure 5.1. Leaf dry matter $\delta^{18}\text{O}$ values of parasitic plants growing in southwestern Australia plotted against the leaf dry matter $\delta^{18}\text{O}$ values of their hosts. Data points below the one-to-one line indicate a lower $\delta^{18}\text{O}$ in the parasite than in the host, whereas those above the line indicate a higher $\delta^{18}\text{O}$.

Parasite/host differences in $\delta^{18}\text{O}$ of leaf cellulose also varied significantly among parasite functional types ($P=0.0002$, $n=34$). In this case, parasite species within functional types was a significant term in this analysis ($P=0.02$). Mistletoe $\delta^{18}\text{O}_c$ values were less than those of their hosts by a mean parasite/host difference of -3.6‰ ($P<0.0001$). There was a significant difference in parasite/host $\delta^{18}\text{O}_c$ differences between the two mistletoe species ($P=0.05$); values are given in Table 5.2. The transpiration modeling exercise based on $\delta^{18}\text{O}_c$ measurements suggested proportional enhancements in transpiration rates for *A. preissii* and *A. miquelii* compared to their hosts of 5.0 and 1.1, respectively.

There was significant variation among parasite functional types in parasite/host differences in leaf water $\delta^{18}\text{O}$ ($P=0.01$, $n=24$), whereas variation among parasite species

Table 5.2. Oxygen isotope composition of parasitic plants and their hosts. Values are given with standard deviations where more than one pair was sampled. The column headed *n* gives the number of parasite/host pairs sampled for leaf dry matter $\delta^{18}\text{O}$, leaf cellulose $\delta^{18}\text{O}$, and leaf water $\delta^{18}\text{O}$, in that order.

Parasite species	Host species	<i>n</i>	Leaf dry matter $\delta^{18}\text{O}$ (‰)			Leaf cellulose $\delta^{18}\text{O}$ (‰)			Leaf water $\delta^{18}\text{O}$ (‰)			
			parasite	host	diff.	parasite	host	diff.	parasite	host	diff.	
Mistletoes:												
<i>Amyema miquelii</i>	<i>Eucalyptus wandoo</i>	10, 6, 4	27.0 ± 1.4	31.6 ± 0.8	-4.6	33.1 ± 2.6	34.6 ± 2.1	-1.5	8.9 ± 0.5	9.4 ± 0.6	-0.5	
<i>Amyema preissii</i>	<i>Acacia acuminata</i>	10, 6, 4	25.9 ± 1.8	29.4 ± 1.6	-3.5	34.5 ± 2.2	40.1 ± 1.4	-5.6	17.1 ± 1.5	16.7 ± 4.7	0.4	
Holoparasites:												
<i>Cassytha</i> sp.	<i>Acacia littorea</i>	3, 1, 2	29.6 ± 2.0	24.0 ± 2.1	5.6	31.4	30.8	0.6	13.4 ± 2.3	12.8 ± 1.6	0.6	
	<i>Exocarpus odoratus</i>	1, 1, 0	24.7	22.6	2.1	29.6	29.2	0.4				
	<i>Leucopogon capitellatus</i>	4, 1, 3	28.2 ± 1.0	26.2 ± 1.6	2.0	32.5	31.2	1.3	9.5 ± 1.7	14.1 ± 1.3	-4.6	
	<i>Spyridium globulosum</i>	2, 1, 1	29.5 ± 0.4	27.7 ± 1.1	1.8	31.5	29.9	1.6	8.8	14.9	-6.1	
	<i>Cuscuta campestris</i>	<i>Cakile maritima</i>	1, 1, 0	22.4	21.5	0.9	28.3	29.1	-0.8			
		<i>Euphorbia paralias</i>	1, 0, 1	29.2	27.9	1.3				5.3	13.1	-7.8
		<i>Muehlenbeckia adpressa</i>	2, 1, 1	25.9 ± 2.9	24.5 ± 3.0	1.4	29.0	28.6	0.4	4.9	10.5	-5.6
		<i>Pecarisonium</i> sp.	1, 1, 0	26.4	23.3	3.1	30.0	27.1	2.9			
	<i>Senecio elegans</i>	1, 0, 1	30.2	24.8	5.4				7.1	9.8	-2.7	
	Unknown host	1, 1, 0	25.6	20.3	5.3	29.2	28.4	0.8				
<i>Orobanche minor</i>	<i>Ribes sanguineum</i>	1, 1, 0	27.2	21.8	5.4	28.8	25.4	3.4				
Root hemiparasites:												
<i>Bartsia trixago</i>	<i>Conocephalum</i> sp.	1, 0, 0	23.9	27.0	-3.1							
	<i>Senecio lautus</i>	1, 0, 0	24.3	22.8	1.5							
<i>Exocarpus odoratus</i>	<i>Bossiaea lynophylla</i>	1, 1, 0	22.6	22.5	0.1	29.2	30.8	-1.6				
	<i>Hibbertia</i> sp.	1, 0, 1	27.1	27.1	0.0				13.3	14.5	-1.2	
<i>Exocarpus sparteus</i>	<i>Spyridium globulosum</i>	3, 2, 1	24.7 ± 1.7	27.2 ± 1.1	-2.5	28.4 ± 0.7	31.7 ± 0.6	-3.3	11.6	13.9	-2.3	
	<i>Pelargonium australe</i>	2, 1, 1	26.2 ± 0.6	24.9 ± 1.1	1.3	32.2	-	-	12.1	9.3	2.8	
	<i>Scaevola nitida</i>	1, 1, 0	24.7	22.2	2.5	30.9	27.2	3.7				
	<i>Spyridium globulosum</i>	2, 1, 1	26.4 ± 0.9	28.1 ± 1.4	-1.7	29.2	30.5	-1.3	11.0	12.2	-1.2	
<i>Olax phyllanthi</i>	<i>Acacia littorea</i>	1, 1, 0	23.4	23.0	0.4	30.9	31.6	-0.7				
	<i>Hibbertia</i> sp.	1, 1, 0	23.1	24.3	-1.2	29.1	31.6	-2.5				
	<i>Leucopogon parviflorus</i>	2, 1, 1	22.5 ± 2.0	25.8 ± 2.3	-3.3	29.3	29.2	0.1	12.3	13.5	-1.2	
	<i>Spyridium globulosum</i>	5, 3, 2	25.7 ± 1.0	27.6 ± 0.7	-1.9	30.6 ± 2.4	32.3 ± 0.8	-1.7	13.7 ± 0.7	12.9 ± 0.4	0.8	
<i>Parentucellia viscosa</i>	<i>Scaevola nitida</i>	1, 1, 0	23.6	21.6	2.0	31.2	28.3	2.9				
	<i>Anthoxanthum odoratum</i>	2, 0, 0	21.6 ± 2.0	25.2 ± 0.1	-3.6							
	<i>Hypochaeris radicata</i>	1, 0, 0	25.1	23.3	1.8							
	<i>Ricinocarpus</i> sp.	1, 0, 0	24.1	25.3	-1.2							
	<i>Senecio</i> sp.	1, 0, 0	22.1	21.1	1.0							

within functional types was not significant ($P=0.64$). However, in contrast to the results for dry matter and cellulose, the mean parasite/host difference in $\delta^{18}\text{O}_L$ for mistletoes was not significantly different from zero ($P=0.96$). Mean $\delta^{18}\text{O}_L$ values for the mistletoes and their hosts are given in Table 5.2.

5.4.2. Mistletoe $\delta^{13}\text{C}$

The contrasting isotopic patterns of the parasite functional types in relation to their hosts was similarly reflected in the $\delta^{13}\text{C}$ of leaf dry matter ($P<0.0001$, $n=64$); data are shown in Figure 5.2. For parasite/host $\delta^{13}\text{C}_p$ differences, there was significant variation among parasite species within parasite functional types ($P=0.003$). Mistletoe $\delta^{13}\text{C}_p$ values were more negative than those of their hosts, showing an average difference of -1.9‰ ($P<0.0001$). This mean difference was significantly different from that of holoparasites ($P<0.0001$), but not root hemiparasites ($P=0.21$). Additionally, the parasite/host difference in $\delta^{13}\text{C}_p$ was significantly different between the two mistletoe species ($P=0.03$); mean values for the two species are given in Table 5.3.

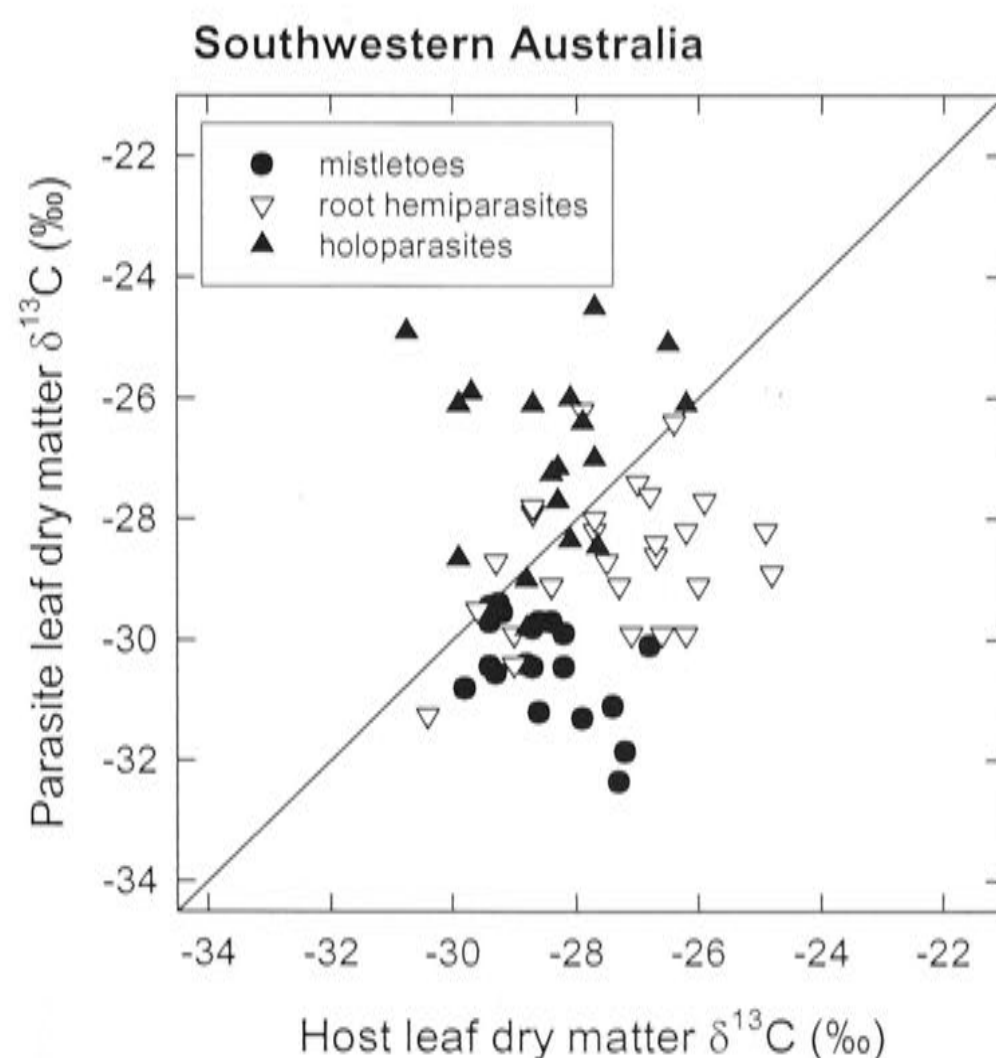


Figure 5.2. Leaf dry matter $\delta^{13}\text{C}$ values of parasitic plants growing in southwestern Australia plotted against the leaf dry matter $\delta^{13}\text{C}$ values of their hosts. Data points below the one-to-one line indicate a more negative $\delta^{13}\text{C}$ in the parasite than in the host, whereas those above the line indicate a less negative $\delta^{13}\text{C}$.

Table 5.3. Carbon isotope composition of parasitic plants and their hosts. Values are given with standard deviations where more than one pair was sampled. The column headed *n* gives the number of parasite/host pairs sampled for leaf dry matter $\delta^{13}\text{C}$ and leaf cellulose $\delta^{13}\text{C}$, in that order.

Parasite species	Host species	<i>n</i>	Leaf dry matter $\delta^{13}\text{C}$ (‰)			Leaf cellulose $\delta^{13}\text{C}$ (‰)		
			parasite	host	diff.	parasite	host	diff.
Mistletoes:								
<i>Amyema miquelii</i>	<i>Eucalyptus wandoo</i>	10, 6	-31.0 \pm 0.7	-28.0 \pm 0.8	-3.0	-27.8 \pm 0.6	-25.5 \pm 0.9	-2.3
<i>Amyema preissii</i>	<i>Acacia acuminata</i>	10, 6	-29.8 \pm 0.4	-29.0 \pm 0.5	-0.8	-27.0 \pm 0.7	-25.0 \pm 0.4	-2.0
Holoparasites:								
<i>Cassytha</i> sp.	<i>Acacia littorea</i>	3, 1	-26.7 \pm 2.1	-29.8 \pm 1.0	3.1	-27.5	-25.2	-2.3
	<i>Exocarpus odoratus</i>	1, 1	-26.1	-26.2	0.1	-24.1	-23.5	-0.6
	<i>Leucopogon capitellatus</i>	4, 1	-27.5 \pm 1.2	-28.5 \pm 0.9	1.0	-24.3	-26.9	2.6
	<i>Spyridium globulosum</i>	2, 1	-28.1 \pm 2.4	-28.4 \pm 0.6	0.3	-25.1	-25.5	0.4
<i>Cuscuta campestris</i>	<i>Cakile maritima</i>	1, 1	-27.2	-28.3	1.1	-26.0	-27.1	1.1
	<i>Euphorbia paralias</i>	1, 0	-25.1	-26.5	1.4			
	<i>Muehlenbeckia adpressa</i>	2, 1	-26.1 \pm 2.3	-28.0 \pm 0.4	1.9	-27.3	-25.6	-1.7
	<i>Pecarisonium</i> sp.	1, 1	-26.0	-28.1	2.1	-25.2	-25.3	0.1
	<i>Senecio elegans</i>	1, 0	-26.1	-28.7	2.6			
	Unknown host	1, 0	-28.7	-29.9	1.2			
<i>Orobanche minor</i>	<i>Ribes sanguineum</i>	1, 1	-27.0	-27.7	0.7	-25.9	-24.9	-1.0
Root hemiparasites:								
<i>Bartsia trixago</i>	<i>Conocephalum</i> sp.	1, 0	-28.7	-29.3	0.6			
	<i>Senecio lautus</i>	1, 0	-29.9	-29.0	-0.9			
<i>Exocarpus odoratus</i>	<i>Bossiaea lynophylla</i>	1, 1	-26.2	-27.9	1.7	-23.5	-25.5	2.0
	<i>Hibbertia</i> sp.	1, 0	-28.7	-27.5	-1.2			
	<i>Spyridium globulosum</i>	3, 2	-28.9 \pm 1.2	-27.1 \pm 0.3	-1.8	-25.0 \pm 1.6	-25.1 \pm 0.2	0.1
<i>Exocarpus sparteus</i>	<i>Pelargonium australe</i>	2, 1	-28.3 \pm 0.1	-25.8 \pm 1.3	-2.5	-24.2	-25.5	1.3
	<i>Scaevola nitida</i>	1, 1	-29.1	-26.0	-3.1	-27.0	-	-
	<i>Spyridium globulosum</i>	2, 1	-29.4 \pm 0.7	-25.5 \pm 1.0	-3.9	-27.8	-24.1	-3.7
<i>Olax phyllanthi</i>	<i>Acacia littorea</i>	1, 1	-27.8	-28.7	0.9	-25.7	-24.9	-0.8
	<i>Hibbertia</i> sp.	1, 1	-28.0	-27.7	-0.3	-25.8	-24.3	-1.5
	<i>Leucopogon parviflorus</i>	2, 1	-28.7 \pm 0.6	-28.1 \pm 0.5	-0.6	-26.5	-25.1	-1.4
	<i>Spyridium globulosum</i>	5, 3	-28.2 \pm 1.3	-26.4 \pm 0.3	-1.8	-23.8 \pm 0.3	-25.7 \pm 1.4	1.9
	<i>Scaevola nitida</i>	1, 1	-27.4	-27.0	-0.4	-24.4	-	-
<i>Parentucellia viscosa</i>	<i>Anthoxanthum odoratum</i>	1, 0	-30.4	-29.0	-1.4			
	<i>Hypochaeris radicata</i>	1, 0	-27.9	-28.7	0.8			
	<i>Ricinocarpus</i> sp.	1, 0	-29.5	-29.6	0.1			
	<i>Senecio</i> sp.	1, 0	-31.3	-30.4	-0.9			

Foliar N concentrations varied significantly between the two mistletoe/host species pairs ($P < 0.0001$, $n = 40$), but not between mistletoes and their hosts ($P = 0.14$). The mean N concentration for leaf dry matter of *Amyema preissii* was $23.6 \pm 8.0 \text{ mg g}^{-1}$ (mean \pm 1SD); that for its host *Acacia acuminata* was $27.5 \pm 3.0 \text{ mg g}^{-1}$. The mean N concentration for leaf dry matter of *Amyema miquelii* was $8.4 \pm 2.2 \text{ mg g}^{-1}$; that for its host *Eucalyptus wandoo* was $8.7 \pm 1.7 \text{ mg g}^{-1}$. The regression line relating mistletoe N concentration to host N concentration was $[N]_{\text{mistletoe}} = 0.83[N]_{\text{host}} + 1.0 \text{ mg g}^{-1}$ ($R^2 = 0.70$, $P < 0.0001$, $n = 20$). Mistletoe/host differences in $\delta^{13}\text{C}_p$ became less negative with increasing host leaf N concentration according to the following equation: $\delta^{13}\text{C}_p(\text{difference}) = 0.11[N]_{\text{host}} - 3.8$ ($R^2 = 0.51$, $P = 0.0002$, $n = 20$).

There was significant variation among parasite functional types in parasite/host differences in $\delta^{13}\text{C}_c$ ($P = 0.02$, $n = 31$). Mistletoe $\delta^{13}\text{C}_c$ values were significantly more negative than those of their hosts ($P = 0.0002$). The mean parasite/host $\delta^{13}\text{C}_c$ difference for mistletoes was -2.2‰ . Interestingly, when cellulose was analyzed instead of leaf dry matter, variation in parasite/host $\delta^{13}\text{C}$ differences was no longer observed among species within parasite functional types ($P = 0.82$). Thus, the two mistletoes species had very similar parasite/host differences in $\delta^{13}\text{C}_c$, in contrast to the results for $\delta^{13}\text{C}_p$ (Table 5.3).

5.4.3. Root hemiparasite $\delta^{18}\text{O}$

Root hemiparasites had $\delta^{18}\text{O}_p$ values that were significantly lower than those of their hosts ($P = 0.04$). The mean parasite/host $\delta^{18}\text{O}_p$ difference for root hemiparasites was -1.0‰ . The difference in $\delta^{18}\text{O}_c$ between root hemiparasites and their hosts was similar to that in $\delta^{18}\text{O}_p$, with a mean value of -0.9‰ ; however, this difference was not statistically significant ($P = 0.31$). I did not observe a significant difference in leaf water $\delta^{18}\text{O}$ between root hemiparasites and their hosts ($P = 0.82$); the mean difference was -0.2‰ . There was no significant variation among parasite species within the root hemiparasite functional type for any of the $\delta^{18}\text{O}$ analyses. Values for individual species are detailed in Table 5.2.

5.4.4. Root hemiparasite $\delta^{13}\text{C}$

Root hemiparasites had $\delta^{13}\text{C}_p$ values more negative than those of their hosts ($P = 0.0006$); the mean parasite/host $\delta^{13}\text{C}_p$ difference was -1.2‰ . There were no

significant differences among individual root hemiparasite species in their $\delta^{13}\text{C}_p$ values relative to their hosts. However, sample sizes were rather small for all but a couple of species (Table 5.3). In contrast to the results for $\delta^{13}\text{C}_p$, values of $\delta^{13}\text{C}_c$ for perennial root hemiparasites did not differ between parasite and host ($P=0.94$); the mean parasite/host $\delta^{13}\text{C}_c$ difference for root hemiparasites was 0.2‰.

5.4.5. Holoparasite $\delta^{18}\text{O}$

Variation in $\delta^{18}\text{O}_p$ between holoparasites and their hosts was opposite in sign to that observed for mistletoes and root hemiparasites (Figure 5.1). The mean parasite/host difference was positive, having a value +3.0‰ ($P<0.0001$); this value was significantly different from that observed for mistletoes ($P<0.0001$) and root hemiparasites ($P<0.0001$). Holoparasite $\delta^{18}\text{O}_c$ was also higher than that of hosts, showing a mean difference of +1.2‰, which was moderately significant ($P=0.06$). In contrast, however, holoparasite tissue water was significantly less enriched in ^{18}O than host leaf water; the parasite/host $\delta^{18}\text{O}_L$ difference was -3.8‰ ($P=0.0003$); mean $\delta^{18}\text{O}_L$ values were 9.1 ± 3.3 ‰ and 12.9 ± 2.0 ‰ for parasite and host, respectively. This was an interesting result because the sign of the difference in $\delta^{18}\text{O}_L$ between holoparasites and their hosts was opposite to that of the differences in $\delta^{18}\text{O}_p$ and $\delta^{18}\text{O}_c$. There were no significant differences among parasite species within the holoparasite functional type for any of the $\delta^{18}\text{O}$ analyses.

5.4.6. Holoparasite $\delta^{13}\text{C}$

Parasite/host variation in $\delta^{13}\text{C}_p$ for holoparasites also differed in sign compared to that observed for mistletoes and root hemiparasites (Figure 5.2). Holoparasites were enriched in ^{13}C compared to their hosts, showing an average parasite/host $\delta^{13}\text{C}_p$ difference of +1.5‰ ($P=0.02$). This mean value differed from that for both mistletoes ($P<0.0001$), and root hemiparasites ($P=0.0005$). However, a similar difference in $\delta^{13}\text{C}$ was not observed in cellulose; holoparasite $\delta^{13}\text{C}_c$ was not different from that of the hosts ($P=0.59$). There were no significant differences among parasite species within the holoparasite functional type for either of the $\delta^{13}\text{C}$ analyses.

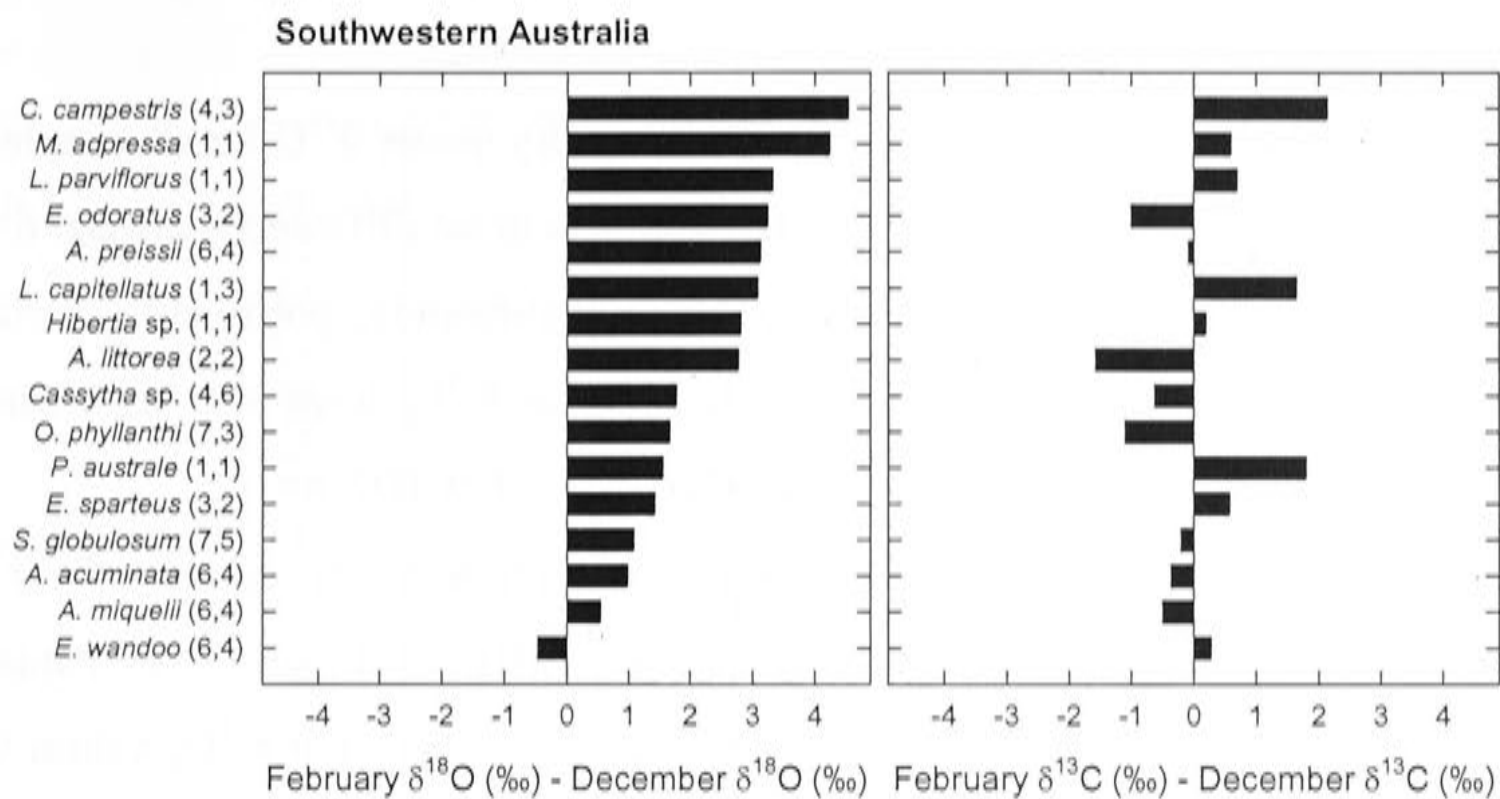


Figure 5.3. The mean difference between leaf dry matter $\delta^8\text{O}$ values sampled in February, 2002 and those sampled in December, 2001 for all species sampled on both dates (A), and the corresponding differences in leaf dry matter $\delta^3\text{C}$ values (B). Values in parentheses are the number of individuals sampled in December, followed by the number of individuals sampled in February.

5.4.7. All species $\delta^8\text{O}$ and $\delta^3\text{C}$

The oxygen isotope ratio of leaf dry matter increased between December and February for all species sampled on both dates except *E. wandoo* (Figure 5.3A). The mean $\delta^{18}\text{O}_p$ for all plants sampled in December was 25.4‰, whereas the mean value for February was 28.0‰. Sampling date (December or February) was a significant term in the analysis of variance in individual $\delta^{18}\text{O}_p$ values ($P<0.0001$, $n=130$). In contrast, $\delta^{13}\text{C}_p$ did not change consistently across species between December and February (Figure 5.3B), with mean values of -28.5‰ and -28.3‰ for the two dates respectively, which were statistically indistinguishable ($P=0.67$, $n=129$).

Leaf cellulose was enriched in ^{18}O compared to leaf dry matter for all of the samples in which both analyses were performed. The mean value for ϵ_{cp} , the difference between $\delta^{18}\text{O}_p$ and $\delta^{18}\text{O}_c$, across all samples was $-6.2 \pm 2.9\text{‰}$ (mean \pm 1 SD). Values of ϵ_{cp} for individual species varied from -11.2‰ for *A. acuminata* to -2.8‰ for *E. wandoo* (Table 5.4). There was a significant, positive correlation between $\delta^{18}\text{O}_p$ and $\delta^{18}\text{O}_c$ ($r=0.63$, $P<0.0001$, $n=67$). Additionally, parasite/host differences in $\delta^{18}\text{O}_p$ were

significantly correlated with parasite/host differences in $\delta^{18}\text{O}_\text{c}$ ($r=0.69$, $P<0.0001$, $n=33$).

Leaf cellulose $\delta^{13}\text{C}$ was less negative than leaf dry matter $\delta^{13}\text{C}$ for all samples in which both analyses were performed, except two. The mean difference between $\delta^{13}\text{C}_\text{p}$ and $\delta^{13}\text{C}_\text{c}$ was $-2.6 \pm 1.1\text{‰}$, with the two being significantly, positively correlated ($r=0.70$, $P<0.0001$, $n=64$). Parasite/host differences in $\delta^{13}\text{C}_\text{p}$ were also significantly correlated with parasite/host differences in $\delta^{13}\text{C}_\text{c}$ ($r=0.55$, $P=0.002$, $n=30$).

There was a general relationship across all parasite/host pairs between the $\delta^{13}\text{C}_\text{p}$ parasite/host difference and the $\delta^{18}\text{O}_\text{p}$ parasite/host difference (Figure 5.4). Parasites with higher $\delta^{13}\text{C}_\text{p}$ values than their hosts also tended to have higher $\delta^{18}\text{O}_\text{p}$ values than their hosts. The holoparasites were a good example of such a pattern. Conversely, parasites such as the mistletoes, which had lower $\delta^{13}\text{C}_\text{p}$ values than their hosts, also tended to have lower $\delta^{18}\text{O}_\text{p}$ values than their hosts.

Table 5.4. Values for ϵ_cp , the difference between total leaf dry matter $\delta^{18}\text{O}$ and leaf cellulose $\delta^{18}\text{O}$, for species sampled in the present study and others available in the literature. Values reported from the present study are limited to species in which 3 or more individuals were sampled, and are given as the mean ± 1 SD. The overall mean is -6.8‰ .

Species	ϵ_cp (‰)	Reference
<i>Acacia acuminata</i>	-11.2 ± 2.2	This study
<i>Amyema miquelii</i>	-6.3 ± 2.5	This study
<i>Amyema preissii</i>	-9.8 ± 1.6	This study
<i>Exocarpus odoratus</i>	-5.6 ± 1.7	This study
<i>Exocarpus sparteus</i>	-5.3 ± 1.7	This study
<i>Eucalyptus wandoo</i>	-2.8 ± 2.1	This study
<i>Gossypium hirsutum</i>	-7.5	Barbour and Farquhar 2000
<i>Olex phyllanthi</i>	-6.4 ± 1.6	This study
<i>Picea abies</i>	-6.4	Jäggi et al. 2003
<i>Spyridium globulosum</i>	-4.4 ± 1.0	This study
<i>Triticum aestivum</i>	-9.1	Barbour et al. 2000

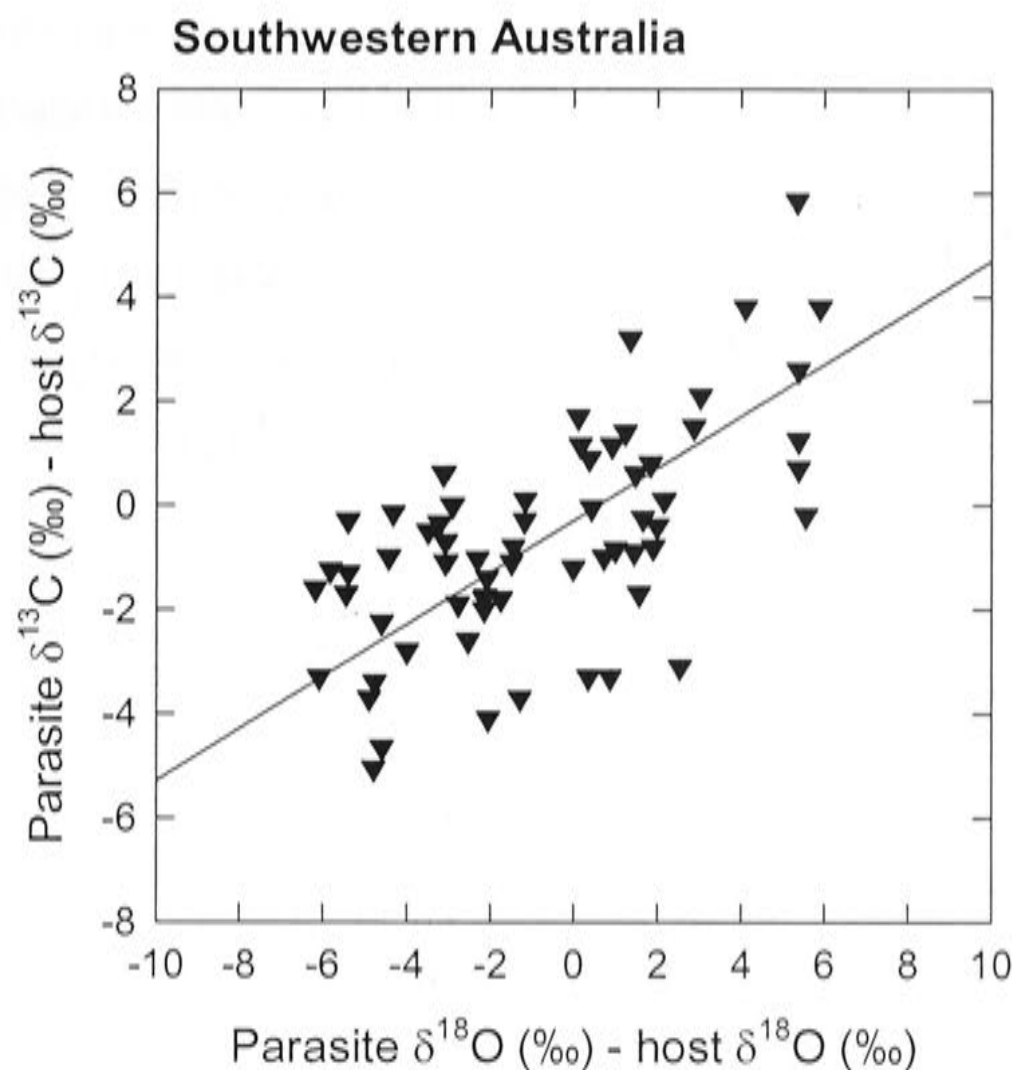


Figure 5.4. Parasite/host differences in leaf dry matter $\delta^{13}\text{C}$ plotted against the corresponding parasite/host difference in leaf dry matter $\delta^{18}\text{O}$. The two parameters are significantly, positively correlated ($r=0.63$, $P<0.0001$, $n=64$). The line drawn on the graph has a slope of 0.5 and a y-intercept of 0.3. These coefficients were calculated using principle components analysis, such that neither parameter was explicitly dependent on the other.

5.5. Discussion

I observed consistent differences in $\delta^{18}\text{O}_p$ and $\delta^{13}\text{C}_p$ between parasitic plants and their hosts within the different parasite functional types. Results for leaf dry matter isotopic analyses generally agreed with those for leaf cellulose, although there were some exceptions. Such variation in isotopic composition suggests contrasting strategies of resource acquisition and use among the various parasitic plants in relation to each other and to their hosts. For example, lower $\delta^{18}\text{O}_p$ and $\delta^{13}\text{C}_p$ in mistletoes and root hemiparasites than their hosts suggests a relatively more liberal use of water and a lower water use efficiency by both functional types in the seasonally dry, mediterranean-type environment of southwestern Australia. However, the three-fold larger parasite/host difference in $\delta^{18}\text{O}_p$ for mistletoes compared to root hemiparasites highlights the greater extent to which mistletoes rely on such a strategy to acquire carbon and nutrients

compared to the root hemiparasites. Additionally, some of the results serve to highlight areas in which the mechanisms leading to isotopic variation among plants have yet to be unraveled, such as the higher $\delta^{18}\text{O}_p$ and $\delta^{13}\text{C}_p$ in holoparasites compared to their hosts. In such cases, the observations presented here may provide a basis for designing experimental systems aimed at elucidating these mechanisms. In the following discussion, I expand upon the implications of my results for understanding the ecology of parasitic plants and the mechanisms underlying their isotopic variations.

5.5.1. Mistletoe $\delta^{18}\text{O}$

The mean differences in $\delta^{18}\text{O}_p$ of -3.5‰ for the mistletoe *A. preissii* growing on *A. acuminata*, and -4.6‰ for the mistletoe *A. miquelii* growing on *E. wandoo*, suggest substantially higher transpiration rates in these two mistletoe species compared to their hosts in southwestern Australia. Transpiration rates of mistletoes growing in Australia were previously observed to be consistently higher than those of their hosts (Hellmuth 1971; Ullmann et al. 1985; Davidson et al. 1989; Davidson and Pate 1992; Marshall et al. 1994b; Tennakoon and Pate 1996a); estimates of the proportional enhancement in mistletoe transpiration rates compared to those of their hosts range from 0.4 to 7.9. Similar observations have been reported for mistletoes in other regions as well (Glatzel 1983; Schulze et al. 1984; Ehleringer et al. 1986; Marshall et al. 1994a). Based on $\delta^{18}\text{O}_p$ measurements, I calculated time-integrated, proportional enhancements in transpiration of 2.8 and 3.9 for *A. preissii* and *A. miquelii* compared to their respective hosts, whereas $\delta^{18}\text{O}_c$ measurements indicated proportional enhancements of 5.0 and 1.1, respectively. Such values are well within the range observed for Australian mistletoes. Nonetheless, the difference in estimates based on $\delta^{18}\text{O}_p$ as compared to $\delta^{18}\text{O}_c$ highlights the need for a mechanistic understanding of processes controlling ε_{cp} , the difference in $\delta^{18}\text{O}$ between dry matter and cellulose.

Because mistletoes are known to assimilate organic solutes from the host's transpiration stream (Raven 1983; Marshall and Ehleringer 1990; Schulze et al. 1991), it is reasonable to ask whether this process might have contributed to the difference that I observed in $\delta^{18}\text{O}_p$ and $\delta^{18}\text{O}_c$ between mistletoes and their hosts. The effect of mistletoe heterotrophy on $\delta^{18}\text{O}_c$ can be included in equation (5.3) as follows:

$$\delta_{c(m)} = \delta_s + (1 - \rho)(\delta_{L(m)} - \delta_s)(1 - p_{ex(m)}p_{x(m)}) + \rho(\delta_{ox} - \varepsilon_{wc} - \delta_s)(1 - p_{ex(ox)}p_{x(m)}) + \varepsilon_{wc} \quad (5.7)$$

The δ terms in equation (5.7) refer to $\delta^{18}\text{O}$. The subscript m refers to the mistletoe, and the subscript ox refers to xylem-borne organic solutes procured from the host's transpiration stream. The ρ is the proportion of photosynthate acquired from the host's xylem sap, and $(1-\rho)$ is the proportion supplied by the mistletoe's own photosynthesis. I assume similar oxygen concentrations in the two pools. In the one case that I am aware of in which the $\delta^{18}\text{O}$ of xylem sap dry matter was measured, it was found to be enriched relative to source water by 34.9‰ in *Lupinus angustifolius* (Chapter 2). In this case, the term $(\delta_{ox} - \epsilon_{wc} - \delta_s)$ would have a value of 7.9‰. The effect of this term on the $\delta^{18}\text{O}$ of mistletoe foliage depends on the terms ρ and $(1 - p_{ex(ox)} p_{x(m)})$. The term ρ has been estimated from measurements of gas exchange and $\delta^{13}\text{C}$ values for some mistletoe species (Marshall and Ehleringer 1990, Marshall et al. 1994b). The term $p_{ex(ox)}$ is not known, but detailed investigation of the chemical composition of xylem-borne solutes and likely pathways for their incorporation into organic material could provide a range of expected values. However, until specific data become available, it is difficult to predict whether heterotrophy should increase, decrease, or not change the $\delta^{18}\text{O}$ of mistletoe leaves.

The consistent difference that I observed in $\delta^{18}\text{O}_p$ of mistletoes compared to their hosts, whereby mistletoes were less enriched in ^{18}O , contrasts with previous results comparing dry matter δD of Australian mistletoes to that of their hosts (Ziegler 1994). For dry matter δD , mean values of -51‰ for mistletoes and -73‰ for hosts were reported. Thus, in the case of deuterium, mistletoes were consistently *more* enriched than their hosts. I assume that the difference in $\delta^{18}\text{O}_p$ between mistletoes and hosts results from a differential enrichment between the two in leaf water isotopes (e.g. Flanagan et al. 1993); because $\delta^{18}\text{O}$ and δD in leaf water are strongly correlated, one might expect that the $\delta^{18}\text{O}$ and δD patterns in dry matter would be similarly correlated. Presumably then, the difference in the direction of mistletoe/host variation in δD as opposed to $\delta^{18}\text{O}$ of leaf dry matter results from variation between the mistletoe and host in post-photosynthetic, biochemical fractionation of δD . To a first approximation, the higher δD for mistletoe dry matter may imply a proportionally larger heterotrophic metabolism than in the host (Yakir 1992).

In the leaf water $\delta^{18}\text{O}$ samples that I examined, I did not observe a statistically significant difference between mistletoes and hosts. However the sample size was rather small ($n=8$) and therefore may not have been sufficient to capture variation

between the two. Whereas the $\delta^{18}\text{O}_p$ and $\delta^{18}\text{O}_c$ values represent integrated measures of the leaf water $\delta^{18}\text{O}$, a single measurement of the leaf water itself represents only a snapshot in time in the dynamic leaf water system. Therefore, one would expect the power to detect differences between two populations to be greater for analyses of $\delta^{18}\text{O}_p$ or $\delta^{18}\text{O}_c$ than for $\delta^{18}\text{O}_L$. For example, in a sampling of 30 *Eucalyptus globulus* Labill. leaves over the course of a diel cycle, the coefficient of variation for $\delta^{18}\text{O}_p$ was 0.03, whereas that for $\delta^{18}\text{O}_L$ was 0.24 (Chapter 6). For samples collected at the same time within that diel cycle, the average coefficient of variation for $\delta^{18}\text{O}_p$ was 0.01, whereas that for $\delta^{18}\text{O}_L$ was 0.13. Similar differences in variability between $\delta^{18}\text{O}_p$ and $\delta^{18}\text{O}_L$ were observed for cotton plants grown at constant humidity (Gan et al. 2002). The situation is analogous to that encountered when one analyzes variation among populations in instantaneous measurements of c_i/c_a , as compared to measurements of $\delta^{13}\text{C}_p$ (e.g. Cernusak and Marshall 2001).

5.5.2. Mistletoe $\delta^{13}\text{C}$

I found a significant variation in the parasite/host $\delta^{13}\text{C}_p$ differences between *A. miquelii* growing on a non-nitrogen fixing *Eucalyptus* host and *A. preissii* growing on a potentially nitrogen fixing *Acacia* host; parasite/host $\delta^{13}\text{C}_p$ differences were -3.0‰ and -0.8‰, respectively. This result is consistent with results for two *Phoradendron* mistletoe species growing on a non-nitrogen fixing host and an *Acacia* host, where the parasite/host $\delta^{13}\text{C}_p$ differences were -3.0‰ and -0.2‰, respectively (Schulze and Ehleringer 1984), and with results from three continents showing a general pattern of smaller parasite/host $\delta^{13}\text{C}_p$ differences on nitrogen fixing hosts than on non-nitrogen fixing hosts (Ehleringer et al. 1985). I observed a significant relationship between mistletoe/host $\delta^{13}\text{C}_p$ differences and host leaf N concentrations, consistent with previous reports (Ehleringer et al. 1985; Schulze et al. 1991; Bannister and Strong 2001).

The observations of $\delta^{18}\text{O}_p$ and $\delta^{18}\text{O}_c$ and foliar N concentration in the present study can be used to formulate hypotheses aimed at explaining the variation in mistletoe/host $\delta^{13}\text{C}_p$ differences. Parasite/host differences in $\delta^{13}\text{C}_p$ between *A. preissii* and *A. miquelii* could suggest a proportionally lower c_i/c_a ratio in *A. preissii* relative to its host compared to that in *A. miquelii* relative to its host. The observations of $\delta^{18}\text{O}_p$ suggest that the parasite/host differences in transpiration rate were similar for the two mistletoe species, whereas observations of $\delta^{18}\text{O}_c$ suggest a larger parasite/host

difference in transpiration for *A. preisii* than *A. miquelii*. These observations indicate that a lower parasite/host difference in c_i/c_a in *A. preisii* compared to *A. miquelii* would have to result from a proportionally higher photosynthetic rate in *A. preisii* relative to its host compared to that in *A. miquelii* relative to its host. However, I found that foliar N concentrations were similar between *A. preisii* and its *Acacia* host, as was the case for *A. miquelii* and its *Eucalyptus* host. Therefore, the inference of a higher photosynthetic rate in *A. preisii* relative to its host compared to *A. miquelii* relative to its host based on measurements of foliar N concentration alone is not justified.

An alternative explanation is that *A. preisii* assimilated a larger amount of dissolved organic carbon from its host's transpiration stream than *A. miquelii*, thereby taking on a higher degree of partial heterotrophy. In a previous study of mistletoes and their hosts in southwestern Australia (Pate et al. 1991), the *Eucalyptus* host of *A. miquelii* was reported to have a xylem sap total amino acid concentration of 0.83 mmol L⁻¹, whereas the *Acacia* host of *A. preisii* had a xylem sap total amino acid concentration of 2.4 mmol L⁻¹, approximately three-fold higher. In the few cases where the $\delta^{13}\text{C}$ of xylem sap dry matter has been measured, it was consistently less negative than that of leaf dry matter from the same plant (Richter et al. 1995; Yoneyama et al. 1998; Chapter 2), with an average difference of 1.0‰ for four *Acacia* species (Richter et al. 1995). Thus, I can hypothesize that the assimilation of a larger amount of amino acids and other compounds relatively enriched in ¹³C and dissolved in the host's transpiration stream caused the $\delta^{13}\text{C}_p$ of *A. preisii* to resemble its host more closely than that of *A. miquelii* did its host.

5.5.3. Root hemiparasite $\delta^{18}\text{O}$ and $\delta^{13}\text{C}$

I found that leaf dry matter of root hemiparasites was less enriched in ¹⁸O and ¹³C than that of their hosts; average parasite/host differences were -1.0‰ for $\delta^{18}\text{O}_p$, and -1.2‰ for $\delta^{13}\text{C}_p$. Results were the same for both annual and perennial root hemiparasites. This suggests a general trend of higher transpiration rates and lower water use efficiency for root hemiparasites when compared to their hosts in southwestern Australia, although notably not to the same extent as the mistletoe species that I examined. Previous assessments of the water use efficiency of root hemiparasites in relation to their hosts have resulted in both lower estimates (Press et al. 1988; Press et al. 1993; Ducharme and Ehleringer 1996; Lechowksi 1996; Pate and Bell 2000), and similar or higher estimates (Pate et al. 1990a; Tennakoon et al. 1997; Loveys et al.

2001). Pate et al. (1990a) previously observed no difference in $\delta^{13}\text{C}_p$ between *O. phyllanthi* and its hosts in the coastal heath near Denmark, Western Australia. In contrast, I observed a difference of -1.0‰ for $\delta^{13}\text{C}_p$, and a corresponding difference of -1.5‰ for $\delta^{18}\text{O}_p$ for *O. phyllanthi* in the same location. The contrasting results might relate to changes in the successional status of the vegetation community, or to temporal variations in resource availability. It is worth noting that root hemiparasites can also gain carbon by assimilating xylem-borne solutes from their host's transpiration stream (Press et al. 1987; Press et al. 1988; Ducharme and Ehleringer 1996; Tennakoon and Pate 1996b), and that such heterotrophy will cause variation in leaf dry matter $\delta^{13}\text{C}$ unrelated to parasite c_i/c_a . However, the likely net effect is to cause parasite $\delta^{13}\text{C}$ to be less negative than it otherwise would be, thereby causing differences in water use efficiency between parasite and host to be underestimated, if anything.

Parasite/host differences in $\delta^{18}\text{O}_c$ appeared to be similar to those in $\delta^{18}\text{O}_p$. In contrast, $\delta^{13}\text{C}_c$ did not show the same parasite/host difference that $\delta^{13}\text{C}_p$ did. It is possible that leaf cellulose $\delta^{13}\text{C}$ contains a signature that is temporally separated from that contained in total leaf dry matter, or that post-photosynthetic fractionations differ between the parasites and their hosts. Further research would be helpful in clarifying the contrasting results between $\delta^{13}\text{C}_p$ and $\delta^{13}\text{C}_c$ for root hemiparasites compared to their hosts.

Our analysis did not detect variation in parasite/host isotopic differences among the different species of root hemiparasites. However sampling frequencies were rather low for most of the species. Thus, an improved experimental design in the future may well show meaningful differences among different species of root hemiparasites in their isotopic behavior in relation to their hosts.

5.5.4. Holoparasite $\delta^{18}\text{O}$

The dry matter and cellulose of holoparasites were enriched in ^{18}O compared to their hosts, showing parasite/host $\delta^{18}\text{O}_p$ and $\delta^{18}\text{O}_c$ differences of $+3.0\text{‰}$ and $+1.2\text{‰}$, respectively. This was not simply a reflection of a more enriched tissue water, as the tissue water in the holoparasites was less enriched than host leaf water by -3.8‰ when sampled at midday. Transpirational water loss is generally very low for holoparasites (Raven 1983); it has been assessed as less than 2% of the host's transpiration rate in *Orobanch*e (Hibberd et al. 1999), and as roughly the same as the amount of water used for tissue growth in *Cuscuta* (Jeschke et al. 1994a; Jeschke et al. 1994b). If one

assumes little or no evaporational enrichment after uptake, the holoparasite tissue water $\delta^{18}\text{O}$ values are consistent with host phloem water being the main water source. Within the host, the phloem water $\delta^{18}\text{O}$ is expected to be intermediate between that of leaf water and that of xylem water (Chapter 2; Chapter 4). A symplastic connection between host sieve elements and haustorial cells in *Cuscuta* was recently demonstrated (Haupt et al. 2001), which would allow direct uptake of host phloem water together with solutes.

Equation (5.3) can be used to construct hypotheses aimed at explaining the enrichment in ^{18}O of holoparasite dry matter and cellulose relative to their hosts. In the case of holoparasites, the terms $\delta^{18}\text{O}_L$ and $\delta^{18}\text{O}_s$ in equation (5.3) would refer to values for the host, and thus would not differ between the two partners. Therefore, I can hypothesize that the difference between parasite and host lies in the term $p_{\text{ex}}p_x$. If the parasite uses exclusively phloem water, this may lead to a lower p_x value in the parasite, because developing cells in the host would be expected to contain a mixture of phloem water and xylem water (Lalonde et al. 2003). Alternatively, p_{ex} may be lower in the parasite than in the host. There is at least one report suggesting that p_{ex} may decrease if sink strength is high and carbohydrate supply is limiting (Barbour and Farquhar 2000). A final hypothesis is that p_x is effectively lower in the parasite, not, however, caused by a difference in use of phloem versus xylem water, but rather by evaporative enrichment of water within the holoparasite. Although evaporation rates are very low compared to the host, some evaporation must occur from the tissue of the holoparasite. The small enrichments in tissue water caused by this evaporation may build up over time because the residence time of water in the holoparasite is likely to be long. In an analogous situation, water in twigs of deciduous trees was observed to increase in $\delta^{18}\text{O}$ by several per mil during the leafless winter months, before returning to the value of soil water when leaves developed (Förstel and Hützen 1983). Notably, the parasite/host trend for $\delta^{18}\text{O}$ in dry matter of holoparasites agrees with the trend for δD ; holoparasites were consistently enriched in dry matter δD compared to their hosts (Ziegler 1994, 1996).

5.5.5. Holoparasite $\delta^{13}\text{C}$

I found that the holoparasites that I analyzed were consistently enriched in $\delta^{13}\text{C}_p$ relative to their hosts. In a previous comparison of holoparasite/host $\delta^{13}\text{C}_p$, it was concluded that the two were not significantly different (Ziegler 1994). I re-analyzed the data presented in Table 19.2 of that report and found that there was one anomalous pair

in the parasite/host comparison that caused the two not to differ statistically; the pair in question lists a value of -24.8‰ for *Cuscuta hyalina* Heyne ex Roth growing on *Zea mays* L. with a value of -14.6‰. This datum is likely erroneous (H. Ziegler, personal communication), because it implies that *Cuscuta* assimilated most of its own carbon via the C₃ photosynthetic pathway. In contrast, *Cuscuta* is known to be a phloem-feeding, obligate holoparasite, and has been shown to assimilate less than 1% of its own carbon by its own photosynthesis (Jeschke et al. 1994a). Excluding this particular datum from the data set results in an average difference between holoparasites and hosts of +1.0‰ ($P=0.007$, $n=27$), similar to the average difference that I observed of +1.5‰. Such results are also consistent with observations of holoparasitic plants in South Africa (de la Harpe et al. 1981). I calculated an average enrichment of +1.4‰ ($P=0.06$, $n=12$), based on data presented in Table 3 of de la Harpe et al.

The less negative holoparasite $\delta^{13}\text{C}_p$ relative to host leaves is consistent with a general pattern of ^{13}C enrichment in heterotrophic plant tissues relative to the leaves supplying them with photosynthate. This pattern has been observed in wood (Craig 1953; Leavitt and Long 1982; Francey et al. 1985), roots (Gebauer and Schulze 1991; Ineson et al. 1996; Syvertsen et al. 1997), fruits (Yoneyama and Ohtani 1983; Chapter 2), and emerging leaves (Terwilliger 1997; Terwilliger et al. 2001). In cases where $\delta^{13}\text{C}_c$ was analyzed, the pattern was generally the same as for $\delta^{13}\text{C}_p$ (Leavitt and Long 1982; Terwilliger et al. 2001). This contrasts with my results for holoparasitic plants, in which $\delta^{13}\text{C}_p$ was less negative than that of the leaves supplying them with photosynthate, but $\delta^{13}\text{C}_c$ was not. It should also be noted that not all holoparasitic plants show less negative $\delta^{13}\text{C}_p$ than their hosts; for example, the holoparasitic mistletoe *Tristerix aphyllus* consistently showed $\delta^{13}\text{C}_p$ values more negative than its hosts (Kraus et al. 1995).

The *Cuscuta* and *Cassytha* holoparasites that I sampled were assumed incapable of net photosynthesis, as has been demonstrated elsewhere by gas exchange measurements (de la Harpe et al. 1981; Jeschke et al. 1994a). However, members of both genera have been reported capable of low rates of $^{14}\text{CO}_2$ fixation (MacLeod 1961; de la Harpe et al. 1979). This photosynthetic capacity allows the plants to refix some respiratory CO_2 in the light. Thus, although there is not a net uptake of CO_2 from the atmosphere, there is a reduced rate of CO_2 efflux from the plants in the light compared to the CO_2 efflux rate in the dark (de la Harpe et al. 1981; Jeschke et al. 1994a). An analogous situation exists in woody tissues, where some respired CO_2 can be refixed in

the light by photosynthetic bark (e.g. Cernusak and Marshall 2000). This process has been shown to result in the retention of carbon having a $\delta^{13}\text{C}$ value more negative than that of the dark-respired CO_2 (Cernusak et al. 2001). The same process would be expected during refixation in holoparasitic plants. However, it would appear that the refixation of CO_2 relatively depleted in ^{13}C is generally not sufficient to counter the process that causes the dry matter of holoparasites to be enriched in ^{13}C compared to their hosts.

5.5.6. All species $\delta^{18}\text{O}$ and $\delta^{13}\text{C}$

I observed an increase of 2.6‰ in $\delta^{18}\text{O}_\text{p}$ between the December sampling and the February sampling averaged across all species; in contrast there was no change in $\delta^{13}\text{C}_\text{p}$ (Figures 5.3A and 5.3B). I previously observed a variation of 4‰ in $\delta^{18}\text{O}_\text{p}$ of *Lupinus angustifolius* L. leaves over the course of a diel cycle (Chapter 2); the variation was attributed to the daily accumulation and export of carbohydrates in equilibrium with $\delta^{18}\text{O}_\text{L}$. Given the apparent plasticity of the $\delta^{18}\text{O}_\text{p}$ of leaves in response to variation in $\delta^{18}\text{O}_\text{L}$, a seasonal shift across most species is not surprising. The magnitude of seasonal variation that I observed in $\delta^{18}\text{O}_\text{p}$ in southwestern Australia agrees well with recent observations for *Picea abies* in Switzerland, where $\delta^{18}\text{O}_\text{p}$ of current-year leaves increased by 2.1‰ from spring to summer (Jäggi et al. 2003).

I observed a large variation among species in ϵ_cp , the difference between $\delta^{18}\text{O}_\text{p}$ and $\delta^{18}\text{O}_\text{c}$ (Table 5.4). This may reflect differences among species in the timing and dynamics of leaf expansion. Other factors such as variation in leaf carbohydrate concentration or composition may also contribute. Until the processes underlying variation in ϵ_cp are better understood, it would be premature to conclude that $\delta^{18}\text{O}_\text{p}$ or $\delta^{18}\text{O}_\text{c}$ is likely to provide a more useful integrated record of $\delta^{18}\text{O}_\text{L}$.

Of the consistent differences that I observed in isotopic composition between parasitic plants and their hosts, some were easily interpretable in terms of mechanisms causing the variations. In other cases, data necessary for testing explanatory hypotheses were not available; these hypotheses await experimental testing in the future. Data describing the chemical and isotopic composition of solutes procured by parasites from the xylem and phloem sap of their hosts would be especially helpful in enabling some of these hypotheses to be tested.

Chapter 6: Environmental and physiological controls over the oxygen and carbon isotope composition of the Tasmanian blue gum, *Eucalyptus globulus*

6.1. Abstract

I measured oxygen isotope ratios ($\delta^{18}\text{O}$) of xylem sap, phloem sap, leaves, wood, and bark of *Eucalyptus globulus* growing in southwestern Australia. Carbon isotope ratios ($\delta^{13}\text{C}$) were measured in dry matter of phloem sap, leaves, and wood. Results were used to test several aspects of a mechanistic model of oxygen isotope enrichment, and additionally provided insights into post-photosynthetic variations in dry matter $\delta^{13}\text{C}$. Xylem water $\delta^{18}\text{O}$ varied little within different parts of the tree crown. Landscape-level variation in xylem water $\delta^{18}\text{O}$ was more pronounced, with plantations near the coast being enriched by up to 3‰ compared to plantations less than 100 km inland. Phloem water was significantly enriched in ^{18}O compared to xylem water in two of three sampling campaigns; mean enrichments were 0.5 and 0.8‰. Phloem sap sugars exported from *E. globulus* leaves closely reflected observed leaf water enrichment when diurnal variation in photosynthesis was taken into account. Photosynthesis was higher in the morning than in the afternoon, whereas leaf water ^{18}O enrichment increased to maximum values in the afternoon. A non-steady state model of leaf water ^{18}O enrichment accurately predicted observed values through a full diel cycle. Mean estimates of the proportion of organic oxygen effectively exchanging with xylem water during cellulose synthesis were very close to 0.40 for both leaves and wood. Carbon isotope ratios of nascent xylem tissues did not differ from those of phloem sap sugars collected concurrently. Nascent leaf tissues, on the other hand, were depleted in ^{13}C compared to phloem sap sugars by 2‰. These $\delta^{13}\text{C}$ results suggest that in *E. globulus*, ^{13}C enrichment of sink tissues compared to source leaves does not result from an enriching process within the sink tissue itself.

6.2. Introduction

Oxygen and carbon stable isotope ratios have become valuable tools for investigating plant ecophysiology and ecosystem processes (Yakir and Sternberg 2000; Adams and Grierson 2001; Dawson et al. 2002; Ehleringer et al. 2002; Maguas and Griffiths 2003). Mechanisms underlying variation in carbon isotope discrimination by

plants are generally well understood (Farquhar et al. 1989a); however, some patterns remain unexplained, such as the frequently observed enrichment of heterotrophic plant tissues in ^{13}C compared to the leaves supplying them with photosynthate (Brugnoli and Farquhar 2000; Hobbie and Werner 2004). Oxygen isotope ratios in plant organic material have been measured far less often than carbon isotope ratios. Although much progress has been made recently toward establishment of a general, synthetic model of oxygen isotope enrichment in plant organic material (Saurer et al. 1997; Farquhar et al. 1998; Barbour and Farquhar 2000; Roden et al. 2000; Helliker and Ehleringer 2002; Barbour et al. in press-b), some theoretical aspects remain untested, especially under field conditions.

In this paper, I present observations of oxygen isotope ratios of xylem sap, phloem sap, leaves, wood, and bark in the Tasmanian blue gum, *Eucalyptus globulus* Labill., growing in several plantations in southwestern Australia. These observations were used to test several aspects of a mechanistic model of oxygen isotope enrichment in plant organic material. Additionally, I present analyses of carbon isotope ratios in phloem sap, leaves, and wood, and discuss results in terms of the process or processes likely to cause ^{13}C enrichment in heterotrophic plant tissues compared to source leaves.

6.3. Theory

Liquid water within leaves becomes enriched in the heavy isotope ^{18}O during transpiration (Gonfiantini et al. 1965). Under steady-state conditions, the ^{18}O enrichment at the evaporative sites within leaves ($\Delta^{18}\text{O}_e$) can be modeled as (Craig and Gordon 1965; Dongmann et al. 1974; Farquhar and Lloyd 1993)

$$\Delta^{18}\text{O}_e = \varepsilon^+ + \varepsilon_k + \left(\Delta^{18}\text{O}_v - \varepsilon_k \right) \frac{e_a}{e_i}, \quad (6.1)$$

where ε^+ is the equilibrium fractionation between liquid water and vapor at the air-water interfaces, ε_k is the kinetic fractionation that occurs during water vapor diffusion from the leaf intercellular air space to the atmosphere, $\Delta^{18}\text{O}_v$ is the isotopic enrichment of vapor in the atmosphere compared to source water, and e_a/e_i is the ratio of ambient to intercellular vapor pressures. The equilibrium fractionation, ε^+ , can be calculated from a regression equation relating it to temperature (T , in K) (Bottinga and Craig 1969):

$$\varepsilon^+ (\text{‰}) = 2.644 - 3.206 \left(\frac{10^3}{T} \right) + 1.534 \left(\frac{10^6}{T^2} \right). \quad (6.2)$$

The T in this application of equation (6.2) refers to leaf temperature. The kinetic fractionation, ε_k , can be calculated as (Farquhar et al. 1989b)

$$\varepsilon_k(\text{‰}) = \frac{32r_s + 21r_b}{r_s + r_b}, \quad (6.3)$$

where r_s and r_b are the stomatal and boundary layer resistances to water vapor diffusion ($\text{m}^2 \text{s mol}^{-1}$), and 32 and 21 are associated fractionation factors scaled to per mil. Note that these fractionation factors have been revised up from values of 28 and 19, respectively, based on new measurements showing the isotope effect for diffusion of H_2^{18}O in air to be 1.032 (Cappa et al. 2003), rather than 1.028 (Merlivat 1978). Throughout this paper, I express the oxygen isotope enrichment of any water or dry matter component ($\Delta^{18}\text{O}$) relative to source water as $\Delta^{18}\text{O} = R/R_s - 1$, where R is $^{18}\text{O}/^{16}\text{O}$ of the sample of interest and R_s is $^{18}\text{O}/^{16}\text{O}$ of source water. Equation (6.1) is a convenient approximation of the mathematically correct form of this particular model, which it underestimates by about 0.1‰ (Farquhar and Lloyd 1993). I consider this bias to be negligible, as discussed in more detail elsewhere (Chapter 4).

The $\Delta^{18}\text{O}$ of water in the leaf mesophyll is expected to be less than that at the evaporative sites due to the influx of relatively unfractionated vein water. Farquhar and Lloyd (1993), and more recently Farquhar and Gan (2003), suggested that the $\Delta^{18}\text{O}$ of average lamina mesophyll water ($\Delta^{18}\text{O}_L$) could be related to $\Delta^{18}\text{O}_e$ as

$$\Delta^{18}\text{O}_L = \frac{\Delta^{18}\text{O}_e (1 - e^{-\wp})}{\wp}, \quad (6.4)$$

where \wp is a lamina radial Péclet number (Farquhar and Gan 2003), defined as $EL/(CD)$, where E is transpiration rate ($\text{mol m}^{-2} \text{s}^{-1}$), L is a scaled effective path length (m), C is the molar concentration of water (mol m^{-3}), and D is the diffusivity of H_2^{18}O in water ($\text{m}^2 \text{s}^{-1}$).

Barbour and Farquhar (2000) related the ^{18}O enrichment of plant cellulose ($\Delta^{18}\text{O}_c$) to $\Delta^{18}\text{O}_L$ as

$$\Delta^{18}\text{O}_c = \Delta^{18}\text{O}_L (1 - p_{\text{ex}} p_x) + \varepsilon_{\text{wc}}, \quad (6.5)$$

where p_{ex} is the proportion of oxygen atoms exchanging with medium water in the developing tissue during cellulose synthesis, p_x is the proportion of unenriched source water in the developing tissue, i.e. water originating from the xylem rather than the leaf mesophyll, and ε_{wc} is the equilibrium fractionation between organic oxygen and medium water, which has a value of +27‰ (Sternberg and DeNiro 1983; Sternberg et

al. 1984; Yakir and DeNiro 1990). The term p_x is expected to be less than unity because enriched water can be transferred from the leaf mesophyll into developing cells by translocation in the phloem (Barbour and Farquhar 2000; Chapter 2; Chapter 4). I suggest that p_x can be calculated as

$$p_x = 1 - \rho \left(\frac{\Delta^{18}O_{pw}}{\Delta^{18}O_L} \right), \quad (6.6)$$

where ρ is the proportion of water in the developing cell coming from phloem as opposed to xylem, and $\Delta^{18}O_{pw}$ is the phloem water enrichment compared to source water. Thus, p_x measures the extent to which water in the developing cell is xylem-like in its oxygen isotope composition. The term ρ is a measure of the deviation from this state caused by the contribution of phloem water; however, phloem water only has an effect if it is enriched, and $(\Delta^{18}O_{pw}/\Delta^{18}O_L)$ is a measure of how enriched, or how mesophyll-like, it is. Equation (6.6) assumes that water in the developing cell is not further enriched by evaporation after it has entered the cell; it may need to be modified for application in leaves if it is found that water in developing leaf cells becomes directly enriched by transpiration while cellulose synthesis is occurring. Barbour and Farquhar (2000) suggested that p_{ex} can be modeled as

$$p_{ex} = 0.2 + y \left(0.6 + \frac{0.2}{2 - y} \right), \quad (6.7)$$

where y is the proportion of hexose phosphates that cycle through to triose phosphates before being incorporated into cellulose. Barbour and Farquhar (2000) further suggested that a term ε_{cp} could be added to the right side of equation (6.5) so that it could be applied to $\Delta^{18}O$ of total dry matter ($\Delta^{18}O_p$), in addition to cellulose:

$$\Delta^{18}O_p = \Delta^{18}O_L (1 - p_{ex} p_x) + \varepsilon_{wc} + \varepsilon_{cp}. \quad (6.8)$$

The term ε_{cp} is an empirical term, and is simply calculated as the difference between $\Delta^{18}O$ for total dry matter and $\Delta^{18}O$ of cellulose extracted from it.

Equation (6.1) predicts evaporative site water enrichment under steady state conditions. Whereas leaves may be likely to reach isotopic steady state in the early afternoon (Harwood et al. 1998), there will undoubtedly be times when leaf water enrichment is not at steady state. Therefore, non-steady state variation must be considered when modeling leaf water ^{18}O enrichment in the field. Farquhar and Cernusak (in preparation) have derived a non-steady state modification of equation (6.4):

$$\Delta^{18}O_{Ln} = \Delta^{18}O_L - \left(\frac{1 - e^{-\phi}}{\phi} \right) \left[\frac{d(W\Delta^{18}O_{Ln})}{dt} \right] \frac{1}{gw_i}, \quad (6.9)$$

where $\Delta^{18}O_{Ln}$ is the non-steady average lamina leaf water ^{18}O enrichment, W is the lamina leaf water concentration (mol m^{-2}), t is time (s), g is the total conductance to water vapor of stomata plus boundary layer ($\text{mol m}^{-2} \text{s}^{-1}$), and w_i is the mole fraction of water vapor in the leaf intercellular air spaces (mol mol^{-1}). Because the term $\Delta^{18}O_{Ln}$ occurs on both sides of equation (6.9), it must be solved iteratively. I suggest that the solver function in Microsoft Excel provides a simple means of achieving this. Equation (6.9) is similar to the non-steady state equation presented for average lamina leaf water in Chapter 2, but differs in the inclusion of the term $(1 - e^{-\phi})/\phi$. The inclusion of this term represents a revision to the derivation, as will be explained by Farquhar and Cernusak (in preparation).

Under field conditions, equation (6.5) should be modified such that the leaf water enrichment term is weighted by photosynthesis:

$$\Delta^{18}O_c = \frac{\int A \Delta^{18}O_L}{\int A} (1 - p_{ex} p_x) + \varepsilon_{wc}, \quad (6.10)$$

where $\int A \Delta^{18}O_L$ is the daily integral of the product of photosynthesis and leaf water enrichment (‰ mol m^{-2}) and $\int A$ is the daily integral of photosynthesis (mol m^{-2}). This modification of equation (6.5) allows for differing diurnal patterns of variation in $\Delta^{18}O_L$ and A . Equation (6.8) can be similarly modified:

$$\Delta^{18}O_p = \frac{\int A \Delta^{18}O_L}{\int A} (1 - p_{ex} p_x) + \varepsilon_{wc} + \varepsilon_{cp}. \quad (6.11)$$

6.4. Materials and Methods

6.4.1. Sampling campaign 1

Samples for $\Delta^{18}O$ analysis were collected from *Eucalyptus globulus* Labill. plantations in southwestern Australia on three occasions. An overview of the sampling sites is shown in Figure 6.1. Locations, year of planting, and sampling date are given in Table 6.1.

The first sampling campaign took place at the Mount Barker plantation on 3 November, 2000. Six trees, approximately 5 m in height, were harvested at two to three

hour intervals beginning at 0500 hrs and finishing at 2000 hrs. Leaves were collected separately for leaf water extraction from the upper and lower canopy. One fully-expanded leaf was collected from each of four sides of the tree, and one half of the lamina quickly separated from the midrib. The four lamina halves were sealed together in a glass tube with a rubber stopper embedded in a screw cap. Sampled leaves had areas of approximately 60 cm². Newly emerged leaves at the apex of the main stem were also collected for water extraction. The upper-most 3 cm of the apices was collected, which included leaves with areas ranging from 0.1 to 3 cm².

Table 6.1. *Locations, year of planting, and time of sampling for E. globulus plantations in southwestern Australia.*

Plantation	Latitude	Longitude	Year of planting	Time of sampling
Denbarker	-34°42'41" S	117°30'22" E	1997	December 2001
Denmark	-34°58'45" S	117°20'06" E	1999	December 2001
Eulup	-34°36'51" S	117°33'04" E	1997	December 2001
Frankland	-34°19'24" S	116°57'26" E	1997	December 2001
Kwornicup	-34°33'24" S	117°24'24" E	1997	December 2001
Mount Barker	-34°32'28" S	117°30'24" E	1999	November 2000, March 2001
Peaceful Bay	-35°01'36" S	116°53'44" E	2000	December 2001
Redmond	-34°54'19" S	117°36'39" E	1997	December 2001
St. Werburghs	-34°39'32" S	117°34'19" E	1997	December 2001

Gas exchange was measured on five to 10 fully-expanded leaves from the upper and lower canopy under ambient conditions with an LCA 4 portable gas exchange system (ADC Bioscientific Ltd, Hoddesdon, Hertfordshire, UK). Leaf temperature of five leaves was measured with a 0.13 mm-diameter chromel-constantan thermocouple (Omega Engineering, Stamford, CT, USA). Ambient air temperature and relative humidity were measured with a Vaisala temperature and humidity probe (Vaisala Inc, Helsinki, Finland).

Phloem sap was collected from the upper and lower main stem, as described previously for *E. globulus* (Pate et al. 1998). Phloem sap droplets were attracted into microcapillary tubes immediately upon exudation and expressed into small vials which were sealed to prevent evaporation. Xylem sap was collected from the upper and lower main stem by a mild-vacuum extraction technique described previously (Jeschke and Pate 1995; Dawson and Pate 1996; Pate and Arthur 2000; Chapter 2). All samples were

frozen upon collection in a portable freezer. Leaf and apex water was later extracted by cryogenic distillation.

6.4.2. *Sampling campaign 2*

The second sampling campaign took place at the Mount Barker plantation on 13 and 14 March, 2001. Five trees, 5 to 6 m tall, were harvested at times varying between 0530 hrs and 1500 hrs. The leaf water sampling scheme was similar to that conducted in the first campaign, except that the canopy was stratified into four levels instead of two. Phloem and xylem sap were collected from four levels of the main stem, as well as from inner and outer branches of canopy level two, where level one was the base of the crown, and level four the top. Xylem wood and bark were also collected from the stem or branch sections from which phloem sap and xylem sap were collected, and quickly sealed in glass tubes. Xylem wood from the stem sections sampled for xylem water by mild-vacuum extraction was later subjected to cryogenic distillation to test whether the non-mobile xylem water in the stem had a different isotopic signature from the mobile xylem water.

6.4.3. *Sampling campaign 3*

The third sampling campaign took place between 5 and 12 December, 2001. The first experiment in this sampling campaign was aimed at examining isotopic fractionation between phloem sap sugar and newly synthesized xylem wood. Phloem sap, newly differentiated xylem tissue, and mature xylem tissue were sampled from six trees at each of six plantations of similar age, and distributed over a rainfall and productivity gradient. These plantations were Denbarker, Eulup, Frankland, Kwormicup, Redmond, and St. Werburghs. Trees in these plantations ranged from approximately 10 to 16 m in height. Phloem sap was collected from near breast height in the manner described previously. A square window of bark, approximately 15 cm by 15 cm, was then removed from the same location. The gelatinous layer of recently differentiated xylem tissue was gently scraped off the inner face of the exposed surface of cambium with a clean razor blade and placed into a vial of ethanol. This sampling procedure has been described previously in more detail (Pate and Arthur 1998). A chisel and hammer were used to quickly remove two to three pieces of mature xylem tissue (approximately 0.75 cm wide by 3 cm long), penetrating radially to approximately 0.75 cm depth from the cambium surface. These tissues were sealed in

glass tubes and frozen. Xylem water was later extracted from these tissues by cryogenic distillation.

The second experiment in the third sampling campaign was aimed at investigating the diel variation in $\Delta^{18}\text{O}$ of leaf water, phloem sap, and leaf dry matter. Sampling took place at the Denmark plantation on 7 and 8 December, 2001. Samples were collected ten times at approximately 3 hr intervals between 1800 hrs on day 1 and 2030 hrs on day 2. For each sample collection time, three uniform trees of approximately 10 m height were selected. Fully-expanded leaves were collected from the lower-middle canopy as described previously. Phloem sap was collected from the main stem at the same canopy height. Xylem water was collected by mild-vacuum extraction from one branch on each tree at the same canopy height. Atmospheric water vapor in the vicinity of the sampled trees was collected by drawing canopy air through an ethanol-dry ice trap at a flow rate of approximately 1 L min^{-1} . Three leaves from each sampled tree were collected and quickly sealed and frozen in glass tubes for gravimetric measurement of leaf water concentrations. Gas exchange was measured on five to 10 leaves, and leaf temperature, air temperature, and relative humidity were measured as described above.

The third component of the third sampling campaign was aimed at investigating variation in bark and xylem water along the length of branches, and at comparing leaf water and dry matter enrichment in expanding versus fully-expanded leaves. Sampling took place on 12 December, 2001 at the Peaceful Bay plantation. Three fully expanded leaves were sampled from the middle canopy of five trees, and half the lamina of each retained for leaf water extraction. Ten expanding leaves were sampled from each of the same trees. These leaves had areas of approximately 10 cm^2 , whereas the fully-expanded leaves had areas of approximately 60 cm^2 . The midrib was quickly cut out with a razor blade and both halves of all ten lamina retained for leaf water extraction. A branch section was cut from each tree from near where the branch joined the main stem. Xylem and bark tissue were separated and quickly sealed and frozen in glass tubes. The procedure was repeated with a branch section from halfway between the branch base and branch tip. The second internode from the branch tip was then collected from eight branches on each tree and quickly separated into bark and xylem, which were sealed in glass tubes and frozen. Water in all these samples was later extracted by cryogenic distillation.

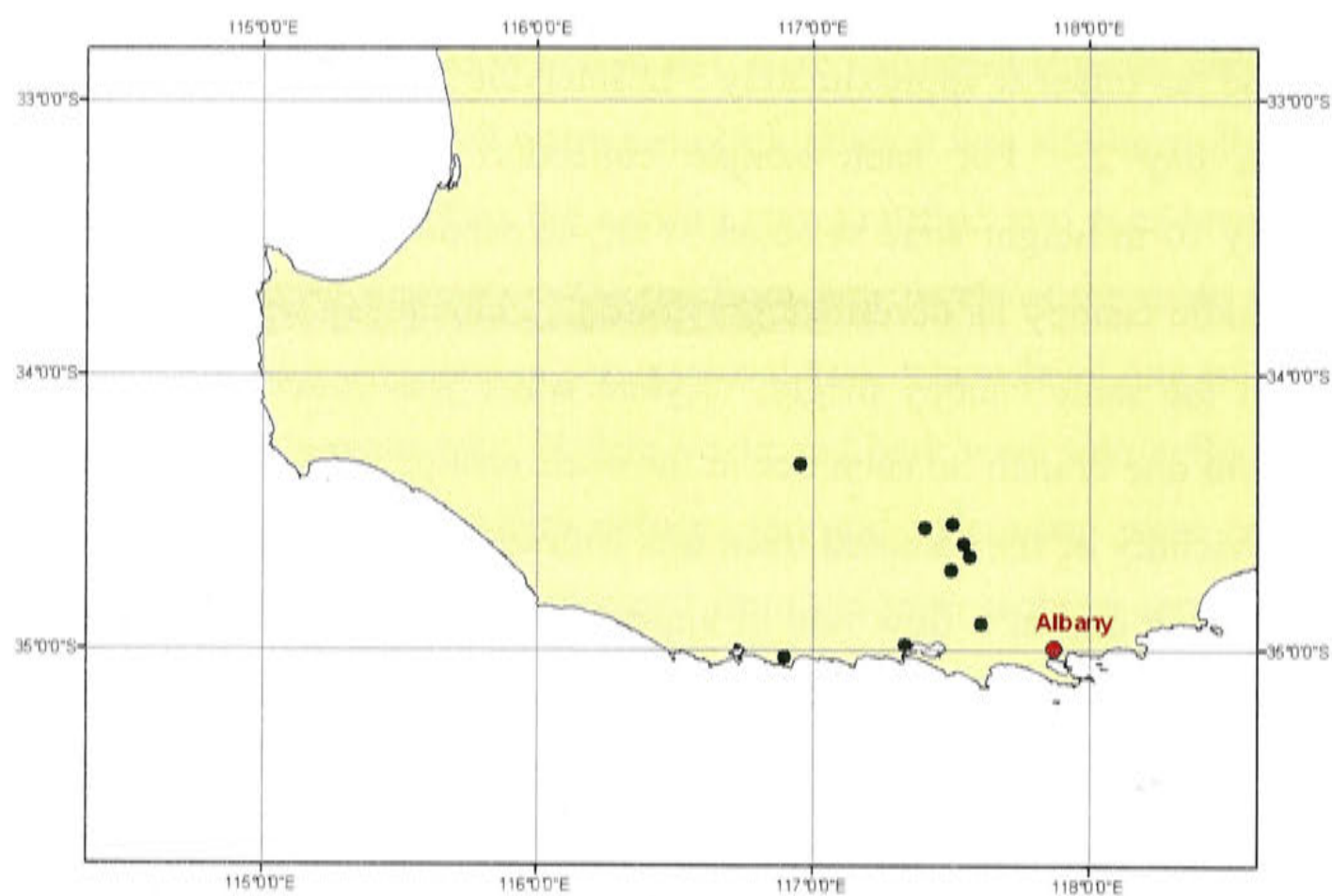


Figure 6.1. A map of southwestern Australia showing the location of sampled *E. globulus* plantations. The town of Albany is shown as a point of reference. Note that the coastline in the vicinity of the sampled plantations is very close to 35°S latitude.

6.4.4. Isotopic analyses

Oxygen isotope ratios of water and dry matter samples were measured as described previously (Farquhar et al. 1997). Analyses took place in an Isochrom mass spectrometer (Micromass, Manchester, UK) following pyrolysis in a Carlo Erba elemental analyzer (CE Instruments, Milan, Italy) or a custom-built furnace. Phloem sap dry matter oxygen isotope ratios were measured on samples that were oven-dried overnight at 60°C. Samples were sealed under argon in tin cups immediately following removal from the drying oven to prevent hydration of the sugars by vapor in the ambient air (Chapter 3). Phloem sap water oxygen isotope ratios were determined as described previously (Chapter 2), based on a technique for determination of the water component of a homogenous mixture of water and dry matter (Gan et al. 2002). Oxygen isotope ratios were obtained in delta notation ($\delta^{18}\text{O}$) expressed relative to Vienna Standard Mean Ocean Water. Precision of analyses, based on repeated measurements of laboratory sucrose and water standards, was $\pm 0.3\text{‰}$. The $\delta^{18}\text{O}$ values of all components except xylem water are expressed as enrichment above xylem water ($\Delta^{18}\text{O}$), calculated as $\Delta^{18}\text{O} = (\delta^{18}\text{O} - \delta^{18}\text{O}_x) / (1 + \delta^{18}\text{O}_x)$, where $\delta^{18}\text{O}$ refers to the sample of interest and $\delta^{18}\text{O}_x$ is the corresponding value for xylem water.

Carbon isotope ratios of dry matter samples were analyzed in an Isochrom mass spectrometer (Micromass, Manchester, UK) following combustion in a Carlo Erba elemental analyzer (CE Instruments, Milan, Italy). Values were obtained in delta notation ($\delta^{13}\text{C}$) relative to the Pee Dee Belemnite standard. The $\delta^{13}\text{C}$ values were then converted to carbon isotope discrimination values ($\Delta^{13}\text{C}$) according to the equation $\Delta^{13}\text{C} = (\delta^{13}\text{C}_a - \delta^{13}\text{C}) / (1 + \delta^{13}\text{C})$, where $\delta^{13}\text{C}$ is the sample of interest and $\delta^{13}\text{C}_a$ is the value for CO_2 in the air. The $\delta^{13}\text{C}_a$ was assumed to be -7.8‰ .

Approximately half the dry matter samples were subjected to α -cellulose extraction. The extraction procedure was as described by Barbour and Farquhar (2000), based on the modified technique of Loader et al. (1997). The α -cellulose samples were analyzed first for $\delta^{18}\text{O}$, then for $\delta^{13}\text{C}$ if sufficient sample remained. The collections of recently differentiated xylem tissues were washed three times in 80% ethanol and oven dried prior to isotopic analyses (Pate and Arthur 1998). Dry matter was then bulked for the six trees from each plantation to provide sufficient material for α -cellulose extraction.

A subset of 10 phloem sap samples was randomly selected and the ionizable solutes removed with a cation/anion exchange resin (Bio-Rad AG 501-X8, Bio-Rad Laboratories, Hercules, CA, USA). The remaining sugar fraction of the sap was oven dried and analyzed for $\delta^{18}\text{O}$. Bulk phloem sap dry matter $\delta^{18}\text{O}$ values did not differ from resin-treated sugar $\delta^{18}\text{O}$ values ($P=0.26$, $n=10$); the mean difference was 0.3‰. A similar result was found for $\delta^{13}\text{C}$ of bulk phloem sap dry matter for *E. globulus* versus $\delta^{18}\text{O}$ of the purified sugar fraction (Pate and Arthur 1998). Based on these results, I concluded that the isotopic composition of the bulk phloem sap dry matter in my samples was representative of phloem sap sugars. No further attempt was made to separate the sugar and non-sugar fractions for isotopic analyses.

6.4.5. Isotopic calculations

The term p_{ex} was calculated for the recently differentiated xylem tissue samples and the stem apices with equation (6.10) by replacing the term $(\int A \Delta^{18}\text{O}_L / \int A)$ with the term $(\Delta^{18}\text{O}_{\text{suc}} - \epsilon_{\text{wc}})$, where $\Delta^{18}\text{O}_{\text{suc}}$ is the oxygen isotope enrichment measured in phloem sap dry matter (Barbour et al. 2000b; Chapter 4). The term p_x was estimated from equation (6.6) by similarly replacing $\Delta^{18}\text{O}_L$ with $(\Delta^{18}\text{O}_{\text{suc}} - \epsilon_{\text{wc}})$. Literature estimates of ρ , the proportion of water in developing cells coming from phloem rather than xylem, range from 0.5 to 0.8 (Schmalstig and Cosgrove 1990; Bret-Harte and Silk 1994; Pritchard et al. 2000). I assumed an intermediate value of 0.65 for calculations of p_x .

An additional estimate of p_{ex} was made for fully-expanded leaf samples by plotting their $\Delta^{18}\text{O}_p$ values against corresponding $\Delta^{18}\text{O}_{\text{suc}}$ for phloem sap collected from the same tree from the same canopy height. Equation (6.11) was modified by replacing $(\int A \Delta^{18}\text{O}_L / \int A)$ with $(\Delta^{18}\text{O}_{\text{suc}} - \epsilon_{\text{wc}})$ and rearranged:

$$\Delta^{18}\text{O}_p = \Delta^{18}\text{O}_{\text{suc}} (1 - p_{\text{ex}} p_x) + \epsilon_{\text{wc}} p_{\text{ex}} p_x + \epsilon_{\text{cp}} \quad (6.12)$$

Using equation (6.12), the term $(1 - p_{\text{ex}} p_x)$ can be estimated from the slope of a regression analysis of the relationship between $\Delta^{18}\text{O}_p$ and $\Delta^{18}\text{O}_{\text{suc}}$. Such an analysis requires some assumptions, namely that xylem water $\delta^{18}\text{O}$ and $\Delta^{18}\text{O}_{\text{suc}}$ are the same as when leaf dry matter was formed. Additionally, the terms $p_{\text{ex}} p_x$ and ϵ_{cp} are assumed constant. These assumptions will be addressed in the discussion.

In the third sampling campaign, during the diel leaf water collections, gas exchange was not measured for the nighttime collection times when the ambient vapor pressure was near saturation. For leaf water modeling at these times, stomatal

conductance was assumed to be $20 \text{ mmol m}^{-2} \text{ s}^{-1}$, based on measurements of nighttime stomatal conductance in another *Eucalyptus* species (L. Cernusak, unpublished data). For leaf water modeling, boundary layer conductance was assumed to be $0.9 \text{ mol m}^{-2} \text{ s}^{-1}$. The scaled effective path length, L , for calculation of the Péclet number in equations (6.4) and (6.9), was estimated from the discrepancy between predicted $\Delta^{18}\text{O}_e$ and observed $\Delta^{18}\text{O}_L$ in early afternoon samples when $\Delta^{18}\text{O}_L$ was assumed to be at steady state.

Variation in isotopic parameters was assessed with analysis of variance, linear regression, or paired *t*-test. In cases where pair-wise comparisons were made following analyses of variance, Tukeys method was used. Statistical analyses were performed in SYSTAT 9.0 (SPSS Inc, Chicago, IL, USA).

6.5. Results

6.5.1. Xylem water $\delta^{18}\text{O}$

The plantations that I sampled were located across a latitudinal gradient that also corresponds to a rainfall gradient (Figure 6.2). Total rainfall for 2001 decreased linearly with south latitude for seven weather stations located in the vicinity of the sampled plantations, and covering approximately the same latitudinal range. As seen in Figure 6.1, the coastline in this part of southwestern Australia runs in an east-west direction, such that distance north from -35° South latitude is effectively a measure of distance from the coast. Locations of the plantations that I sampled thus varied from very near the coast to approximately 80 km inland. Annual rainfall decreases sharply as one progresses inland, and there is a corresponding, and linearly related variation in xylem water $\delta^{18}\text{O}$ (Figure 6.3). Plantations nearer the coast during the December 2001 sampling campaign had xylem water that was enriched in ^{18}O by as much as 3‰ compared to plantations furthest inland.

There was a slight tendency for xylem water in upper stems to be enriched in ^{18}O relative to that in lower stems in the trees sampled at the Mount Barker plantation in November 2000. Mean values were -3.6 and -4.0 ‰, respectively; the difference was moderately significant ($P=0.05$, $n=6$). A similar tendency was observed at the same plantation in March 2001, with xylem water $\delta^{18}\text{O}$ increasing from -3.7 ‰ at the base of the stem to -3.2 ‰ at the top of the stem (Table 6.2); this difference was not statistically significant. There was a tendency for xylem water sampled from branch tips at the

Peaceful Bay plantation to be enriched by about 1‰ compared to xylem water sampled from the middle and bases of branches (Table 6.3).

The $\delta^{18}\text{O}$ of mobile xylem water extracted from stem xylem tissues by mild-vacuum extraction did not differ from that of non-mobile xylem water extracted later from the same tissues by cryogenic distillation ($P=0.34$, $n=20$). Mean values were -3.5‰ and -3.7‰ , respectively. Bark water $\delta^{18}\text{O}$ did not differ from xylem water $\delta^{18}\text{O}$ ($P=0.59$, $n=14$).

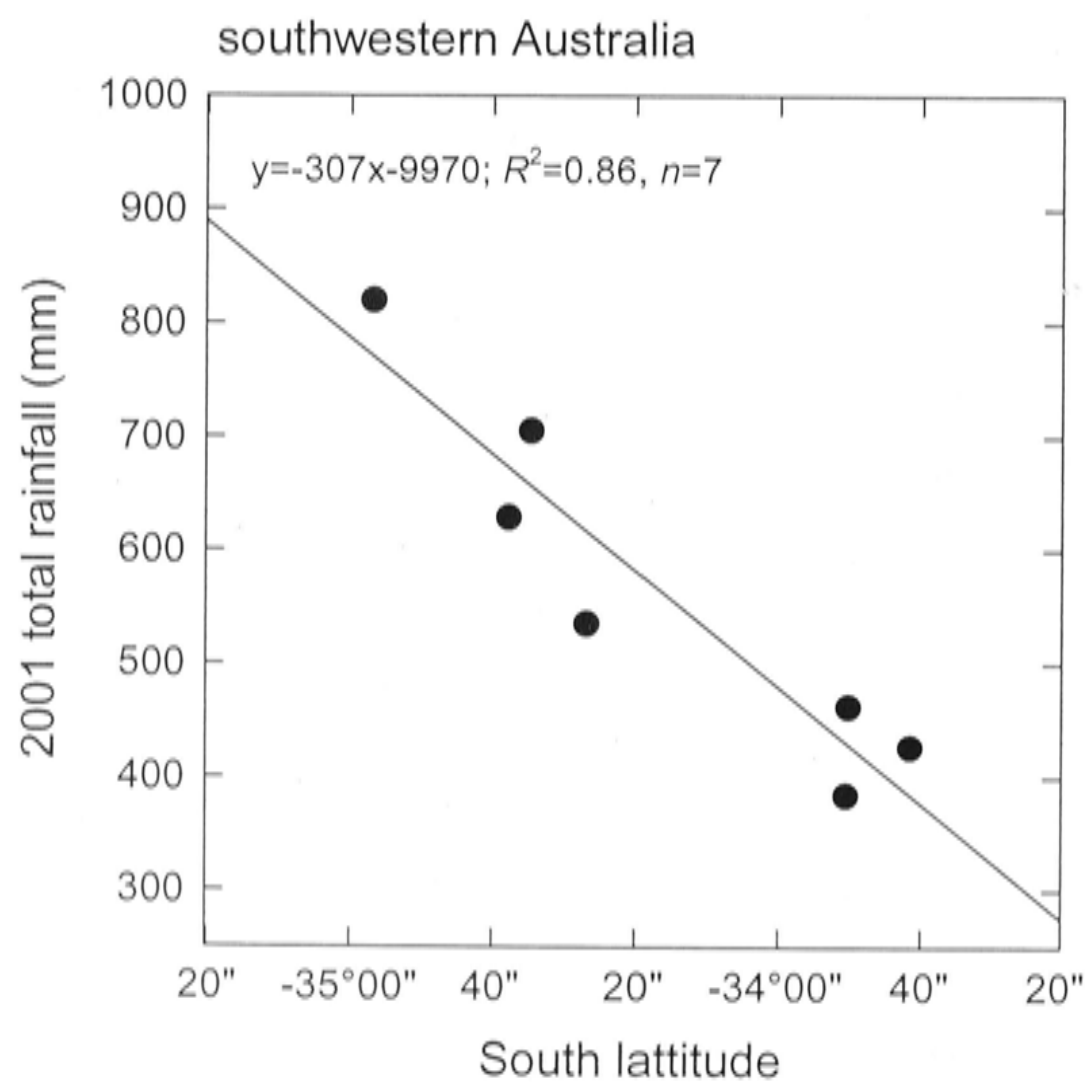


Figure 6.2. Annual rainfall for 2001 plotted against south latitude for seven weather stations in the vicinity of the sampled plantations, and covering approximately the same latitudinal range.

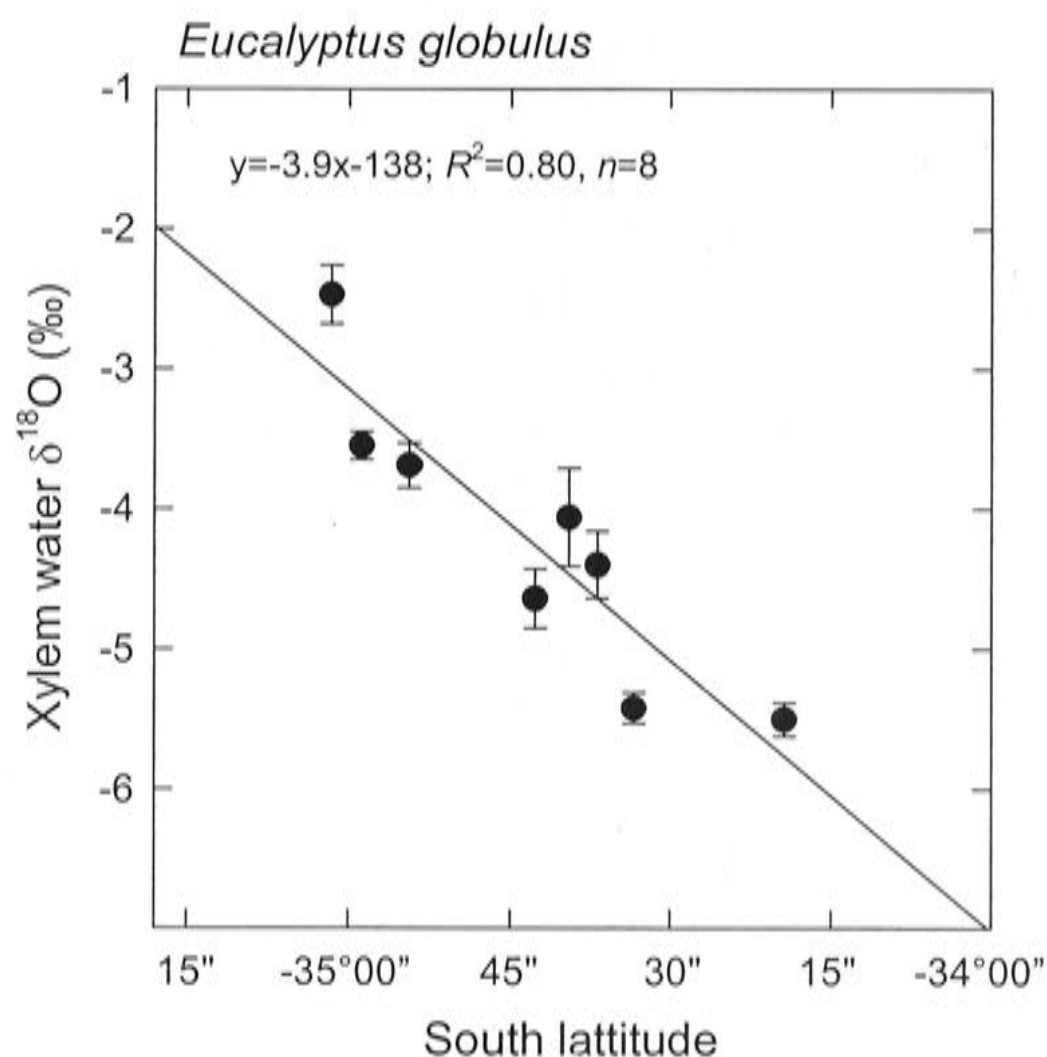


Figure 6.3. Mean xylem water $\delta^{18}\text{O}$ of sampled *E. globulus* plantations plotted against south latitude. At least five trees were sampled within each plantation; samples were collected in December 2001. Error bars represent 1 SE.

6.5.2. Leaf water $\Delta^{18}\text{O}$

Observed leaf water ^{18}O enrichment for fully-expanded leaves ranged from 6.3 to 19.7‰. It was consistently lower than predicted $\Delta^{18}\text{O}_e$ during the day, and higher at night (Tables 6.3, 6.4 and 6.5; Figure 6.4). I did not observe a pronounced variation in observed $\Delta^{18}\text{O}_L$ of fully-expanded leaves among different crown positions (Tables 6.4 and 6.5). Enrichment of water extracted from stem apices was less than that observed in fully-expanded leaves by values ranging from 2.2 to 10.6‰, and showed a dampened diurnal cycle compared to observed $\Delta^{18}\text{O}_L$ for fully-expanded leaves (Table 6.4). Expanding leaves collected at the Peaceful Bay plantation had $\delta^{18}\text{O}_L$ values that were higher than those for fully-expanded leaves by 1.7‰; however this difference was reduced to 0.7‰ and was no longer significant when leaf water $\delta^{18}\text{O}_L$ values were expressed as enrichment above xylem water (Table 6.3).

Table 6.2. Variation in isotopic parameters within the crown in *E. globulus* trees sampled at the Mount Barker plantation in March 2001. Values in parentheses are 1 SE ($n=5$). Values within a row followed by different letters are significantly different at $P<0.05$. Branches were sampled from the lower, middle crown.

Isotopic parameter (‰)	Main stem				Branches	
	Lower	Lower, middle	Upper, middle	Upper	Inner	Outer
Xylem water $\delta^{18}\text{O}$	-3.7 (0.3) a	-3.5 (0.1) a	-3.4 (0.1) a	-3.2 (0.2) a	-3.0 (0.4) a	-3.5 (0.2) a
Phloem sap $\Delta^{18}\text{O}_{\text{suc}}$	43.0 (0.6) a	42.4 (0.5) a	42.3 (0.4) a	41.8 (0.6) a	43.0 (0.8) a	42.0 (0.1) a
Mature xylem $\Delta^{18}\text{O}_p$	32.2 (0.7) a	30.7 (0.4) ab	31.0 (0.4) a	30.9 (0.3) a	28.7 (0.5) b	30.5 (0.4) ab
Bark $\Delta^{18}\text{O}_p$	30.7 (0.5) a	30.6 (0.2) a	29.8 (0.7) ab	28.2 (0.5) ab	27.4 (0.9) b	28.8 (0.5) ab
Leaf $\Delta^{18}\text{O}_p$	33.7 (0.4) a	33.7 (0.3) a	34.1 (0.4) a	33.2 (0.2) a		
Phloem sap $\Delta^{13}\text{C}$	15.4 (0.3) a	15.2 (0.2) a	15.0 (0.1) a	14.8 (0.1) a		
Mature xylem $\Delta^{13}\text{C}_p$	17.3 (0.5) a	17.4 (0.3) a	16.6 (0.5) a	16.0 (0.5) a		
Leaf $\Delta^{13}\text{C}_p$	19.6 (0.2) a	19.4 (0.3) ab	18.5 (0.2) b	16.5 (0.3) c		

Table 6.3. Xylem water $\delta^{18}\text{O}$ in different branch sections of *E. globulus*, along with observed lamina leaf water $\delta^{18}\text{O}$. Values in parentheses are 1 SE ($n=5$). Values within a row followed by different letters are significantly different at $P<0.05$. Note that the observed leaf water $\delta^{18}\text{O}$ is different between fully-expanded leaves on the middle of branches and expanding leaves at the tips; however, the difference disappears when leaf water $\delta^{18}\text{O}$ is expressed as enrichment above xylem water ($\Delta^{18}\text{O}_L$). Samples were collected between 1300 and 1400 hrs at the Peaceful Bay plantation in December 2001.

Isotopic composition (‰)	Position on branch		
	Base	middle	tip
Xylem water $\delta^{18}\text{O}$	-2.5 (0.3) a	-2.4 (0.1) a	-1.5 (0.4) a
Observed leaf water $\delta^{18}\text{O}$		10.8 (0.6) a	12.5 (0.5) b
Observed $\Delta^{18}\text{O}_L$		13.3 (0.6) a	14.0 (0.6) a
Predicted $\Delta^{18}\text{O}_e$		15.4	15.4

Table 6.4. Observed leaf water enrichment in samples collected at the Mount Barker plantation in November 2000. Also shown is the predicted steady-state evaporative site water enrichment at the times of collection.

Leaf water ^{18}O enrichment (‰)	Time of day					
	0500	0800	1100	1400	1700	2000
Observed upper canopy $\Delta^{18}\text{O}_L$	10.3	9.5	11.1	19.7	16.2	12.5
Observed lower canopy $\Delta^{18}\text{O}_L$	9.2	9.1	10.9	16.5	16.6	12.4
Observed stem apices $\Delta^{18}\text{O}_L$	6.9	6.9	7.2	9.1	10.3	8.6
Predicted steady-state $\Delta^{18}\text{O}_e$	2.1	11.7	22.9	24.0	12.7	0.8

Table 6.5. Observed lamina leaf water enrichment in samples collected at the Mount Barker plantation in March 2001. Also shown is the predicted steady-state evaporative site water enrichment at the times of collection.

Leaf water ^{18}O enrichment (‰)	Time, day 1			Time, day 2	
	1000	1200	1500	0530	1000
Observed upper canopy $\Delta^{18}\text{O}_L$	11.5	13.2	19.6	12.0	16.2
Observed upper, middle canopy $\Delta^{18}\text{O}_L$	9.4	13.2	18.8	11.9	15.4
Observed lower, middle canopy $\Delta^{18}\text{O}_L$	6.8	13.3	18.4	14.3	14.7
Observed lower canopy $\Delta^{18}\text{O}_L$	7.9	14.6	17.3	15.1	14.4
Predicted steady-state $\Delta^{18}\text{O}_e$	18.6	21.9	26.7	3.5	23.1

Departures from steady-state predictions of $\Delta^{18}\text{O}_L$ were especially apparent at night, whereas non-steady state predictions using equation (6.9) were close to observed $\Delta^{18}\text{O}_L$ values throughout a full diel cycle (Figure 6.4). The $\delta^{18}\text{O}$ values for atmospheric water vapor during the diel leaf water sampling at the Denmark plantation ranged from -10.8 to -14.0‰ , yielding $\Delta^{18}\text{O}_v$ values ranging from -7.3 to -10.5‰ . Leaf water concentrations ranged from 10.4 to 13.9 mol m^{-2} . Xylem water $\delta^{18}\text{O}$ values did not show a diel trend, and averaged $-3.5 \pm 0.1\text{‰}$ (mean \pm 1SE). Relative humidity and air temperature ranged from 0.51 to 0.95 , and from 6.5 to 20.3°C , respectively. Leaf temperatures were generally within 1°C of air temperature. Transpiration ranged from 0 to $1.9 \text{ mmol m}^{-2} \text{ s}^{-1}$ on a projected leaf area basis. The scaled effective path length for *E. globulus* leaves was estimated to be 54 mm , using the revised values for ϵ_k , or 25 mm , using the previously accepted values for ϵ_k .

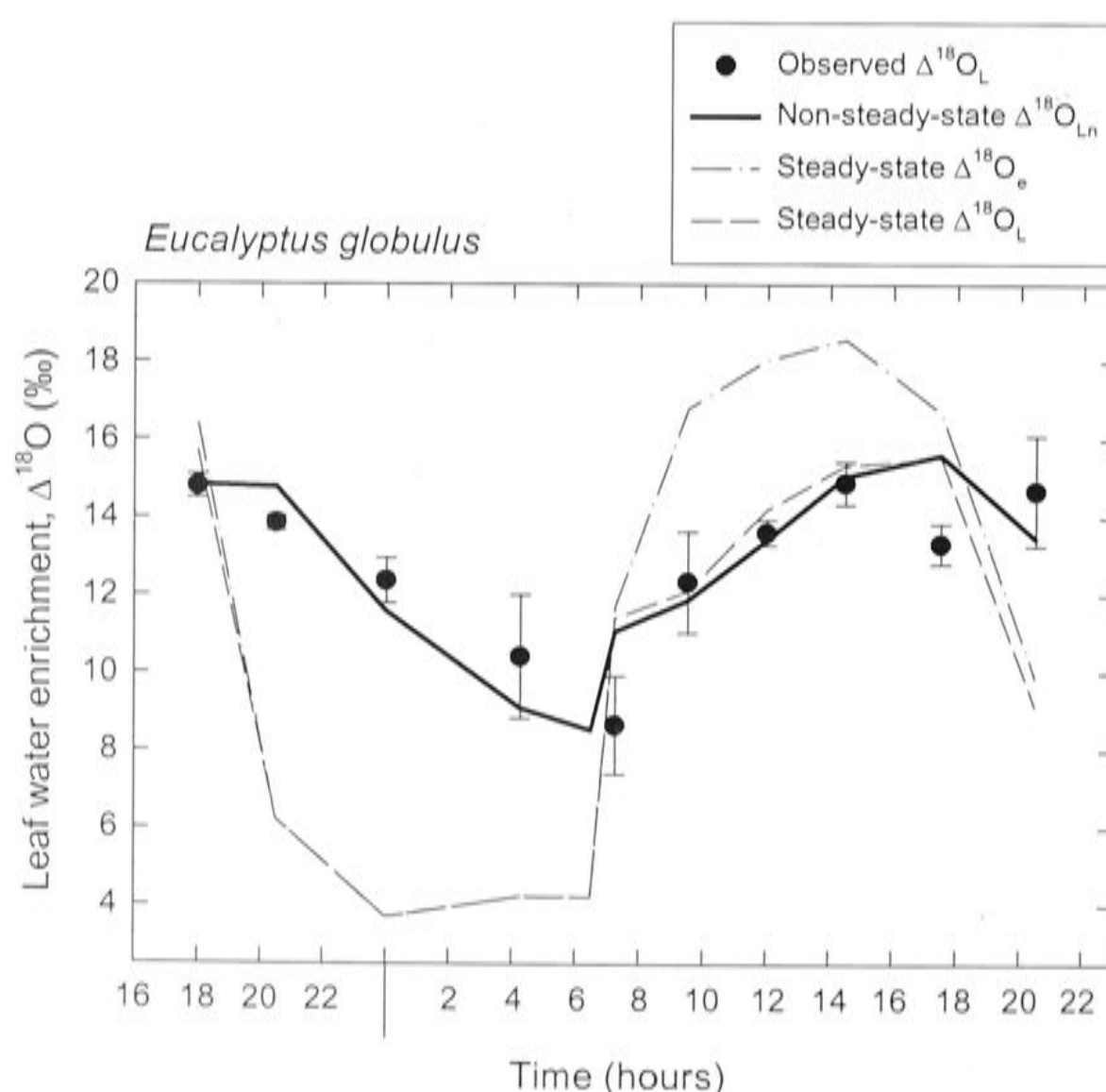


Figure 6.4. Diel variation in observed and predicted oxygen isotope enrichment of *E. globulus* leaf water. The $\Delta^{18}\text{O}_L$ refers to average lamina leaf water, and $\Delta^{18}\text{O}_e$ to evaporative site water. Lines are model predictions, and points are observed values. Model formulations and details of input parameters are given in the text. Sampling took place at the Denmark plantation in December 2001.

6.5.3. *Phloem sap* $\Delta^{18}\text{O}_{\text{pw}}$

Phloem water enrichment varied significantly among sampling dates ($P=0.006$, $n=98$); the mean value for March 2001 differed from that for November 2000 ($P=0.02$) and December 2001 ($P=0.01$), whereas values for November 2000 and December 2001 did not differ ($P=0.69$). For phloem sap samples collected in November 2000, phloem water was significantly enriched compared to xylem water ($P=0.02$); mean $\Delta^{18}\text{O}_{\text{pw}}$ was $0.8 \pm 0.4\text{‰}$ (mean \pm 1SE). In March 2001, phloem water was not significantly enriched compared to xylem water ($P=0.17$). In December 2001, phloem water was enriched compared to xylem water by a mean value of $0.5 \pm 0.1\text{‰}$ ($P=0.001$). Phloem water enrichment values for plantations at which recently differentiated xylem tissues were sampled in December 2001 are shown in Table 6.6. The mean value for the Denmark plantation, at which diel collections were made, was $0.3 \pm 0.2\text{‰}$.

6.5.4. *Phloem sap* $\Delta^{18}\text{O}_{\text{suc}}$

Observed phloem sugar ^{18}O enrichment values ranged from 34.5 to 44.7‰, with a mean value of 40.1‰ ($n=101$). These enrichments correspond to inferred photosynthesis rate-weighted leaf water enrichments ranging from 7.5 to 17.7‰. I did not observe a pronounced variation in $\Delta^{18}\text{O}_{\text{suc}}$ at different canopy heights (Table 6.2). There was variation in $\Delta^{18}\text{O}_{\text{suc}}$ among plantations sampled in December 2001 (Table 6.6). There appeared to be some variation in $\Delta^{18}\text{O}_{\text{suc}}$ of phloem sap samples collected at different times over the diel cycle at the Denmark plantation, with values increasing by about 1 to 2‰ during the night. There was little variation in $\Delta^{18}\text{O}_{\text{suc}}$ at the Mount Barker plantation between samples collected in November 2000 and March 2001; mean values were 42.3 and 42.4‰, respectively.

Observed $\Delta^{18}\text{O}_{\text{suc}}$ values accurately reflected observed $\Delta^{18}\text{O}_{\text{L}}$ values when the latter were weighted by photosynthesis rates, taking into account the fractionation between water and organic molecules of 27‰ (Table 6.7). Photosynthetic rates consistently decreased from morning to late afternoon (Figure 6.5A). I estimated that approximately 50% of daily photosynthesis occurred before 1100 hrs. In contrast, leaf water enrichment continued to increase well into the afternoon (Tables 6.4 and 6.5; Figures 6.4 and 6.5B). As a result, the leaf water signal that was recorded in the phloem sap sugars was less enriched than the maximum leaf water enrichment achieved in the late afternoon.

Table 6.6. Mean isotopic composition of xylem and phloem sap, new xylem wood, and mature xylem wood at six *E. globulus* plantations in southwestern Australia. Samples were collected in December 2001. Values in parentheses are 1 SE (n=6). Values within a row followed by different letters are significantly different at $P < 0.05$. New xylem tissue was bulked for each plantation for cellulose extraction, giving only a single value for $\Delta^{18}\text{O}_c$ and $\Delta^{13}\text{C}_c$.

Isotopic parameter (‰)	Plantation					
	Redmond	Denbarker	St. Werburghs	Eulup	Kwornicup	Frankland
Xylem water $\delta^{18}\text{O}$	-3.7 (0.4) a	-4.6 (0.2) bc	-4.1 (0.4) ab	-4.4 (0.2) ab	-5.4 (0.1) c	-5.5 (0.1) c
Phloem sap $\Delta^{18}\text{O}_{\text{pw}}$	0.9 (0.6) a	0.1 (0.4) a	0.3 (0.2) a	0.8 (0.5) a	2.1 (0.8) a	0.5 (0.3) a
Phloem sap $\Delta^{18}\text{O}_{\text{suc}}$	38.5 (0.5) a	39.5 (0.8) ab	37.2 (0.7) a	38.7 (0.2) a	37.8 (0.6) a	41.4 (0.8) b
New xylem $\Delta^{18}\text{O}_p$	26.7 (0.3) a	28.6 (0.5) b	27.8 (0.3) ab	28.1 (0.4) ab	28.2 (0.4) ab	29.0 (0.2) b
New xylem $\Delta^{18}\text{O}_c$	31.7	34.3	34.5	32.7	36.2	36.6
Mature xylem $\Delta^{18}\text{O}_p$	29.8 (0.3) a	31.1 (0.4) ab	31.0 (0.3) ab	31.1 (0.4) ab	31.7 (0.5) b	31.6 (0.4) b
Mature xylem $\Delta^{18}\text{O}_c$	35.1 (0.2) a	36.3 (0.3) ab	35.8 (0.4) ab	35.2 (0.4) a	37.1 (0.3) b	37.0 (0.4) b
Phloem sap $\Delta^{13}\text{C}$	20.7 (0.3) a	20.0 (0.3) ab	18.9 (0.3) bc	17.7 (0.3) c	18.5 (0.3) bc	19.1 (0.7) ac
New xylem $\Delta^{13}\text{C}_p$	21.4 (0.2) a	19.2 (0.4) b	18.6 (0.2) bc	17.7 (0.2) c	17.9 (0.3) bc	18.8 (0.5) bc
New xylem $\Delta^{13}\text{C}_c$	21.0	19.1	19.3	17.8	17.9	18.1
Mature xylem $\Delta^{13}\text{C}_p$	22.0 (0.4) a	20.1 (0.4) b	19.5 (0.2) b	18.8 (0.2) b	19.4 (0.1) b	19.9 (0.4) b
Mature xylem $\Delta^{13}\text{C}_c$	21.5 (0.5) a	19.7 (0.4) b	19.0 (0.2) b	18.3 (0.2) b	19.0 (0.2) b	19.1 (0.4) b

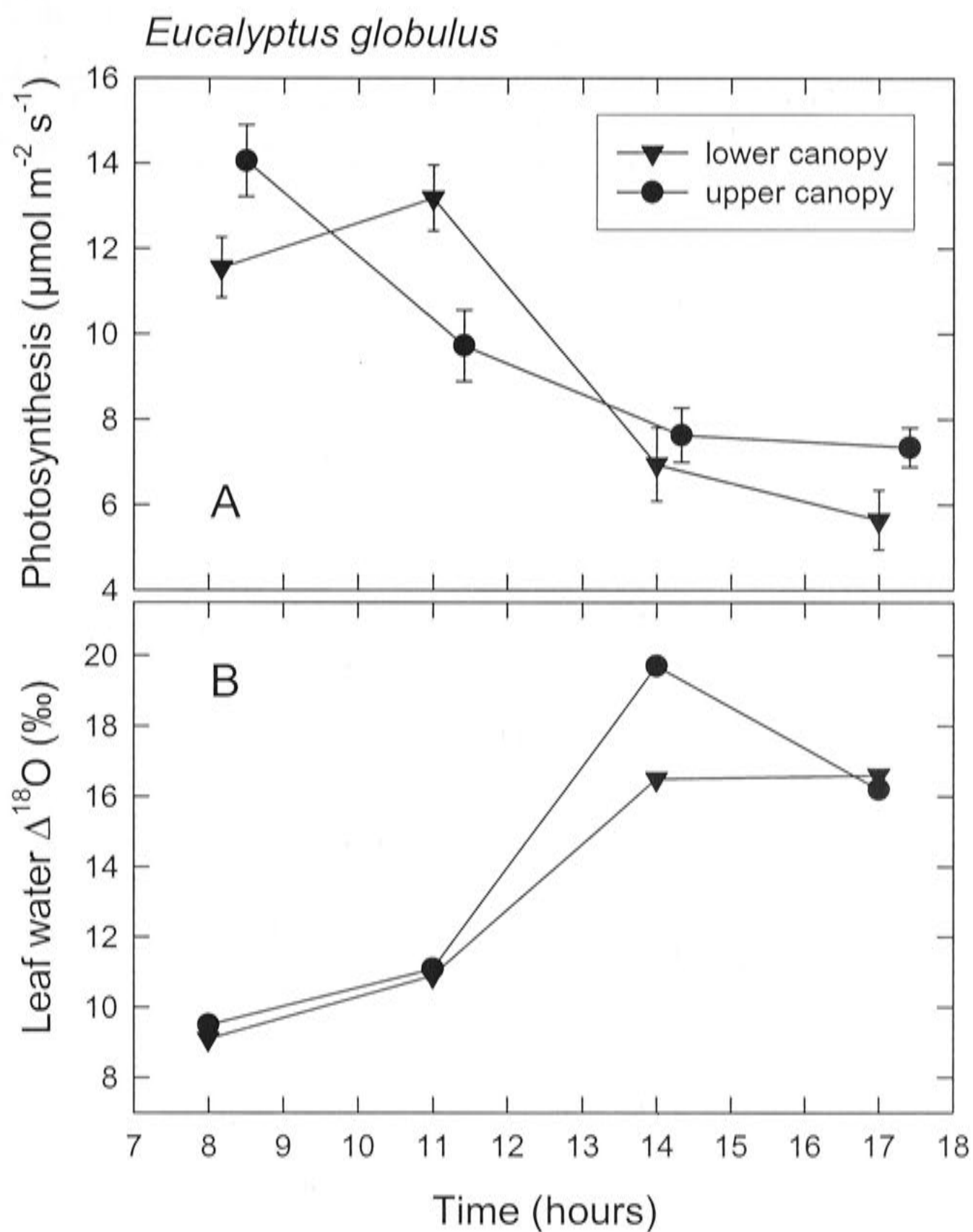


Figure 6.5. Diurnal variation in (A) photosynthesis and (B) leaf water ^{18}O enrichment in *E. globulus*. Measurements were made at the Mount Barker plantation in November 2000. Error bars in (A) represent 1 SE. Note the differential patterns of diurnal variation between photosynthesis and leaf water $\Delta^{18}\text{O}$.

Table 6.7. Observed photosynthesis rate-weighted lamina leaf water ^{18}O enrichment compared to observed phloem sap sugar ^{18}O enrichment. Phloem sap values are the mean of several samples collected throughout the day; values in parentheses are 1 SE. The expected difference between ^{18}O enrichment of phloem sap sugars and lamina leaf water is 27.4‰.

Sampling date	Photosynthesis-weighted $\Delta^{18}\text{O}_\text{L}$ (‰)	Phloem sap $\Delta^{18}\text{O}_\text{suc}$ (‰)	$\Delta^{18}\text{O}_\text{suc}$ minus $\Delta^{18}\text{O}_\text{L}$ (‰)
November 2000	13.8	42.3 (0.5)	28.5
March 2001	14.0	42.4 (0.2)	28.4
December 2001	12.5	39.0 (0.2)	26.5
Average			27.8

6.5.5. Leaf $\Delta^{18}\text{O}_\text{p}$ and $\Delta^{18}\text{O}_\text{c}$

Leaf dry matter $\Delta^{18}\text{O}$ values for fully-expanded leaves ranged from 28.3 to 34.8‰, with a mean value of 32.2‰ ($n=67$). Leaf $\Delta^{18}\text{O}_\text{p}$ for expanding leaves at the Peaceful Bay plantation was similar to that for fully-expanded leaves ($P=0.77$, $n=5$); mean values were 29.6 and 29.9‰, respectively. The $\Delta^{18}\text{O}_\text{p}$ for stem apices at the Mount Barker plantation was less than $\Delta^{18}\text{O}_\text{p}$ for fully-expanded leaves from the same trees ($P<0.001$, $n=6$); mean values were 32.1 and 33.9‰, respectively. I did not observe a pronounced variation in leaf $\Delta^{18}\text{O}_\text{p}$ with crown position in the March 2001 sampling at the Mount Barker plantation (Table 6.2). In the sampling at the Denmark plantation in December 2001, there appeared to be a diel variation in $\Delta^{18}\text{O}_\text{p}$ of about 1.5‰ that coincided with observed variation in $\Delta^{18}\text{O}_\text{L}$.

Leaf $\Delta^{18}\text{O}$ for cellulose of fully-expanded leaves was rather more variable than that of the corresponding dry matter; $\Delta^{18}\text{O}_\text{c}$ values ranged from 25.0 to 38.0‰, with a mean value of 31.3‰ ($n=17$). The $\Delta^{18}\text{O}_\text{c}$ values for fully-expanded leaves at the Peaceful Bay plantation were correlated with those of expanding leaves from the same trees ($r=0.88$, $P=0.05$, $n=5$); mean values were 28.4 and 31.0‰, respectively. The $\Delta^{18}\text{O}_\text{c}$ of fully-expanded leaves at the Mount Barker plantation was significantly lower than $\Delta^{18}\text{O}_\text{c}$ of stem apices of the same trees ($P=0.01$, $n=5$); mean values were 32.5 and 36.5‰, respectively. This difference was opposite in sign to the difference in $\Delta^{18}\text{O}_\text{p}$ between fully-expanded leaves and apices.

The parameter ε_cp , the difference between leaf $\Delta^{18}\text{O}_\text{p}$ and leaf $\Delta^{18}\text{O}_\text{c}$, was variable among different developmental stages of leaves. The mean value for fully-

expanded leaves was $1.4 \pm 0.7\text{‰}$ (mean \pm 1SE, $n=17$). The mean value for expanding leaves at the Peaceful Bay plantation was $-1.4 \pm 2.0\text{‰}$ ($n=5$). The mean value for stem apices at the Mount Barker plantation was $-4.6 \pm 0.5\text{‰}$ ($n=6$).

Leaf $\Delta^{18}\text{O}_p$ was significantly correlated with $\Delta^{18}\text{O}_{\text{suc}}$ in samples for which phloem sap was collected at the same time as leaves (Figure 6.6). The slope of the relationship was 0.59 ± 0.07 , indicating a mean value for $p_{\text{ex}}p_x$ of 0.41 ± 0.07 , if interpreting the relationship according to equation (6.12). The slope of the relationship between $\delta^{18}\text{O}_p$ and $\delta^{18}\text{O}_{\text{suc}}$ for the same samples was 0.58 ± 0.07 , indicating that the analysis of $\Delta^{18}\text{O}_p$ on $\Delta^{18}\text{O}_{\text{suc}}$ was not influenced by variation in xylem water $\delta^{18}\text{O}$.

Calculation of $p_{\text{ex}}p_x$ for the stem apices sampled at the Mount Barker plantation yielded a value of 0.38 ± 0.03 (mean \pm 1SE, $n=6$). The mean value calculated for p_x for trees from which apices were sampled was 0.95 ± 0.03 , such that the mean value for p_{ex} for stem apices was 0.40 ± 0.04 .

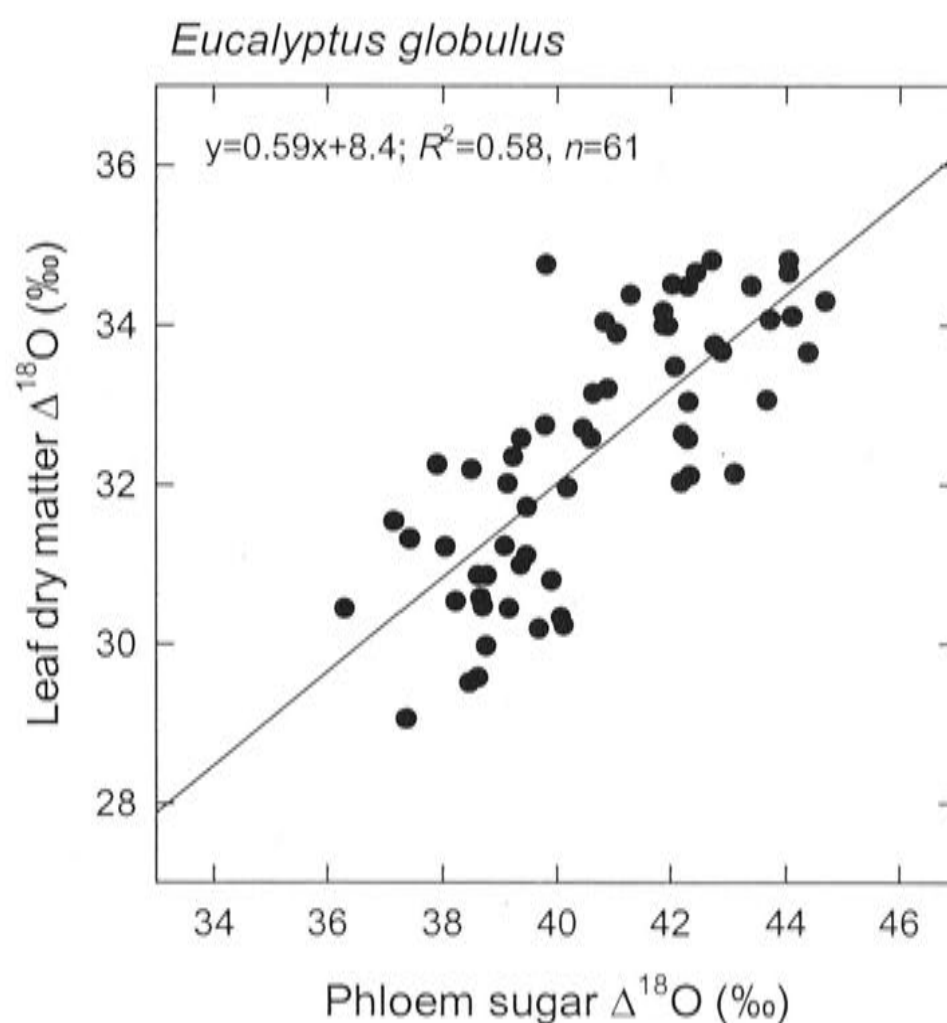


Figure 6.6. Leaf dry matter ^{18}O enrichment plotted against that for phloem sap sugars collected from the main stem at the same canopy height as leaves. Samples were collected from the Mount Barker and Denmark plantations.

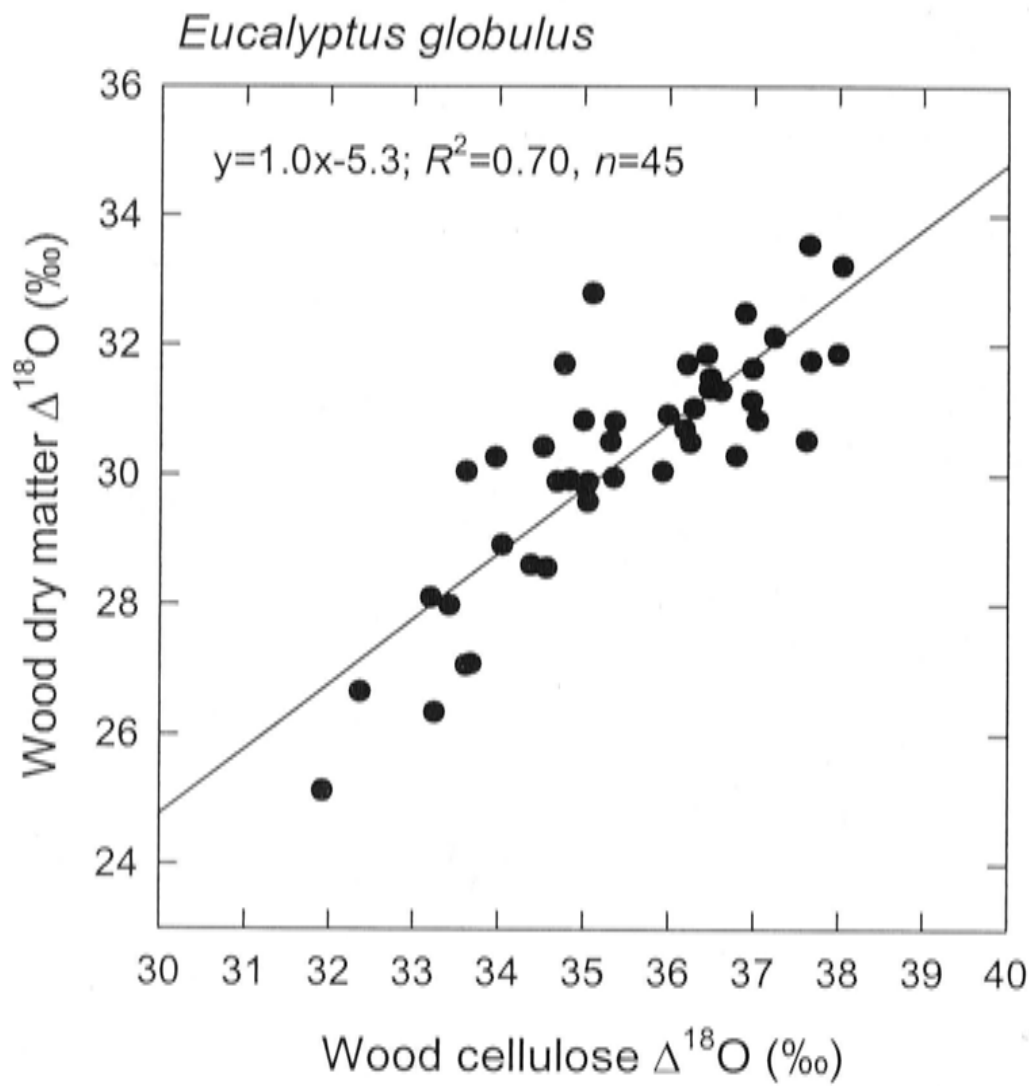


Figure 6.7. Total dry matter ^{18}O enrichment of mature xylem wood plotted against ^{18}O enrichment of α -cellulose extracts. Samples were collected across seven plantations in December 2001.

6.5.6. Wood and bark $\Delta^{18}\text{O}_p$ and $\Delta^{18}\text{O}_c$

The $\Delta^{18}\text{O}_p$ values for mature xylem wood ranged from 24.6 to 33.8‰, and had a mean value of 30.3‰ ($n=71$). There was variation among plantations in xylem wood $\Delta^{18}\text{O}_p$ (Table 6.6), as well as among different positions within trees (Table 6.2). Mature xylem $\Delta^{18}\text{O}_p$ was correlated with $\Delta^{18}\text{O}_c$ for cellulose extracted from the same tissue (Figure 6.7). The mean ε_{cp} value for mature xylem tissues was $-5.3 \pm 0.1\text{‰}$ (mean \pm 1SE, $n=45$).

The $\Delta^{18}\text{O}_p$ of bark was significantly correlated with the $\Delta^{18}\text{O}_p$ of underlying wood (Figure 6.8). However, bark $\Delta^{18}\text{O}_p$ was lower than wood $\Delta^{18}\text{O}_p$ ($P<0.001$, $n=45$); mean values were 28.0 and 29.5‰, respectively. Bark $\Delta^{18}\text{O}_c$ was also less than wood $\Delta^{18}\text{O}_c$ ($P<0.001$, $n=10$); mean values were 29.2 and 33.4‰, respectively. The ε_{cp} for bark was $-3.7 \pm 0.7\text{‰}$ ($n=10$).

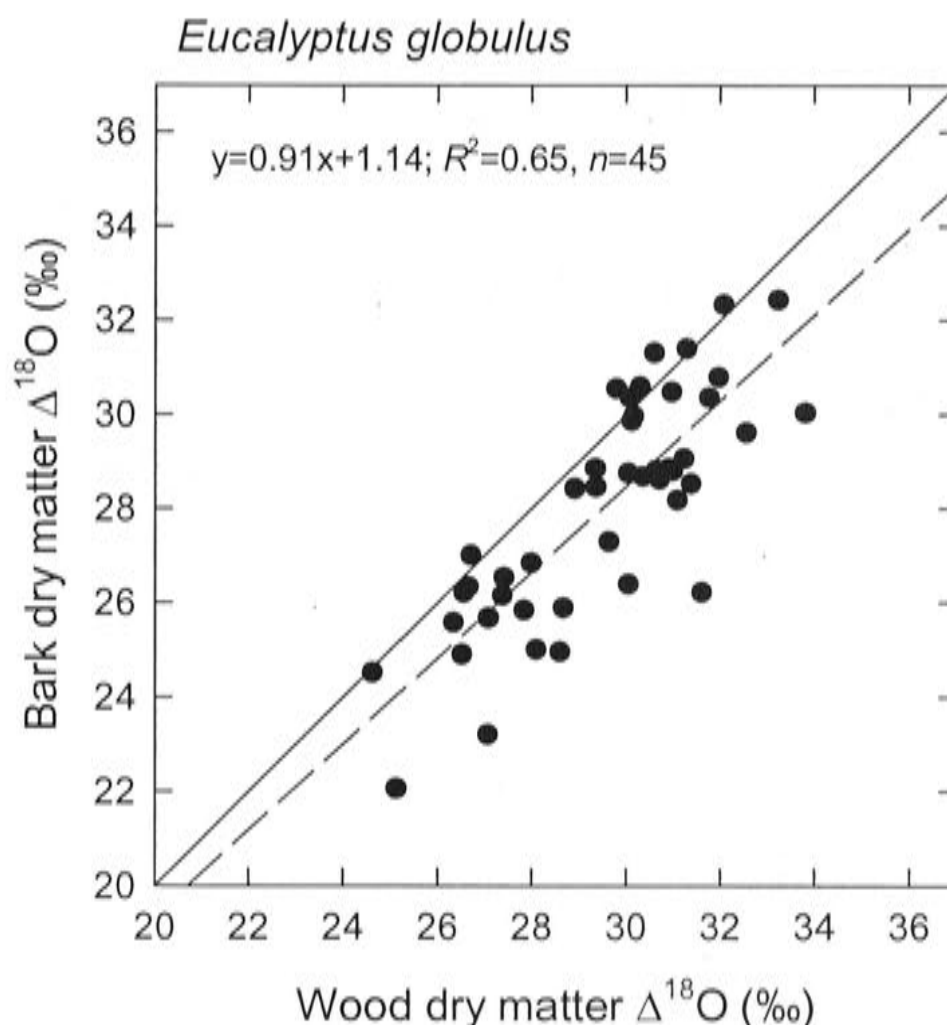


Figure 6.8. Bark dry matter ^{18}O enrichment plotted against ^{18}O enrichment of underlying wood. Samples were collected from main stems and branches in the Mount Barker and Peaceful Bay plantations. The solid line is the one-to-one line; the broken line is a regression line.

Recently differentiated xylem tissues had $\Delta^{18}\text{O}_p$ and $\Delta^{18}\text{O}_c$ values that were generally lower than corresponding values for mature xylem tissues (Table 6.6). The ϵ_{cp} for recently differentiated xylem tissue was $-6.3 \pm 0.6\text{‰}$ (mean \pm 1SE, $n=6$). The $\Delta^{18}\text{O}_p$ of recently differentiated xylem tissue was significantly correlated with $\Delta^{18}\text{O}_{\text{suc}}$ of phloem sap dry matter ($r=0.49$, $P=0.003$, $n=36$). The mean value of p_{ex} calculated for recently differentiated xylem tissue, using equation (6.10) but replacing the term $(\int A \Delta^{18}\text{O}_L / \int A)$ with $(\Delta^{18}\text{O}_{\text{suc}} - \epsilon_{wc})$, was 0.39 ± 0.07 (mean \pm 1SE, $n=6$). Mean p_x for the same trees was 0.95 ± 0.02 .

6.5.7. Phloem sap, leaf, and wood $\Delta^{13}\text{C}$

The $\Delta^{13}\text{C}$ of phloem sap sugars ranged from 14.6 to 21.6‰, with a mean value of 18.7‰ ($n=94$). There was variation in phloem sap $\Delta^{13}\text{C}$ among plantations sampled in December 2001 (Table 6.6), and seasonally between the November and March sampling dates at the Mount Barker plantation (Figure 6.9).

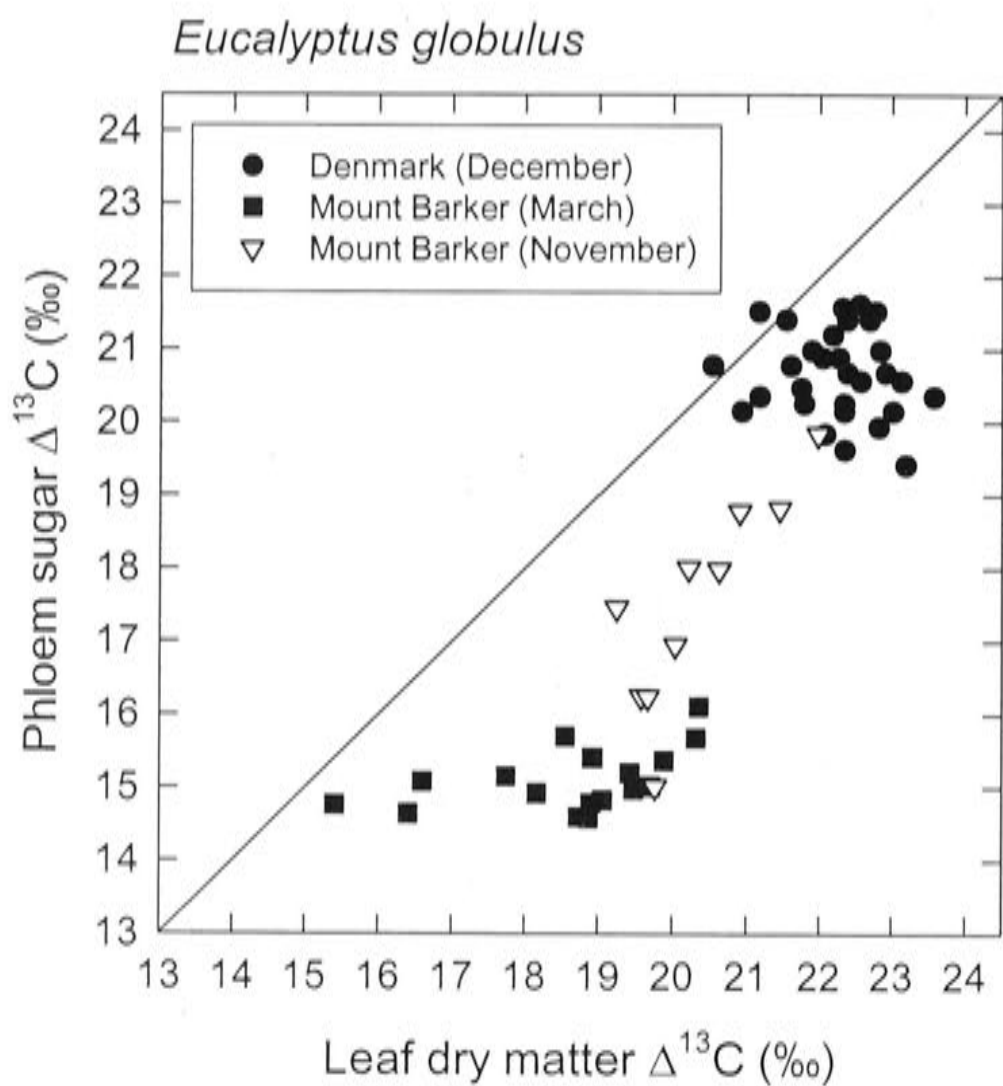


Figure 6.9. Phloem sugar carbon isotope discrimination plotted against leaf dry matter carbon isotope discrimination from the same canopy height. The solid line is the one-to-one line.

Leaf $\Delta^{13}\text{C}_p$ ranged from 15.4 to 23.6‰, with a mean value of 20.7‰ ($n=72$). There was significant variation in leaf $\Delta^{13}\text{C}_p$ among different canopy positions in the March 2001 sampling at the Mount Barker plantation (Table 6.2); leaf $\Delta^{13}\text{C}_p$ decreased with increasing canopy height. Leaf $\Delta^{13}\text{C}_p$ also varied seasonally between the November and March collections at the Mount Barker plantation (Figure 6.9). Leaf $\Delta^{13}\text{C}_p$ was correlated with, but consistently higher than, phloem sap $\Delta^{13}\text{C}$ for samples collected at the same time and from the same height in the canopy (Figure 6.9). The difference between leaf $\Delta^{13}\text{C}_p$ and phloem sap $\Delta^{13}\text{C}$ ranged from -0.3 to 4.6‰, with a mean value of 2.3‰ ($n=57$).

Stem apices collected at the Mount Barker plantation in November 2000 had a mean $\Delta^{13}\text{C}_p$ value of 19.2 ± 0.3 ‰ (mean \pm 1SE, $n=10$), whereas the $\Delta^{13}\text{C}$ of phloem sap sugars collected concurrently had a mean value of 17.2 ± 0.4 ‰ ($n=6$). Thus, stem

apices had significantly higher $\Delta^{13}\text{C}$ than phloem sap sugars at the time of collection ($P=0.01$, $n=6$).

The $\Delta^{13}\text{C}_p$ of recently differentiated xylem tissue was not significantly different from the $\Delta^{13}\text{C}$ of phloem sap sugars collected concurrently ($P=0.44$, $n=36$). Variation between the two was closely correlated (Figure 6.10B). In contrast, mature xylem tissue $\Delta^{13}\text{C}_p$ was found to be higher than that of $\Delta^{13}\text{C}$ of phloem sap sugars by 0.8‰ ($P<0.001$, $n=36$; Figure 6.10A), and similarly higher than recently differentiated xylem tissue $\Delta^{13}\text{C}_p$ by 1.0‰ ($P<0.001$, $n=36$; Figure 6.10C).

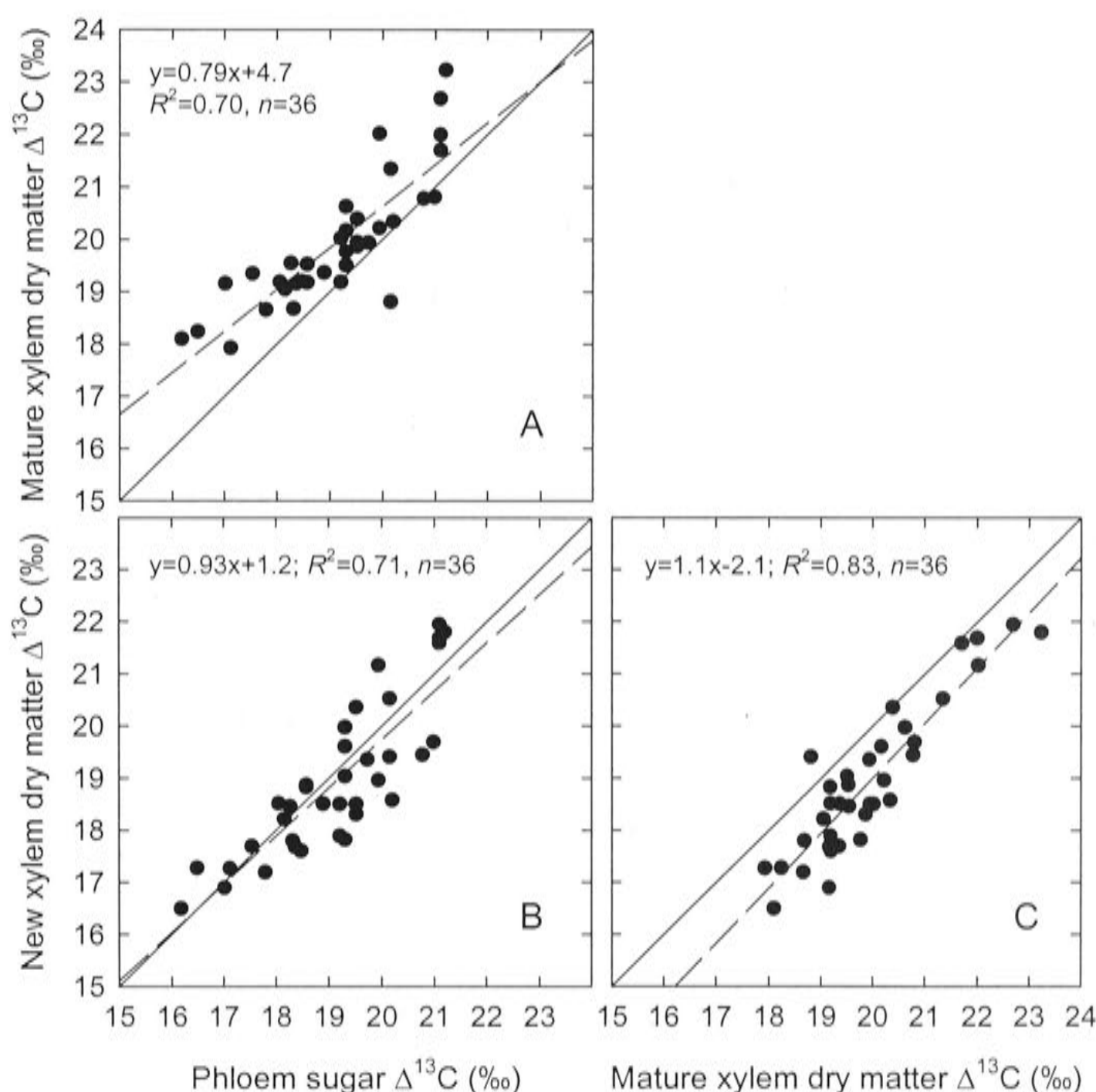


Figure 6.10. Carbon isotope discrimination of mature xylem dry matter (A) and newly differentiated xylem dry matter (B) plotted against carbon isotope discrimination of phloem sap sugars. Also shown is carbon isotope discrimination of newly differentiated xylem dry matter plotted against that of mature xylem dry matter (C). Solid lines show one-to-one lines; broken lines are regression lines. Samples were collected from six trees at each of six *E. globulus* plantations in December 2001.

Mature xylem $\Delta^{13}\text{C}_p$ and $\Delta^{13}\text{C}_c$ were closely correlated (Figure 6.11). The mean difference between $\Delta^{13}\text{C}_p$ and $\Delta^{13}\text{C}_c$ for mature xylem wood was $0.5 \pm 0.04\text{‰}$ (mean \pm 1SE, $n=45$). In contrast the $\Delta^{13}\text{C}_c$ for cellulose extracted from recently differentiated xylem tissues did not differ from $\Delta^{13}\text{C}_p$ of the same tissue ($P=0.72$, $n=6$). Variation among plantations in mature and recently differentiated xylem $\Delta^{13}\text{C}_p$ and $\Delta^{13}\text{C}_c$ is detailed in Table 6.6.

Mature xylem $\Delta^{13}\text{C}_p$ was consistently less than leaf $\Delta^{13}\text{C}_p$ for samples collected from the same canopy position ($P=0.001$, $n=24$); the mean difference between the two was 1.0‰. For samples collected at the Mount Barker plantation in March 2001, the difference between leaf $\Delta^{13}\text{C}_p$ and stem wood $\Delta^{13}\text{C}_p$ appeared to decrease with increasing height in the canopy (Table 6.2).

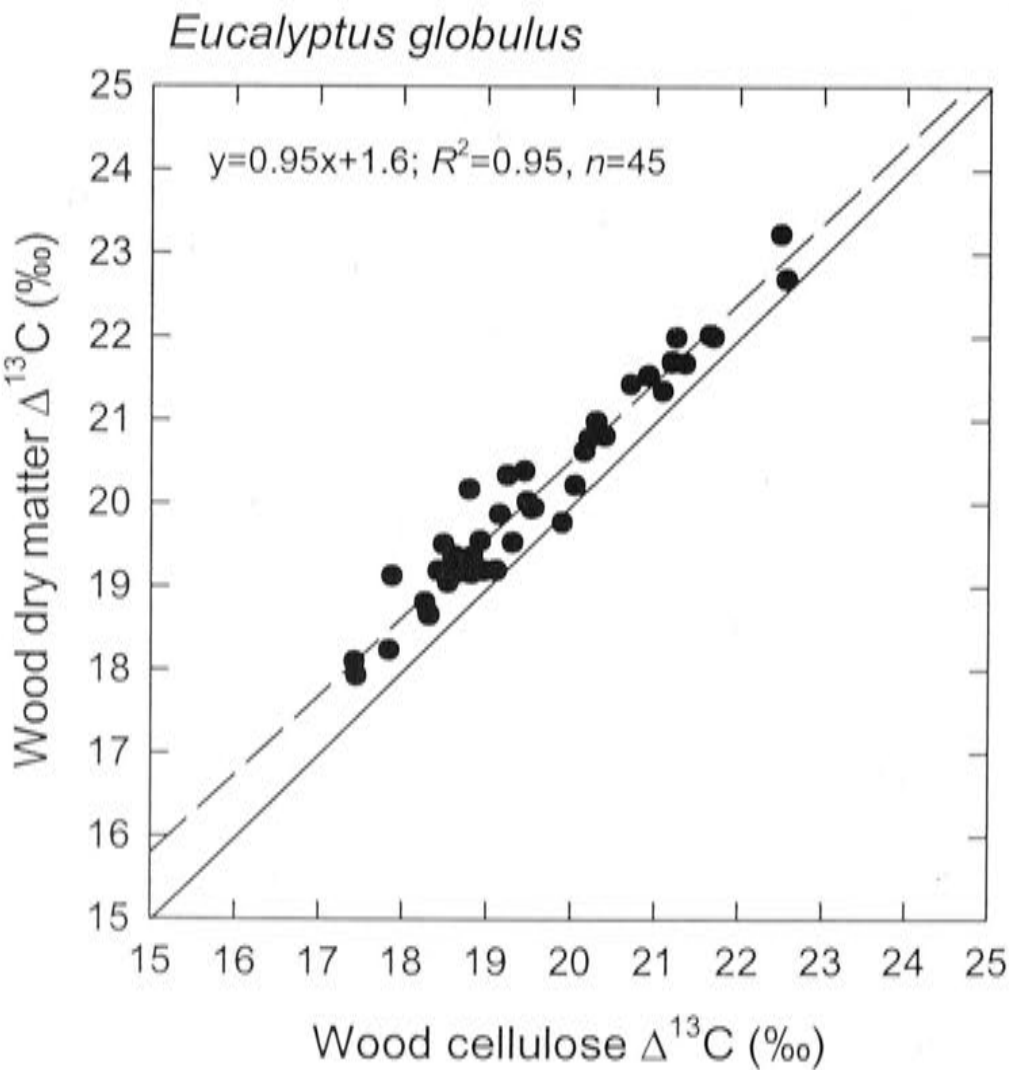


Figure 6.11. The relationship between carbon isotope discrimination in wood dry matter and wood cellulose. Samples were collected in December 2001 from seven *E. globulus* plantations. The solid line is the one-to-one line; the broken line is a regression line.

6.5.8. Correlations between $\Delta^{18}\text{O}$ and $\Delta^{13}\text{C}$

Variation in $\Delta^{18}\text{O}$ of phloem sap sugars was significantly related to variation in their $\Delta^{13}\text{C}$ according to the equation $\Delta^{18}\text{O}_{\text{suc}} = -0.62\Delta^{13}\text{C}_{\text{suc}} + 51$ ($R^2 = 0.40$, $P < 0.001$, $n = 94$). Leaf $\Delta^{18}\text{O}_p$ was related to leaf $\Delta^{13}\text{C}_p$ by the equation $\Delta^{18}\text{O}_p = -0.61\Delta^{13}\text{C}_p + 45$ ($R^2 = 0.35$, $P < 0.001$, $n = 72$). Finally, variation in mature xylem wood $\Delta^{18}\text{O}_p$ was significantly related to variation in mature xylem wood $\Delta^{13}\text{C}_p$ by the equation $\Delta^{18}\text{O}_p = -0.38\Delta^{13}\text{C}_p + 38$ ($R^2 = 0.19$; $P < 0.001$, $n = 64$).

If the oxygen and carbon isotope ratios were expressed using little delta notation, the two were still correlated, indicating that correlations between $\Delta^{18}\text{O}$ and $\Delta^{13}\text{C}$ were not caused by variation in xylem water $\delta^{18}\text{O}$. The regression equation describing the relationship between $\delta^{18}\text{O}$ and $\delta^{13}\text{C}$ of phloem sap sugars was $\delta^{18}\text{O}_{\text{suc}} = 0.67\delta^{13}\text{C}_{\text{suc}} + 53$ ($R^2 = 0.36$, $P < 0.001$, $n = 94$). For leaf dry matter, the relationship between $\delta^{18}\text{O}$ and $\delta^{13}\text{C}$ was $\delta^{18}\text{O}_p = 0.62\delta^{13}\text{C}_p + 46$ ($R^2 = 0.51$, $P < 0.001$, $n = 72$). Finally, for wood dry matter $\delta^{18}\text{O}$ versus $\delta^{13}\text{C}$, the relationship was $\delta^{18}\text{O}_p = 0.41\delta^{13}\text{C}_p + 37$ ($R^2 = 0.45$; $P < 0.001$, $n = 64$). Note that the slopes of the regression equations are positive when little delta values are used, because $\delta^{13}\text{C}$ and $\Delta^{13}\text{C}$ are opposite in sign.

6.6. Discussion

Data presented in this chapter provide a means for critically examining several aspects of the $\Delta^{18}\text{O}$ theory presented after the introduction. The non-steady state leaf water model performed well in comparison with observed variation in $\Delta^{18}\text{O}_L$ over a full diel cycle (Figure 6.4). I confirmed that the leaf water $\Delta^{18}\text{O}_L$ signal is recorded by sugars exported from leaves in phloem sap. Importantly, it was the photosynthesis-weighted average leaf water signal that was exported (Table 6.7). I confirmed that enriched leaf water can be exported from *E. globulus* leaves in the phloem, but found that $\Delta^{18}\text{O}_{\text{pw}}$ was generally rather small in this species, yielding p_x estimates close to unity. Mean values for the proportion of exchangeable oxygen during cellulose synthesis for both leaf and xylem tissues were observed to be close to 0.40, as has been observed in other species. In addition to these interpretations relating to $\Delta^{18}\text{O}$, variations in $\Delta^{13}\text{C}$ between phloem sap sugars and leaf and xylem tissues can be interpreted in terms of post-photosynthetic processes influencing the carbon isotope composition of plant dry matter. These concepts, in addition to some others, will be examined in more detail below.

6.6.1. Xylem water $\delta^{18}\text{O}$

I observed a linear decrease in xylem water $\delta^{18}\text{O}$ with decreasing south latitude from approximately -35.0°S to approximately -34.3°S . A corresponding linear decrease in annual precipitation amount occurred over this latitudinal gradient. This spatial variation in xylem water $\delta^{18}\text{O}$ might then be explained by variation in the isotopic composition of rainfall, caused by the ‘continental effect’ (Rozanski et al. 1993). The ‘continental effect’ describes a process by which rainfall becomes progressively depleted in heavy isotopes as storms track inland from the coast. This is because heavy isotopes preferentially move from the gaseous to liquid phase, as indicated by positive values for the equilibrium fractionation factor, ε^+ . The variation that I observed in xylem water $\delta^{18}\text{O}$ of approximately 3‰ over a transect extending approximately 80 km inland is similar to variation in xylem water $\delta^{18}\text{O}$ recently observed over a similar transect in the northwestern United States (Bowling et al. 2003a).

In addition to the possible influence of the continental effect on xylem water $\delta^{18}\text{O}$, some of the spatial variation that I observed could have been caused by differential use of groundwater relative to soil water in the inland plantations compared to those near the coast. Dawson and Pate (1996) found that ground water in the Mount Barker region of southwestern Australia was depleted in deuterium compared to soil water. Assuming the pattern is the same for $\delta^{18}\text{O}$, use of groundwater in the low rainfall end of the transect could have caused lower xylem water $\delta^{18}\text{O}$.

I found only weak evidence for any appreciable variation in xylem water $\delta^{18}\text{O}$ within different parts of the tree crown. There was a tendency for xylem water in the upper stem to be slightly enriched in ^{18}O compared to that in the lower stem, and similarly for xylem water in branch tips to be slightly enriched compared to that in the middle and base of branches. Xylem water in branch tips has been previously observed to be enriched in deuterium compared to xylem water in more proximal branch sections (Dawson and Ehleringer 1993). The enrichment was ascribed to evaporative water loss from non-suberized woody tissues. A similar enrichment may also occur in ^{18}O in *E. globulus* branch tips.

6.6.2. Leaf water $\Delta^{18}\text{O}$

The leaf water ^{18}O enrichment that I observed during the day was consistently less than steady-state predictions of evaporative site water enrichment. This is a

common feature among many leaf water investigations (Flanagan 1993; Wang et al. 1998). The Péclet effect, summarized in equation (6.4), offers a potential explanation for this discrepancy. Application of equation (6.4) requires an estimate of L , the scaled effective path length. I estimated this term by assuming that observed leaf water enrichment was at steady-state in the afternoon. The L was then fitted to minimize the difference between predicted $\Delta^{18}\text{O}_L$ and observed $\Delta^{18}\text{O}_L$. The L value that I estimated for *E. globulus* was 54 mm. This value is large compared to previous estimates for some species (Flanagan et al. 1993; Flanagan et al. 1994; Barbour et al. 2000b; Chapter 4), but well within the range of values estimated for 90 different species, which was 4 to 166 mm (Wang et al. 1998). The value of L that I estimated for *E. globulus* was partly influenced by my use of new coefficients in the calculation of ε_k for prediction of $\Delta^{18}\text{O}_e$. If the previously accepted value of 1.028 for the kinetic isotope effect during diffusion of H_2^{18}O in air (Merlivat 1978) is used instead of the recently reported value of 1.032 (Cappa et al. 2003), then my estimated L value for *E. globulus* would be 25 mm, which agrees well with some other observations (Flanagan et al. 1993).

Nighttime steady-state predictions of $\Delta^{18}\text{O}_e$ and $\Delta^{18}\text{O}_L$ were consistently less than observed leaf water enrichment. Similar results have been observed previously in other species (Flanagan and Ehleringer 1991; Chapter 2). Application of a non-steady state modification of the leaf water enrichment model resulted in improved prediction of nighttime leaf water enrichment, both in this and a previous study (Chapter 2).

6.6.3. *Phloem sap* $\Delta^{18}\text{O}_{pw}$

I observed small but consistent enrichments in phloem water compared to xylem water for phloem sap samples collected in November 2000 and December 2001, but no phloem water enrichment for samples collected in March 2001. March is normally a time of peak water stress in the Mediterranean-type environment of southwestern Australia. This was likely to have been the case in 2001, as indicated by the low $\Delta^{13}\text{C}$ that I observed in phloem sap sugars at this time (Figure 6.9). During times of high water stress, phloem sap flow velocities are likely to be low due to low photosynthetic rates (i.e. low rates of sugar production) and high phloem sap sugar concentrations (Chapter 3). Under such conditions, the residence time of phloem sap in sieve tubes may be long, allowing for extensive mixing between phloem water and xylem water across sieve tube membranes, and consequent dilution of ^{18}O enrichment in phloem water. The same mechanism may explain the generally low $\Delta^{18}\text{O}_{pw}$ that I observed in *E.*

globulus compared with observations in herbaceous plants (Chapter 2; Chapter 4). Translocation over longer distances in trees than in herbaceous plants probably results in longer phloem sap residence times, and therefore lower $\Delta^{18}\text{O}_{\text{pw}}$.

6.6.4. Phloem sap $\Delta^{18}\text{O}_{\text{suc}}$

Phloem sap $\Delta^{18}\text{O}_{\text{suc}}$ reflected leaf water enrichment to a very good approximation in *E. globulus* when observed leaf water enrichments were weighted by observed photosynthetic rates. The precise relationship between $\Delta^{18}\text{O}_{\text{suc}}$ and $\Delta^{18}\text{O}_{\text{L}}$ is expected to be $\Delta^{18}\text{O}_{\text{suc}} = 1.027\Delta^{18}\text{O}_{\text{L}} + 27\text{‰}$ (Chapter 4). Applying this relationship to $\Delta^{18}\text{O}_{\text{L}}$ data presented in Table 6.7, a mean difference between $\Delta^{18}\text{O}_{\text{suc}}$ and $\Delta^{18}\text{O}_{\text{L}}$ of 27.4‰ is predicted. This agrees very well with the observed mean difference of 27.8‰ (Table 6.7). A similar result was found for *Ricinus communis*, where $\Delta^{18}\text{O}_{\text{suc}}$ of phloem sap sugars reflected almost perfectly the average lamina leaf water enrichment under carefully controlled conditions (Chapter 4). For *E. globulus* in the field, I observed that photosynthesis was highest in the morning and decreased through the day, whereas $\Delta^{18}\text{O}_{\text{L}}$ was relatively low in the morning and increased to a maximum in the afternoon. The same contrasting diurnal patterns in photosynthesis and leaf water enrichment have been observed in other species under field conditions (Harwood et al. 1998; Chapter 2). These results suggest that appropriate weighting by diurnal variation in photosynthetic rates may be important for interpreting organic matter ^{18}O enrichment in terms of leaf water enrichment, and factors affecting leaf water enrichment such as humidity. Additionally, results presented in Table 6.7 provide validation of my use of $(\Delta^{18}\text{O}_{\text{suc}} - \varepsilon_{\text{wc}})$ in place of $(\int A \Delta^{18}\text{O}_{\text{L}} / \int A)$ in calculations of p_{ex} .

In my analysis, I have neglected any possible effect of daytime starch storage followed by nighttime degradation and export on the oxygen isotope composition of translocated photosynthate. Further research is necessary to fully understand this process, and to assess its possible effect on the oxygen isotope composition of phloem sap sugars.

6.6.5. Leaf $\Delta^{18}\text{O}_{\text{p}}$ and $\Delta^{18}\text{O}_{\text{c}}$

I observed a reasonably strong relationship between leaf dry matter $\Delta^{18}\text{O}_{\text{p}}$ and phloem sap sugar $\Delta^{18}\text{O}_{\text{suc}}$ among samples collected at the Mount Barker plantation and the Denmark plantation (Figure 6.6). I used this relationship to estimate $p_{\text{ex}}p_{\text{x}}$ for *E.*

globulus leaves. As noted in the methods section, this analysis assumed that the $\Delta^{18}\text{O}_{\text{suc}}$ that I observed was the same as that at the time when the leaf dry matter was formed, and that xylem water $\delta^{18}\text{O}$ was also the same. I suggest that those assumptions need not be strictly met to provide an accurate estimate of $p_{\text{ex}}p_{\text{x}}$ if $\Delta^{18}\text{O}_{\text{suc}}$ and xylem water $\delta^{18}\text{O}$ covary through time to the same extent among the different trees sampled. If this were the case, the relationship between leaf $\Delta^{18}\text{O}_{\text{p}}$ and phloem sap $\Delta^{18}\text{O}_{\text{suc}}$ would have the same slope regardless of when the two were sampled, whereas the intercept would be expected to vary. The mean value of $p_{\text{ex}}p_{\text{x}}$ that I estimated from the relationship between leaf $\Delta^{18}\text{O}_{\text{p}}$ and phloem sap $\Delta^{18}\text{O}_{\text{suc}}$ was 0.41. The mean value for p_{x} that I estimated over all the phloem sap samples was 0.98. Assuming this value for p_{x} , a mean p_{ex} value of 0.42 is calculated based on the relationship between leaf $\Delta^{18}\text{O}_{\text{p}}$ and phloem sap $\Delta^{18}\text{O}_{\text{suc}}$. This value is very close to the mean p_{ex} value of 0.40 that I calculated for the stem apices sampled at the Mount Barker plantation; the two values were calculated from independent data by different methods. Both values also compare favorably with the mean p_{ex} that I calculated for recently differentiated xylem tissue of 0.39.

Table 8 compares the observations that I made of p_{ex} in *E. globulus* with values presented elsewhere in the literature. There is a surprising consistency among mean p_{ex} estimates over a wide range of species and growth conditions when the substrate for tissue synthesis is carbohydrate; the mean p_{ex} value among all such entries in Table 6.8 is 0.42.

In reviewing the literature, I found that there was one p_{ex} value that deviated substantially from this overall mean value; this was an estimate of 1.0 for sprouting potato shoots (DeNiro and Cooper 1989). A slope of 1.0 was calculated for the relationship between shoot cellulose and tuber water, apparently indicating complete exchange between organic oxygen and medium water during shoot cellulose synthesis. Tuber water $\delta^{18}\text{O}$ values ranged from -11 to -3‰. I suggest that this variation in tuber water $\delta^{18}\text{O}$ was too small to provide an accurate estimate of p_{ex} from the regression slope. An alternative is to estimate the $\delta^{18}\text{O}$ value of organic oxygen in equilibrium with tuber water by adding 27‰ to the tuber water $\delta^{18}\text{O}$ value. In doing this, one quickly recognizes that the shoot cellulose $\delta^{18}\text{O}$ values in Table 2 of DeNiro and Cooper (1989) generally lie about halfway between those of tuber starch and those

Table 6.8. Mean $p_{\text{ex}}p_x$ and p_{ex} values for analyses in the present study and in the literature. The dotted line separates those samples in which the substrate for cellulose synthesis was lipids or glycerol from those for which it was some form of carbohydrate. Values from the present study are given as mean ± 1 SE.

Species	Growth environment	Substrate	Mean $p_{\text{ex}}p_x$	Mean p_{ex}	Reference
<i>Arachis hypogaea</i>	dark	lipid		0.72	Luo and Sternberg 1992
<i>Ricinus communis</i>	dark	lipid		0.69	Luo and Sternberg 1992
<i>Ricinus communis</i>	dark	lipid		0.76	Sternberg <i>et al.</i> 1986
<i>Daucus carota</i>	dark	glycerol		0.77	Sternberg <i>et al.</i> 1986
<i>Daucus carota</i>	dark	sucrose		0.47	Sternberg <i>et al.</i> 1986
<i>Hordeum vulgare</i>	dark	starch		0.38	Luo and Sternberg 1992
<i>Lemna gibba</i>	dark	sucrose		0.38	Yakir and Deniro 1990
<i>Solanum tuberosum</i>	dark or light	starch		0.50 ± 0.04^a	DeNiro and Cooper 1989
<i>Triticum aestivum</i>	dark	starch		0.31	Luo and Sternberg 1992
<i>Triticum aestivum</i>	dark	starch		0.43	Sternberg <i>et al.</i> 2003
<i>Quercus robur</i>	4 hour incubation of stem tissue	glucose		0.53	Hill <i>et al.</i> 1995
10 grass species	normal day/night	sucrose	0.25	$\sim 0.40^b$	Helliker and Ehleringer 2002a
<i>Lolium multiflorum</i>	normal day/night	sucrose	0.22	0.35	Helliker and Ehleringer 2002b
<i>Gossypium hirsutum</i>	normal day/night	sucrose	0.38	$\sim 0.44^c$	Barbour and Farquhar 2000
<i>Alnus</i> sp., <i>Betula occidentalis</i> , <i>Populus</i> sp.	normal day/night	sucrose	0.42	$\sim 0.44^d$	Roden <i>et al.</i> 2000
<i>Eucalyptus globulus</i> (stem wood)	normal day/night	sucrose/raffinose	0.38 ± 0.07	0.39 ± 0.07	This study
<i>Eucalyptus globulus</i> (stem apex)	normal day/night	sucrose/raffinose	0.38 ± 0.03	0.40 ± 0.04	This study
<i>Eucalyptus globulus</i> (leaves)	normal day/night	sucrose/raffinose	0.41 ± 0.07	0.42 ± 0.07	This study

^aValues are based on a re-analysis of data presented in DeNiro and Cooper (1989). See text for details.

^bCalculated assuming a p_x value of 0.62, based on data presented in Helliker and Ehleringer (2002b).

^cCalculated with a p_x value of 0.87, assuming $\Delta^{18}\text{O}_{\text{pw}}$ was 4.0‰ (Cernusak *et al.* 2003) and average $\Delta^{18}\text{O}_L$ was 20‰.

^dCalculated assuming p_x was 0.95, based on $\Delta^{18}\text{O}_{\text{pw}}$ measurements presented in the present paper.

expected for organic oxygen in equilibrium with tuber water. The p_{ex} for each potato shoot can then be calculated according to the equation, $p_{\text{ex}} = (\delta^{18}\text{O}_{\text{ts}} - \delta^{18}\text{O}_{\text{sc}}) / (\delta^{18}\text{O}_{\text{ts}} - \delta^{18}\text{O}_{\text{tw}+27})$, where $\delta^{18}\text{O}_{\text{ts}}$ refers to tuber starch, $\delta^{18}\text{O}_{\text{sc}}$ to shoot cellulose, and $\delta^{18}\text{O}_{\text{tw}+27}$ to tuber water plus 27‰. One potato sample in Table 2 of DeNiro and Cooper (1989), potato number 21, cannot be analyzed in this way because the difference between $\delta^{18}\text{O}_{\text{ts}}$ and $\delta^{18}\text{O}_{\text{tw}+27}$ is only 0.1‰. Among the other 20 samples, this difference ranges from 4.6 to 8.8‰. The mean p_{ex} for these 20 samples is 0.50 ± 0.04 (mean \pm 1 SE). I suggest that the anomalous p_{ex} estimate of 1.0 (DeNiro and Cooper 1989) can thus be satisfactorily reconciled with the other values in Table 6.8 by considering this alternative approach to calculating p_{ex} .

In my calculations of p_{ex} in this paper, I have assumed that the fractionation between organic oxygen and water is 27‰, regardless of the intra-molecular position of oxygen atoms when they exchange. Sternberg et al. (2003) recently estimated a fractionation factor of 48.8 ± 20 ‰ for the oxygen atom bound to the second carbon of glucose moieties during heterotrophic cellulose synthesis. The authors suggested that this may indicate variation in fractionation factors between organic oxygen and water, depending on where the oxygen atom is located within the organic molecule. However, as noted by Sternberg et al. (2003), the error around the estimate of 48.8‰ is very large (1 SE=20‰), and the analytical precision will have to be improved before this conclusion can be firmly asserted. However, if this is shown to be the case, theory relating to p_{ex} , as it currently stands, will have to be reconsidered.

I observed apparent differences in the term ϵ_{cp} , the difference between leaf $\Delta^{18}\text{O}_{\text{p}}$ and $\Delta^{18}\text{O}_{\text{c}}$, among different developmental stages of leaves. Among the youngest leaves, those emerging from the stem apices, the mean value was -4.6 ‰. In expanding leaves, the mean ϵ_{cp} increased to -1.4 ‰. Finally, the mean value for fully-expanded leaves was 1.4 ‰. This can be contrasted with the average value of -6.8 ‰ observed for a range of species (Chapter 5). The trend with leaf age may reflect an increase in storage of non-structural carbohydrates in leaves as they develop; such compounds would be expected to have higher $\Delta^{18}\text{O}$ than leaf cellulose because none of their oxygen atoms would have had an opportunity to exchange with unenriched source water.

In addition to the apparent variation in ϵ_{cp} with leaf developmental stage, I also observed a rather large variation in ϵ_{cp} among fully-expanded leaves. This large variability may partly reflect differences in leaf age. Because xylem water $\delta^{18}\text{O}$ was

probably lower in the winter than in the summer, due to precipitation being relatively depleted in ^{18}O (Rozanski et al. 1993), and leaf water $\Delta^{18}\text{O}$ was probably also lower, due to humidity being relatively high, leaves expanding during winter could have lower cellulose $\delta^{18}\text{O}$ values than those expanding during summer. The cellulose $\delta^{18}\text{O}$ signal is not expected to change after cellulose synthesis. In contrast, some components of the leaf dry matter, such as soluble carbohydrates, turn over regularly, and are therefore expected to reflect the current leaf water $\delta^{18}\text{O}$ value. The diurnal variation in leaf $\Delta^{18}\text{O}_p$ in correspondence with variation in leaf water $\Delta^{18}\text{O}$, in this and a previous study (Chapter 2), provides evidence in support of this concept. Thus, I suggest that there is some fraction of leaf dry matter that progressively tracks and incorporates the current leaf water isotopic signal. By this reasoning, a leaf that expanded when xylem water $\delta^{18}\text{O}$ or $\Delta^{18}\text{O}_L$ was lower than at the time of sampling would be expected to have a smaller absolute difference between leaf $\Delta^{18}\text{O}_p$ and $\Delta^{18}\text{O}_c$ than one that expanded under conditions similar to those at the time of sampling.

6.6.6. Wood and bark $\Delta^{18}\text{O}_p$ and $\Delta^{18}\text{O}_c$

I observed that bark $\Delta^{18}\text{O}_p$ was consistently less than wood $\Delta^{18}\text{O}_p$ in *E. globulus* (Figure 6.8). Similar results were observed for cellulose, with bark $\Delta^{18}\text{O}_c$ being consistently less than wood $\Delta^{18}\text{O}_c$ by an average value of 4.2‰. I suggest that this pattern reflects the influence of re-fixation, a process by which some of the CO_2 respired by woody tissues is re-assimilated by photosynthetic cells in the bark (Cernusak and Marshall 2000; Pfanz et al. 2002; Damesin 2003). The bark cortex of *E. globulus* is noticeably green when one peels away the outer-most layer of the bark. In contrast to leaf water, I observed no enrichment in *E. globulus* bark water in comparison to xylem water. Photosynthate produced by chlorophyllous cells in the bark would therefore be expected to have a $\Delta^{18}\text{O}$ value of 27‰, whereas that produced in leaves had values ranging from 35 to 45‰. It was observed previously that re-fixation by bark could have a significant effect on the carbon isotope signature of underlying wood (Cernusak et al. 2001). I suggest that the oxygen isotope signature of wood might be similarly influenced by re-fixation, with the extent of influence depending on the proportion of re-fixed photosynthate being incorporated into the wood. Differential re-fixation rates in different parts of the crown might reduce wood $\Delta^{18}\text{O}$ by varying degrees, and this might

explain the apparently coordinated variation in mature xylem wood and bark $\Delta^{18}\text{O}_p$ within the crown of *E. globulus* (Table 6.2).

I observed a small variation in ε_{cp} between recently differentiated xylem tissues and mature xylem tissues; values were -6.3 and -5.3‰ , respectively. This variation was much smaller than that observed between recently differentiated leaf tissue and mature leaf tissue. The ε_{cp} for mature xylem wood of *E. globulus* can be compared to mean values of -3.6‰ and -3.9‰ for many *Quercus* and *Pinus* sp., respectively (Barbour et al. 2001).

6.6.7. Phloem sap, leaf, and wood $\Delta^{13}\text{C}$

The carbon isotope results that I present in this chapter serve generally to confirm and reinforce those presented previously for *E. globulus* in southwestern Australia (Pate and Arthur 1998). The observation that $\Delta^{13}\text{C}$ of newly synthesized wood matches very closely that of phloem sap sugars agrees with previous results (Pate and Arthur 1998). I observed that $\Delta^{13}\text{C}$ of cellulose extracted from recently differentiated xylem tissues also matched that of simultaneously collected phloem sap sugars. This suggests that the consistent difference in $\Delta^{13}\text{C}$ between cellulose and wood dry matter for mature xylem tissues (Figure 6.11) might result from lignification during xylem maturation (Loader et al. 2003), because lignin is known to be depleted in ^{13}C compared to cellulose (Wilson and Grinsted 1977). My observation that phloem sap sugar $\Delta^{13}\text{C}$ is consistently less than that of dry matter of mature leaves is also consistent with the previous report (Pate and Arthur 1998), as is the observation that leaf dry matter $\Delta^{13}\text{C}$ is consistently greater than wood dry matter $\Delta^{13}\text{C}$.

Wood dry matter $\Delta^{13}\text{C}$ has been observed to be less than leaf dry matter $\Delta^{13}\text{C}$ in many tree species (Craig 1953; Leavitt and Long 1982; Francey et al. 1985; Guehl et al. 1998; Miller et al. 2001). This observation fits a more general pattern of ^{13}C enrichment in heterotrophic plant tissues relative to the leaves supplying them with photosynthate (Brugnoli and Farquhar 2000; Hobbie et al. 2002; Hobbie and Werner 2004; Chapter 5). It was recently suggested that emerging leaves in two neotropical tree species have lower $\Delta^{13}\text{C}$ than mature leaves due to a greater proportional carbon fixation by PEP-carboxylase in emerging leaves than in mature source leaves (Terwilliger et al. 2001). This hypothesis suggests that the process that causes heterotrophic tissues to be ^{13}C enriched compared to source leaves takes place within the sink tissue. Present and previous observations in *E. globulus* (Pate and Arthur 1998)

and *Lupinus angustifolius* (Chapter 2) do not appear to support this hypothesis. I find that sink tissues in these species generally reflect, to a very close approximation, the $\Delta^{13}\text{C}$ of carbon delivered to them in phloem sap.

An exception to this general pattern in the present study was that the $\Delta^{13}\text{C}$ for stem apices at the Mount Barker plantation was greater than incoming phloem sap $\Delta^{13}\text{C}$. However, this trend is in the opposite direction to the hypothesis proposed by Terwilliger et al. (2001). It suggests, if anything, a depletion in ^{13}C of carbon in new leaves compared to incoming phloem sap carbon. This could reflect a carbon contribution to the new leaf tissue from photosynthesis in the new leaves taking place at relatively high c_i/c_a , thereby producing sugars with higher $\Delta^{13}\text{C}$ than incoming phloem sap sugars. This would be consistent with the observations of Terwilliger et al. (2001) concerning c_i/c_a in emerging leaves. I suggest that the consistent differences in $\Delta^{13}\text{C}$ between source leaves and heterotrophic tissues reflect a fractionation in the partitioning of carbon in the source leaf between that which remains in the leaf and that which is exported in the phloem. I acknowledge, however, that multiple processes may be operating simultaneously, such that a single unifying mechanism causing the widespread ^{13}C enrichment of heterotrophic tissues compared to source leaves may not exist. More experiments along the lines of that conducted by Terwilliger et al. (2001), and including analyses of phloem sap $\Delta^{13}\text{C}$, would be helpful for resolving this issue.

6.6.8. Correlations between $\Delta^{18}\text{O}$ and $\Delta^{13}\text{C}$

I observed that $\Delta^{18}\text{O}$ was negatively correlated with $\Delta^{13}\text{C}$ in phloem sap sugars, leaf dry matter, and wood dry matter of *E. globulus* growing in southwestern Australia. Farquhar et al. (1994) and Yakir and Israeli (1995) suggested that the combination of $\Delta^{13}\text{C}$ and $\Delta^{18}\text{O}$ analyses allows interpretation of $\Delta^{13}\text{C}$ in terms of effects on c_i/c_a caused either by variation in photosynthetic capacity or by variation in stomatal conductance. If variation in $\Delta^{13}\text{C}$ is caused by variation in photosynthetic capacity, no relationship is expected between $\Delta^{13}\text{C}$ and $\Delta^{18}\text{O}$. In contrast, if $\Delta^{13}\text{C}$ varies as a function of variation in stomatal conductance, $\Delta^{13}\text{C}$ and $\Delta^{18}\text{O}$ should be negatively correlated. The negative correlations that I observed between $\Delta^{13}\text{C}$ and $\Delta^{18}\text{O}$ of phloem sap sugars, leaf tissue, and wood in *E. globulus* suggest that variation in $\Delta^{13}\text{C}$ among trees and plantations was at least partly caused by variation in stomatal conductance. This is consistent with measurements of stomatal conductance and $\Delta^{13}\text{C}$ in the Mount Barker and Denmark

plantations (Chapter 3), and is not surprising given the large variation in annual rainfall among the plantations that I sampled.

Chapter 7: Measurement and interpretation of the oxygen isotope composition of carbon dioxide respired by leaves in the dark

7.1. Abstract

I measured the oxygen isotope composition ($\delta^{18}\text{O}$) of CO_2 respired by *Ricinus communis* leaves in the dark. Experiments were conducted at low CO_2 partial pressure, and at normal atmospheric CO_2 partial pressure. Across both experiments, the $\delta^{18}\text{O}$ of dark-respired CO_2 (δ_{R}) ranged from 44 to 324‰ (VSMOW scale). This seemingly implausible range of values reflects the large flux of CO_2 that diffuses into leaves, equilibrates with leaf water via the catalytic activity of carbonic anhydrase, then diffuses out of the leaf, leaving the net CO_2 efflux rate unaltered. The impact of this process on δ_{R} is modulated by the $\delta^{18}\text{O}$ difference between CO_2 inside the leaf and in the air, and by variation in the CO_2 partial pressure inside the leaf relative to that in the air. I developed theoretical equations to calculate $\delta^{18}\text{O}$ of CO_2 in leaf chloroplasts (δ_{c}), the assumed location of carbonic anhydrase activity, during dark respiration. Their application led to sensible estimates of δ_{c} , suggesting that the theory adequately accounted for the labeling of CO_2 by leaf water in excess of that expected from the net CO_2 efflux. The δ_{c} values were strongly correlated with $\delta^{18}\text{O}$ of water at the evaporative sites within leaves. I estimated that approximately 80% of CO_2 in chloroplasts had completely exchanged oxygen atoms with chloroplast water during dark respiration, whereas approximately 100% had exchanged during photosynthesis. Incorporation of the $\delta^{18}\text{O}$ of leaf dark respiration into ecosystem and global scale models of C^{18}OO dynamics could affect model outputs and their interpretation.

7.2. Introduction

Variations in the oxygen isotope composition of CO_2 in the atmosphere have the potential to reveal vital information about the global carbon cycle (Francey and Tans, 1987; Farquhar et al., 1993; Ciais et al., 1997). Furthermore, measurements of $\delta^{18}\text{O}$ of CO_2 in canopy air may allow differentiation of CO_2 fluxes into photosynthetic and respiratory components (Yakir and Wang, 1996). It was also recently suggested that nighttime measurements of $\delta^{18}\text{O}$ in canopy air could be used to partition nocturnal

ecosystem respiration between leaves and soil (Bowling et al., 2003a, 2003b). Leaf dark respiration is an important component of carbon cycling between vegetation and the atmosphere. An understanding of the factors controlling the $\delta^{18}\text{O}$ of CO_2 respired by leaves in the dark could therefore be important for interpreting the $\delta^{18}\text{O}$ of atmospheric CO_2 at local, regional, and global scales.

The net rate of CO_2 efflux from a leaf in the dark can be thought of as the difference between two one-way diffusional fluxes; one from the atmosphere to the leaf, and the other from the leaf to the atmosphere. For example, if the net respiratory CO_2 efflux (\mathcal{R}_n) is defined as $\mathcal{R}_n = g_c(c_i - c_a)$, where g_c is the leaf conductance to CO_2 , and c_i and c_a are CO_2 mole fractions in the intercellular air spaces and atmosphere respectively, the one-way flux from leaf to atmosphere becomes $g_c c_i$ and that from atmosphere to leaf becomes $g_c c_a$. The difference between \mathcal{R}_n and $g_c c_i$ will depend on the magnitude of the CO_2 concentration difference between c_i and c_a ; this difference will in turn depend on the leaf conductance to CO_2 and the CO_2 production rate inside the leaf. If the CO_2 concentration difference between c_i and c_a is very large, then the magnitude of the net CO_2 efflux will approach that of the one-way CO_2 efflux from leaf to atmosphere. However, if the CO_2 concentration inside the leaf is only a little larger than that in the atmosphere, the net CO_2 efflux from the leaf will be much smaller than the one-way CO_2 efflux from the leaf.

It has previously been recognized that one of the primary controls over the $\delta^{18}\text{O}$ of CO_2 diffusing out of leaves in the dark should be the oxygen isotope composition of leaf water (Flanagan et al., 1997; Flanagan et al., 1999). This is because gaseous CO_2 exchanges oxygen atoms with water during inter-conversion between CO_2 and bicarbonate. In plant tissues, this inter-conversion is catalyzed by the enzyme carbonic anhydrase. The rate constant for carbonic anhydrase is very fast, such that CO_2 diffusing out of leaves is expected to reflect nearly complete oxygen isotope exchange with leaf water. There is an equilibrium fractionation that takes place during the exchange reaction, such that at 25°C , the $\delta^{18}\text{O}$ of CO_2 will be enriched by $\sim 41\text{‰}$ compared to the $\delta^{18}\text{O}$ of water with which it has equilibrated.

In this chapter, I present measurements of the $\delta^{18}\text{O}$ of CO_2 respired by *Ricinus communis* L. leaves in the dark. I theorized that it should be the one-way flux of CO_2 out of a respiring leaf that is labeled with the leaf water $\delta^{18}\text{O}$ signal, rather than the net CO_2 efflux. This led me to hypothesize that the effect of a respiring leaf on the $\delta^{18}\text{O}$ of

CO₂ in air passing over the leaf could be much greater than predicted by considering the net CO₂ efflux alone.

7.3. Theory

Natural abundance oxygen isotope ratios are commonly expressed relative to the value of a standard:

$$\delta_X = \frac{R_X}{R_{Std}} - 1, \quad (7.1)$$

where δ_X represents the proportional deviation of R_X , the ¹⁸O/¹⁶O of material X , from R_{Std} , the ¹⁸O/¹⁶O of a standard. Using δ notation, I present the following equation for the oxygen isotope composition of CO₂ respired by leaves in the dark (δ_R):

$$\delta_R = \frac{\theta[\delta_e(1 + \varepsilon_w) + \varepsilon_w] + (1 - \theta)\delta_{c0} - \frac{C_a}{C_c}(\delta_a - \bar{a}) - \bar{a}}{(1 + \bar{a})\left(1 - \frac{C_a}{C_c}\right)}, \quad (7.2)$$

where θ is the proportion of CO₂ in the chloroplast that has completely exchanged oxygen atoms with chloroplast water, δ_e is the oxygen isotope composition of water at the evaporating sites within the leaf, ε_w is the equilibrium fractionation between water and CO₂, δ_{c0} is the oxygen isotope composition of CO₂ in the chloroplast that has not exchanged oxygen atoms with chloroplast water, C_a is the ambient carbon dioxide partial pressure, C_c is the chloroplastic CO₂ partial pressure, δ_a is the oxygen isotope composition of ambient CO₂, and \bar{a} is the weighted mean isotopic discrimination against C¹⁸OO during diffusion from the chloroplast to the atmosphere. A summary of all symbols used in the text is given in Table 7.1. A derivation of equation (7.2) is presented in Appendix 7.1. As described for photosynthesizing leaves by Gillon and Yakir (2000b), I make the assumption that CO₂ inside the leaf comprises a mixture of CO₂ completely equilibrated with leaf water (of proportion θ) and CO₂ that has undergone no equilibration with leaf water (of proportion $1-\theta$). The diffusional discrimination, \bar{a} , can be calculated as (Farquhar and Lloyd 1993)

$$\bar{a} = \frac{(C_c - C_i)a_w + (C_i - C_s)a + (C_s - C_a)a_b}{C_c - C_a}, \quad (7.3)$$

Table 7.1. Symbols used in Chapter 7.

A	Net photosynthesis rate
a	Weighted mean discrimination against $C^{18}OO$ for diffusion from chloroplast to atmosphere
a	Discrimination against $C^{18}OO$ during diffusion through stomata
a_b	Discrimination against $C^{18}OO$ during diffusion through leaf boundary layer
a_w	Summed discriminations against $C^{18}OO$ during liquid phase diffusion and dissolution
a^{13}	Discrimination against $^{13}CO_2$ during diffusion through stomata
a_b^{13}	Discrimination against $^{13}CO_2$ during diffusion through leaf boundary layer
a_w^{13}	Summed discrimination against $^{13}CO_2$ during dissolution and liquid phase diffusion
α_w	Equilibrium oxygen isotope effect between CO_2 and water
b	Discrimination against $^{13}CO_2$ by carboxylating enzymes
b^{18}	Discrimination against $C^{18}OO$ by Rubisco
C	Molar concentration of water
C_a	Partial pressure of CO_2 in atmosphere
C_c	Partial pressure of CO_2 in chloroplast
C_i	Partial pressure of CO_2 in leaf intercellular air spaces
C_{in}	Partial pressure of CO_2 in dry air entering leaf chamber
C_s	Partial pressure of CO_2 at the leaf surface
c_i	Mole fraction of CO_2 in intercellular air spaces
c_a	Mole fraction of CO_2 in atmosphere
D	Diffusivity of $H_2^{18}O$ in water
Δ_A	Discrimination against ^{13}C or ^{18}O during net CO_2 uptake by photosynthesis
Δ_{ca}	Discrimination against $C^{18}OO$ between chloroplast and atmosphere
Δ_e	^{18}O enrichment at evaporative sites in leaves compared to source water
Δ_{ca}	Discrimination against $C^{18}OO$ in CO_2 in equilibrium with chloroplast water compared to atmosphere
Δ_i	Discrimination against $^{13}CO_2$ that would occur if g_i were infinite and photorespiration and day respiration did not discriminate
Δ_L	^{18}O enrichment of average lamina leaf water compared to source water
Δ_{obs}	Observed discrimination against $^{13}CO_2$ during photosynthesis
Δ_v	^{18}O enrichment of vapor in atmosphere compared to source water
δ_A	$\delta^{18}O$ of CO_2 taken up by net photosynthesis (VSMOW scale)
δ_a	$\delta^{18}O$ of CO_2 in atmosphere (VSMOW scale)
δ_c	$\delta^{18}O$ of net CO_2 in chloroplast (VSMOW scale)
δ_{c0}	$\delta^{18}O$ of CO_2 in chloroplast that has not equilibrated with chloroplast water (VSMOW scale)
δ_e	$\delta^{18}O$ of water at evaporative sites in leaves (VSMOW scale)
δ_{in}	$\delta^{18}O$ of CO_2 in air entering leaf chamber (VSMOW scale)
δ_R	$\delta^{18}O$ of net CO_2 efflux during dark respiration (VSMOW scale)
δ_s	$\delta^{18}O$ of source water (VSMOW scale)
E	Transpiration rate
e	Discrimination against ^{13}C during day respiration
e_a	Vapor pressure in atmosphere
e_i	Vapor pressure in leaf intercellular air spaces
ε^+	Equilibrium ^{18}O fractionation between liquid water and vapor
ε_k	Kinetic fractionation during diffusion of $H_2^{18}O$ from leaf intercellular air spaces to atmosphere

ε_w	Equilibrium ^{18}O fractionation between CO_2 and water
f	Discrimination against ^{13}C during photorespiration
g_t	Conductance to H_2O from leaf intercellular air space to atmosphere
g_i	Conductance to CO_2 from leaf intercellular air spaces to sites of carboxylation
g_{tc}	Conductance to CO_2 from chloroplast to atmosphere
k	Carboxylation efficiency
L	Scaled effective path length for calculation of ϕ
P	Atmospheric pressure
ϕ	Péclet number
θ	Proportion of chloroplast CO_2 isotopically equilibrated with chloroplast water
R_A	$^{13}\text{C}/^{12}\text{C}$ or $^{18}\text{O}/^{16}\text{O}$ of net CO_2 uptake by photosynthesis
R_a	$^{13}\text{C}/^{12}\text{C}$ or $^{18}\text{O}/^{16}\text{O}$ of CO_2 in atmosphere
R_{ce}	$^{18}\text{O}/^{16}\text{O}$ of CO_2 in equilibrium with chloroplast water
R_{c0}	$^{18}\text{O}/^{16}\text{O}$ of chloroplast CO_2 that has not equilibrated with chloroplast water
R_e	$^{18}\text{O}/^{16}\text{O}$ of water at evaporative sites in leaves
R_R	$^{18}\text{O}/^{16}\text{O}$ of net CO_2 efflux during dark respiration
R_{Std}	$^{18}\text{O}/^{16}\text{O}$ of VSMOW standard
r_s	Stomatal resistance to water vapor diffusion
r_b	Leaf boundary layer resistance to water vapor diffusion
\mathfrak{R}_d	Day respiration rate
\mathfrak{R}_n	Net CO_2 efflux rate during dark respiration
ρ	Ratio of rates of carboxylation and CO_2 hydration in chloroplast
Γ^*	CO_2 compensation point in absence of day respiration
u	Flow rate of air through leaf chamber
w_i	Mole fraction of water vapor in the leaf intercellular air spaces
W	Leaf lamina water concentration
Λ	Area of leaf in leaf chamber

where C_i is the CO_2 partial pressure in the intercellular air spaces, and C_s is that at the leaf surface. The term a_w describes the summed discrimination against C^{18}O during liquid phase diffusion and dissolution (0.8‰); a is the discrimination during diffusion through the stomata (8.8‰); and a_b is the discrimination during diffusion through the leaf boundary layer (5.8‰). I note that equation (7.3) is precisely the same as the equation given for a by Farquhar and Lloyd (1993); I have simply multiplied both their numerator and denominator by -1 . The equilibrium fractionation between water and CO_2 can be calculated as (Brenninkmeijer et al. 1983)

$$\varepsilon_w(\text{‰}) = \frac{17604}{T} - 17.93, \quad (7.4)$$

where T is leaf temperature in K.

The oxygen isotope composition of CO_2 in the chloroplast of a respiring leaf (δ_c) can be calculated from the following equation:

$$\delta_c = \delta_R \left(1 + \bar{a}\right) \left(1 - \frac{C_a}{C_c}\right) + \frac{C_a}{C_c} (\delta_a - \bar{a}) + \bar{a}; \quad (7.5)$$

derivation of equation (7.5) is presented in Appendix 7.1. Equations (A7.5) and (A7.6) can be combined, and, after dividing through by R_{Std} , give

$$\delta_c = \delta_e \theta (1 + \varepsilon_w) + \theta \varepsilon_w + \delta_{c0} (1 - \theta). \quad (7.6)$$

For a series of measurements made at different values of δ_e , δ_c can be calculated from equation (7.5) and plotted against δ_e . According to equation (7.6), the slope of the relationship between δ_c and δ_e , m , is then equal to $\theta(1 + \varepsilon_w)$, such that θ can be calculated as $\theta = m/(1 + \varepsilon_w)$. The intercept of the relationship, I , is equal to $\theta \varepsilon_w + \delta_{c0}(1 - \theta)$, such that δ_{c0} can be calculated as $\delta_{c0} = (I - \theta \varepsilon_w)/(1 - \theta)$. I note that such an analysis assumes that only δ_e varies across the series of measurements; thus, θ and δ_{c0} are assumed invariant.

The oxygen isotope enrichment at the evaporative sites in leaves (Δ_e) can be calculated as (Craig and Gordon 1965; Dongmann et al. 1974; Farquhar and Lloyd 1993)

$$\Delta_e = \varepsilon^+ + \varepsilon_k + (\Delta_v - \varepsilon_k) \frac{e_a}{e_i}, \quad (7.7)$$

where ε^+ is the equilibrium fractionation that occurs during the phase change from liquid to vapor, ε_k is the kinetic fractionation that occurs during diffusion of vapor from the leaf intercellular air space to the atmosphere, Δ_v is the isotopic enrichment of vapor in the atmosphere, and e_a/e_i is the ratio of ambient to intercellular vapor pressures. The

Δ_e and Δ_v are defined with respect to source water, such that $\Delta_e = R_e/R_s - 1$ and $\Delta_v = R_v/R_s - 1$, where R_e is $^{18}\text{O}/^{16}\text{O}$ of water at the evaporating sites, R_s is $^{18}\text{O}/^{16}\text{O}$ of source water, and R_v is $^{18}\text{O}/^{16}\text{O}$ of vapor in the atmosphere. The term δ_e can be calculated from Δ_e as

$$\delta_e = \Delta_e (1 + \delta_s) + \delta_s, \quad (7.8)$$

where δ_s is the oxygen isotope composition of source water relative to a standard. The parameter Δ_v in equation (7.6) can be calculated from measurements of the oxygen isotope composition of vapor in the atmosphere (δ_v) and source water as $\Delta_v = (\delta_v - \delta_s)/(1 + \delta_s)$. The equilibrium fractionation between liquid and vapor, ε^+ , can be calculated as (Bottinga and Craig 1969)

$$\varepsilon^+ (\text{‰}) = 2.644 - 3.206 \left(\frac{10^3}{T} \right) + 1.534 \left(\frac{10^6}{T^2} \right), \quad (7.9)$$

where T is leaf temperature in K. The kinetic fractionation, ε_k , can be calculated as (Farquhar et al. 1989b)

$$\varepsilon_k (\text{‰}) = \frac{32r_s + 21r_b}{r_s + r_b}, \quad (7.10)$$

where r_s and r_b are the stomatal and boundary layer resistances to water vapor diffusion ($\text{m}^2 \text{ s mol}^{-1}$), and 32 and 21 are associated fractionation factors scaled to per mil. These fractionation factors have been revised up from values of 28 and 19, respectively, based on recent measurements showing the isotope effect for diffusion of H_2^{18}O in air to be 1.032 (Cappa et al. 2003), rather than 1.028 (Merlivat 1978).

7.4. Methods

7.4.1. Plant material and gas exchange measurements

Ricinus communis L. plants were grown from seeds in 10 L pots for 8 to 12 weeks in a temperature and humidity controlled glasshouse. Growth conditions were essentially the same as those described in Chapter 4. Daytime temperature and humidity were $27 \pm 2^\circ\text{C}$ and $40 \pm 10\%$, respectively. Nighttime temperature was 20°C , with the same humidity as during the day. Measurements were made on fully expanded leaves of plants that were approximately 1 m tall. Projected areas of measured leaves ranged from approximately 400 to 800 cm^2 . The configuration of the gas exchange system was described previously (Chapter 4). The through-flow rate of air in the leaf chamber was approximately 3 L min^{-1} . Chamber air cycled continuously through a by-pass drying loop to remove water vapor. The flow rate through the by-pass drying loop

was varied between 5 and 45 L min⁻¹ to achieve different vapor pressures within the chamber, and therefore different values of e_a/e_i , and consequently of δ_e . Air entering the leaf chamber was generated by mixing 79% dry nitrogen with 21% dry oxygen using two mass flow controllers. Carbon dioxide was added to this air stream from a cylinder of 10% CO₂ in air. Leaf temperature was measured with eight thermocouples arrayed across the underside of the leaf, and the average of these measurements used in gas-exchange and isotopic calculations. Gas-exchange calculations were performed according to the equations of Caemmerer and Farquhar (1981).

After gas exchange conditions in the leaf chamber stabilized for a time period judged long enough for leaf water to reach isotopic steady state, CO₂ was cryogenically trapped from air exiting the chamber, as described previously (Evans et al., 1986; Caemmerer and Evans, 1991). Trapping continued until approximately 50 μ mol of CO₂ was obtained. The time period sufficient for leaf water to reach isotopic steady state was assumed to be three times the residence time of lamina leaf water (Förstel, 1978). The residence time of lamina leaf water was calculated as $W/g_t w_i$, where W is the lamina water concentration (mol m⁻²), g_t is the total conductance of boundary layer plus stomata to water vapor (mol m⁻² s⁻¹), and w_i is the mole fraction of water vapor in the leaf intercellular air spaces (mol mol⁻¹). The term W was determined to be 6.3 ± 0.4 mol m⁻² (mean \pm 1 SD) from measurements of the difference between fresh weight and dry weight for one leaf from each of five plants. This mean value of W was assumed for all leaves in the experiment; g_t and w_i were calculated continuously for each leaf being measured. Time periods calculated in this way for leaf water to reach isotopic steady state after a step change in humidity ranged from approximately 0.5 to 3.5 hrs.

Three experiments were conducted, two in the dark and one in the light. In the first dark experiment, air entering the leaf chamber was free of CO₂. All CO₂ in the air exiting the chamber was therefore derived from the leaf. Measurements were conducted on one leaf from each of five plants. Each leaf was subject to two or three different chamber vapor pressures, and CO₂ collected after gas exchange had stabilized for the requisite amount of time at each vapor pressure. Chamber air temperature was maintained at approximately 30°C. The second dark experiment was similar to the first, but differed in that CO₂ was added to the air entering the chamber, such that the partial pressure within the chamber was approximately 350 μ bar. The third experiment was in the light. Irradiance varied between 300 and 800 μ mol PAR m⁻² s⁻¹, and chamber air

temperature varied between 25 and 30°C. The CO₂ partial pressure within the chamber was approximately 350 µbar.

7.4.2. Isotope measurements

The carbon and oxygen isotope composition of CO₂ exiting the leaf chamber was determined on an Isoprime mass spectrometer (Micromass, Manchester, UK) operating in dual inlet mode. Repeated analyses of the same gas sample generally showed a precision of better than 0.1‰ (1SD, $n=10$) for $\delta^{13}\text{C}$ and $\delta^{18}\text{O}$. The carbon and oxygen isotopic composition of the gas used as a reference for the dual inlet measurements was calibrated against standard gases supplied by the International Atomic Energy Agency (Vienna, Austria). Oxygen isotope ratios in this paper are presented relative to Vienna Standard Mean Ocean Water (VSMOW); carbon isotope ratios are presented relative to the Vienna Pee Dee Belemnite standard (VPDB). The oxygen isotope composition of irrigation water fed to the plants was determined with an Isochrom mass spectrometer (Micromass, Manchester, UK) operating in continuous flow mode (Farquhar et al., 1997). The water samples were pyrolysed in a custom-built furnace at 1300°C prior to entering the mass spectrometer. Precision of analyses, based on repeated measurements of a laboratory standard water sample, was 0.3‰ (1SD, $n=10$). The $\delta^{18}\text{O}$ of the irrigation water was found to be $-7.2 \pm 0.2\text{‰}$ (mean \pm 1SE; $n=6$).

We assumed that the only source of N₂O in the leaf chamber was the compressed air that the CO₂ was mixed into, and that the concentration of N₂O in this air was 300 nmol mol⁻¹. The CO₂ concentration was 10%, giving a ratio of N₂O to CO₂ of 3×10^{-6} . This ratio could have been doubled during photosynthesis measurements, when the CO₂ concentration exiting the chamber was as little as half that entering it, giving a ratio of 6×10^{-6} . Using the empirical equations of Mook and van der Hoek (1983), this ratio of N₂O to CO₂ would result in measurement biases of 0.002‰ for both $\delta^{13}\text{C}$ and $\delta^{18}\text{O}$. This bias was considered negligible, and no attempt was made to account for contamination of CO₂ samples by N₂O.

7.4.3. Calculation of the oxygen isotope composition of dark-respired CO₂

In the first dark experiment, where air entering the leaf chamber was free of CO₂, the oxygen isotope composition of respired CO₂, δ_{R} , was assumed equal to that of CO₂ exiting the chamber, δ_{a} . In the second dark experiment, where air entering the

chamber had a CO₂ concentration sufficient to bring the concentration inside the chamber to near 350 μmol mol⁻¹, δ_R was calculated as

$$\delta_R = \frac{C_a \delta_a - C_{in} \delta_{in}}{C_a - C_{in}}, \quad (7.11)$$

where C_a is the CO₂ partial pressure (μbar) of air within the chamber when dried, δ_a is δ¹⁸O of CO₂ within the chamber, C_{in} is the CO₂ partial pressure (μbar) of dry air entering the chamber, and δ_{in} is the δ¹⁸O of CO₂ entering the chamber. A derivation of equation (7.11) is provided in Appendix 7.2. The terms C_a and δ_a are measured in gas exiting the leaf chamber, due to effective stirring of air within the chamber.

7.4.4. Calculation of photosynthetic discrimination against ¹³C and ¹⁸O

For measurements in the light, I calculated carbon and oxygen isotope discrimination during photosynthesis as described by Evans et al. (1986):

$$\Delta_A = \frac{R_a}{R_A} - 1 = \frac{\xi(\delta_a - \delta_{in})}{1 + \delta_a - \xi(\delta_a - \delta_{in})}, \quad (7.12)$$

where R_a is ¹³C/¹²C or ¹⁸O/¹⁶O of CO₂ within the leaf chamber, R_A is ¹³C/¹²C or ¹⁸O/¹⁶O of CO₂ removed from the chamber by photosynthesis, δ_a is δ¹³C or δ¹⁸O of CO₂ within the leaf chamber, δ_{in} is δ¹³C or δ¹⁸O of CO₂ entering the chamber, and ξ is defined as $C_{in}/(C_{in}-C_a)$, where C_{in} and C_a refer to CO₂ partial pressures in dry air. I calculated the oxygen isotope composition of chloroplast CO₂ during photosynthesis by rearranging the C¹⁸OO discrimination equation presented by Farquhar and Lloyd (1993):

$$\Delta_{ca} = \frac{\Delta_A - \bar{a}}{(1 + \Delta_A) \left(\frac{C_c}{C_a - C_c} \right)}, \quad (7.13)$$

where Δ_A is discrimination against C¹⁸OO during photosynthesis, as defined above, and Δ_{ca} is defined as $(R_c/R_a)-1$, where R_c is ¹⁸O/¹⁶O of chloroplast CO₂. I then calculated δ_c as $\delta_c = \Delta_{ca}(1 + \delta_a) + \delta_a$.

For the photosynthesis measurements that comprised my third experiment, I compared the regression approach to calculating θ, as described above in the theory relating to dark respiration, to the method suggested by Gillon and Yakir (2000b), whereby θ can be calculated separately for each individual photosynthesis measurement:

$$\theta = \frac{\Delta_{ca} + \bar{a} \left(1 - \frac{C_c}{C_a} \right)}{\Delta_{ea} + \bar{a} \left(1 - \frac{C_c}{C_a} \right)}, \quad (7.14)$$

where Δ_{ea} is the value of Δ_{ca} expected if chloroplastic CO_2 were in full oxygen isotope equilibrium with δ_e . The Δ_{ea} was calculated as

$$\Delta_{ea} = \frac{\delta_e (1 + \varepsilon_w) + \varepsilon_w - \delta_a}{1 + \delta_a}. \quad (7.15)$$

Equation (14) incorporates an assumption that is not applied in the regression approach to calculating θ that I described above for dark respiration. The assumption is that the $\delta^{18}\text{O}$ of CO_2 in the chloroplast that has not equilibrated with leaf water can be calculated from the equation $R_{c0} = R_a [1 - a(1 - C_c/C_a)]$ (Gillon and Yakir, 2000b), which can be replaced, to a close approximation, by $\delta_{c0} = \delta_a - a(1 - C_c/C_a)$. Defining δ_{c0} in this way assumes no discrimination against C^{18}OO by Rubisco; it also ignores any possible effect of photorespiration or day respiration on δ_{c0} .

7.4.5. Calculation of the conductance from c_i to c_c

The CO_2 conductance from leaf intercellular air spaces to the sites of carboxylation in chloroplasts (g_i) was calculated from ^{13}C discrimination measurements during photosynthesis using the method of Evans et al. (1986):

$$\Delta_i - \Delta_{obs} = \frac{(b - a_w^{13})}{g_i} \left(\frac{A}{C_a} \right) - \frac{\frac{e\mathcal{R}_d}{k} + f\Gamma_*}{C_a}, \quad (7.16)$$

where Δ_{obs} is the observed ^{13}C discrimination, b is the discrimination against $^{13}\text{CO}_2$ during carboxylation (taken as 29‰), a_w^{13} is the sum of discriminations against $^{13}\text{CO}_2$ during dissolution of CO_2 and liquid phase diffusion (1.8‰), A is the net photosynthetic rate ($\mu\text{mol CO}_2 \text{ m}^{-2} \text{ s}^{-1}$), C_a is the ambient CO_2 partial pressure (μbar), \mathcal{R}_d is day respiration ($\mu\text{mol CO}_2 \text{ m}^{-2} \text{ s}^{-1}$), e is the associated discrimination against $^{13}\text{CO}_2$, k is the carboxylation efficiency ($\text{mol m}^{-2} \text{ s}^{-1} \text{ bar}^{-1}$), Γ_* is the CO_2 compensation point in the absence of \mathcal{R}_d (μbar), and f is the discrimination against $^{13}\text{CO}_2$ associated with photorespiration. The term Δ_i represents the discrimination that would occur if g_i were infinite, and if photorespiration and day respiration did not discriminate (Farquhar et al. 1982):

$$\Delta_i = a_b^{13} \left(\frac{C_a - C_s}{C_a} \right) + a^{13} \left(\frac{C_s - C_i}{C_a} \right) + b \left(\frac{C_i}{C_a} \right), \quad (7.17)$$

where a_b^{13} is the discrimination against $^{13}\text{CO}_2$ during diffusion through the boundary layer (2.8‰), C_s is the CO_2 partial pressure at the leaf surface, and a^{13} is the discrimination against $^{13}\text{CO}_2$ during diffusion through the stomata (4.4‰). The term $(b - a_w^{13})/g_i$ was calculated from the slope, m^{13} , of a plot of $\Delta_i - \Delta_{\text{obs}}$ against A/C_a . The term g_i was then calculated as $(b - a_w^{13})/m^{13}$. The value of m^{13} is independent of values assigned to f and e in equation (16), because varying these parameters affects the intercept of the regression rather than the slope. Therefore, there is no need to assign values to f and e for calculation of g_i .

7.4.6. Calculation of the oxygen isotope composition of average lamina leaf water

I estimated the average lamina leaf water ^{18}O enrichment (Δ_L) of leaves during CO_2 collections from a model relating Δ_L to Δ_e (Farquhar and Lloyd 1993):

$$\Delta_L = \frac{\Delta_e (1 - e^{-\wp})}{\wp}, \quad (7.18)$$

where Δ_e is as calculated in equation (7.7), and \wp is a lamina radial Péclet number (Farquhar and Gan 2003). The term \wp is defined as $EL/(CD)$, where E is transpiration rate ($\text{mol m}^{-2} \text{s}^{-1}$), L is a scaled effective path length (m), C is the molar concentration of water ($5.55 \times 10^4 \text{ mol m}^{-3}$), and D is the diffusivity of H_2^{18}O in water ($2.66 \times 10^{-9} \text{ m}^2 \text{s}^{-1}$). In a previous experiment, I found that the scaled effective path length for *Ricinus communis*, grown and measured under the same conditions as in the present experiment, was $15.0 \pm 3.5 \text{ mm}$ (mean \pm 1SD; $n=5$) (Chapter 4). This mean value was used to calculate Δ_L . The term δ_L was calculated as $\delta_L = \Delta_L(1 + \delta_s) + \delta_s$. In the previous experiment (Chapter 4), I found that the ethanol-dry ice traps on the by-pass drying loop of the gas exchange system were not quite efficient enough to remove all of the water vapor from the air cycling back to the chamber. Due to fractionation during condensation of the vapor in the traps, vapor in the air returning to the chamber was slightly enriched compared to that retained in the traps. As a result, Δ_v for the air exiting the chamber was found to be $1.2 \pm 0.5\text{‰}$ (mean \pm 1SE; $n=5$). This mean value was used in calculations of Δ_e .

7.5. Results

7.5.1. Dark respiration with CO₂ free air entering the leaf chamber

In the first dark respiration experiment, air entering the leaf chamber was free of CO₂, and air exiting the leaf chamber had a mean CO₂ partial pressure of 47 μ bar. The CO₂ exiting the leaf chamber was collected and analyzed for its isotopic composition. A summary of gas exchange parameters measured just prior to each CO₂ collection is presented in Table 7.2. The dark respiration rates of the leaves ranged from 0.8 to 2.0 μ mol CO₂ m⁻² s⁻¹ on a projected leaf area basis, with a mean value of 1.5. The C_a/C_i values ranged from 0.46 to 0.93, with a mean value of 0.81.

Isotopic parameters derived by combining the results of the gas exchange measurements with results of analyses of the isotopic composition of CO₂ exiting the leaf chamber, and of irrigation water fed to the plants, are given in Table 7.2; these parameters are δ_e , δ_L , and δ_c . Results for δ_a , the $\delta^{18}\text{O}$ of CO₂ exiting the leaf chamber, are also given in Table 7.2. The observed δ_R values, which are equal to δ_a in the first experiment, ranged from 43.8 to 59.0‰, with a mean value of 51.6‰. All $\delta^{18}\text{O}$ values in this chapter are reported relative to VSMOW. The δ_c values were significantly, positively correlated with corresponding values of δ_e (Figure 7.1); the Pearson correlation coefficient (r) between the two was 0.96 ($P < 0.0001$, $n = 11$). The δ_c values were also significantly correlated with values of δ_L ($r = 0.90$, $P = 0.0001$, $n = 11$), but the relationship was not as strong as that between δ_c and δ_e . The slope of the regression relating δ_c to δ_e was 0.82, yielding an estimate for θ of 0.79. Thus, I estimated, by applying equation (6), that 79% of the CO₂ in the chloroplasts had equilibrated with chloroplast water during dark respiration in the first experiment. The intercept of the regression relating δ_c to δ_e was 39.4‰; this intercept yields an estimate for δ_{c0} of 36.2‰. This is the mean $\delta^{18}\text{O}$ estimated for CO₂ not equilibrated with chloroplast water.

By applying the mean value of g_i derived from carbon isotope discrimination measurements during photosynthesis (see results below), I generated estimates of C_c and a . These values are detailed in Table 7.2. Estimates of C_a/C_c ranged from 0.45 to 0.88, with a mean value 0.78. When these values for C_a/C_c and a were inserted into equation (7.2), along with the values of θ and δ_{c0} described above, a mean *modeled* δ_R of 51.9‰ was predicted, in good agreement with the mean observed δ_R of 51.6‰. The range of *modeled* δ_R can be compared with the range of observed δ_R in Table 7.2.

Table 7.2. Gas exchange and isotopic characteristics for *R. communis* leaves. Values are given as the mean, with the total range in parentheses, for the three experiments conducted. Symbols are as defined in Table 7.1. Modeled δ_R values were calculated using equation (7.2) and the empirically determined coefficients for θ and δ_{c0} for experiments 1 and 2. Modeled Δ_A values were calculated using equation (7.13) and assuming $\Delta_{ca} = \Delta_{ea}$; the term Δ_{ea} was calculated as in equation (7.15).

Parameter	Experiment 1: Dark respiration at low CO ₂ concentration	Experiment 2: Dark respiration at atmospheric CO ₂ concentration	Experiment 3: Photosynthesis at atmospheric CO ₂ concentration
	<i>n</i>	<i>n</i>	<i>n</i>
g_s (mol m ⁻² s ⁻¹)	0.28 (0.04 to 0.55)	0.13 (0.03 to 0.28)	0.50 (0.18 to 0.77)
E (mmol m ⁻² s ⁻¹)	4.4 (1.2 to 7.8)	2.7 (1.3 to 4.0)	8.8 (5.7 to 15.1)
T_{leaf} (°C)	29.3 (27.3 to 31.2)	30.2 (29.3 to 30.8)	27.2 (24.0 to 30.1)
C_a (μbar)	47 (24 to 66)	347 (324 to 365)	363 (328 to 395)
C_i (μbar)	63 (27 to 125)	357 (328 to 401)	285 (250 to 317)
C_c (μbar)	66 (28 to 128)	360 (330 to 403)	249 (207 to 287)
e_a/e_i	0.53 (0.13 to 0.92)	0.41 (0.11 to 0.73)	0.51 (0.30 to 0.78)
a (‰)	6.6 (5.4 to 8.4)	5.9 (3.7 to 8.3)	6.0 (5.0 to 7.5)
δ_a (‰ vs. VSMOW)	51.6 (43.8 to 59.0)	43.5 (37.7 to 51.2)	42.3 (40.1 to 45.4)
δ_e (‰ vs. VSMOW)	16.9 (5.0 to 29.2)	20.5 (10.8 to 29.8)	17.5 (9.4 to 23.9)
δ_L (‰ vs. VSMOW)	12.4 (4.3 to 26.5)	17.2 (8.4 to 27.4)	9.5 (4.1 to 16.4)
δ_c (‰ vs. VSMOW)	53.3 (44.8 to 63.2)	51.4 (44.6 to 60.7)	59.6 (50.4 to 70.7)
δ_R (‰ vs. VSMOW)	51.6 (43.8 to 59.0)	277 (233 to 324)	
modeled δ_R	51.9 (34.0 to 64.4)	291 (149 to 476)	
Δ_A (‰ vs. VSMOW)			44.6 (32.4 to 78.5)
modeled Δ_A			43.4 (30.6 to 62.9)

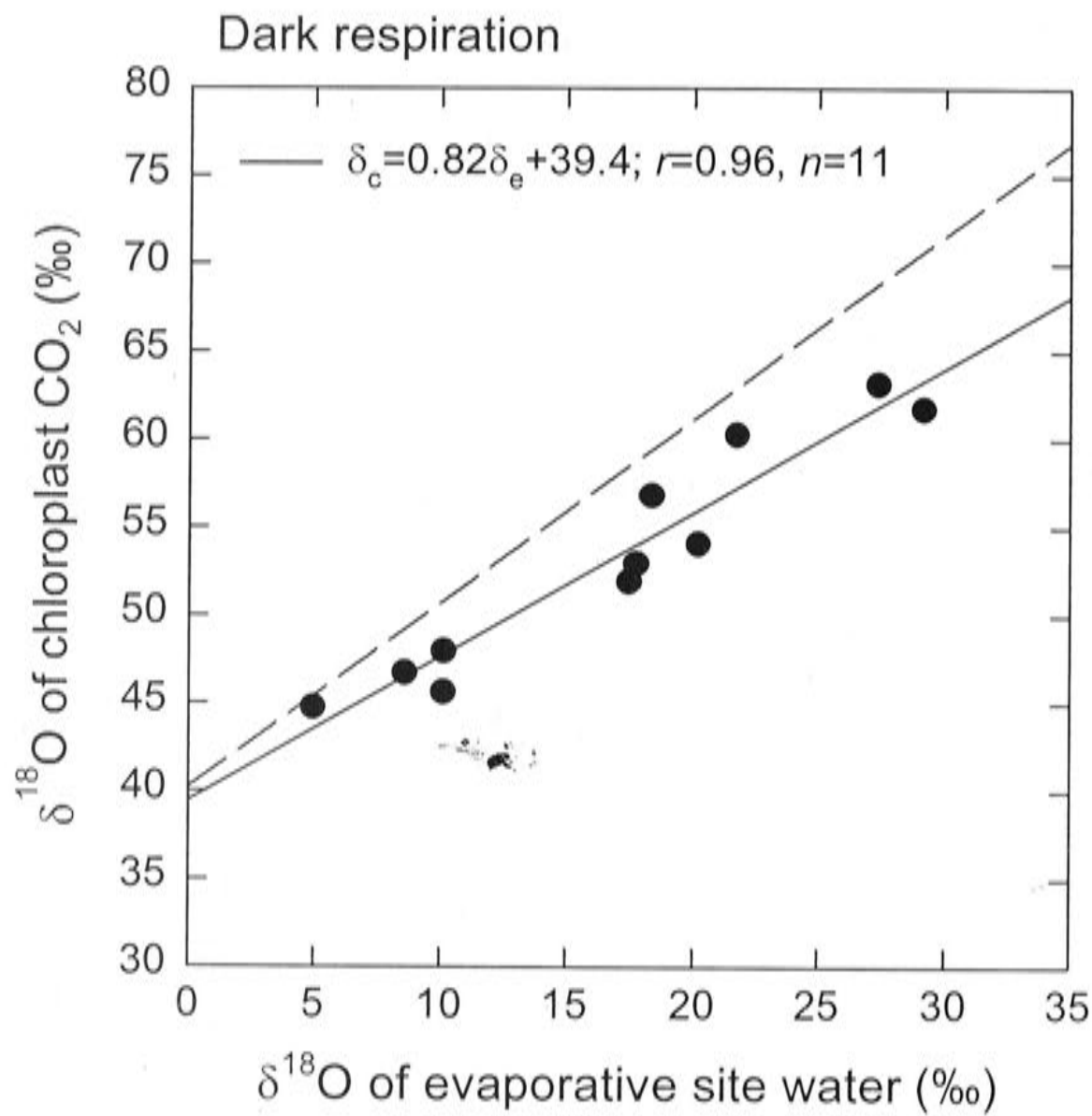


Figure 7.1. The $\delta^{18}\text{O}$ of chloroplast CO_2 plotted against the $\delta^{18}\text{O}$ of water at evaporative sites in *R. communis* leaves during dark respiration. In this experiment, air entering the leaf chamber was free of CO_2 , and the CO_2 partial pressure of air exiting the chamber averaged 47 μbar . The $\delta^{18}\text{O}$ of chloroplast CO_2 was calculated from measurements of the $\delta^{18}\text{O}$ of CO_2 exiting the chamber and gas exchange parameters, as described in the theory section of this chapter. The broken line on the graph represents the relationship expected if chloroplast CO_2 were in full oxygen isotope equilibrium with water at evaporative sites. The $\delta^{18}\text{O}$ values are presented relative to VSMOW. The $\delta^{18}\text{O}$ of irrigation water fed to the plants was -7.2‰ .

7.5.2. Dark respiration at atmospheric CO₂ concentration

In the second dark respiration experiment, the partial pressure of CO₂ in the air entering the leaf chamber was adjusted such that the air exiting the chamber had a partial pressure of approximately 350 μ bar. Under these conditions, leaf dark respiration rates were similar to those observed in the first experiment, ranging from 1.0 to 2.0 μ mol CO₂ m⁻² s⁻¹, with a mean value of 1.4. Stomatal conductance was lower than in the first experiment, having a mean value less than half that observed in the first experiment (Table 7.2). This presumably reflects a response to the increased CO₂ partial pressure within the leaf chamber. Although stomatal conductance was lower, C_a/C_i values were higher than in the first experiment due to the increase in C_a ; values ranged from 0.91 to 0.99, with a mean of 0.97. The $\delta^{18}\text{O}$ of CO₂ in air entering the leaf chamber was $19.1 \pm 0.1\text{‰}$ (mean \pm 1SE; $n=5$). The mean $\delta^{18}\text{O}$ of CO₂ exiting the chamber was 43.5‰.

The most striking difference between the first and second dark respiration experiments was the difference in observed δ_R . The mean observed δ_R in the second experiment was 277‰, which can be compared with 52‰ for the first experiment (Table 7.2). Mean values for δ_e , δ_L , and δ_c were similar between the two experiments (Table 7.2). Differences between δ_e and δ_L in the second experiment were slightly less than in the first experiment, reflecting the lower transpiration rates (Table 7.2). As in the first experiment, variation in δ_c was significantly correlated with variation in δ_e (Figure 7.2), showing an r value of 0.95 ($P<0.0001$, $n=10$). It was also correlated with δ_L , with a slightly lower correlation coefficient ($r=0.94$, $P<0.0001$, $n=10$). The regression slope of the relationship between δ_c and δ_e was 0.82, resulting in an estimate for θ of 0.79, suggesting that 79% of the CO₂ in chloroplasts had equilibrated with chloroplast water during dark respiration in the second experiment. This θ value is the same as the value of 0.79 estimated in the first experiment. The value of the intercept of the regression of δ_c on δ_e was 34.6‰, yielding an estimate for δ_{c0} of 14.3‰; this value is lower than the δ_{c0} of 36.2‰ estimated in the first experiment.

Values of C_a/C_c in the second experiment did not differ from values for C_a/C_i when calculated to two decimal places; the range was from 0.91 to 0.99, with a mean of 0.97. This mean of 0.97 is considerably higher than the mean C_a/C_c of 0.78 observed in the first experiment. Mean estimates for a were similar between the two experiments (Table 7.2). When the empirically determined coefficients for θ and δ_{c0} for the second

experiment were inserted into equation (7.2), along with the other relevant parameters, the mean value of *modeled* δ_R was 291‰, which compares reasonably well with the mean observed δ_R of 277‰. The relatively small difference between the two presumably reflects variation around the regression line in Figure 7.2, which was used to estimate θ and δ_{c0} .

A comparison of *modeled* δ_R values across both experiments with observed δ_R showed that *modeled* δ_R accounted for 80% of variation in observed δ_R . The regression line relating the two was $\delta_R(\text{observed}) = 0.72\delta_R(\text{modeled}) + 39.5$ ($R^2 = 0.80$, $P < 0.0001$, $n = 21$).

7.5.3. Carbon and oxygen isotope discrimination during photosynthesis

In the third experiment, *R. communis* leaves were placed in the leaf chamber in the light, and gas exchange and isotopic analyses were conducted. Photosynthesis rates ranged from 8.5 to 30.9 $\mu\text{mol CO}_2 \text{ m}^{-2} \text{ s}^{-1}$, with a mean value of 20.4. The CO_2 partial pressure of air exiting the chamber ranged from 328 to 395 μbar , whereas the CO_2 partial pressure of incoming air ranged from 533 to 967 μbar ; this gave rise to ξ values ranging from 1.5 to 3.0. Stomatal conductance was approximately 4-fold larger in the light than in the dark at similar CO_2 partial pressure (Table 7.2). The C_i/C_a ranged from 0.66 to 0.90, with a mean of 0.79. The $\delta^{18}\text{O}$ of CO_2 entering the leaf chamber was $19.1 \pm 0.1\text{‰}$ (mean \pm 1SE; $n = 5$); the $\delta^{13}\text{C}$ of CO_2 entering the leaf chamber was $-33.1 \pm 0.2\text{‰}$ (mean \pm 1SE; $n = 5$). The $\delta^{18}\text{O}$ of CO_2 exiting the leaf chamber ranged from 40.1 to 45.4‰; the $\delta^{13}\text{C}$ of CO_2 exiting the chamber ranged from -25.3 to -19.3‰ .

The mean observed oxygen isotope discrimination during photosynthesis (Δ_A) was 44.6‰; the range is given in Table 7.2. The δ_c values for the photosynthesis experiment were somewhat higher than for the dark respiration experiment at similar CO_2 concentration, presumably reflecting a higher proportion of chloroplast CO_2 equilibrated with chloroplast water (i.e., higher θ). Differences between δ_c and δ_L were larger in the photosynthesis experiment than in the dark respiration experiments, reflecting the higher transpiration rates (Table 7.2). Variation in δ_c was significantly correlated with variation in δ_e ($r = 0.97$, $P < 0.0001$, $n = 8$), as shown in Figure 7.3. The δ_c was also correlated with δ_L ($r = 0.91$, $P = 0.001$, $n = 8$), but the correlation was not as strong as with δ_e . The slope of the relationship between δ_c and δ_e was 1.31; using equation (6), this indicates a value for θ of 1.25. However, this slope estimate was

strongly influenced by one outlying data point; this datum is identified by an arrow in Figure 7.3. If this outlying datum is excluded from the analysis, the slope of the relationship between δ_c and δ_e becomes 1.11, yielding an estimate for θ of 1.06. The individual θ values calculated according to the method of Gillon and Yakir (2000b) ranged from 0.93 to 1.24, with a mean value of 1.02. If the outlying data point identified with the arrow in Figure 7.3 is excluded, these individual θ estimates ranged from 0.93 to 1.06, with a mean of 0.99. Because the θ values were very close to 1.0, we did not estimate a δ_{c0} value for the photosynthesis experiment.

Observed carbon isotope discrimination values, Δ_{obs} , ranged from 19.4 to 25.2‰, whereas values predicted for infinite g_i and no discrimination by photorespiration or day respiration, Δ_i , ranged from 20.6 to 26.5‰. The slope of the relationship between $\Delta_i - \Delta_{\text{obs}}$ and A/C_a was 47.8 ± 14.6 (slope $\pm 1\text{SE}$), yielding a mean g_i estimate of $0.57 \text{ mol m}^{-2} \text{ s}^{-1} \text{ bar}^{-1}$.

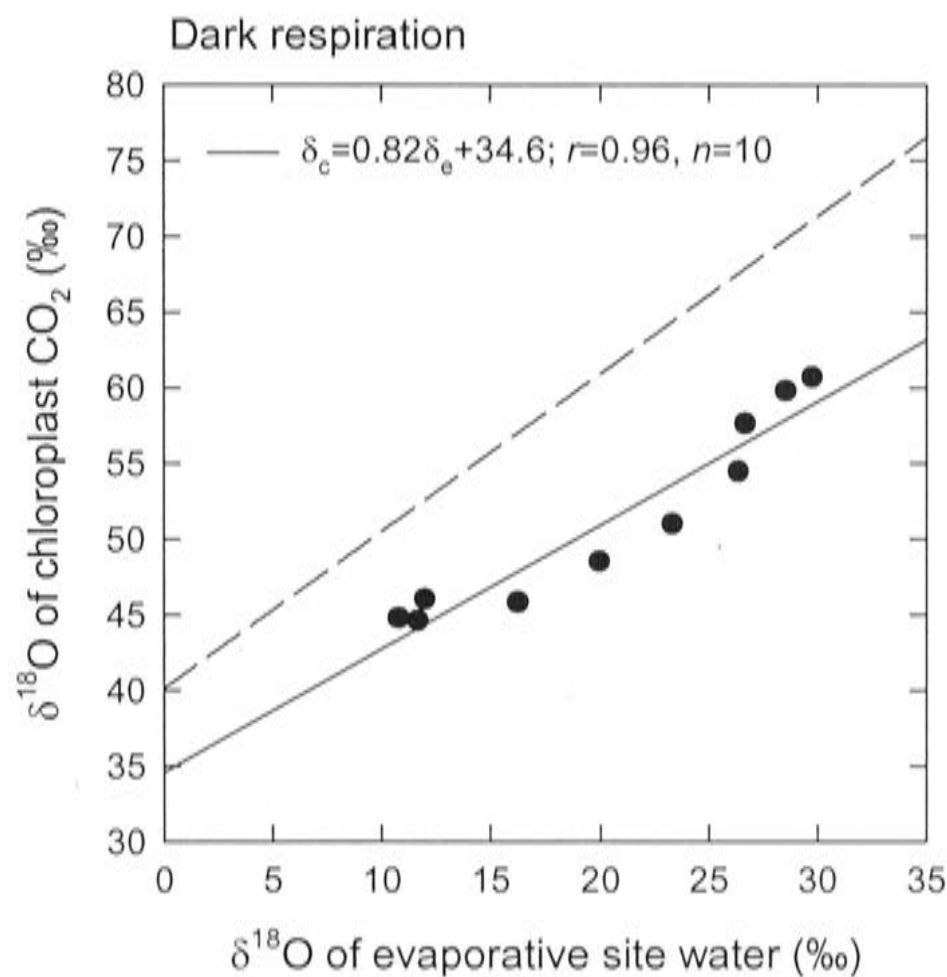


Figure 7.2. The $\delta^{18}\text{O}$ of chloroplast CO_2 plotted against the $\delta^{18}\text{O}$ of water at evaporative sites in *R. communis* leaves during dark respiration. In this experiment, air entering the leaf chamber had an average CO_2 partial pressure of 314 μbar , and air exiting the chamber had an average CO_2 partial pressure of 347 μbar . The broken line on the graph represents the relationship expected if chloroplast CO_2 were in full oxygen isotope equilibrium with water at the evaporative sites. The $\delta^{18}\text{O}$ values are presented relative to VSMOW. The $\delta^{18}\text{O}$ of irrigation water fed to the plants was -7.2‰ .

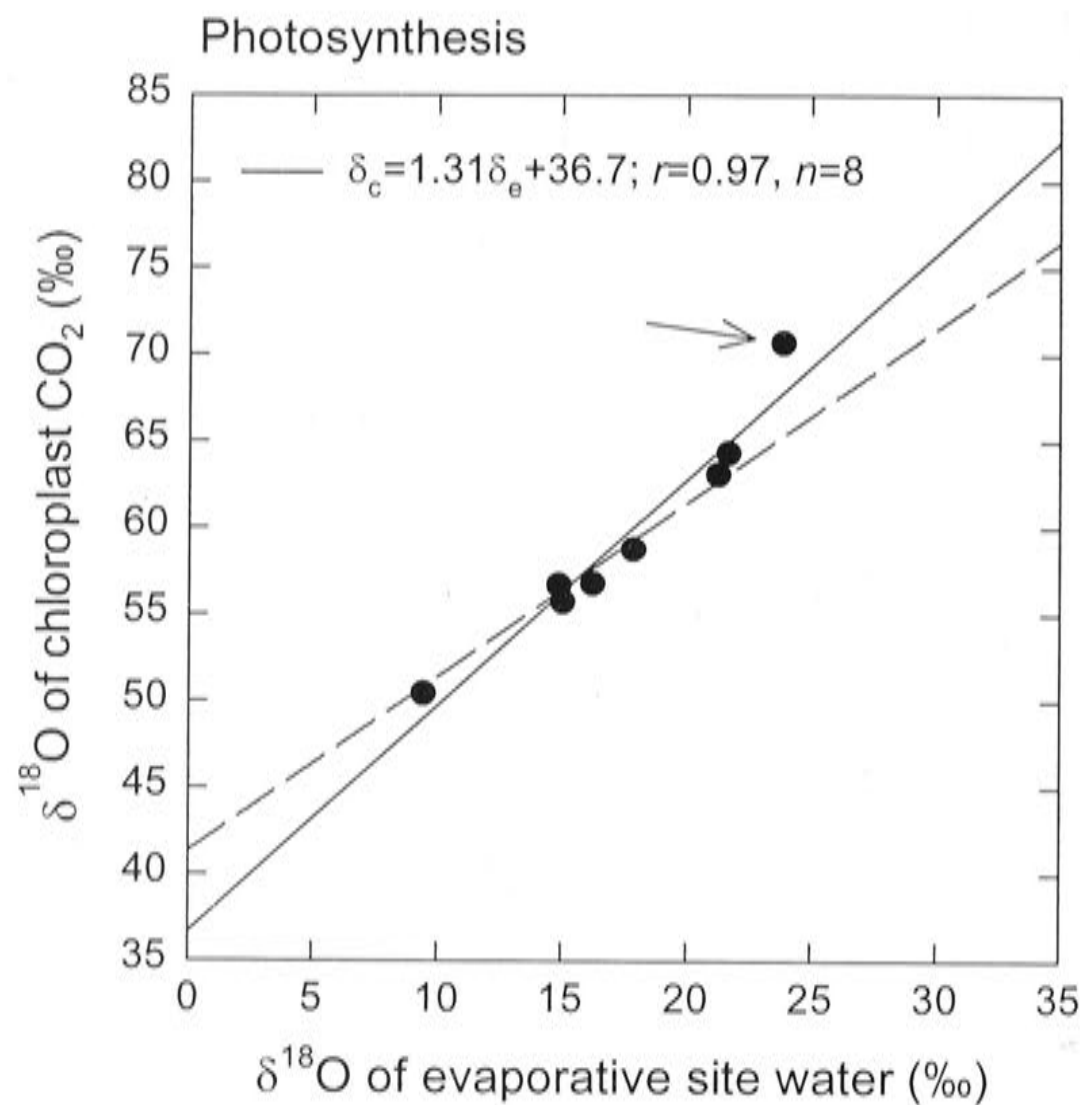


Figure 7.3. The $\delta^{18}\text{O}$ of chloroplast CO_2 plotted against the $\delta^{18}\text{O}$ of water at evaporative sites in *R. communis* leaves during photosynthesis. In this experiment, air entering the leaf chamber had an average CO_2 partial pressure of 833 μbar , and air exiting the chamber had an average CO_2 partial pressure of 363 μbar . Irradiance varied from 300 to 800 $\mu\text{mol PAR m}^{-2} \text{s}^{-1}$, and chamber air temperature varied between 25 and 30°C. The $\delta^{18}\text{O}$ of chloroplast CO_2 was calculated as described in the theory section of the main text. The broken line on the graph represents the relationship expected if chloroplast CO_2 were in full oxygen isotope equilibrium with water at the evaporative sites. The $\delta^{18}\text{O}$ values are presented relative to VSMOW. The $\delta^{18}\text{O}$ of irrigation water fed to the plants was -7.2‰ . The arrow on the graph indicates an outlying datum that strongly influenced the slope of the regression between δ_c and δ_e . Excluding this datum resulted in a slope between δ_c and δ_e of 1.10.

7.6. Discussion

The most important result of this study is that I have shown that it is the one-way CO_2 efflux from a respiring leaf that is labeled with the leaf water $\delta^{18}\text{O}$ signal, rather than the net CO_2 efflux. The one-way efflux can be calculated as $g_{\text{tc}}C_c/P$, where g_{tc} is the total conductance to CO_2 from chloroplast to atmosphere ($\text{mol m}^{-2} \text{s}^{-1}$), and P is atmospheric pressure (bar). In my second dark respiration experiment, where C_a

averaged 347 μbar , values for $g_{\text{tc}}C_e/P$ ranged from 7.4 to 50.1 $\mu\text{mol CO}_2 \text{ m}^{-2} \text{ s}^{-1}$, whereas the net respiratory efflux, \mathcal{R}_n , ranged from 1.0 to 2.0 $\mu\text{mol CO}_2 \text{ m}^{-2} \text{ s}^{-1}$; the ratio of $g_{\text{tc}}C_e/P$ to \mathcal{R}_n averaged 16.9. Thus, in cases where the CO_2 diffusing out of a respiring leaf has a $\delta^{18}\text{O}$ different from CO_2 in canopy air, the effect of δ_R on δ_a could be significantly underestimated if one assumes that only the net CO_2 efflux is influenced by the isotopic composition of leaf water. The analogous requirement for considering one-way CO_2 fluxes when calculating the effect of photosynthesizing leaves on $\delta^{18}\text{O}$ of atmospheric CO_2 was discerned by Farquhar et al. (1993).

Previous attempts to model the effect of leaf dark respiration on the $\delta^{18}\text{O}$ of CO_2 in canopy air have considered only the net respiratory CO_2 efflux. I will refer to this method as the ‘net flux model’. In the net flux model, δ_R is calculated as $\delta_R = \delta_e + \epsilon_w - a$, where a is usually taken as 8.8‰. The C^{18}OO isoflux is then calculated as the product of \mathcal{R}_n and δ_R . For the purposes of this discussion, I define an isoflux as the product of a net CO_2 flux and its $\delta^{18}\text{O}$. The net flux model has been used to interpret nighttime measurements of $\delta^{18}\text{O}$ in canopy CO_2 (Flanagan et al., 1997; Flanagan et al., 1999; Mortazavi and Chanton, 2002; Bowling et al., 2003a, 2003b), and in global simulations of $\delta^{18}\text{O}$ dynamics in atmospheric CO_2 (Cuntz et al., 2003a; Cuntz et al., 2003b). Earlier global studies did not differentiate leaf respiration from soil respiration, and thus did not define δ_R for leaves (Farquhar et al., 1993; Ciais et al., 1997). A slightly different version of the net flux model, with a modified term for diffusional fractionation, has also been applied at the leaf level (Yakir et al., 1994; Yakir 1998). If I apply the net flux model to data from my second experiment, where C_a was near that found in the atmosphere, predicted values for δ_R range from 42 to 61‰. These values can be compared to observed δ_R values ranging from 233 to 324‰. Thus, in the second dark respiration experiment, the net flux model underestimated the observed δ_R by 180 to 266‰. Note that these observed δ_R values are effective values that result when one treats the modification of $\delta^{18}\text{O}$ of CO_2 in air passing over the leaf as if it resulted from the net CO_2 efflux alone. Thus, using these observed δ_R values, the C^{18}OO isoflux is still calculated as $\mathcal{R}_n\delta_R$, and the large difference between \mathcal{R}_n and $g_{\text{tc}}C_e/P$ becomes manifested in the δ_R term.

If I apply the net flux model to my first experiment, where air entering the leaf chamber was free of CO_2 , it predicts δ_R values ranging from 36 to 60‰. Observed δ_R values in this experiment ranged from 44 to 59‰, in good agreement with predictions

from the net flux model. The difference in the performance of the net flux model between the first and second dark respiration experiments can be effectively understood by examining an alternative formulation of equation (7.2). If the definition of δ_c from equation (7.6) is substituted into equation (2), and the term $(1+a)$ in the denominator of equation (2) is assumed equal to unity, equation (2) can be rewritten as

$$\delta_R = \delta_c - \bar{a} + (\delta_c - \delta_a) \left(\frac{C_a}{C_c - C_a} \right). \quad (7.19)$$

$\uparrow \quad \uparrow \quad \underbrace{\hspace{1.5cm}}_{\text{III}}$

 I II

Equation (7.19) is informative in that terms I and II on the right side are analogous to the net flux model; the difference is that in equation (7.19) δ_c is defined as in equation (7.6), whereas in the net flux model δ_c is defined as $\delta_c + \varepsilon_w$. Term III on the right side of equation (7.19) reflects the proportion of CO_2 that diffuses into the leaf and equilibrates with leaf water, then diffuses out of the leaf, thereby altering the isotopic composition of CO_2 in the leaf chamber while leaving the net CO_2 efflux rate unaltered. This process is analogous to the invasion effect that has been described for soil respiration (Tans, 1998; Miller et al., 1999; Stern et al., 2001). In the first dark respiration experiment, where air entering the leaf chamber was free of CO_2 , this process was also occurring, but had a much smaller impact on δ_R than in the second experiment. This is because $(\delta_c - \delta_a)$ was small in the first experiment, having a mean value of 1.8‰; in contrast, $(\delta_c - \delta_a)$ in the second experiment had a mean value of 7.9‰. Additionally, $[C_a/(C_c - C_a)]$ was much smaller in the first experiment than in the second, having a mean value of 4.8 in the former versus 47.7 in the latter. As a result, the mean value for term III in equation (7.19), which can be thought of as the invasion term, was 5.2‰ for the first dark respiration experiment, and 234‰ for the second dark respiration experiment.

Equation (7.19) can be used to highlight the conditions under which large departures in δ_R from values predicted by the net flux model can be expected at the ecosystem level under natural conditions. For example, if δ_c is very similar to δ_a , term III will be small. Additionally, if stomata are tightly closed, $[C_a/(C_c - C_a)]$ will be small, and term III will also be small. Thus, the largest departures in δ_R from the predictions of the net flux model should occur when there is a relatively large difference between δ_c and δ_a , and when stomata are relatively open, such that $[C_a/(C_c - C_a)]$ is large. The approximation in equation (7.19) that $(1+a)$ equals unity introduces a very small bias into calculations with this equation; however, this bias is less than 1% and is therefore

negligible. Thus, equation (7.19), in combination with equation (7.6), can be used in place of equation (7.2), if so desired.

Photosynthesis enriches the atmosphere in $C^{18}OO$ due to exchange of CO_2 with evaporatively enriched leaf water in the chloroplast, whereas soil respiration is generally thought of as depleting the atmosphere in $C^{18}OO$, because soil CO_2 exchanges with water in soil that has generally not been enriched by evaporation (Flanagan and Ehleringer, 1998). In this study, I have observed that leaf dark respiration is capable of enriching air passing over a leaf in $C^{18}OO$ to as great an extent as photosynthesis. The mean $\delta^{18}O$ value of CO_2 exiting the leaf chamber in the respiration measurements at atmospheric CO_2 partial pressure was 43.5‰; the mean value for photosynthesis measurements at similar C_a was 42.3‰. The $\delta^{18}O$ of incoming CO_2 in both experiments was 19.1‰, and flow rates through the chamber were similar between the two experiments. Thus, dark respiration had as marked an effect as photosynthesis on the $\delta^{18}O$ of CO_2 passing over the leaves, even though the net exchange of CO_2 between the leaf and ambient air is roughly an order of magnitude less, and in the opposite direction, during dark respiration.

The effect of both photosynthesis and respiration on $\delta^{18}O$ of CO_2 in canopy air is partly controlled by the isotopic composition of leaf water. In natural systems, nighttime leaf water $\delta^{18}O$ is typically intermediate between daytime leaf water $\delta^{18}O$ and the $\delta^{18}O$ of source water (Dongmann et al., 1974; Förstel, 1978; Zundel et al., 1978; Förstel and Hützen, 1983; Flanagan and Ehleringer, 1991; Flanagan et al., 1993; Flanagan et al., 1999; Cernusak et al., 2002; Mortazavi and Chanton, 2002). I therefore expect nighttime leaf respiration to impart a $C^{18}OO$ signal on the atmosphere that is intermediate between the soil respiration signal and the photosynthesis signal.

Accurate prediction of the oxygen isotope composition of leaf water is important for interpreting vegetation effects on $\delta^{18}O$ of atmospheric CO_2 . Equation (7.7) can be used to calculate δ_e under steady state conditions. However, leaf water $\delta^{18}O$ is unlikely to be at steady state at night (Flanagan and Ehleringer, 1991; Harwood et al., 1998; Chapter 2). In Chapter 2, I applied a non-steady state equation for $\delta^{18}O$ in leaf water, derived by Farquhar and Cernusak (in preparation), and found good agreement between predicted and observed nighttime values. The combination of the non-steady state leaf water equation and the model that I have provided here for δ_R should allow reasonable predictions to be made of the impact of leaf dark respiration on $\delta^{18}O$ of atmospheric CO_2 .

Stomatal conductance will be an important parameter in the prediction of both δ_e and δ_R during the night. However, little attention has been paid historically to nighttime stomatal conductance. Snyder et al. (2003) recently observed nighttime stomatal conductance to water vapor ranging from 10 to 150 $\text{mmol m}^{-2} \text{s}^{-1}$ for 17 plant species in the western United States. However, a mechanistic framework for interpreting such variation does not currently exist. Further investigation into the patterns and processes controlling nighttime stomatal conductance will lead to more accurate prediction of nighttime δ_e and δ_R . I note that the mean stomatal conductance that I observed in the dark for *Ricinus communis* at normal atmospheric CO_2 concentration was 130 $\text{mmol m}^{-2} \text{s}^{-1}$ (Table 7.2), near the high end of values observed by Snyder et al. (2003) at night in the field. My measurements were made during the day, and it is likely that stomatal conductance was influenced by circadian rhythms, causing it to be higher than it would be in the dark at night.

The mean value of θ for the photosynthesis experiment calculated by the method described by Gillon and Yakir (2000b) was very close to 1.0. If the outlying data point, indicated by an arrow in Figure 7.3, was excluded from the analysis, the regression method resulted in a similar estimate of 1.06. Thus, both calculations suggested θ values close to unity for photosynthesizing *R. communis* leaves. A quick examination of Figure 3 shows that observed δ_e estimates lie very close to those expected for full equilibrium, with the exception of the one outlier, which is several per mil above the value expected for full equilibrium. I am unable to find a satisfactory explanation for why this particular datum should differ so markedly from the others. Results have been reported for a number of other C_3 species in which the CO_2 diffusing out of photosynthesizing leaves appeared to be very close to full equilibrium with δ_e (Farquhar et al. 1993; Gillon and Yakir 2001). Interestingly the θ values that I observed during dark respiration in *R. communis* were lower than those observed during photosynthesis, having values close to 0.80. Further research is necessary to determine the cause of this apparent discrepancy between θ in the light and in the dark.

Gillon and Yakir (2000b) suggested that during photosynthesis δ_{c0} , the $\delta^{18}\text{O}$ of CO_2 in the chloroplast not equilibrated with chloroplast water, can be calculated, to a close approximation, as $\delta_{c0} = \delta_a - a(1 - C_c/C_a)$. This definition assumes no discrimination against C^{18}OO by Rubisco during photosynthesis, and neglects any influence of photorespiration or day respiration on δ_{c0} . The latter statement is tantamount to saying

that CO_2 evolved from the mitochondria in the light has the same oxygen isotope composition as CO_2 in the chloroplast. In that case, any addition of mitochondrial CO_2 will have no impact upon the $\delta^{18}\text{O}$ of chloroplast CO_2 . The photosynthesis data set that I collected for *R. communis* did not allow me to test these assumptions because θ was very close to 1.0; thus, the δ_{c0} signal was completely washed out by the activity of carbonic anhydrase.

However, this was not the case for dark respiration, during which θ was approximately 0.80. The method of Gillon and Yakir (2000b) leads to mean δ_{c0} values for the first and second dark respiration experiments of 55.2 and 43.7‰, respectively. These values can be compared to the mean δ_{c0} values generated by the regression method of 30.8 and 14.3‰, respectively. Although the regression method makes no *a priori* assumptions about the controls on δ_{c0} , we caution against over-interpretation of these latter values for the following reason: the regression analysis, as summarized in equation (7.6), assumes no variation in θ and δ_{c0} among individual measurements in each experiment. The δ_{a} values varied among measurements according to how the leaf was modifying the $\delta^{18}\text{O}$ of CO_2 in the leaf chamber. Therefore, to the extent that δ_{c0} is controlled by δ_{a} , δ_{c0} could also have varied among individual measurements.

Nonetheless, the large variation between δ_{c0} calculated as suggested by Gillon and Yakir (2000b) and the apparent δ_{c0} values observed in the dark respiration experiments warrants some discussion. There are three possible sources for the oxygen in CO_2 evolved in mitochondria during either dark respiration or photosynthesis: atmospheric O_2 , organic oxygen from respiratory substrates, and oxygen from leaf water. Atmospheric O_2 has a $\delta^{18}\text{O}$ near 23.5‰ (VSMOW scale), and discrimination against ^{18}O during respiration in plant tissues ranges from about 17 to 26‰ (Guy et al., 1992). I would therefore expect the $\delta^{18}\text{O}$ of respiratory CO_2 deriving its oxygen atoms from O_2 to be in the range of 0 to 5‰. Assuming the O_2 tank used in our experiments had a $\delta^{18}\text{O}$ similar to atmospheric O_2 , this range of values would apply. Organic oxygen in phloem sap sugars of the *R. communis* plants that I studied had a mean $\delta^{18}\text{O}$ of 27.5 ± 0.6 ‰ (mean \pm 1SD; $n=10$). Generally, this oxygen pool is expected to have a $\delta^{18}\text{O}$ enriched by 27‰ compared to δ_{L} at the time of photosynthesis (Chapter 4). Oxygen atoms derived from water during respiratory reactions would also be expected to be enriched by 27‰ compared to the $\delta^{18}\text{O}$ of the water source. The difference between the $\delta^{18}\text{O}$ of CO_2 derived from any of these three sources and that of

CO₂ diffusing into the leaf from the atmosphere, prior to equilibration with leaf water, would depend on δ_a and, in the case of organic oxygen and oxygen from water, δ_L . However, it seems likely that under most circumstances the effect of incomplete equilibration between CO₂ evolved from mitochondria and leaf water would be to decrease δ_{c0} below the value predicted by the formulation given by Gillon and Yakir (2000). More experiments like those conducted by Yakir et al. (1994) would be helpful for resolving this issue.

Farquhar and Lloyd (1993) discussed the departure of δ_c from that predicted for equilibrium with δ_e during photosynthesis in terms of the ratio of the rate of carboxylation by Rubisco to the rate of CO₂ hydration by carbonic anhydrase. This ratio was termed ρ . A simplified non-equilibrium equation for discrimination against C¹⁸OO during photosynthesis, neglecting the possible effects of photorespiration and day respiration, was presented as (Farquhar and Lloyd, 1993)

$$\Delta_A = \frac{\bar{a}(1 + 3\rho) + \left(\frac{C_c}{C_a - C_c}\right)(\Delta_{ea} + 3\rho b^{18})}{1 - \left(\frac{C_c}{C_a - C_c}\right)\Delta_{ea} + 3\rho\left(\frac{C_a}{C_a - C_c}\right)}, \quad (7.20)$$

where b^{18} is discrimination against C¹⁸OO by Rubisco. Using this equation, and assuming $b^{18}=0$, I calculated a mean ρ value for my photosynthesis measurements of -0.002 ± 0.009 (mean \pm 1SD; $n=8$); if the outlier in Figure 3 is excluded, the mean ρ value becomes 0.001 ± 0.006 (mean \pm 1SD; $n=7$). These values can be compared to a mean ρ value calculated for *Phaseolus vulgaris* of 0.025 (Flanagan et al., 1994). Thus, the ρ values that I observed for *R. communis* were somewhat smaller than those observed previously for *P. vulgaris*. These values can be compared to a theoretical prediction for ρ of ~ 0.05 (Cowan, 1986).

In my calculations I have assumed that the $\delta^{18}\text{O}$ of chloroplast water is equivalent to δ_e . One might expect chloroplast water to be slightly less enriched than δ_e due to the Péclet effect (Farquhar and Lloyd, 1993), which describes the interplay between advection of water toward the evaporative sites and diffusion of heavy isotopes away from the evaporative sites. I found that correlations between δ_c and δ_e were generally stronger than between δ_c and δ_L . This agrees with previous results (Flanagan et al., 1994), and suggests that δ_e is a more relevant parameter for predicting $\delta^{18}\text{O}$ of CO₂ diffusing out of leaves than δ_L .

Gillon and Yakir (2000a) suggested that the CO_2 partial pressure at the chloroplast surface (C_{cs}) is a more appropriate parameter for predicting discrimination against C^{18}OO during photosynthesis than that at the sites of carboxylation by Rubisco (C_c). They reconstructed C_{cs} by combining measurements of C^{18}OO discrimination and carbonic anhydrase activity. I did not measure carbonic anhydrase activity directly, and so could not modify my calculations to take into account C_{cs} . In cases where the total resistance from the chloroplast to the atmosphere in the dark is dominated by the stomatal resistance, use of C_{cs} in place of C_c will likely not alter predictions of δ_R to a very large extent. However, if stomata are relatively open and $(\delta_c - \delta_a)$ is large, such that the invasion term in equation (7.19) is large, a variation between C_c and C_{cs} of as little as 2 μbar could have a significant effect on predicted δ_R . In such cases it may prove helpful to use C_{cs} in place of C_c , if possible.

Farquhar et al. (1993) found that a globally averaged leaf water $\delta^{18}\text{O}$ of 4.4‰ satisfactorily balanced the global budget for $\delta^{18}\text{O}$ of atmospheric CO_2 . In the most recent study of the global budget for $\delta^{18}\text{O}$ of atmospheric O_2 , a globally averaged leaf water $\delta^{18}\text{O}$ of between 6.1 and 6.8‰ was estimated (Hoffmann et al., 2004). Gillon and Yakir (2001) suggested that the globally averaged leaf water $\delta^{18}\text{O}$ could be as much as 3‰ more than the estimate of Farquhar et al. (1993), in agreement with the requirement for balancing the Dole effect (global ^{18}OO budget); the global C^{18}OO budget could then be maintained by incomplete equilibration of chloroplast CO_2 with chloroplast water (i.e., $\theta < 1$). They estimated a globally averaged θ of 0.80. The results presented in this study provide an additional reason that the apparent leaf water signals required to balance the global C^{18}OO and ^{18}OO budgets should not be expected to resolve into a single value. The apparent leaf water signal relevant to the global $\delta^{18}\text{O}$ budget for O_2 is the average daytime leaf water $\delta^{18}\text{O}$, weighted by diurnal (daytime) variation in photosynthetic oxygen evolution rates. In contrast, the apparent leaf water signal relevant to the global $\delta^{18}\text{O}$ budget for CO_2 is the 24-hour average leaf water $\delta^{18}\text{O}$, weighted by diel (day and night) variation in $g_{\text{tc}}C_c/P$. Thus, the apparent leaf water $\delta^{18}\text{O}$ signals relevant to the global C^{18}OO and ^{18}OO budgets are fundamentally different.

In conclusion, I observed a very large variation in the $\delta^{18}\text{O}$ of CO_2 respired by leaves in the dark, with observed values ranging from 44‰ to as high as 324‰. I have shown that this large range of δ_R values can be satisfactorily explained by taking into

account the flux of CO_2 that enters the leaf, equilibrates with leaf water, and diffuses out of the leaf without affecting the net CO_2 efflux. Incorporation of the correct expression for $\delta^{18}\text{O}$ of leaf dark respiration into ecosystem and global scales models of C^{18}OO dynamics could affect model outputs and their interpretation.

7.7. Appendix

7.7.1. Predicting the $\delta^{18}\text{O}$ of dark-respired CO_2

I begin by writing an equation for the total CO_2 flux from the leaf interior to the atmosphere in the dark in the steady state:

$$\mathfrak{R}_n = g_{tc} \left(\frac{C_c - C_a}{P} \right), \quad (\text{A7.1})$$

where \mathfrak{R}_n is the net CO_2 efflux ($\mu\text{mol m}^{-2} \text{s}^{-1}$), g_{tc} is the total conductance to CO_2 from chloroplast to atmosphere ($\text{mol m}^{-2} \text{s}^{-1}$), C_c and C_a are the CO_2 partial pressures in the chloroplast and atmosphere, respectively (μbar), and P is atmospheric pressure (bar). I make the assumption that, in C_3 plants, carbonic anhydrase resides primarily in the chloroplasts (Everson 1970; Jacobson et al. 1975; Tsuzuki et al. 1985), and that it is therefore the chloroplastic CO_2 concentration that should be considered when calculating the C^{18}OO efflux from the leaf. I further assume that the chloroplasts in C_3 plants are appressed against the intercellular air spaces in the leaf, and that CO_2 evolved in mitochondria interacts with chloroplasts during diffusion out of the leaf. These assumptions may need to be reassessed for application of the model to C_4 plants. Equation (A7.1) can be written for C^{18}OO as

$$\mathfrak{R}_n R_R = \frac{g_{tc}}{1+a} \left(\frac{C_c R_c - C_a R_a}{P} \right), \quad (\text{A7.2})$$

where R_R is the $^{18}\text{O}/^{16}\text{O}$ of dark-respired CO_2 , a is the weighted mean diffusional fractionation from chloroplast to atmosphere [calculated as described in equation (7.3) of the main text], R_c is $^{18}\text{O}/^{16}\text{O}$ of chloroplastic CO_2 , and R_a is $^{18}\text{O}/^{16}\text{O}$ of ambient CO_2 . Equations (A7.1) and (A7.2) can be combined to give

$$R_R (C_c - C_a) = \frac{1}{1+a} (C_c R_c - C_a R_a). \quad (\text{A7.3})$$

Dividing equation (A7.3) by the $^{18}\text{O}/^{16}\text{O}$ of a standard, R_{Std} , and applying the relationship $R_X/R_{\text{Std}} = \delta_X + 1$ leads to

$$(1 + \delta_R)(C_c - C_a) = \frac{1}{1+a} [C_c(1 + \delta_c) - C_a(1 + \delta_a)]. \quad (\text{A7.4})$$

Solving (A7.4) for δ_c leads to equation (7.5) of the main text:

$$\delta_c = \delta_R \left(1 + \bar{a}\right) \left(1 - \frac{C_a}{C_c}\right) + \frac{C_a}{C_c} (\delta_a - \bar{a}) + \bar{a} .$$

To write an expression for δ_R , I apply an assumption proposed by Gillon and Yakir (2000b), under which the CO_2 within the chloroplast can be divided into two pools: one pool, of proportion θ , has completely exchanged oxygen atoms with chloroplast water and therefore has an $^{18}\text{O}/^{16}\text{O}$ composition of R_{ce} ; the other pool, of proportion $1-\theta$, has not exchanged oxygen atoms with chloroplast water and retains its initial $^{18}\text{O}/^{16}\text{O}$ composition of R_{c0} . I note that the term R_{c0} could describe a mixture of mitochondrial CO_2 and CO_2 that has diffused into the leaf from ambient air. Therefore, I do not define R_{c0} solely as a function of CO_2 diffusing into the leaf from the atmosphere, as was done previously for photosynthesis (Gillon and Yakir 2000b). The term R_c is then written as

$$R_c = \theta R_{ce} + (1 - \theta) R_{c0} . \quad (\text{A7.5})$$

The term R_{ce} can be calculated from the equilibrium fractionation between CO_2 and water:

$$\alpha_w = \frac{R_{ce}}{R_e} = 1 + \varepsilon_w , \quad (\text{A7.6})$$

where R_e is $^{18}\text{O}/^{16}\text{O}$ of chloroplast water, which I assume to be equal to $^{18}\text{O}/^{16}\text{O}$ of water at the evaporative sites. Combining equations (A7.3), (A7.5), and (A7.6) leads to

$$R_R (C_c - C_a) (1 + \bar{a}) = C_c [R_e \alpha_w \theta + R_{c0} (1 - \theta)] - C_a R_a . \quad (\text{A7.7})$$

Dividing through by R_{std} , and substituting $1 + \varepsilon_w$ for α_w , gives

$$(1 + \delta_R) (C_c - C_a) (1 + \bar{a}) = C_c [(1 + \delta_e) (1 + \varepsilon_w) \theta + (1 + \delta_{c0}) (1 - \theta)] - C_a (1 + \delta_a) . \quad (\text{A7.8})$$

Solving equation (A7.8) for δ_R leads to equation (7.2) of the main text, which is

$$\delta_R = \frac{\theta [\delta_e (1 + \varepsilon_w) + \varepsilon_w] + (1 - \theta) \delta_{c0} - \frac{C_a}{C_c} (\delta_a - \bar{a}) - \bar{a}}{\left(1 + \bar{a}\right) \left(1 - \frac{C_a}{C_c}\right)} .$$

7.7.2. Calculating δ_R from on-line gas-exchange measurements

Under steady-state conditions, the increase in CO_2 concentration in air flowing through a gas-exchange cuvette containing a respiring leaf can be described as

$$u \frac{C_a}{P} = u \frac{C_{in}}{P} + \Lambda \mathfrak{R}_n, \quad (\text{A7.9})$$

where u is the flow rate through the cuvette (mol s^{-1}), Λ is the area of the leaf in the cuvette (m^2), C_a and C_{in} are CO_2 partial pressures of dry air exiting and entering the cuvette (μbar), P is atmospheric pressure (bar), and \mathfrak{R}_n is the respiration rate of the leaf ($\mu\text{mol CO}_2 \text{ m}^{-2} \text{ s}^{-1}$). The corresponding mass balance for C^{18}OO can be written as

$$u R_a \frac{C_a}{P} = u R_{in} \frac{C_{in}}{P} + \Lambda R_R \mathfrak{R}_n. \quad (\text{A7.10})$$

Combining equations (A7.9) and (A7.10) gives

$$R_R = \frac{1}{C_a - C_{in}} (R_a C_a - R_{in} C_{in}). \quad (\text{A7.11})$$

Dividing through by the isotope ratio of a standard, R_{Std} , and substituting from the relationship $R_X/R_{\text{Std}} = \delta_X + 1$ gives

$$\delta_R + 1 = \frac{1}{C_a - C_{in}} [(\delta_a + 1)C_a - (\delta_{in} + 1)C_{in}]. \quad (\text{A7.12})$$

Canceling common terms leads to equation (7.11) of the main text, which is

$$\delta_R = \frac{C_a \delta_a - C_{in} \delta_{in}}{C_a - C_{in}}.$$

I note that the equations derived in Appendices 7.1 and 7.2 can also be applied in the light. Thus, for photosynthesis, the term δ_R in equations (7.2), (7.5), and (7.11) of the main text can simply be replaced with the term δ_A . The term δ_A relates to Δ_A by the relationship $\Delta_A = (\delta_a - \delta_A)/(1 + \delta_A)$.

Chapter 8: General Conclusions

The aim of this thesis was to provide a better understanding of the biological and physical fractionation of stable isotopes of carbon and oxygen during some physiological processes in plants. In this context, six research questions were posed in Chapter 1. I now provide conclusions to those questions based on results presented in Chapters 2 through 7.

8.1. Conclusions to Questions Posed in Chapter 1

8.1.1. Question 1

Is water enriched in ^{18}O by transpiration exported from leaves in phloem sap? If so, is the level of enrichment such that this process should be considered when interpreting variation in $^{18}\text{O}/^{16}\text{O}$ of plant organic material?

I found that phloem sap collected from pod tips of *Lupinus angustifolius* showed the highest ^{18}O enrichment in phloem water of the three phloem bleeding species examined. Phloem water enrichment was as much as 17‰ compared to source water in the afternoon in *L. angustifolius* (Chapter 2). In contrast, *Eucalyptus globulus* showed the smallest phloem water ^{18}O enrichments, with average values less than 1‰ (Chapter 6). Phloem water ^{18}O enrichment in *Ricinus communis* was intermediate, showing an average value of 4‰ (Chapter 4). The large variation among species is interesting, and could well represent an equally large variation in phloem ultra-structure and phloem loading mechanisms. However, because the variation is so large, it poses some difficulty for incorporating phloem water ^{18}O enrichment into general models of organic material $^{18}\text{O}/^{16}\text{O}$. In answer to the second part of question 1, the results in Chapters 2, 4, and 6 seem to suggest the following: in large woody plants, in which the residence time of water in sieve tubes is likely to be long, phloem water ^{18}O enrichment appears to be considerably dampened by mixing with un-enriched xylem water; it could thus be safely excluded from models of organic material $^{18}\text{O}/^{16}\text{O}$. However, in herbaceous plants, phloem water enrichments appear to persist during translocation, and the possible implications should be considered when interpreting $^{18}\text{O}/^{16}\text{O}$ of organic material.

8.1.2. Question 2

Can leaf water $^{18}\text{O}/^{16}\text{O}$ be predicted under field conditions using a steady state model over a full diel cycle? If not, can the model be modified to take into account non-steady state variation?

I found that observed leaf water enrichments during the day were generally close to those predicted by the steady state leaf water model when the Péclet effect was taken into account (Chapters 2, 4, and 6). In contrast, nighttime leaf water enrichment was poorly predicted by the steady state leaf water model (Chapters 2 and 6). Modification of the steady state model to take into account non-steady state effects resulted in improved predictions of nighttime leaf water enrichments (Chapters 2 and 6). As noted in Chapter 7, accurate prediction of nighttime leaf water enrichment is important for predicting the impact of leaf dark respiration on the $\delta^{18}\text{O}$ of atmospheric CO_2 . The non-steady state modification of the leaf water model should thus be considered when predicting nighttime leaf water ^{18}O enrichment.

8.1.3. Question 3

What is the physiological basis for the previously-observed, strong correlation between phloem sap sugar concentration and $^{13}\text{C}/^{12}\text{C}$ of phloem sap sugars?

I showed in Chapter 3 that variation in both phloem sap sugar concentration and phloem sap sugar $^{13}\text{C}/^{12}\text{C}$ could be related to variation in plant water potential. Thus, there appears to be a strong physiological basis for the correlated variation between the two parameters. Application of this result could enable inferences about plant water relations to be made from simple, field-based measurements of phloem sap sugar concentration.

8.1.4. Question 4

Is the fractionation of $^{18}\text{O}/^{16}\text{O}$ between leaf water and sugars exported from leaves in the phloem sap predictable based on a known isotope effect between organic molecules and the water in which they form?

The equilibrium fractionation between organic molecules and water was previously assessed to be 27‰, based on measurements of $\delta^{18}\text{O}$ in cellulose from aquatic plants and the water in which they grew, and on measurements of the $\delta^{18}\text{O}$ of oxygen in acetone and the water with which it had equilibrated (Sternberg and DeNiro 1983). However, it was not previously known whether organic molecules exported

from leaves in the phloem sap (mainly sucrose) show the same fractionation with respect to average lamina leaf water. In Chapters 4 and 6, I show that the organic molecules exported in phloem sap of *Ricinus communis* and *Eucalyptus globulus* do indeed show a fractionation with respect to average lamina leaf water that is very close to 27‰. This result enables improved confidence in interpretations of $\delta^{18}\text{O}$ in organic material, particularly with regard to the relationship with leaf water ^{18}O enrichment.

8.1.5. Question 5

Can the models that are currently available for carbon and oxygen isotope discrimination be applied to plants in the field that are taxonomically and functionally very diverse, and still provide sensible interpretations in terms of physiological processes?

In Chapter 5, I present measurements of carbon and oxygen isotope ratios in parasitic plants and their hosts growing in southwestern Australia. The plants that were sampled represented a very diverse group in terms of plant form and function, ranging from xylem-tapping mistletoes to holoparasitic plants entirely dependent on their hosts for resources. Some results matched expectations in terms of variation in $\delta^{18}\text{O}$ and $\delta^{13}\text{C}$ between parasites and hosts, such as those for mistletoes. Other results were not readily interpretable with the current models of $\delta^{18}\text{O}$ and $\delta^{13}\text{C}$ variation in plants. In some cases, this represented a lack of availability of ancillary data for parameterizing the models, such as the chemical and isotopic composition of xylem sap solutes of the host. In other cases, there appeared to be processes at work that may not be currently represented in the isotope models, such as the process or processes causing ^{13}C enrichment of heterotrophic plant tissues relative to source leaves. In these cases, I suggest that data presented in Chapter 5 provide a useful context for designing experiments aimed at testing hypotheses about such processes.

8.1.6. Question 6

What are the controls over the oxygen isotope composition of carbon dioxide respired by leaves in the dark? Can a theoretical model be developed that explains observed variation in $^{18}\text{O}/^{16}\text{O}$ of leaf dark respiration?

In Chapter 7, I present measurements and interpretation of the $\delta^{18}\text{O}$ of CO_2 respired by *Ricinus communis* leaves in the dark. I show that the observed variations in the effect of respiring leaves on the oxygen isotope composition of CO_2 passing over

the leaves can be satisfactorily explained by taking account of the leaf water ^{18}O enrichment and gas exchange characteristics. The theory presented as part of this analysis should prove useful for interpreting variations in the $\delta^{18}\text{O}$ of CO_2 in the atmosphere.

8.2. Future Research Questions

Several interesting issues arise as a result of research presented in this thesis; these issues may in turn form the basis of future research projects. I will outline below three future research questions that I consider to be important outcomes of the research that I have conducted.

The impact of daytime starch storage and subsequent nighttime starch export from leaves on the $^{13}\text{C}/^{12}\text{C}$ and $^{18}\text{O}/^{16}\text{O}$ ratios of plant organic material has not been explored. In the case of $^{13}\text{C}/^{12}\text{C}$, starch extracted from leaves has typically been found to be enriched in ^{13}C relative to leaf soluble sugars (Gleixner et al. 1993; Gleixner et al. 1998; Brugnoli and Farquhar 2000). This could suggest a $^{13}\text{C}/^{12}\text{C}$ fractionation in the partitioning of carbon between starch and soluble sugars that are subsequently utilized in leaf metabolism. The isotopically heavier carbon that is stored as starch may then be exported from leaves at night, causing the isotopic composition of total carbon exported from the leaf over a 24-hour cycle to be enriched in ^{13}C compared to that utilized by the leaf in its own metabolism over the same period. This hypothesis may explain the frequently observed ^{13}C enrichment in phloem sap carbon and heterotrophic plant tissues compared to source leaves that is discussed in Chapters 5 and 6. If so, it would be an important process to include in models of $^{13}\text{C}/^{12}\text{C}$ dynamics in plant organic material. With regard to $^{18}\text{O}/^{16}\text{O}$ effects during starch export, the leaf water with which organic oxygen atoms exchange during sucrose synthesis at night should be less enriched in ^{18}O than that during the day. This may cause sucrose derived from starch and exported at night to have a lower $\delta^{18}\text{O}$ signal than that exported during the day. If so, the potential consequences for interpretation of $^{18}\text{O}/^{16}\text{O}$ variations in plant organic material should be considered.

The observations presented in Chapter 7, about the influence of leaf dark respiration on the $\delta^{18}\text{O}$ of atmospheric CO_2 , emphasize the need for a better understanding of the controls over stomatal conductance at night. This topic is nearly unexplored in the plant physiology literature, and yet it may prove to be an important parameter in carbon cycle models constrained by C^{18}OO data.

The impact of mitochondrial CO_2 evolution on the oxygen isotope composition of CO_2 diffusing out of leaves during the day and night is not known. This topic was discussed in Chapter 7. Any experiments that shed light on the relative importance, or unimportance, of including this process in models of C^{18}OO dynamics would be most useful.

Bibliography

- Adams MA, Grierson PF (2001) Stable isotopes at natural abundance in terrestrial plant ecology and ecophysiology: an update. *Plant Biol.* 3:299-310
- Adar EM, Gev I, Lipp J, Yakir D, Gat J, Cohen Y (1995) Utilization of oxygen-18 and deuterium in stem flow for the identification of transpiration sources: soil water versus groundwater in sand dune terrain. *Application of Tracers in Arid Zone Hydrology* (Proceedings of the Vienna Symposium, August 1994) IAHS No. 232:329-338
- Allison GB, Gat JR, Leaney FWJ (1985) The relationship between deuterium and oxygen-18 delta values in leaf water. *Chem. Geol.* 58:145-156
- Bannister P, Strong GL (2001) Carbon and nitrogen isotope ratios, nitrogen content and heterotrophy in New Zealand mistletoes. *Oecologia* 126:10-20
- Barbour MM, Andrews JT, Farquhar GD (2001) Correlations between oxygen isotope ratios of wood constituents of *Quercus* and *Pinus* samples from around the world. *Aust. J. Plant Physiol.* 28:335-348
- Barbour MM, Cernusak LA, Farquhar GD (in press-a) Factors affecting the oxygen isotope ratio of plant organic material. In: Flanagan LB, Ehleringer JR (eds) *Stable isotopes in biosphere-atmosphere interactions*. Academic Press, San Diego
- Barbour MM, Farquhar GD (2000) Relative humidity- and ABA-induced variation in carbon and oxygen isotope ratios of cotton leaves. *Plant Cell Environ.* 23:473-485
- Barbour MM, Fischer RA, Sayre KD, Farquhar GD (2000a) Oxygen isotope ratio of leaf and grain material correlates with stomatal conductance and grain yield in irrigated wheat. *Aust. J. Plant Physiol.* 27:625-637
- Barbour MM, Roden JS, Farquhar GD, Ehleringer JR (in press-b) Expressing leaf water and cellulose oxygen isotope ratios as enrichment above source water reveals evidence of a Péclet effect. *Oecologia*
- Barbour MM, Schurr U, Henry BK, Wong S-C, Farquhar GD (2000b) Variation in the oxygen isotope ratio of phloem sap sucrose from castor bean. Evidence in support of the Péclet effect. *Plant Physiol.* 123:671-679
- Bariac T, Gonzalezdunia J, Katerji N, Bethenod O, Bertolini JM, Mariotti A (1994) Spatial variation of the isotopic composition of water (^{18}O , ^2H) in the soil-plant-atmosphere system, 2. Assessment under field conditions. *Chem. Geol.* 115:317-333

- Bariac T, Jusserand C, Mariotti A (1990) Evolution spatio-temporelle de la composition isotopique de l'eau dans le continuum sol-plante-atmosphere. *Geochim. Cosmochim. Acta* 54:413-424
- Bariac T, Rambal S, Jusserand C, Berger A (1989) Evaluating water fluxes of field-grown alfalfa from diurnal observations of natural isotope concentrations, energy budget and ecophysiological parameters. *Agricultural and Forest Meteorology* 48:263-283
- Behboudian MH, Ma Q, Turner NC, Palta JA (2000) Discrimination against $^{13}\text{CO}_2$ in leaves, pod walls, and seeds of water-stressed chickpea. *Photosynthetica* 38:155-157
- Bender M (1968) Mass spectrometric studies of carbon 13 variations in corn and other grasses. *Radiocarbon* 10:468-472
- Bender M, Sowers T, Labeyrie L (1994) The Dole effect and its variations during the last 130,000 years as measured in the Vostok ice core. *Global Biogeochem. Cycles* 8:363-376
- Borella S, Leuenberger M, Saurer M (1999) Analysis of $\delta^{18}\text{O}$ in tree rings: Wood-cellulose comparison and method dependent sensitivity. *J. Geophys. Res.* 104:19,267-19,273
- Bottinga Y, Craig H (1969) Oxygen isotope fractionation between CO_2 and water, and the isotopic composition of marine atmospheric CO_2 . *Earth Planet. Sci. Lett.* 5:285-295
- Bowling DR, McDowell NG, Bond BJ, Law BE, Ehleringer JR (2002) C-13 content of ecosystem respiration is linked to precipitation and vapor pressure deficit. *Oecologia* 131:113-124
- Bowling DR, McDowell NG, Welker JM, Bond BJ, Law BE, Ehleringer JR (2003a) Oxygen isotope content of CO_2 in nocturnal ecosystem respiration. 1. Observations in forests along a precipitation transect in Oregon, USA. *Global Biogeochem. Cycles* 17:1120
- Bowling DR, McDowell NG, Welker JM, Bond BJ, Law BE, Ehleringer JR (2003b) Oxygen isotope content of CO_2 in nocturnal ecosystem respiration. 2. Short-term dynamics of foliar and soil component fluxes in an old-growth ponderosa pine forest. *Global Biogeochem. Cycles* 17:1124
- Brenninkmeijer C, Kraft P, Mook W (1983) Oxygen isotope fractionation between CO_2 and H_2O . *Isotope Geoscience* 1:181-190

- Bret-Harte MS, Silk WK (1994) Nonvascular, symplastic diffusion of sucrose cannot satisfy the carbon demands of growth in the primary root tip of *Zea mays* (L.). *Plant Physiol.* 105:19-33
- Brugnoli E, Farquhar GD (2000) Photosynthetic fractionation of carbon isotopes. In: Leegood RC, Sharkey TC, von Caemmerer S (eds) *Photosynthesis: physiology and metabolism*. Kluwer Academic Publishers, The Netherlands, pp 399-434
- Brugnoli E, Hubick KT, von Caemmerer S, Wong SC, Farquhar GD (1988) Correlation between the carbon isotope discrimination in leaf starch and sugars of C₃ plants and the ratio of intercellular and atmospheric partial pressures of carbon dioxide. *Plant Physiol.* 88:1418-1424
- Caemmerer S, Farquhar GD (1981) Some relationships between the biochemistry of photosynthesis and the gas exchange of leaves. *Planta* 153:376-387
- Caemmerer Sv, Evans JR (1991) Determination of the average partial pressure of CO₂ in chloroplasts from leaves of several C₃ plants. *Aust. J. Plant Physiol.* 18:287-305
- Cappa CD, Hendricks MB, DePaulo DJ, Cohen RC (2003) Isotopic fractionation of water during evaporation. *J. Geophys. Res.* 108:4525
- Cernusak LA, Marshall JD (2000) Photosynthetic refixation in branches of Western White Pine. *Funct. Ecol.* 14:300-311
- Cernusak LA, Marshall JD (2001) Responses of foliar $\delta^{13}\text{C}$, gas exchange, and leaf morphology to reduced hydraulic conductivity in *Pinus monticola* branches. *Tree Physiol.* 21:1215-1222
- Cernusak LA, Marshall JD, Comstock JP, Balster NJ (2001) Carbon isotope discrimination in photosynthetic bark. *Oecologia* 128:24-35
- Christy AL, Ferrier JM (1973) A mathematical treatment of Münch's pressure-flow hypothesis of phloem translocation. *Plant Physiol.* 52:531-538
- Ciais P, Denning AS, Tans PP, Berry JA, Randall DA, Collatz GJ, Sellers PJ, White JWC, Troler M, Meijer HAJ, Francey RJ, Monfray P, Heimann M (1997) A three dimensional synthesis study of $\delta^{18}\text{O}$ in atmospheric CO₂. 1. Surface fluxes. *J. Geophys. Res.* 102:5857-5872
- Cowan IR (1986) Economics of carbon fixation in higher plants. In: Givnish TJ (ed) *On the economy of plant form and function*. Cambridge University Press, Cambridge, pp 133-170

- Craig H (1953) The geochemistry of the stable carbon isotopes. *Geochim. Cosmochim. Acta* 3:53-92
- Craig H (1957) Isotopic standards for carbon and oxygen and correction factors for mass-spectrometric analysis of carbon dioxide. *Geochim. Cosmochim. Acta* 12:133-149
- Craig H, Gordon LI (1965) Deuterium and oxygen-18 variations in the ocean and the marine atmosphere. In: Tongiorgi E (ed) *Proceedings of a conference on stable isotopes in oceanographic studies and palaeotemperatures*. Lischi and Figli, Pisa, pp 9-130
- Cuntz M, Ciais P, Hoffmann G, Allison CE, Francey R, Knorr W, Tans P, White JWC, Levin I (2003a) A comprehensive global three-dimensional model of $\delta^{18}\text{O}$ in atmospheric CO_2 : 2. Mapping the atmospheric signal. *J. Geophys. Res.* 108:4528
- Cuntz M, Ciais P, Hoffmann G, Knorr W (2003b) A comprehensive global three-dimensional model of $\delta^{18}\text{O}$ in atmospheric CO_2 : 1. Validation of surface processes. *J. Geophys. Res.* 108:4527
- Damesin C (2003) Respiration and photosynthesis characteristics of current-year stems of *Fagus sylvatica*: from the seasonal pattern to an annual balance. *New Phytol.* 158:465-475
- Damesin C, Rambal S, Joffre R (1998) Seasonal and annual changes in leaf $\delta^{13}\text{C}$ in two co-occurring Mediterranean oaks: relations to leaf growth and drought progression. *Funct. Ecol.* 12:778-785
- Daudet FA, Lacoïnte A, Gaudillère JP, Cruiziat P (2002) Generalized Münch coupling between sugar and water fluxes for modelling carbon allocation as affected by water status. *J. Theor. Biol.* 214:481-498
- Davidson NJ, Pate JS (1992) Water relations of the mistletoe *Amyema fitzgeraldii* and its host *Acacia acuminata*. *J. Exp. Bot.* 43:1549-1555
- Davidson NJ, True KC, Pate JS (1989) Water relations of the parasite: host relationship between the mistletoe *Amyema linophyllum* (Fenzl) Tieghem and *Casuarina obesa* Miq. *Oecologia* 80:321-330
- Dawson TE, Ehleringer JR (1993) Isotopic enrichment of water in the "woody" tissues of plants: Implications for plant water source, water uptake, and other studies which use the stable isotopic composition of cellulose. *Geochim. Cosmochim. Acta* 57:3487-3491

- Dawson TE, Mambelli S, Plamboeck AH, Templer PH, Tu KP (2002) Stable isotopes in plant ecology. *Ann. Rev. Ecol. Syst.* 33:507-559
- Dawson TE, Pate JS (1996) Seasonal water uptake and movement in root systems of Australian phreatophytic plants of dimorphic root morphology - a stable isotope investigation. *Oecologia* 107:13-20
- de la Harpe AC, Visser JH, Grobbelaar N (1979) The chlorophyll concentration and photosynthetic activity of some parasitic flowering plants. *Zeitschrift für Pflanzenphysiologie* 93:83-87
- DeNiro MJ, Cooper LW (1989) Post-photosynthetic modification of oxygen isotope ratios of carbohydrates in the potato: implications for paleoclimatic reconstruction based upon isotopic analysis of wood cellulose. *Geochim. Cosmochim. Acta* 53:2573-2580
- Dongmann G, Nurnberg HW, Förstel H, Wagener K (1974) On the enrichment of $H_2^{18}O$ in the leaves of transpiring plants. *Radiat. Environ. Biophys.* 11:41-52
- Ducharme LA, Ehleringer JR (1996) Gas exchange, $\delta^{13}C$, and heterotrophy for *Castilleja linarifolia* and *Orthocarpus tolmiei*, facultative root hemiparasites on *Artemisia tridentata*. *Great Basin Naturalist* 56:333-340
- Ehleringer JR (1993) Gas-exchange implications of isotopic variation in arid-land plants. In: Griffiths H, Smith J (eds) *Plant responses to water deficit*. BIOS Scientific Publishers, London, pp 265-284
- Ehleringer JR, Bowling DR, Flanagan LB, Fessenden JE, Helliker BR, Martinelli LA, Ometto JP (2002) Stable isotopes and carbon cycle processes in forests and grasslands. *Plant Biol.* 4:181-189
- Ehleringer JR, Cook CS, Tieszen LL (1986) Comparative water use and nitrogen relationships in a mistletoe and its host. *Oecologia* 68:279-284
- Ehleringer JR, Schulze E-D, Ziegler H, Lange OL, Farquhar GD, Cowan IR (1985) Xylem-tapping mistletoes: water or nutrient parasites? *Science* 227:1479-1481
- Evans JR, Sharkey TD, Berry JA, Farquhar GD (1986) Carbon isotope discrimination measured concurrently with gas exchange to investigate CO_2 diffusion in leaves of higher plants. *Aust. J. Plant Physiol.* 13:281-292
- Everson RG (1970) Carbonic anhydrase and CO_2 fixation in isolated chloroplasts. *Phytochemistry* 9:25-32
- Farquhar GD, Barbour MM, Henry BK (1998) Interpretation of oxygen isotope composition of leaf material. In: Griffiths H (ed) *Stable isotopes: integration of*

- biological, ecological, and geochemical processes. BIOS Scientific Publishers Ltd., Oxford, pp 27-48
- Farquhar GD, Condon AG, Masle J (1994) Use of carbon and oxygen isotope composition and mineral ash content in breeding for improved rice production under favorable, irrigated conditions. In: Cassman KG (ed) *Breaking the yield barrier*. International Rice Research Institute, Manila, pp 95-101
- Farquhar GD, Ehleringer JR, Hubick KT (1989a) Carbon isotope discrimination and photosynthesis. *Annu. Rev. Plant Physiol. Plant Mol. Biol.* 40:503-537
- Farquhar GD, Gan KS (2003) On the progressive enrichment of the oxygen isotopic composition of water along leaves. *Plant Cell Environ.* 26:801-819
- Farquhar GD, Henry BK, Styles JM (1997) A rapid on-line technique for determination of oxygen isotope composition of nitrogen-containing organic matter and water. *Rapid Commun. Mass Spectrom.* 11:1554-1560
- Farquhar GD, Hubick KT, Condon AG, Richards RA (1989b) Carbon isotope discrimination and water-use efficiency. In: Rundel PW, Ehleringer JR, Nagy KA (eds) *Stable isotopes in ecological research*. Springer-Verlag, New York, pp 21-46
- Farquhar GD, Lloyd J (1993) Carbon and oxygen isotope effects in the exchange of carbon dioxide between terrestrial plants and the atmosphere. In: Ehleringer JR, Hall AE, Farquhar GD (eds) *Stable isotopes and plant carbon-water relations*. Academic Press, San Diego, pp 47-70
- Farquhar GD, Lloyd J, Taylor JA, Flanagan LB, Syvertsen JP, Hubick KT, Wong SC, Ehleringer JR (1993) Vegetation effects on the isotope composition of oxygen in atmospheric CO₂. *Nature* 363:439-443
- Farquhar GD, O'Leary MH, Berry JA (1982) On the relationship between carbon isotope discrimination and the intercellular carbon dioxide concentration in leaves. *Aust. J. Plant Physiol.* 9:121-137
- Farquhar GD, Richards RA (1984) Isotopic composition of plant carbon correlates with water-use efficiency in wheat genotypes. *Aust. J. Plant Physiol.* 11:539-552
- Flanagan LB (1993) Environmental and biological influences on the stable oxygen and hydrogen isotopic composition of leaf water. In: Ehleringer JR, Hall AE, Farquhar GD (eds) *Stable isotopes and plant carbon-water relations*. Academic Press, San Diego, pp 71-89

- Flanagan LB, Brooks JR, Varney GT, Ehleringer JR (1997) Discrimination against $C^{18}O^{16}O$ during photosynthesis and the oxygen isotope ratio of respired CO_2 in boreal forest ecosystems. *Global Biogeochem. Cycles* 11:83-98
- Flanagan LB, Ehleringer JR (1991) Effects of mild water stress and diurnal changes in temperature and humidity on the stable oxygen and hydrogen isotopic composition of leaf water in *Cornus stolonifera* L. *Plant Physiol.* 97:298-305
- Flanagan LB, Ehleringer JR (1998) Ecosystem-atmosphere CO_2 exchange: interpreting signals of change using stable isotope ratios. *Trends Ecol. Evol.* 13:10-14
- Flanagan LB, Kubien DS, Ehleringer JR (1999) Spatial and temporal variation in the carbon and oxygen stable isotope ratio of respired CO_2 in a boreal forest ecosystem. *Tellus* 51:367-384
- Flanagan LB, Marshall JD, Ehleringer JR (1993) Photosynthetic gas exchange and the stable isotope composition of leaf water - comparison of a xylem-tapping mistletoe and its host. *Plant Cell Environ.* 16:623-631
- Flanagan LB, Phillips SL, Ehleringer JR, Lloyd J, Farquhar GD (1994) Effect of changes in leaf water oxygen isotopic composition on discrimination against $C^{18}O^{16}O$ during photosynthetic gas exchange. *Aust. J. Plant Physiol.* 21:221-234
- Förstel H (1978) Contribution of oxygen isotope fractionation during the transpiration of plant leaves to the biogeochemical oxygen cycle. In: Knumboin WE (ed) *Proc. 3rd International Symposium on Environmental Biogeochemistry and Geomicrobiology*. AnnArbor Press, pp 811-824
- Förstel H, Hütten H (1983) $^{18}O/^{16}O$ ratio of water in a local ecosystem as a basis of climate record Palaeoclimates and palaeowaters: a collection of environmental isotope studies. IAEA, Vienna, pp 67-81
- Francey RJ, Gifford RM, Sharkey TD, Weir B (1985) Physiological influences on carbon isotope discrimination in huon pine (*Lagarostrobos franklinii*). *Oecologia* 66:211-218
- Francey RJ, Tans PP (1987) Latitudinal variation in oxygen-18 of atmospheric CO_2 . *Nature* 327:495-497
- Francey RJ, Tans PP, Allison CE, Enting IG, White JWC, Troler M (1995) Changes in oceanic and terrestrial carbon uptake since 1982. *Nature* 373:326-330
- Gan KS, Wong SC, Farquhar GD (in press) Oxygen isotope analysis of plant water without extraction procedure. In: de Groot PA (ed) *Handbook of Stable Isotope Analytical Techniques*, Volume 1. Elsevier

- Gan KS, Wong SC, Yong JWH, Farquhar GD (2002) ^{18}O spatial patterns of vein xylem water, leaf water, and dry matter in cotton leaves. *Plant Physiol.* 130:1008-1021
- Gat JR (1971) Comments on the stable isotope method in regional groundwater investigations. *Water Resources Research* 7:980-993
- Gebauer G, Schulze E-D (1991) Carbon and nitrogen isotope ratios in different compartments of a healthy and declining *Picea abies* forest in the Fichtelgebirge, NE Bavaria. *Oecologia* 87:198-207
- Gessler A, Schrempp S, Matzarakis A, Mayer H, Rennenberg H, Adams MA (2001) Radiation modifies the effect of water availability on the carbon isotope composition of beech (*Fagus sylvatica*). *New Phytol.* 150:653-664
- Gillon JS, Yakir D (2000a) Internal conductance to CO_2 diffusion and C^{18}OO discrimination in C_3 leaves. *Plant Physiol.* 123:201-213
- Gillon JS, Yakir D (2000b) Naturally low carbonic anhydrase activity in C_4 and C_3 plants limits discrimination against C^{18}OO during photosynthesis. *Plant Cell Environ.* 23:903-915
- Gillon JS, Yakir D (2001) Influence of carbonic anhydrase activity in terrestrial vegetation on the ^{18}O content of atmospheric CO_2 . *Science* 291:2584-2587
- Glatzel G (1983) Mineral nutrition and water relations of hemiparasitic mistletoes: a question of partitioning. Experiments with *Loranthus europaeus* on *Quercus petraea* and *Quercus robur*. *Oecologia* 56:193-201
- Gleixner G, Danier HJ, Werner RA, Schmidt HL (1993) Correlations between the ^{13}C content of primary and secondary plant products in different cell compartments and that in decomposing basidiomycetes. *Plant Physiol.* 102:1287-1290
- Gleixner G, Scrimgeour C, Schmidt HL, Viola R (1998) Stable isotope distribution in the major metabolites of source and sink organs of *Solanum tuberosum* L.: a powerful tool in the study of metabolic partitioning in intact plants. *Planta* 207:241-245
- Goeschl JD, Magnuson CE, DeMichele DW, Sharpe PJH (1976) Concentration-dependent unloading as a necessary assumption for a closed form mathematical model of osmotically driven pressure flow in phloem. *Plant Physiol.* 58:556-562
- Gonfiantini R, Gratzia S, Tongiorgi E (1965) Oxygen isotope composition of water in leaves. *Isotopes and radiation in soil-plant nutrition studies*. IAEA, Vienna, pp 405-410

- Griffiths H, ed. 1998. Stable isotopes: integration of biological, ecological, and geochemical processes. BIOS Scientific Publishers Ltd, Oxford, UK.
- Guehl JM, Domenach AM, Bereau M, Barigah TS, Casabianca H, Ferhi A, Garbaye J (1998) Functional diversity in an Amazonian rainforest of French Guyana: a dual isotope approach ($\delta^{15}\text{N}$ and $\delta^{13}\text{C}$). *Oecologia* 116:316-330
- Guy RD, Berry J, Fogel ML, Turpin DH, Weger HG (1992) Fractionation of the stable isotopes of oxygen during respiration by plants - the basis of a new technique to estimate partitioning to the alternative path. In: Lambers H, van der Plas LHW (eds) Molecular, biochemical, and physiological aspects of plant respiration. Academic Publishing, The Hague, pp 443-453
- Hall SM, Milburn JA (1973) Phloem transport in *Ricinus*: Its dependence on the water balance of the tissues. *Planta* 109:1-10
- Harwood KG, Gillon JS, Griffiths H, Broadmeadow MSJ (1998) Diurnal variation of $\Delta^{13}\text{CO}_2$, $\Delta\text{C}^{18}\text{O}^{16}\text{O}$, and evaporative site enrichment of $\delta\text{H}_2^{18}\text{O}$ in *Piper aduncum* under field conditions in Trinidad. *Plant Cell Environ.* 21:269-283
- Haupt S, Oparka KJ, Sauer N, Neumann S (2001) Macromolecular trafficking between *Nicotiana tabacum* and the holoparasite *Cuscuta reflexa*. *J. Exp. Bot.* 52:173-177
- Helliker BR, Ehleringer JR (2002a) Differential ^{18}O enrichment of leaf cellulose in C_3 versus C_4 grasses. *Funct. Plant Biol.* 29:435-442
- Helliker BR, Ehleringer JR (2002b) Grass blades as tree rings: environmentally induced changes in the oxygen isotope ratio of cellulose along the length of grass blades. *New Phytol.* 155:417-424
- Hellmuth EO (1971) Eco-physiological studies on plants in arid and semi-arid regions in Western Australia. IV. Comparison of the field physiology of the host, *Acacia grasbyi*, and its hemi-parasite, *Amyema nestor*, under optimal and stress conditions. *J. Ecol.* 59:351-363
- Hibberd JM, Quick WP, Press MC, Scholes JD, Jeschke WD (1999) Solute fluxes from tobacco to the parasitic angiosperm *Orobanche cernua* and the influence of infection on host carbon and nitrogen relations. *Plant Cell Environ.* 22:937-947
- Hill SA, Waterhouse JS, Field EM, Switsur VR, apRees T (1995) Rapid recycling of triose phosphates in oak stem tissue. *Plant Cell Environ.* 18:931-936

- Hobbie EA, Tingey DT, Rygielwicz PT, Johnson MG, Olszyk DM (2002) Contributions of current year photosynthate to fine roots estimated using a ^{13}C depleted CO_2 source. *Plant and Soil* 247:233-242
- Hobbie EA, Werner RA (2004) Intramolecular, compound-specific, and bulk carbon isotope patterns in C_3 and C_4 plants: a review and synthesis. *New Phytol.* 161:371-385
- Hocking PJ, Pate JS, Atkins CA, Sharkey PJ (1978) Diurnal patterns of transport and accumulation of minerals in fruiting plants of *Lupinus angustifolius* L. *Ann. Bot.* 42:1277-1290
- Hoffmann G, Cuntz M, Weber C, Ciais P, Friedlingstein P, Heimann M, Jouzel J, Kaduk J, Maier-Reimer E, Seibt U, Six K (2004) A model of the Earth's Dole effect. *Global Biogeochem. Cycles* 18:1008
- Ineson P, Cotrufo MF, Bol R, Harkness DD, Blum H (1996) Quantification of soil carbon inputs under elevated CO_2 : C_3 plants in a C_4 soil. *Plant and Soil* 187:345-350
- Jacobson BS, Fong F, Heath RL (1975) Carbonic anhydrase of spinach. *Plant Physiol.* 55:468-474
- Jäggi M, Saurer M, Fuhrer J, Siegwolf R (2003) Seasonality of $\delta^{18}\text{O}$ in needles and wood of *Picea abies*. *New Phytol* 158:51-59
- Jeschke WD, Baumel P, Rath N, Czygan F-C, Proksch P (1994a) Modeling of the flows and partitioning of carbon and nitrogen in the holoparasite *Cuscuta reflexa* Roxb. and its host *Lupinus albus* L. II. Flows between host and parasite and within the parasitized host. *J. Exp. Bot.* 45:801-812
- Jeschke WD, Rath N, Baumel P, Czygan F-C, Proksch P (1994b) Modeling the flow and partitioning of carbon and nitrogen in the holoparasite *Cuscuta reflexa* Roxb. and its host *Lupinus albus* L. 1. Methods for estimating net flows. *J. Exp. Bot.* 45:791-800
- Jeschke WD, Pate JS (1995) Mineral nutrition and transport in xylem and phloem of *Banksia prionotes* (Proteaceae), a tree with dimorphic root morphology. *J. Exp. Bot.* 46:895-905
- Jouzel J, Koster RD, Suozzo RJ, Russell GL, White JWC, Broecker WS (1991) Simulations of the HDO and H_2^{18}O atmospheric cycles using the NASA/GISS general circulation model: Sensitivity experiments for present-day conditions. *J. Geophys. Res.* 96:7495-7507

- Kraus R, Trimborn P, Ziegler H (1995) *Tristerix aphyllus*, a holoparasitic Loranthacea. *Naturwissenschaften* 82:150-151
- Kuijt J (1969) The biology of parasitic flowering plants. University of California Press, Berkeley
- Lalonde S, Tegeder M, Throne-Holst M, Frommer WB, Patrick JW (2003) Phloem loading and unloading of sugars and amino acids. *Plant Cell Environ.* 26:37-56
- Lang A, Thorpe MR (1986) Water potential, translocation and assimilate partitioning. *J. Exp. Bot.* 37:495-503
- Leaney F, Osmond C, Allison G, Ziegler H (1985) Hydrogen-isotope composition of leaf water in C₃ and C₄ plants: its relationship to the hydrogen-isotope composition of dry matter. *Planta* 164:215-220
- Leavitt SW, Long A (1982) Evidence for ¹³C/¹²C fractionation between tree leaves and wood. *Nature* 298:742-744
- Lechowski Z (1996) Gas exchange in leaves of the root hemiparasite *Melampyrum arvense* L. before and after attachment to the host. *Biologia Plantarum* 38:85-93
- Lloyd J, Farquhar GD (1994) ¹³C discrimination during CO₂ assimilation by the terrestrial biosphere. *Oecologia* 99:201-215
- Loader NJ, Robertson I, Barker AC, Switsur VR, Waterhouse JS (1997) An improved technique for the batch processing of small wholewood samples to α-cellulose. *Chem. Geol.* 136:313-317
- Loader NJ, Robertson I, McCarroll D (2003) Comparison of stable carbon isotope ratios in the whole wood, cellulose and lignin of oak tree-rings. *Palaeogeography Palaeoclimatology Palaeoecology* 196:395-407
- Loveys BR, Loveys BR, Tyerman SD (2001) Water relations and gas exchange of the root hemiparasite *Santalum acuminatum* (quandong). *Aust. J. Bot.* 49:479-486
- Luo Y-H, Sternberg LSL (1992) Hydrogen and oxygen isotopic fractionation during heterotrophic cellulose synthesis. *J. Exp. Bot.* 43:47-50
- MacLeod D (1961) Photosynthesis in *Cuscuta*. *Experientia* 17:542-543
- Maguas C, Griffiths H (2003) Applications of stable isotopes in plant ecology. *Prog. Bot.* 64:472-505
- Majoube M (1971) Fractionnement en oxygen-18 et en deuterium entre l'eau et sa vapeur. *Journal de Chimie et Physique* 68:1423-1436
- Marshall JD, Ehleringer JR (1990) Are xylem-tapping mistletoes partially heterotrophic? *Oecologia* 84:244-248

- Marshall JD, Dawson TE, Ehleringer JR (1994a) Integrated nitrogen, carbon, and water relations of a xylem-tapping mistletoe following nitrogen fertilization of the host. *Oecologia* 100:430-438
- Marshall JD, Ehleringer JR, Schulze E-D, Farquhar GD (1994b) Carbon isotope composition, gas exchange and heterotrophy in Australian mistletoes. *Funct. Ecol.* 8:237-241
- Merlivat L (1978) Molecular diffusivities of H_2^{16}O , HD^{16}O , and H_2^{18}O in gases. *J. Chem. Phys.* 69:2864-2871
- Milburn JA (1970) Phloem exudation from Castor bean: induction by massage. *Planta* 95:272-276
- Milburn JA (1980) The measurement of turgor pressure in sieve tubes. *Berichte der Deutschen Botanischen Gesellschaft* 93:153-166
- Miller JB, Yakir D, White JWC, Tans PP (1999) Measurement of $^{18}\text{O}/^{16}\text{O}$ in the soil-atmosphere CO_2 flux. *Global Biogeochem. Cycles* 13:761-774
- Miller JM, Williams RJ, Farquhar GD (2001) Carbon isotope discrimination by a sequence of *Eucalyptus* species along a subcontinental rainfall gradient in Australia. *Funct. Ecol.* 15:222-232
- Mook W, Van der Hoek S (1983) The N_2O correction in the carbon and oxygen isotopic analysis of atmospheric CO_2 . *Isotope Geoscience* 1:237-242
- Mortazavi B, Chanton JP (2002) Carbon isotopic discrimination and control of nighttime canopy $\delta^{18}\text{O}-\text{CO}_2$ in a pine forest in the southeastern United States. *Global Biogeochem. Cycles* 16:1008
- Münch E (1930) *Die Stoffbewegungen in der Pflanze*. Fisher, Jena
- Nobel PS (1991) *Physicochemical and Environmental Plant Physiology*. Second Edition. Academic Press, San Diego, California
- Pate JS (1986) Xylem-to-phloem transfer - vital component of the nitrogen-partitioning system of a nodulated legume. In: Cronshaw J, Lucas WJ, Giaquinta RT (eds) *Phloem Transport*. A.R. Liss Inc., New York, pp 445-462
- Pate JS (2001) Haustoria in action: case studies of nitrogen acquisition by woody xylem-tapping hemiparasites from their hosts. *Protoplasma* 215:204-217
- Pate JS, Bell TL (2000) Host associations of the introduced annual root hemiparasite *Parentucellia viscosa* in agricultural and bushland settings in Western Australia. *Ann. Bot.* 85:203-213

- Pate J, Arthur D (1998) $\delta^{13}\text{C}$ analysis of phloem sap carbon: novel means of evaluating seasonal water stress and interpreting carbon isotope signatures of foliage and trunk wood of *Eucalyptus globulus*. *Oecologia* 117:301-311
- Pate JS, Arthur DJ (2000) Uptake, partitioning and utilization of carbon and nitrogen in the phloem bleeding tree, Tasmanian blue gum (*Eucalyptus globulus*). *Aust. J. Plant Physiol.* 27:869-884
- Pate JS, Atkins CA, Perry MW (1980) Significance of photosynthesis produced at different stages of growth as a carbon source for fruit filling and seed reserve accumulation in *Lupinus angustifolius* L. *Aust. J. Plant Physiol.* 7:283-297
- Pate JS, Davidson NJ, Kuo J, Milburn JA (1990a) Water relations of the root hemiparasite *Olex phyllanthi* (Labill) R.Br. (Olacaceae) and its multiple hosts. *Oecologia* 84:186-193
- Pate JS, Jeschke WD, Aylward MJ (1995) Hydraulic architecture and xylem structure of the dimorphic root systems of South-west Australian species of Proteaceae. *J. Exp. Bot.* 46:907-915
- Pate JS, Kuo J, Davidson NJ (1990b) Morphology and anatomy of haustorium of the root hemi parasite *Olex phyllanthi* (Labill.) R. Br. (Olacaceae) with special reference to the haustorial interface. *Ann. Bot.* 65:425-436
- Pate JS, Pate SR, Kuo J, Davidson NJ (1990c) Growth, resource allocation and haustorial biology of the hemiparasite *Olex phyllanthi* (Olacaceae). *Ann. Bot.* 65:437-449
- Pate JS, Sharkey PJ, Atkins CA (1977) Nutrition of a developing legume fruit: functional economy in terms of carbon, nitrogen, water. *Plant Physiol.* 59:506-510
- Pate JS, Sharkey PJ, Lewis OAM (1974) Phloem bleeding from legume fruits- a technique for study of fruit nutrition. *Planta* 120:229-243
- Pate J, Shedley E, Arthur D, Adams M (1998) Spatial and temporal variations in phloem sap composition of plantation-grown *Eucalyptus globulus*. *Oecologia* 117:312-322
- Pate JS, Stewart GR, Unkovich M (1993) ^{15}N natural abundance of plant and soil components of a *Banksia* woodland ecosystem in relation to nitrate utilization, life form, mycorrhizal status and N_2 -fixing abilities of component species. *Plant Cell Environ.* 16:365-373

- Pate JS, True KC, Rasins E (1991) Xylem transport and storage of amino acids by SW Australian mistletoes and their hosts. *J. Exp. Bot.* 42:441-451
- Pate JS, Williams W, Farrington P (1985) Lupins (*Lupinus* spp.). In: Summerfield RJ, Roberts EH (eds) Grain Legume Crops. Collins, London, pp 699-746
- Pfanz H, Aschan G, Langenfeld-Heyser R, Wittmann C, Loose M (2002) Ecology and ecophysiology of tree stems: corticular and wood photosynthesis. *Naturwissenschaften* 89:147-162
- Prentice IC, Farquhar GD, Fasham MJR, Goulden ML, Heinman M, Jaramillo VJ, Khashgi HS, Le Quéré C, Scholes RJ, Wallace DWR (2001) The carbon cycle and atmospheric carbon dioxide. In: Houghton JT, Ding Y, Griggs DJ, Noguer M, van der Linden PJ, Dai X, Maskell K, Johnson CA (eds) Climate Change 2001: The Scientific Basis. Contribution of Working Group 1 to the Third Assessment Report of the Intergovernmental Panel on Climate Change. Cambridge University Press, Cambridge, United Kingdom and New York, NY, USA, pp 183-237
- Press MC, Graves JD, Stewart GR (1988) Transpiration and carbon acquisition in root hemiparasitic angiosperms. *J. Exp. Bot.* 39:1009-1014
- Press MC, Parsons AN, Mackay AW, Vincent CA, Cochrane V, Seel WE (1993) Gas exchange characteristics and nitrogen relations of two Mediterranean root hemiparasites: *Bartsia trixago* and *Parentucellia viscosa*. *Oecologia* 95:145-151
- Press MC, Tuohy JM, Stewart GR (1987) Carbon isotope ratios demonstrate carbon flux from C₄ host to C₃ parasite. *Plant Physiol.* 85:1143-1145
- Pritchard J (1996) Aphid stylectomy reveals an osmotic step between sieve tube and cortical cells in barley roots. *J. Exp. Bot.* 47:1519-1524
- Pritchard J, Winch S, Gould N (2000) Phloem water relations and root growth. *Aust. J. Plant Physiol.* 27:539-548
- Raven JA (1983) Phytophages of xylem and phloem: a comparison of animal and plant sap-feeders. *Adv. Ecol. Res.* 13:136-239
- Revesz K, Woods PH (1990) A method to extract soil water for stable isotope analysis. *J. Hydrol.* 115:397-406
- Richter A, Popp M, Mensen R, Stewart GR, von Willert DJ (1995) Heterotrophic carbon gain of the parasitic angiosperm *Tapinanthus oleifolius*. *Aust. J. Plant Physiol.* 22:537-544

- Robinson D (2001) $\delta^{15}\text{N}$ as an integrator of the nitrogen cycle. *Trends Ecol. Evol.* 16:153-162
- Roden JS, Ehleringer JR (1999) Observations of hydrogen and oxygen isotopes in leaf water confirm the Craig-Gordon model under wide-ranging environmental conditions. *Plant Physiol.* 120:1165-1173
- Roden JS, Lin GG, Ehleringer JR (2000) A mechanistic model for interpretation of hydrogen and oxygen isotope ratios in tree-ring cellulose. *Geochim. Cosmochim. Acta* 64:21-35
- Rozanski K, Araguas-Araguas L, Gonfiantini R (1993) Isotopic patterns in modern global precipitation. In: Swart PK, Lohmann KC, McKenzie J, Savin S (eds) *Climate Change in Continental Isotopic Records*. American Geophysical Union, Washington, pp 1-36
- Saurer M, Aellen K, Siegwolf R (1997) Correlating $\delta^{13}\text{C}$ and $\delta^{18}\text{O}$ in cellulose of trees. *Plant Cell Environ.* 20:1543-1550
- Saurer M, Cherubini P, Siegwolf R (2000) Oxygen isotopes in tree rings of *Abies alba*: The climatic significance of interdecadal variations. *J. Geophys. Res.* 105:12,461-12,470
- Saurer M, Schweingruber F, Vaganov EA, Shiyatov SG, Siegwolf R (2002) Spatial and temporal oxygen isotope trends at the northern tree-line in Eurasia. *Geophys. Res. Lett.* 29:10.1-10.4
- Saurer M, Siegwolf R, Scheidegger Y (2001) Canopy gradients in $\delta^{18}\text{O}$ of organic matter as ecophysiological tool. *Isotope Environ. Health Stud.* 37:13-24
- Scheidegger Y, Saurer M, Bahn M, Siegwolf R (2000) Linking stable oxygen and carbon isotopes with stomatal conductance and photosynthetic capacity: a conceptual model. *Oecologia* 125:350-357
- Schmalstig JG, Cosgrove DJ (1990) Coupling of solute transport and cell expansion in pea stems. *Plant Physiol.* 94:1625-1633
- Scholander PF, Hammel HT, Bradstreet ED, Hemmingsen EA (1965) Sap pressure in vascular plants. *Science* 148:339-345
- Schulze E-D, Ehleringer JR (1984) The effect of nitrogen supply on growth and water-use efficiency of xylem-tapping mistletoes. *Planta* 162:268-275
- Schulze E-D, Lange OL, Ziegler H, Gebauer G (1991) Carbon and nitrogen isotope ratios of mistletoes growing on nitrogen and non-nitrogen fixing hosts and on

- CAM plants in the Namib desert confirm partial heterotrophy. *Oecologia* 88:457-462
- Schulze E-D, Turner NC, Glatzel G (1984) Carbon, water and nutrient relations of two mistletoes and their hosts: A hypothesis. *Plant Cell Environ.* 7:293-299
- Sharkey PJ, Pate JS (1976) Translocation from leaves to fruits of a legume, studied by a phloem bleeding technique: diurnal changes and effects of continuous darkness. *Planta* 128:63-72
- Sheehy JE, Mitchell PL, Durand J-L, Gastal F, Woodward FI (1995) Calculation of translocation coefficients from phloem anatomy for use in crop models. *Ann. Bot.* 76:263-269
- Smith JAC, Milburn JA (1980) Phloem turgor and the regulation of sucrose loading in *Ricinus communis* L. *Planta* 148:42-48
- Smith KC, Magnuson CE, Goeschl JD, DeMichele DW (1980) A time-integrated mathematical expression of the Münch hypothesis of phloem transport. *J. Theor. Biol.* 86:493-505
- Snyder KA, Richards JH, Donovan LA (2003) Night-time conductance in C₃ and C₄ species: do plants lose water at night? *J. Exp. Bot.* 54:861-865
- Stern LA, Amundson R, Baisden WT (2001) Influence of soils on oxygen isotope ratio of atmospheric CO₂. *Global Biogeochem. Cycles* 15:753-759
- Sternberg L, DeNiro M (1983) Biogeochemical implications of the isotopic equilibrium fractionation factor between the oxygen atoms of acetone and water. *Geochim. Cosmochim. Acta* 47:2271-2274
- Sternberg L, DeNiro M, Savidge R (1986) Oxygen isotope exchange between metabolites and water during biochemical reactions leading to cellulose synthesis. *Plant Physiol.* 82:423-427
- Sternberg LSL, Anderson WT, Morrison K (2003) Separating soil and leaf water ¹⁸O isotopic signals in plant stem cellulose. *Geochim. Cosmochim. Acta* 67:2561-2566
- Sternberg LSL, DeNiro M, Keeley JE (1984) Hydrogen, oxygen, and carbon isotope ratios of cellulose from submerged aquatic crassulacean acid metabolism and non-crassulacean acid metabolism plants. *Plant Physiol.* 76:68-70
- Stewart GR, Press MC (1990) The physiology and biochemistry of parasitic angiosperms. *Annu. Rev. Plant Physiol. Plant Mol. Biol.* 41:127-151

- Syvertsen JP, Smith ML, Lloyd J, Farquhar GD (1997) Net carbon dioxide assimilation, carbon isotope discrimination, growth, and water-use efficiency of *Citrus* trees in response to nitrogen status. *J. Amer. Soc. Hort. Sci.* 122:226-232
- Tans PP (1998) Oxygen isotopic equilibrium between carbon dioxide and water in soils. *Tellus* 50B:163-178
- Tennakoon KU, Pate JS (1996a) Effects of parasitism by a mistletoe on the structure and functioning of branches of its host. *Plant Cell Environ.* 19:517-528
- Tennakoon KU, Pate JS (1996b) Heterotrophic gain of carbon from hosts by the xylem-tapping root hemiparasite *Olex phyllanthi* (Olacaceae). *Oecologia* 105:369-376
- Tennakoon KU, Pate JS, Arthur D (1997) Ecophysiological aspects of the woody root hemiparasite *Santalum acuminatum* (R. Br.) A. DC and its common hosts in southwestern Australia. *Ann. Bot.* 80:245-256
- Terwilliger VJ (1997) Changes in the $\delta^{13}\text{C}$ values of trees during a tropical rainy season: some effects in addition to diffusion and carboxylation by Rubisco? *Am. J. Bot.* 84:1693-1700
- Terwilliger VJ, Kitajima K, Le Roux-Swarthout DJ, Mulkey S, Wright SJ (2001) Intrinsic water-use efficiency and heterotrophic investment in tropical leaf growth of two Neotropical pioneer tree species as estimated from $\delta^{13}\text{C}$ values. *New Phytol.* 152:267-281
- Townley LR, Turner JV, Barr AD, Trefry MG, Wright KD, Gailitis V, Harris CJ, Johnston CD (1993) Interaction between lakes, wetlands and unconfined aquifers Wetlands of the Swan Coastal Plain. Environmental Protection Authority of Western Australia and Water Authority of Western Australia
- Tsuzuki M, Miyachi S, Edwards GE (1985) Localization of carbonic anhydrase in mesophyll cells of terrestrial C_3 plants in relation to CO_2 assimilation. *Plant Cell Physiol.* 26:881-891
- Tyree MT, Christy AL, Ferrier JM (1974) A simpler iterative steady state solution of Münch pressure flow systems applied to long and short translocation paths. *Plant Physiol.* 54:589-600
- Ullmann I, Lange OL, Ziegler H, Ehleringer JR, Schulze E-D, Cowan IR (1985) Diurnal courses of leaf conductance and transpiration of mistletoes and their hosts in central Australia. *Oecologia* 67:577-587
- Vitousek PM, Howarth RW (1991) Nitrogen limitation on land and in the sea: how can it occur? *Biogeochemistry* 13:87-115

- Yakir D, DeNiro MJ (1990) Oxygen and hydrogen isotope fractionation during cellulose metabolism in *Lemna gibba* L. *Plant Physiol.* 93:325-332
- Yakir D, Israeli Y (1995) Reduced solar irradiance effects on net primary productivity (NPP) and the $\delta^{13}\text{C}$ and $\delta^{18}\text{O}$ values in plantations of *Musa* sp. *Musaceae*. *Geochim. Cosmochim. Acta* 59:2149-2151
- Yakir D, Sternberg LdL (2000) The use of stable isotopes to study ecosystem gas exchange. *Oecologia* 123:297-311
- Yakir D, Ting I, DeNiro M (1994b) Natural abundance $^2\text{H}/^1\text{H}$ ratios of water storage in leaves of *Peperomia congesta* HBK during water stress. *J. Plant Physiol.* 144:607-612
- Yakir D, Wang X-F (1996) Fluxes of CO_2 and water between terrestrial vegetation and the atmosphere estimated from isotope measurements. *Nature* 380:551-517
- Yoneyama T, Fujiwara H, Engelaar W (2000) Weather and nodule mediated variations in $\delta^{13}\text{C}$ and $\delta^{15}\text{N}$ values in field-grown soybean (*Glycine max* L.) with special interest in the analyses of xylem fluids. *J. Exp. Bot.* 51:559-566
- Yoneyama T, Fujiwara H, Wilson JM (1998) Variations in fractionation of carbon and nitrogen isotopes in higher plants: N metabolism and partitioning in phloem and xylem. In: Griffiths H (ed) *Stable isotopes: integration of biological, ecological, and geochemical processes*. BIOS Scientific Publishers Ltd, Oxford, pp 99-109
- Yoneyama T, Handley LL, Scrimgeour CM, Fisher DB, Raven JA (1997) Variations of the natural abundances of nitrogen and carbon isotopes in *Triticum aestivum*, with special reference to phloem and xylem exudates. *New Phytol.* 137:205-213
- Yoneyama T, Ohtani T (1983) Variations of natural ^{13}C abundances in leguminous plants. *Plant Cell Physiol.* 24:971-977
- Ziegler H (1994) Deuterium content in organic material of hosts and their parasites. In: Schulze E-D, Caldwell M (eds) *Ecophysiology of photosynthesis*. Springer, Berlin, pp 393-408
- Ziegler H (1996) Stable isotopes in interactions of parasites and hosts within higher plants. *Isotopenpraxis* 32:129-140
- Zimmerman MH (1960) Transport in the phloem. *Ann. Rev. Plant Physiol.* 11:167-190
- Zundel G, Miekeley W, Grisi BM, Förstel H (1978) The H_2^{18}O enrichment in the leaf water of tropic trees: Comparison of species from the tropical rain forest and the semi-arid region in Brazil. *Radiat. Environ. Biophys.* 15:203-212

- Walker CD, Lance RC (1991) The fractionation of ^2H and ^{18}O in leaf water of barley. *Aust. J. Plant Physiol.* 18:411-425
- Walker CD, Leaney FW, Dighton JC, Allison GB (1989) The influence of transpiration on the equilibration of leaf water with atmospheric water vapor. *Plant Cell Environ.* 12:221-234
- Wang JH (1954) Theory of self diffusion of water in protein solutions: a new method for studying the hydration and shape of protein molecules. *J. Am. Chem. Soc.* 76:4755-4763
- Wang XF, Yakir D, Avishai M (1998) Non-climatic variations in the oxygen isotopic composition of plants. *Global Change Biol.* 4:835-849
- Warren CR, McGrath JF, Adams MA (2001) Water availability and carbon isotope discrimination in conifers. *Oecologia* 127:476-486
- Weast RC, Lide DR, eds. 1989. *CRC Handbook of Chemistry and Physics*. CRC Press, Boca Raton, Florida.
- White JWC, Gedzelman SD (1984) The isotopic composition of atmospheric water vapor and the concurrent meteorological conditions. *J. Geophys. Res.* 89:4937-4939
- Wilson AT, Grinsted MJ (1977) $^{13}\text{C}/^{12}\text{C}$ in cellulose and lignin as palaeothermometers. *Nature* 265:133-135
- Yakir D (1992) Variations in the natural abundance of oxygen-18 and deuterium in plant carbohydrates. *Plant Cell Environ.* 15:1005-1020
- Yakir D (1992) Water compartmentation in plant tissue: Isotopic evidence. In: Somero GN, Osmond CB, Bolis L (eds) *Water and Life*. Springer-Verlag, Berlin, pp 205-221
- Yakir D (1998) Oxygen-18 of leaf water: a crossroad for plant associated isotopic signals. In: Griffiths H (ed) *Stable isotopes: integration of biological, ecological, and geochemical processes*. BIOS Scientific Publishers, Oxford, pp 147-188
- Yakir D, Berry JA, Giles L, Osmond CB (1994a) Isotopic heterogeneity of water in transpiring leaves: identification of the component that controls the $\delta^{18}\text{O}$ of atmospheric O_2 and CO_2 . *Plant Cell Environ.* 17:73-80
- Yakir D, DeNiro M, Gat J (1990) Natural deuterium and oxygen-18 enrichment in leaf water of cotton plants grown under wet and dry conditions: Evidence for water compartmentation and its dynamics. *Plant Cell Environ.* 13:49-56